FUNDAMENTAL STUDY OF STRUCTURAL FEATURES AFFECTING ENZYMATIC HYDROLYSIS OF LIGNOCELLULOSIC BIOMASS

A Dissertation

by

LI ZHU

Submitted to the Office of Graduate Studies of
Texas A&M University
in partial fulfillment of the requirements for the degree of

DOCTOR OF PHILOSOPHY

August 2005

Major Subject: Chemical Engineering

FUNDAMENTAL STUDY OF STRUCTURAL FEATURES AFFECTING ENZYMATIC HYDROLYSIS OF LIGNOCELLULOSIC BIOMASS

A Dissertation

by

LI ZHU

Submitted to the Office of Graduate Studies of
Texas A&M University
in partial fulfillment of the requirements for the degree of

DOCTOR OF PHILOSOPHY

Approved by:

Chair of Committee,	Mark T. Holtzapple
Committee Members,	Richard R. Davison
	Cady R. Engler
	Daniel F. Shantz
Head of Department,	Kenneth R. Hall

August 2005

Major Subject: Chemical Engineering

ABSTRACT

Fundamental Study of Structural Features Affecting Enzymatic Hydrolysis of Lignocellulosic Biomass. (August 2005)

Li Zhu, B.S., Beijing University of Chemical Technology, P. R. China;

M.S., Research Institute of Petroleum Processing, SINOPEC, P. R. China

Chair of Advisory Committee: Dr. Mark T. Holtzapple

Lignocellulose is a promising and valuable alternative energy source. Native lignocellulosic biomass has limited accessibility to cellulase enzyme due to structural features; therefore, pretreatment is an essential prerequisite to make biomass accessible and reactive by altering its structural features.

The effects of substrate concentration, addition of cellobiase, enzyme loading, and structural features on biomass digestibility were explored. The addition of supplemental cellobiase to the enzyme complex greatly increased the initial rate and ultimate extent of biomass hydrolysis by converting the strong inhibitor, cellobiose, to glucose. A low substrate concentration (10 g/L) was employed to prevent end-product inhibition by cellobiose and glucose. The rate and extent of biomass hydrolysis significantly depend on enzyme loading and structural features resulting from pretreatment, thus the hydrolysis and pretreatment processes are intimately coupled because of structural features.

Model lignocelluloses with various structural features were hydrolyzed with a variety of cellulase loadings for 1, 6, and 72 h. Glucan, xylan, and total sugar conversions at 1, 6, and 72 h were linearly proportional to the logarithm of cellulase loadings from approximately 10% to 90% conversion, indicating that the simplified HCH-1 model is valid for predicting lignocellulose digestibility. Carbohydrate conversions at a given time versus the natural logarithm of cellulase loadings were plotted to obtain the slopes and intercepts which were correlated to structural features

(lignin content, acetyl content, cellulose crystallinity, and carbohydrate content) by both parametric and nonparametric regression models.

The predictive ability of the models was evaluated by a variety of biomass (corn stover, bagasse, and rice straw) treated with lime, dilute acid, ammonia fiber explosion (AFEX), and aqueous ammonia. The measured slopes, intercepts, and carbohydrate conversions at 1, 6, and 72 h were compared to the values predicted by the parametric and nonparametric models. The smaller mean square error (MSE) in the parametric models indicates more satisfactorily predictive ability than the nonparametric models. The agreement between the measured and predicted values shows that lignin content, acetyl content, and cellulose crystallinity are key factors that determine biomass digestibility, and that biomass digestibility can be predicted over a wide range of cellulase loadings using the simplified HCH-1 model.

DEDICATION

To God, whom I love and trust in everything.
To my loving husband, Victor, and my family for their love, encouragement, and support.

ACKNOWLEDGEMENTS

I would like to express my deepest appreciation to my advisor, Dr. Mark Holtzapple for his continuous guidance, encouragement, and financial support. I would like to thank the other members of the committee, Dr. Richard Davison, Dr. Cady Engler, and Dr. Daniel Shantz, for patiently reading through this dissertation and providing helpful comments.

I would like to express special thanks for my colleague, Jonathan O'Dwyer for providing half of the data in this project and helping me improve my oral English. I would also like to thank Dr. Cesar Granada for his tremendous help on the HPLC analysis. These thanks are also extended to the other members of my research group: Sehoon Kim, Guillermo Coward-Kelly, Frank Agbogbo, Zhihong Fu, Maxine Jones, and Rocio Sierra.

I would like to thank Andrew and Sophia Chan for providing me the chance to know God and their continuous prayers for me during my studies. I also would like to thank many sisters and brothers in Chinese Worship at Grace Bible Church and CCCF for their love and encouragement.

Finally, my sincerest gratitude is to my husband Victor and my family. Without their love, encouragement, and support, I would not have been able to accomplish this dissertation and obtain the doctorate degree.

TABLE OF CONTENTS

LIST OF FIGURES

FIGURE Page

FIGURE Page

FIGURE Page

FIGURE Page

LIST OF TABLES

TABLE Page

CHAPTER I

INTRODUCTION

The conversion of lignocellulosic biomass to liquid fuels has long been pursued for its potential to provide an alternative, renewable energy source that substitutes for fossil fuels. Compared to fossil fuels, lignocellulose-derived biofuels have advantages such as reduced greenhouse gas emissions. Using waste biomass as an energy resource can dispose of forestry wastes, agriculture residues, portions of municipal solid waste, and various industrial wastes. Therefore, the development and implementation of such technologies can dramatically improve our environment and economy.

BIOMASS CONVERSION TO ALCOHOL

Lignocellulosic biomass is among the most promising alternative energy sources because it is inexpensive, renewable, widely available, and environmentally friendly. Generally, there are two types of biological processes that convert lignocellulosic biomass to alcohols (Figure I-1).

In the traditional process, biomass is converted to ethanol by two separate steps: (1) the hydrolysis (saccharification) of biomass to fermentable sugars by enzymes, and (2) the fermentation of sugars to ethanol by yeast. Separate hydrolysis and fermentation (SHF) allows operation at the optimal temperature for each process. Combining saccharification and fermentation into a single step is called simultaneous saccharification fermentation (SSF). The primary advantage of SSF is that the immediate consumption of sugars by microorganisms results in low glucose and cellobiose concentrations in the fermentor. Compared to SHF, SSF significantly reduces enzyme inhibition to improve the kinetics (Takagi et al., 1977) and economics (Wright et al., 1988) of biomass conversion.

This dissertation follows the style and format of Biotechnology and Bioengineering.

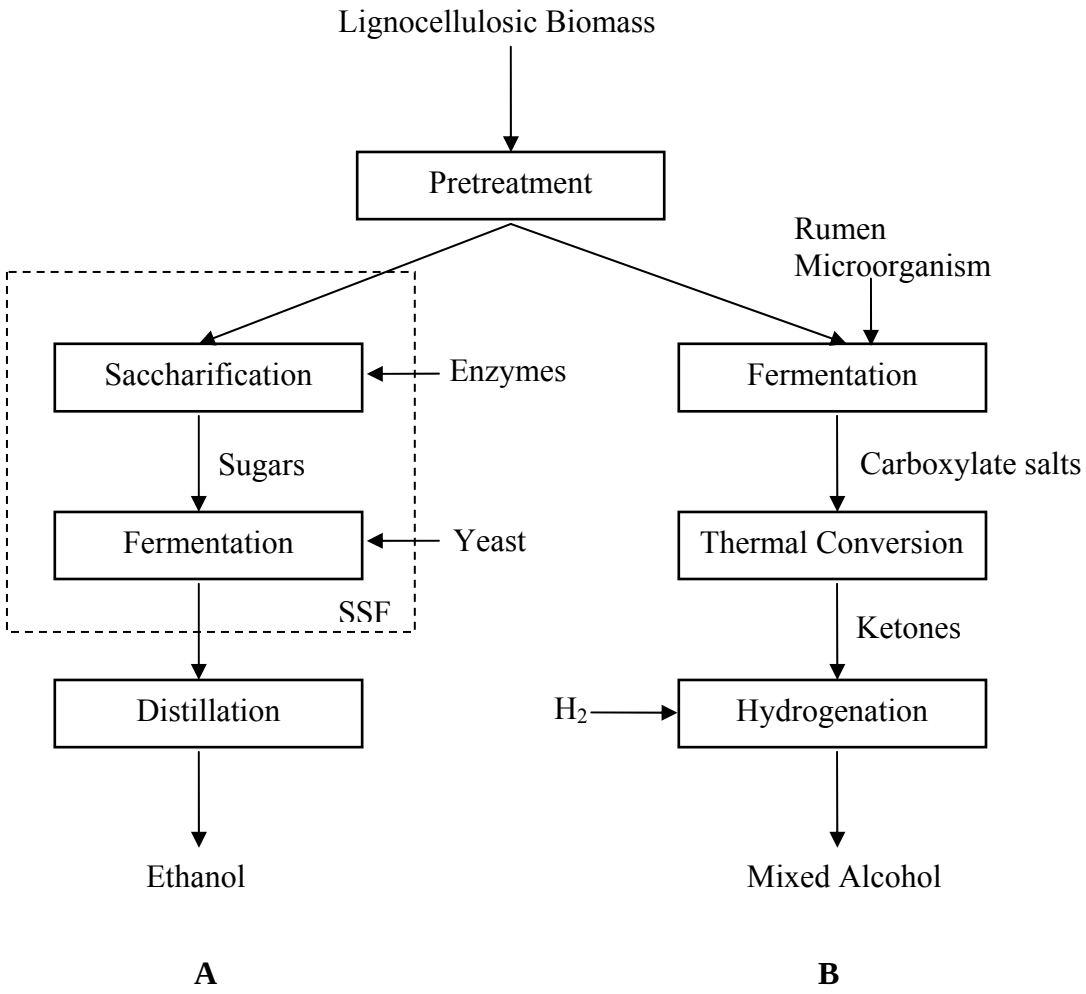

Figure I-1. Schematics of biomass conversion to alcohols: (A) traditional process; (B) MixAlco process.

There are two basic approaches to degrading biomass to sugars: enzymatic hydrolysis and dilute acid hydrolysis. Compared to dilute acid hydrolysis, enzymatic approach is promising because it can achieve high sugar yields and eliminate the need for large quantities of chemicals and the formation of inhibitory by-products during dilute acid hydrolysis (Pfeifer et al., 1984; Tran and Chambers, 1986). Cellulase, the enzyme that catalyzes cellulose degradation to glucose, is actually a complex mixture of several enzymes including endoglucanase, exoglucanase, and β-glucosidase (Figure I-2). Endoglucanase randomly attacks internal bonds in the cellulose chain and acts mainly on the amorphous cellulose. Exoglucanase (cellobiohydrolase) hydrolyzes from the chain ends and produces predominately cellobiose, and it can degrade crystalline cellulose. Cellobiose is cleaved to form two glucose molecules by β-glucosidase (cellobiase).

In the MixAlco process, biomass is converted directly to carboxylate salts by rumen microorganisms (Holtzapple et al., 1997). The carboxylate salts are thermally converted to ketones that are then hydrogenated to mixed alcohols (C_2–C_{13}). The MixAlco process has advantages over the traditional process, for example, no requirements for expensive extracellular enzymes or sterile conditions.

STRUCTURE OF LIGNOCELLULOSIC BIOMASS

Lignocellulose generally consists of about 30–45% cellulose, 25–30% lignin, 25–30% hemicellulose, and extractives. Cellulose forms a skeleton that is surrounded by hemicellulose and lignin functioning as matrix and encrusting materials, respectively. Cellulose, hemicellulose, and lignin are closely associated and covalent cross linkages occur between lignin and polysaccharides (Ingram and Doran, 1995).

Cellulose, the world's most abundant renewable material, is a linear homopolymer of β-1,4-D-glucose with the degree of polymerization (DP) of 500 to 15 000 (Holtzapple, 1993a). The β-1,4 orientation of the glucosidic bonds results in the potential formation of intramolecular and intermolecular hydrogen bonds, which make native cellulose highly crystalline, insoluble, and resistant to enzyme and microbial attack.

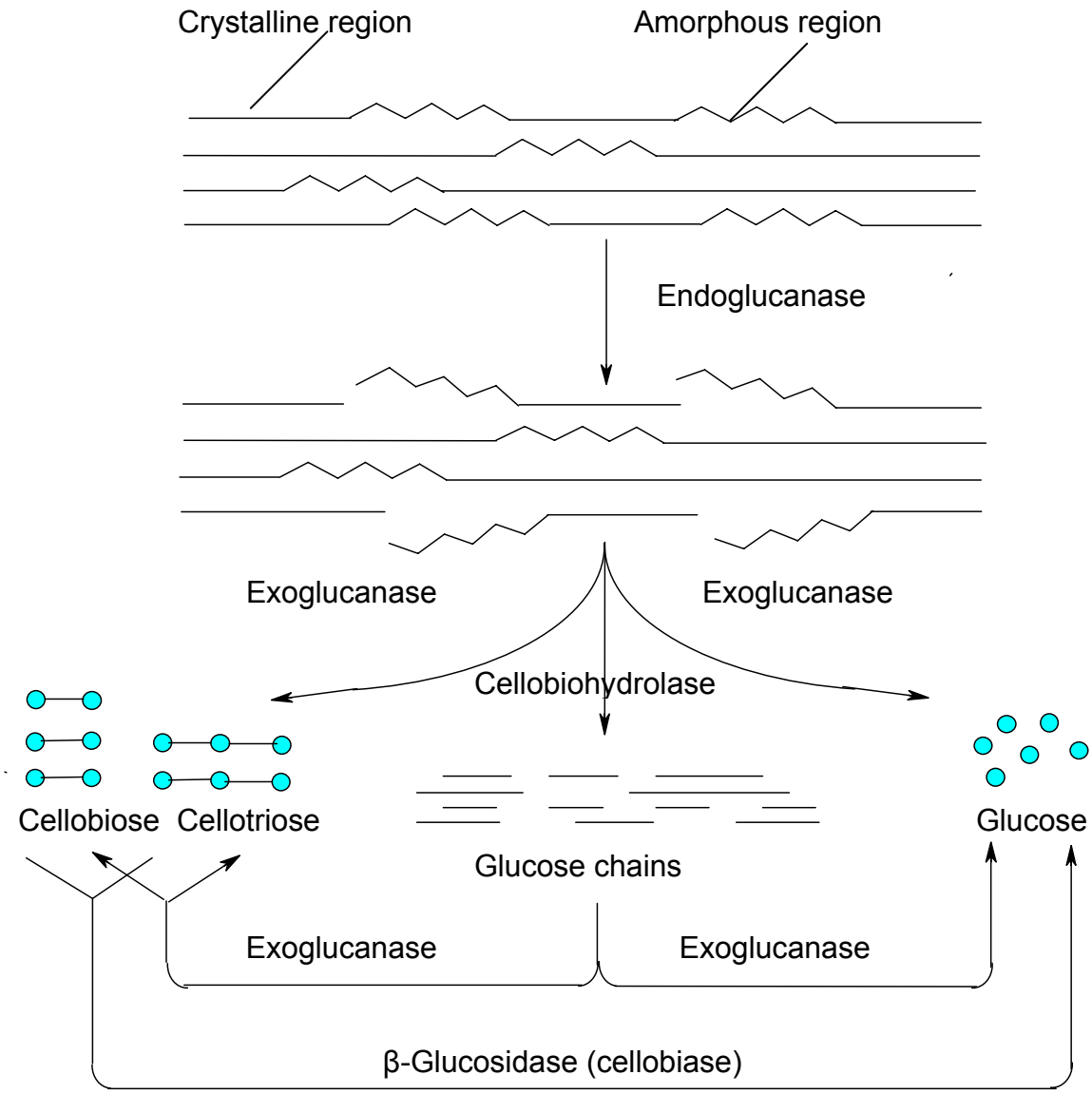

Figure I-2. Mode of cellulolytic enzyme action.
(www.gmu.edu/departments/biology/385-Ch13-biomass2/sld032.htm)

Hemicellulose is a short, highly branched polymer of pentoses and hexoses with a DP of 50 to 200. D-xylose and L-arabinose are the major constituents of the pentosans, whereas D-manose, D-galactose, and D-glucose are the constituents of the hexosans (Holtzapple, 1993b). Hemicellulose has acetate groups randomly attached with ester linkages to the hydroxyl groups of the sugar rings. Its branched chain renders hemicellulose amorphous and relatively easy to hydrolyze to its constituent sugars. However, acetate groups interfere with enzyme recognition thereby slowing the hemicellulose hydrolysis rate, which blocks access to cellulose. The role of hemicellulose is to provide a linkage between lignin and cellulose.

Lignin is a complex, amorphous, and cross-linked polymer consisting of phenyl-propane-based monomeric units (Holtzapple, 1993c). Lignin hinders enzyme accessibility to cellulose and hemicelluose during enzymatic hydrolysis (Mooney et al., 1998) because it encrusts the carbohydrate polymer matrix of cellulose and hemicellulose. One of the major roles of lignin is to maintain fiber integrity and structural rigidity.

EFFECTS OF STRUCTURAL FEATURES ON BIOMASS DIGESTIBILITY

The enzymatic hydrolysis of lignocellulose is affected by many factors. The limiting factors have been traditionally divided into two groups: those related to lignocellulose structural features and those related to the mechanism and interactions of the cellulolytic enzymes. However, the heterogeneous nature of lignocellulose and the multiplicity of enzymes make it difficult to fully understand the interactions between enzyme and lignocellulose; furthermore, the interactions change as hydrolysis proceeds. Therefore, it is apparent that the rate and extent of biomass hydrolysis are inextricably linked to biomass structural features.

Generally, structural features can be categorized into two groups: physical and chemical. Physical structural features include cellulose crystallinity, degree of cellulose polymerization, pore volume, accessible surface area, and particle size. Chemical

structural features include the contents of lignin, hemicellulose, and acetyl groups. Although these structural features are divided into two groups, interactions exist among the structural features in two groups. For example, lignin removal changes the percentage of cellulose and hemicellulose, pore volume, and accessible surface area. Table I-1 summarizes the relationship between structural features and biomass digestibility.

Table I-1. Summary of relationship between structural features and digestibility

Structural Features		Relationship between structural features and digestibility	Reference
Physical	Surface Area	Positive	Grethlein, 1985; Sinitsyn et al., 1991
	Crystallinity	Negative	Caulfield and Moore, 1974; Fan et al., 1981
		No correlation	Grethlein, 1985; Puri, 1984
	Degree of polymerization	Negative	Puri, 1984
		No correlation	Sinitsyn et al., 1991
	Pore volume	Positive	Grethlein, 1985; Weimer and Weston, 1985
	Particle size	No correlation	Draude et al., 2001; Sinitsyn et al., 1991
Chemical	Lignin	Negative	Draude et al., 2001; Mooney et al., 1998
	Hemicellulose	Negative	Grohmann et al., 1989; Kim et al., 2003
	Acetyl group	Negative	Grohmann et al., 1989; Kong et al., 1992

Lignin Content

Lignin plays a significant role in the rate and extent of lignocellulose hydrolysis. Literature results have all shown that cellulose digestibility enhances with increasing lignin removal (Chang and Holtzapple, 2000; Draude et al., 2001; Gharpuray et al., 1983; Thompson and Chen, 1992). The major inhibitory role of lignin has been attributed to nonspecific adsorption of enzyme to lignin (Ooshima et al., 1990; Sewalt et al., 1997) and enzyme inaccessibility to cellulose due to steric hindrance (Mooney et al., 1998; Meunier-Goddik et al., 1999).

Acetyl Content

Xylan backbones in native plant cell walls are extensively acetylated (Holtzapple, 1993b). Several studies showed that the removal of acetyl groups from hemicellulose reduced the steric hindrance of enzymes and greatly enhanced cellulose and xylan digestibility (Grohmann et al., 1989; Kong et al., 1992; Mitchell et al., 1990). The acetate groups interfere with enzyme recognition thereby slowing the hydrolysis rate.

Crystallinity

It is broadly accepted that highly crystalline cellulose is less accessible to cellulase attack than amorphous cellulose; therefore, crystallinity affects the efficiency of enzyme contact with cellulose (Chang and Holtzapple, 2000). Although a negative relationship between crystallinity and digestibility has been reported (Fan et al., 1981; Gharpuay et al. , 1983; Koullas et al., 1990; Sinitsyn et al., 1991; Thompson and Chen, 1992), some researchers proposed that the effect of reduced crystallinity on hydrolysis rate might be a consequence of increased surface area (Gharpuray et al., 1983) or decreased particle size (Grethlein, 1985), because ball milling tends to decrease the particle size and crystallinity of biomass and increase the specific surface area simultaneously (Caulfield and Moore, 1974). Several investigations have shown that further reduction of particle size below 40 mesh did not enhance the hydrolysis rate (Chang et al., 1997; Draude et al., 2001). Decrease in both crystallinity and specific surface area were observed when cellulose was ball milled for 96 h, whereas the extent of hydrolysis still increased significantly (Fan et al., 1981).

Accessible Surface Area

Accessible surface area of lignocellulosic biomass is a crucial factor that affects digestibility. There is a positive correlation between accessible surface area and biomass digestibility (Fan et al*.,* 1981; Grethlein, 1985; Thompson and Chen, 1992; Sinitsyn et al*.,* 1991). However, accessible surface area was not considered as a dependent factor that affects cellulose digestibility (Millet et al., 1976), because it may correlate with

cellulose crystallinity (Sinitsyn et al., 1991) or lignin removal. In addition, accessible surface area is intimately coupled with pore volume. Thompson and Chen (1992) measured three types of specific surface area: total specific surface area and specific surface area available to a 3.8- and 5.1-nm solute. Only the specific surface area available to 5.1-nm solute correlated with biomass digestibility.

Among all of these structural features, lignin content, acetyl content, and crystallinity are key structural features that affect biomass digestibility because they are characteristic factors of the three main components of lignocellulose (lignin, hemicellulose, and cellulose). Furthermore, these parameters can be independently manipulated in pretreatment processes and are easy to measure. This does not rule out other factors, which also affect biomass digestibility. For example, several researchers correlated the hydrolysis rate to pore volume (Mooney et al., 1998; Weimer and Weston, 1985), degree of polymerization (Puri, 1984; Sinitsyn et al., 1991), and particle size (Caulfield and Moore, 1974; Draude et al., 2001; Sinitsyn et al., 1991).

PRETREATMENTS

Enzymatic hydrolysis of biomass to sugars is a promising technology because nearly theoretical sugar yields are possible. However, native lignocellulosic biomass has limited accessibility to enzymes due to structural features. Therefore, pretreatment, is an essential prerequisite to make biomass accessible and reactive by altering its structural features. The goal of pretreating biomass is to achieve high product yields in subsequent enzymatic hydrolysis and fermentation operations with minimal costs.

In general, pretreatment techniques can be grouped into three categories: physical, chemical, and biological. Table I-2 summarizes the change in biomass compositional features for various pretreatment processes (Lynd et al., 2002). Most pretreatment methods are aimed at removing hemicellulose or lignin to increase accessible surface area. Among various technologies, hydrolysis methods with dilute acid or alkali have been intensively studied because they are relatively capital and

Table I-2. Change in biomass compositional features for various pretreatment techniques

Pretreatment	Compositional features			Advantage	Disadvantage	References
	Cellulose	Hemicellulose	Lignin			
Ball-milling	Intensive decrystallization	No removal	No removal	Intensive decrystallization	Energy-intensive	Chang and Holtzapple, 2000; Koullas et al., 1990
Steam explosion	Some depolymerization	80–100% solubilization	Little solubilization, more redistribution	Energy efficient, no recycling cost	Xylan degradation, by-product inhibition	Grethlein and Converse, 1991
Dilute-acid	Some depolymerization	80–100% solubilization	Little solubilization, more redistribution	Mild condition, high xylose yields	Acid recovery, corrosive, relatively expensive	Torget, 1991; Grethlein and Converse, 1991
AFEX	Decrystallization	Up to 60% solubilization	10–20% solubilization	Less xylan loss, no inhibitor formation	Ammonia recovery, not effective for high lignin	Dale and Moreira, 1982; Holtzapple et al., 1991
Sodium hydroxide	Substantial swelling, type I $\rightarrow$ type II	Substantial solubilization	Substantial solubilization (>50%)	Effective ester removal	Expensive reagent, alkali recovery	Millett et al., 1976
ARP	Less than 5% depolymerization	~50% solubilization	~70% solubilization	Effective delignification	Alkali recovery, relatively expensive	Yoon et al,, 1995; Kim et al., 2003
Lime	Little depolymerization	Significant solub-ilization (to 30%)	Partial solubilization (~ 40%)	Effective lignin & acetyl removal, inexpensive	Less effective due to poor solubility of lime	Chang et al., 1997
Ozonolysis	Almost no depolymerization	Little solubilization	Up to 70% solubilization	Effective delignification, mild condition	Expensive, need more ozone	Vidal and Molinier, 1988
Organo-solvlysis	Significant swelling	Substantial, can be nearly complete	Substantial, can be nearly complete	High xylose yields, effective delignification	Solvent recovery expensive	Chum et al., 1988
Biological	20–30% depolymerization	Up to 80% depolymerization	~ 40 % delignification	Low energy requirement, effective delignification	Cellulose loss, slow hydrolysis rate	Kirk and Farrell, 1987; Datta, 1981

AFEX: Ammonia Fiber Explosion; ARP: Ammonia Recycled Percolation.

energy efficient. However, the effect of pretreatment technologies on biomass may vary, depending on substrate and pretreatment conditions. Detailed descriptions of various pretreatment technologies are reviewed by Hsu (1996).

Dilute acid pretreatment usually involves H_2SO_4 or HCl at concentrations of 0.3% to 1.1% (w/w) to hydrolyze hemicellulose. Although lignin is also solubilized during acid hydrolysis, it recondenses forming an altered lignin polymer (Torget et al., 1991). Dilute acid pretreatment increases the surface area and the pore volume by removing hemicellulose. There is no consistent observance of the effect of chemical pretreatments on biomass crystallinity (Grethlein and Converse, 1991; Thompson and Chen, 1992). Actually, chemical treatments have a dual effect on biomass crystallinity: (1) they remove amorphous lignin and hemicellulose components to increase biomass crystallinity, and (2) they loosen the highly packed crystalline structure through swelling to decrease crystallinity (Gharpuray et al., 1983), therefore the change in biomass crystallinity during chemical pretreatment depends on the predominance of these two effects. Although dilute acid pretreatment can significantly improve cellulose hydrolysis and achieve high xylose yields, its cost is usually high compared to steam explosion and AFEX due to acid recovery and the need for corrosion-resistant materials for reactors.

Alkaline pretreatment techniques are delignification processes (Millett et al., 1976) with significant solubilization of hemicellulose as well. The mechanism of alkaline hydrolysis is saponification of intermolecular ester bonds crosslinking hemicellulose and lignin. Dilute NaOH pretreatment causes swelling, leading to an increase in internal surface area, a decrease in DP and crystallinity, and disruption of lignin structure (Fan et al., 1987). In comparison with dilute acid pretreatment, the high cost of caustic soda is the main obstacle to its large-scale implementation. Therefore, aqueous ammonia and lime (calcium hydroxide) pretreatments have been developed to reduce the cost of chemicals. These two kinds of alkali are effective in removing lignin and acetyl groups in biomass. Lime is a promising chemical because it is inexpensive, safe, and can be recovered by carbonating wash water (Chang et al., 1997).

ENZYMATIC HYDROLYSIS MODELS

Models that elucidate the enzymatic hydrolysis of cellulosic and lignocellulosic biomass can be divided into two categories: mechanistic and empirical. Most mechanistic models are Michaelis-Menten models with inhibition (Holtzapple et al., 1984; Schell et al., 1999), enzyme adsorption step (Holtzapple et al., 1984), thermal deactivation of enzyme (Gusakov et al., 1985; Schell et al., 1999), and adsorption of enzyme on lignin (Gusakov et al., 1992; South et al., 1995). Semi-empirical models have been developed based on the assumption that the enzymatic reaction between cellulase and cellulose can be described by summing pseudo-first-order reactions (Nidetzky and Steiner, 1993; Sattler et al., 1989; Wald et al., 1984). Unfortunately, no model can conclusively predict the digestibility of various biomass types satisfactorily due to enzyme complexity, heterogeneous lignocellulose structural features, observed changes in adsorption of enzymes on biomass with time, and enzyme inhibition by hydrolysis products. A good prediction requires fundamental studies of factors that affect biomass digestibility.

The pretreatment and hydrolysis processes are major contributors to the total production cost of ethanol from biomass (~ 60%) when using an enzyme-based process (Nguyen and Saddler, 1991). These two processes are intimately coupled because of structural features. The rate and extent of hydrolysis depend significantly on enzyme loading and structural features resulting from pretreatment (Figure I-3). To some extent, the effect of a poor pretreatment can be overcome by higher enzyme loading; an excellent pretreatment can reduce the required enzyme substantially. It is desirable to develop a mathematical model that correlates biomass digestibility with structural features and predicts its digestibility from specific structural features so as to do economic optimization. Table I-3 summarizes empirical models that have been used for decades (Fan et al.; 1981, Gharpuray et al.; 1983, Koullas et al., 1992; Thompson and Chen, 1992). However, the proposed models are subject to the following problems:

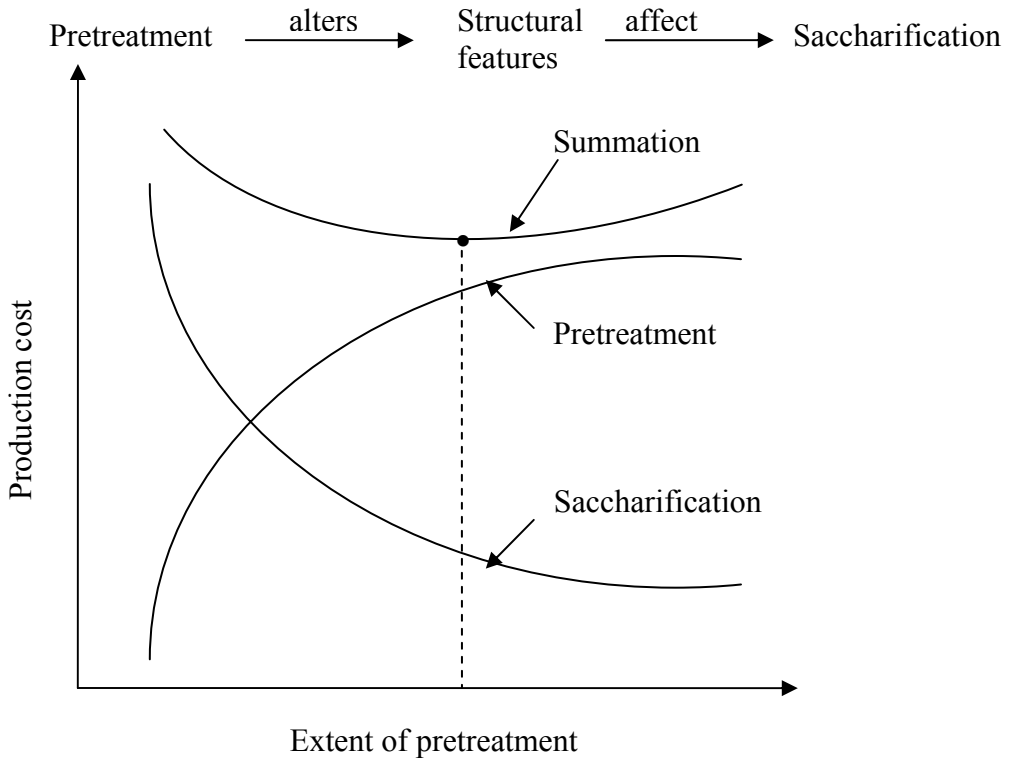

Figure I-3. Relationship between pretreatment and production cost.

Table I-3. Summary of empirical models correlating structural features and digestibility

Biomass	No. of Sample	Spectrum of structural features			Model expression	Reference
		L (%)	CrI (%)	SSA (m^2/g)		
Solka Floc	19	n/a	36.5–88.8	1.15–106.2	$D = 0.38(SSA)^{0.195}\ (100\text{-}CrI)^{1.04}$	Fan, 1981
Wheat straw	18	1.33–11.53	13.9–69.6	0.64–2.9	$D = 2.044(100\text{-}CrI)^{0.257}(SSA)^{0.988}\ (L)^{-0.388}$	Gharpuray, 1983
Avicel Wheat straw	18	n/a	n/a	n/a	$D = 122\text{-}0.21CrI\text{+}0.59\ DL\text{-}0.013\ CrI^2\text{-}0.011DL^2\text{+}0.015CrI{\cdot}DL$	Koullas, 1992
Mixed hardwoods	13	11.12–24.90	68.4–85.8	14.8–128	$D = 0.444(100\text{-}CrI)^{0.293}(G/L)^{0.247}\ (SSA)^{0.827}$	Thompson, 1992

L: lignin content; CrI: biomass crystallinity index; SSA: specific surface area; D: digestibility; DL: extent of deliginification; n/a: no reported data.

1. The number of tested samples was small. The number of tested samples used to develop each of these four models was less than 20, which is too small for deriving a reliable statistical model.
2. The spectrum of investigated structural features was relatively narrow. For example, the crystallinity of mixed hardwoods ranged only from 68.4% to 85.8% (Thompson and Chen, 1992), the specific surface area of wheat straw tested by Gharpuray (1983) was in a narrow range of 0.64 to 2.9 m^2/g.
3. The interaction of structural features was neglected. During a pretreatment, the removal of an individual component such as lignin or hemicellulose influences the composition of the residual material. For example, hemicellulose is altered by many lignin-removal procedures; therefore, a simultaneous study of all major features is necessary to establish a reliable relationship between structural features and digestibility.
4. Some structural features were not independent. As described above, almost all of the pretreatment techniques increase specific surface area. Specific surface area is not an independent variable, because it can be correlated with cystallinity (Sinitsyn et al., 1991). To develop a reliable correlation model, the intercorrelation among independent variables should be eliminated.
5. The enzymatic hydrolysis conditions were not appropriately chosen. The model samples were only hydrolyzed for one hydrolysis time with one enzyme loading (Fan et al., 1981; Gharpuray et al., 1983; Thompson and Chen, 1992). For example, the hydrolysis time employed by Fan (1981) and Gharpuray (1983) was 8 h, which was not long enough for complete hydrolysis.
6. The predictive ability of these models was not evaluated. A satisfactory model should have the ability to predict the digestibility of a variety of biomass types treated by different techniques. Unfortunately, these models have not been applied to biomass type or pretreatment techniques other than those from which they were derived.

To establish a reliable relationship between these structural features and digestibility, it is necessary to employ a large number of biomass samples with a wide spectrum of structural features treated by various techniques. In a previous study (Chang and Holtzapple, 2000), lignin content, acetyl content, and biomass crystallinity were considered as the major structural features that affect biomass digestibility because they are independently controllable and are easy to measure. Selective delignification, deacetylation, and decrystallization were used to prepare model lignocellulose samples to minimize cross effect between structural features. A total of 147 model samples with a variety of lignin contents, acetyl contents, and biomass crystallinities were hydrolyzed with one cellulase loading (5 FPU/g dry biomass), and hydrolysis sugars (glucose, xylose) were measured after 1 h and 3 d. A mathematical model was developed to correlate the initial rate and ultimate conversion of biomass hydrolysis with lignin, acetyl content, and crystallinity, which had the following functional forms:

$$X_G = \frac{a_0 + a_1(A/G) + a_2(A/G)^2 + a_3(A/G)^3}{1 + \exp\left(\frac{b - L/G}{c}\right)} + \frac{d_0 + d_1(A/G) + d_2(A/G)^2 + d_3(A/G)^3}{1 + \exp\left(\frac{e - CrI_B}{f}\right)}$$

$$+ \frac{g_0 + g_1(A/G) + g_2(A/G)^2 + g_3(A/G)^3}{\left(1 + \exp\left(\frac{b - L/G}{c}\right)\right)\left(1 + \exp\left(\frac{e - CrI_B}{f}\right)\right)} \qquad \text{(I-1)}$$

$$X_X = a_0' + a_1' \exp[a_2'(A/X)] + b'(L/X) + c' CrI_B + d'(L/X)^2 + e' CrI_B{}^2 + f'(L/X) \cdot CrI_B \qquad \text{(I-2)}$$

where G = glucan content (%)

X = xylan content (%)

L = lignin content (%)

A = acetyl content (%)

CrI_B = biomass crystallinity index (%)

X_G = 1-h or 3-d glucan conversion (%)

X_X = 1-h or 3-d xylan conversion (%)

a_0–a_3, b, c, d_0–d_3, e, f, g_0–g_3, a_0'–a_2', b', c', d', e', and f' are constants.

Table Curve 3D and SPSS were used to determine the best empirical equations that fit the data. These models showed that crystallinity and lignin content dominated biomass digestibility, whereas acetylation had a less effect. Crystallinity had a significant effect on the initial hydrolysis rate. The mathematical model predicted the initial hydrolysis rate and ultimate conversion of α-cellulose and lime-treated switch grass, poplar wood, and bagasse.

The mathematical model derived by Chang and Holtzapple (2000) can only be used to predict biomass digestibility with one cellulase loading (5 FPU/g dry biomass), which was excessive for biomass with low lignin content and low crystallinity. It is desirable to investigate a wide range of cellulase loadings to reduce the enzyme cost and attain higher sugar conversions.

It has been reported that the relationship between carbohydrate conversion and enzyme loading fit the following equation (Holtzapple et al., 1994; Mandels et al., 1981; Reese and Mandels, 1971).

$$Y = A \cdot \ln(X) + B \tag{I-3}$$

where Y = carbohydrate conversion

X = enzyme loading

A and B are empirical constants

This equation is identical to the simplified model equation derived from the assumption of high enzyme loading in the HCH-1 model (Holtzapple et al., 1984 and 1994) when ϕ is assumed to be 1:

$$-\frac{dG_x}{dt} = \frac{\kappa G_x E i}{\alpha + \phi G_x + \varepsilon E} \tag{I-4}$$

where G_x = cellulose concentration

E = enzyme concentration

ϕ = fraction of cellulose surface which is free to be hydrolyzed ($\phi \cong 1$)

κ, α, and ε = parameters describing the degree of substrate reactivity

i = inhibition parameter ($i \rightarrow 1$ at high activity of cellobiase)

The quantity of enzyme required to achieve the desired conversion of a given biomass and the predicted conversion at given enzyme loading within a selected time can be determined from Figure I-4. Therefore, mathematical models correlating the slope (A) and intercept (B) of the straight line with lignin content, acetyl content, and crystallinity can predict biomass digestibility and help optimize the design of pretreatment and hydrolysis processes.

OBJECTIVES

In this study, model lignocelluloses (Chang and Holtzapple, 2000) with various structural features were hydrolyzed at a variety of cellulase loadings for fixed incubation periods (1, 6, and 72 h). Carbohydrate conversions at a given time versus the natural logarithm of cellulase loadings were plotted to obtain the slopes and intercepts of the straight lines. Mathematical models were developed using both parametric and nonparametric regression approaches to correlate slopes and intercepts with lignin content, acetyl content, crystallinity, and carbohydrate content of biomass. The predictive abilities of these models were evaluated using the digestibility of various biomass types treated by the following methods: lime, dilute acid, ammonia fiber explosion (AFEX), and aqueous ammonia. The overall objective of this research was to fundamentally understand the relative importance of structural features that affect digestibility by developing mathematical models that correlate digestibility with structural features. These mathematical models can be exploited to develop cost-effective pretreatments that required relatively low enzyme loading to achieve high sugar yields; therefore, costs can

be significantly reduced to accelerate commercialization of biomass bioconversion technology.

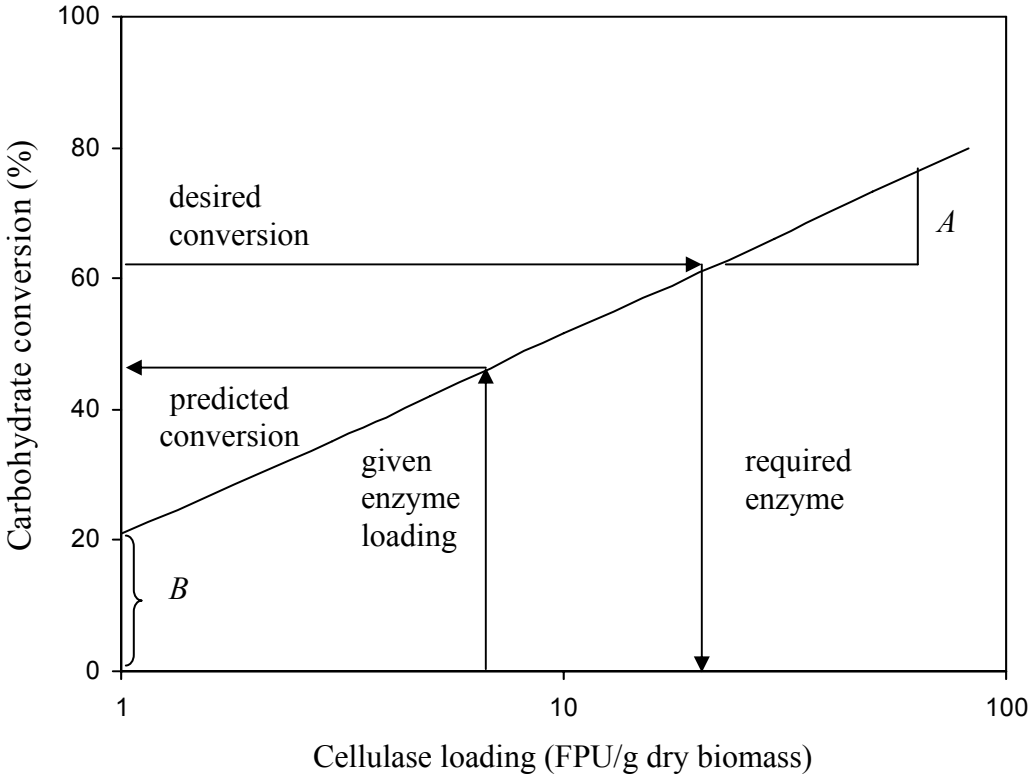

Figure I-4. Schematic diagram of utilization of equation I-3.

CHAPTER II

MATERIALS AND METHODS

This chapter describes the preparation of model lignocellulose samples and the enzymatic hydrolysis of these samples to determine digestibility. Analytical methods for analyzing biomass structural features and carbohydrate contents are also described. The modeling approach for correlating digestibility and structural features is explained.

SUBSTRATE PREPARATION

A total of 147 model samples of poplar wood with a variety of lignin contents, acetyl contents, and crystallinities were prepared via selective delignification with peracetic acid, selective deacetylation with potassium hydroxide, and selective decrystallization with ball milling (Chang and Holtzapple, 2000). The detailed studies of delignification, deacetylation, and decrystallizaton were investigated by Chang and Holtzapple (2000). The treatment conditions are illustrated in Table II-1.

Table II-1. Treatment conditions for preparing model lignocelluloses

Condition	Delignification	Deacetylation	Decrystallization
Temperature	Room	Room	Room
Time[a]	24 and 48 h	24 h	3 and 6 d
Reagent or method	Peracetic acid	Potassium hydroxide	Ball milling (0.375-in zirconia + 300-mL porcelain jar)
Reagent loading	0.1, 0.2, 0.3, 0.5, 1.0, and 5.0 g/g dry biomass	0.07, 0.15, 0.35, 0.55, 0.75, and 1.5 mmol/g dry biomass	43 g grinding media/g dry biomass
Biomass concentration[b]	0.05 and 0.1 g solid/g liquid	0.1 g solid/g liquid	---------

[a] 24 h is used for reagent loading at 5.0 g/g dry biomass.

[b] 0.05 g solid/g liquid is used for reagent loading at 5.0 g/g dry biomass.

ENZYMES

Hydrolysis experiments were performed using cellulase enzyme Spezyme CP, lot 301-00348-257 in combination with a commercial β-glucosidase (Sigma, G-0395). Cellulase was provided by National Renewable Energy Laboratory (NREL) and had an activity of 65 FPU/mL determined according to NREL standard procedure No. 006 (2004). The cellulase activity was improved to 88 FPU/mL when the same amount of cellobiase (cellulase/cellobiase = 1:1 (v/v)) was supplemented (Coward-Kelly et al., 2003). Cellobiase (β-glucosidase) activity was 321 CBU/mL based on the company's assay. The cellulase activity was checked every month to ensure that the cellulase loading for each model lignocellulose was consistent. Throughout this dissertation, the standard NREL procedure was used to characterize cellulose activity.

ENZYMATIC HYDROLYSIS

Enzymatic hydrolysis of pretreated model lignocellulose was performed in 50-mL Erlenmeyer flasks at 50°C in a shaking air bath agitated at 100 rpm. The hydrolysis experiments were performed at 10-g/L solid concentration in 0.05-M citrate buffer (pH 4.8) supplemented with 0.01-g/mL sodium azide to prevent microbial contamination; the final volume was 20 mL. A low substrate concentration (10 g/L) was employed to reduce end-product inhibition. The enzymatic hydrolysis of each model lignocellulose was performed for three incubation periods (1, 6, and 72 h) and three cellulase loadings for each incubation period. The cellulase loadings depended on structural features. One-hour samples indicated the initial hydrolysis rate, 72-h samples indicated the extent of hydrolysis or ultimate carbohydrate conversion, and 6-h samples indicated approximately the average digestibility at 1 and 72 h.

The Erlenmeyer flasks labeled with cellulase loading and incubation period were preheated in the shaking air bath for 1 h. Hydrolysis was initiated by adding 0.2 mL of appropriately diluted cellulase supplemented with 0.05 mL of cellobiase (81.25 CBU/g dry biomass) to prevent end-product inhibition by cellobiose (Holtzapple et al., 1990).

After set incubation periods (1, 6, and 72 h), the Erlenmeyer flasks were removed from the shaking air bath and boiled for 15 min in the sealed Erlenmeyer flasks to denature enzymes to prevent further hydrolysis. Glucose and xylose concentrations were measured using HPLC. The detailed procedure for enzymatic hydrolysis is described in Appendix B.

ANALYTICAL METHODS

Sugar Analysis

The total reducing sugars were measured by a dinitrosalicylic acid (DNS) procedure (Miller, 1959) using glucose as a standard. Other colorimetric assays for sugar measurements including phenol-sulfuric acid, glucose oxidase/peroxidase, chromatropic acid, and phloroglucinol were explored. They were not selected for sugar analysis due to the interference of glucose and xylose by each other and the instability of color development. The detailed procedures and preliminary results of these assays are given in Appendix D. The hydrolysis products, glucose, xylose, and cellobiose were determined by high performance liquid chromatography (HPLC), because it is more specific, analyzes more compounds simultaneously and continuously, and gives reproducible results.

The HPLC system used a Biorad Aminex HPX-87P column and 0.2-μm filtered reverse osmosis deionized water as the mobile phase. The column temperature was 85ºC and flow rate was 0.6 mL/min. Elution of the samples was monitored by a refractive index detector (Lab Alliance, Series 200). The samples were filtered through 0.2-μm filters (Fisher, USA) and a volume of 20 μL was loaded using Spectra System AS 3500 autoinjector (Spectra-Physics, CA, USA). The step-by-step procedure for sugar analysis using HPLC is given in Appendix E.

Structural Carbohydrates and Lignin Analysis

A two-step acid hydrolysis was used to degrade biomass into forms that were more easily quantified. The biomass sample was taken through a primary 72% (w/w)

sulfuric acid hydrolysis at 30ºC for 1 h, followed by a secondary dilute acid (4%, w/w) hydrolysis at 121ºC for 1 h. The resulting sugar monomers and acetyl content were analyzed using HPLC with Bio-Rad Aminex HPX-87P and HPX-87H columns, respectively. The acid-soluble lignin was measured by UV-Vis spectroscopy. The acid-insoluble lignin was determined using gravimetric analysis at 105^{o}C and 575^{o}C. The total lignin content was the summation of acid-insoluble lignin and acid-soluble lignin. This method is based on NREL standard procedure No. 002 (2004), with the detailed procedure given in Appendix F.

Crystallinity Measurements

Biomass crystallinity was measured in the XRD Laboratory, Deapartment of Chemistry, Texas A&M University (College Station, TX) using a D8 Advance Powder X-ray Diffractomer (Brucker Co). The sample was scanned at 2°/min from 2θ = 10° to 26° with a step size of 0.05°. The crystallinity index (CrI) was determined as the percentage of crystalline material in biomass (Segal et al., 1959), as shown in Figure II-1.

$$CrI = \frac{I_{002} - I_{am}}{I_{002}} \times 100 \qquad \text{(II-1)}$$

where CrI = relative degree of crystallinity

I_{002} = intensity of the diffraction from the 002 plane at 2θ = 22.5°

I_{am} = intensity of the background scatter at 2θ = 18.7°

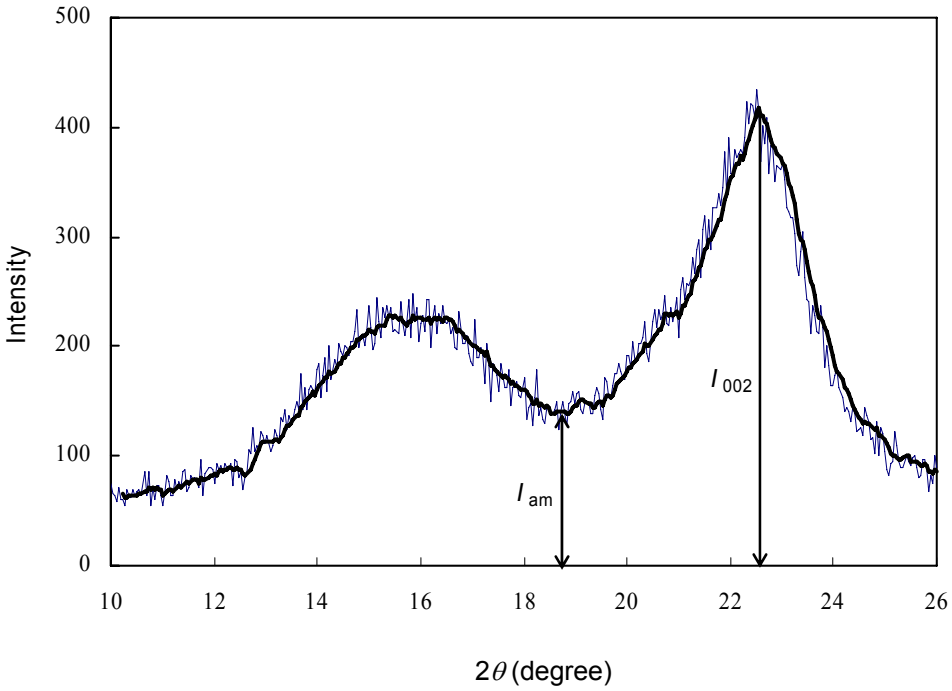

Figure II-1. X-ray diffraction pattern of poplar wood.

Calculation of Carbohydrate Conversion

Using enzymes, glucan and xylan were hydrolyzed to glucose and xylose as follows:

$$[C_6H_{10}O_5]_n + nH_2O \longrightarrow nC_6H_{12}O_6 \quad \text{(II-2)}$$

Glucan — Glucose

Mw 162.2 — *Mw* 180.2

$$[C_5H_8O_4]_n + nH_2O \longrightarrow nC_5H_{10}O_5 \quad \text{(II-3)}$$

Xylan — Xylose

Mw 132.1 — *Mw* 150.1

Knowing the carbohydrate contents in each model lignocellulose, glucan, xylan, and total sugar conversions can be calculated as follows:

$$X_G = \frac{\text{mg glucose}}{\text{mg glucan}} \times \frac{162.2}{180.2} \times 100$$

$$= \frac{([G]\text{-}[G]_0) \times V \times 0.9}{W \times \text{glucan content} \times 1000 \text{ mg/g}} \times 100 \quad \text{(II-4)}$$

$$X_X = \frac{\text{mg xylose}}{\text{mg xylan}} \times \frac{132.1}{150.1} \times 100$$

$$= \frac{([X]\text{-}[X]_0) \times V \times 0.88}{W \times \text{xylan content} \times 1000 \text{ mg/g}} \times 100 \quad \text{(II-5)}$$

$$X_T = \frac{\text{glucose yield} + \text{xylose yield}}{\text{theoretical glucose yield} + \text{theoretical xylose yield}} \times 100$$

$$= \frac{X_G \times \frac{\text{glucan content}}{0.9} + X_X \times \frac{\text{xylan content}}{0.88}}{\frac{\text{glucan content}}{0.9} + \frac{\text{xylan content}}{0.88}} \times 100 \quad \text{(II-6)}$$

where X_G = glucan conversion (%)

X_X = xylan conversion (%)

X_T = total sugar conversion (%)

$[G]$ = glucose concentration in hydrolysis liquid (mg/mL)

$[G]_0$ = initial glucose concentration, can be assumed as 0 (mg/mL)

$[X]$ = xylose concentration in hydrolysis liquid (mg/mL)

$[X]_0$ = initial xylose concentration, can be assumed as 0 (mg/mL)

V = initial volume of biomass slurry (mL)

W = initial dry weight of biomass (g)

0.9 = conversion factor of glucose to equivalent glucan

0.88 = conversion factor of xylose to equivalent xylan

MODELING APPROACH

After carbohydrate conversions of each model lignocellulose were determined, carbohydrate conversions at a given time versus the natural logarithm of cellulase loadings were plotted to obtain the slopes and intercepts of the straight lines. Mathematical models were developed to correlate the slopes and intercepts with lignin content, acetyl content, crystallinity, and carbohydrate content. Schematics of the modeling approach are shown in Figure II-2.

$$\text{Slope } (A) = f(\text{Lignin, Acety, CrI, Carbohydrate}) \quad \text{(II-7)}$$

$$\text{Intercept } (B) = f(\text{Lignin, Acetyl, CrI, Carbohydrate}) \quad \text{(II-8)}$$

where carbohydrate is glucan, xylan, or total sugar.

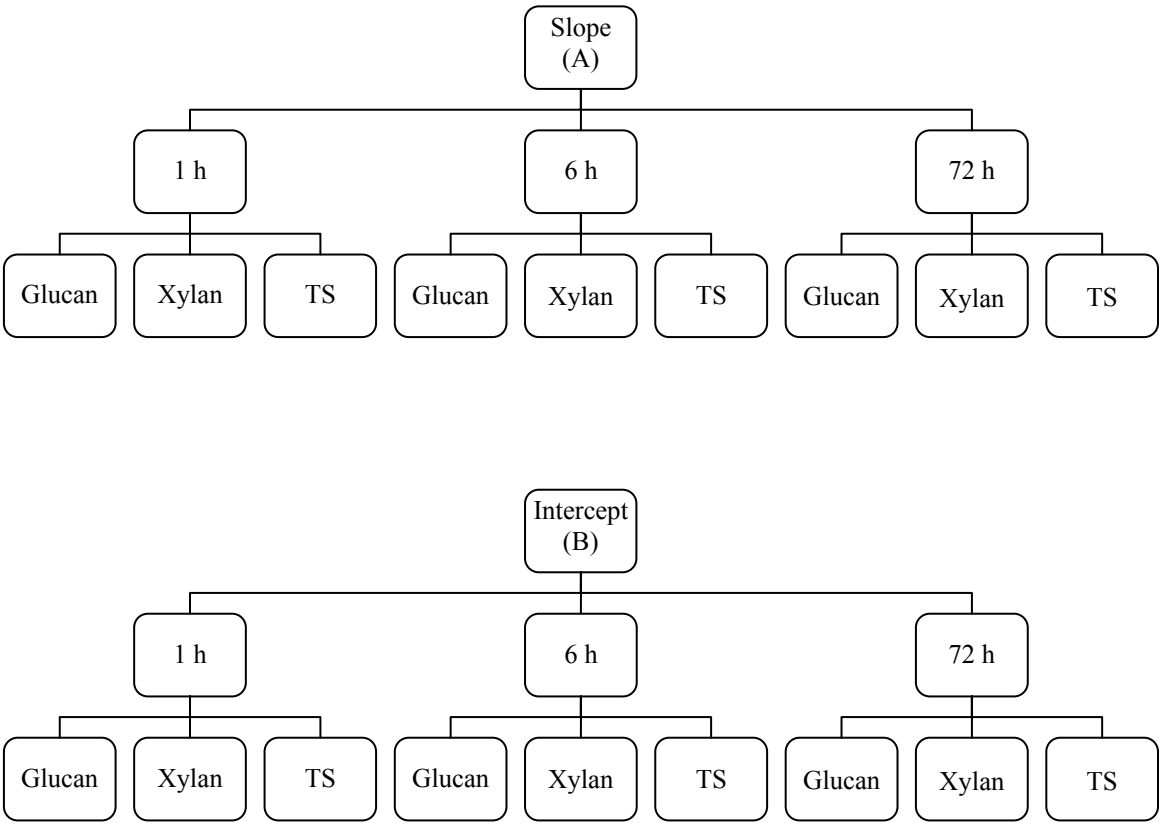

TS: total sugar = glucan + xylan

Figure II-2. Schematic diagram of modeling approach.

CHAPTER III

MATHEMATICAL MODELS FOR DATA CORRELATION

This chapter briefly introduces the concepts of parametric and nonparametric regression approaches, which are widely used to correlate data. Then, the multiple linear regression (parametric) and optimal nonparametric transformations for data regression – called *alternating conditional expectations* (ACE) – are described. Finally, a synthetic example is presented to illustrate the ability of optimal transformation of data using ACE.

DATA REGRESSION

Data regression analysis is a statistical technique for investigating and modeling the relationship between the dependent variable (response) y and the independent variable (regressor) x. The relationship is usually described by a function or regression curve. The general regression model for a bivariate case is expressed as

$$y = f(x) + \varepsilon \tag{III-1}$$

where y = independent variable
x = dependent variable
f = regression function
ε = random error

There are two approaches to determining the regression function f: parametric and nonparametric regression. The conventional parametric regression approach requires *a priori* assumption regarding functional forms. However, nonparametric is only based on data without assumptions of functional forms; therefore, parametric regression is model-driven whereas nonparametric regression is data-driven.

Parametric Regression

A simple example of parametric regression is a linear regression model with a single independent variable. The linear relationship between the dependent variable y and independent variable x can be expressed by the following form:

$$y = \beta_0 + \beta_1 x + \varepsilon \tag{III-2}$$

where β_0 is the intercept, β_1 is the slope, and ε is random error.

The regression parameters β_0 and β_1 can be determined using the observations of the dependent variable $\{y_1, y_2,\ldots, y_n\}$ and the independent variable $\{x_1, x_2, \ldots, x_n\}$ based on least squares error. Once β_0 and β_1 are quantified, this model can be used to predict y within a certain range of a given x.

Nonparametric Regression

The nonparametric approach to determining a regression function is usually achieved by data smoothing techniques such as moving average, kernel function, spline smoothing (Eubank, 1988), and supersmoother (Breiman and Friedman, 1985).

For a given set $\{y_1, y_2,\ldots, y_n\}$ and $\{x_1, x_2,\ldots, x_n\}$ in a bivariate case, the moving average can be defined as

$$f(x_i|k) = \frac{1}{k}\sum_{j=i-k/2}^{i+k/2} y_j, \quad i = 1,\ldots n \tag{III-3}$$

where $f(x_i|k)$ is the smoothed value and k is the window span and is chosen as an odd number. The regression function f determined by the nonparametric approach is not necessarily an analytical function. The moving average is the simplest data smoothing technique, and the smoothness of the function is controlled by the span k. Larger values of k give smoother averaging functions. As an example, Figure III-1 illustrates data

correlation by nonparametric regression using biomass crystallinity data. The thick curve is a moving average of the scatter points with a span of 15.

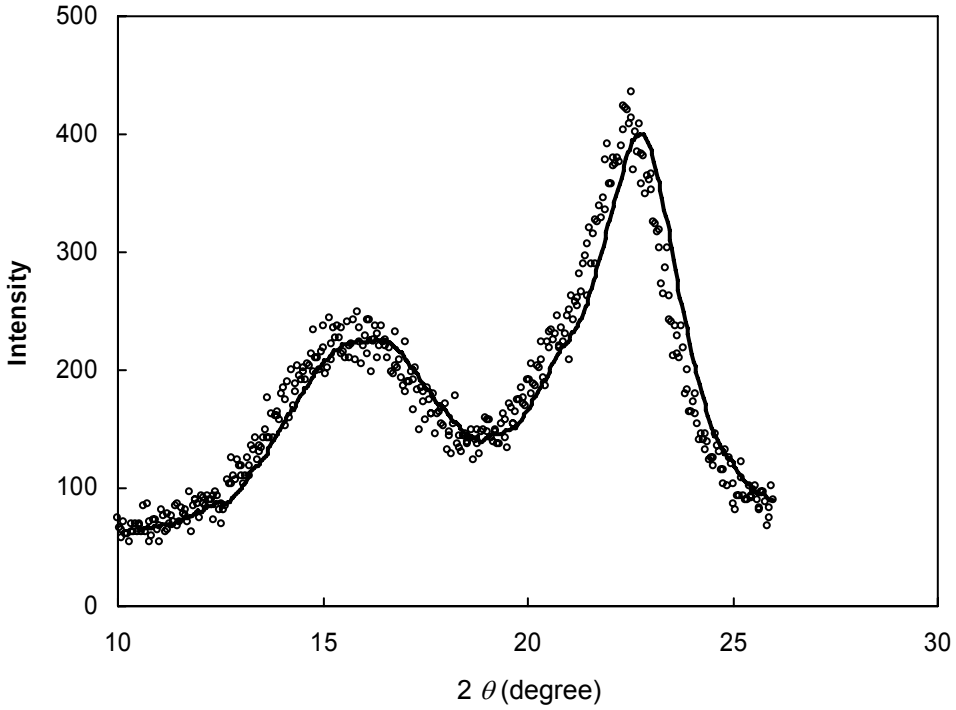

Figure III-1. An example of nonparametric regression using x-ray crystallinity data.

Each approach has its own advantages when used for data correlation. The primary advantage of parametric regression is easy to understand and is easy to use, but it has limitations in multivariate regression because it is difficult to assume the proper functional form for each individual variable. The most important advantage of nonparametric regression is its ability to provide good correlation between the dependent and independent variables in multivariate regression based on data measurements without an assumption of functional forms. The flexibility of nonparametric regression is extremely helpful when there is no clue to functional forms for the variables involved.

MULTIPLE LINEAR REGRESSION

Multiple linear regression is the most popular parametric regression model used to correlate data when multiple independent variables x_1, x_2, …, x_k are involved. Similar to Equation III-2, the multiple (parametric) linear regression model can be expressed as

$$y = \beta_0 + \beta_1 x_1 + \beta_2 x_2 + ... + \beta_k x_k + \varepsilon \quad \text{(III-4)}$$

where k is the number of independent variables. β_0, β_1, β_2,…, β_k are regression parameters that can be determined by observing the dependent and independent variables.

Models that are more complex in structure than Equation III-4 may still be analyzed by multiple linear regression techniques. Such multiple linear regression models can be written as:

$$g(y) = \beta_1 f_1(x_1) + \beta_2 f_2(x_2) + ... + \beta_k f_k(x_k) + \varepsilon \quad \text{(III-5)}$$

where g and $f_1, f_2,\ldots, f_p$ are various functions or transformations assigned *a priori* to the dependent and independent variables. For example, models that include second-order polynomial and interaction effect with two independent variables (x_1 and x_2) may take the following form:

$$y = \beta_0 + \beta_1 x_1 + \beta_2 x_2 + \beta_{11} x_1^2 + \beta_{22} x_2^2 + \beta_{12} x_1 x_2 + \varepsilon \quad \text{(III-6)}$$

Let $x_3 = x_1^2$, $x_4 = x_2^2$, $x_5 = x_1 x_2$, $\beta_3 = \beta_{11}$, $\beta_4 = \beta_{22}$, and $\beta_5 = \beta_{12}$, then Equation III-6 can be written as a multiple linear regression model as follows:

$$y = \beta_0 + \beta_1 x_1 + \beta_2 x_2 + \beta_3 x_3 + \beta_4 x_4 + \beta_5 x_5 + \varepsilon \quad \text{(III-7)}$$

A more general form of multiple linear regression model can be written as

$$Y = X\beta + \varepsilon \qquad \text{(III-8)}$$

where $Y = n \times 1$ vector of the dependent variables

$X = n \times p$ matrix of the independent variables

$\beta = p \times 1$ vector of the regression parameters

$\varepsilon = n \times 1$ vector of random error.

The least squares criterion leads to normal equations

$$X'X\hat{\beta} = X'Y \qquad \text{(III-9)}$$

Solving Equation III-9 for the least-squares estimator of β (provided X′X is non singular)

$$\hat{\beta} = (X'X)^{-1}X'Y \qquad \text{(III-10)}$$

Multiple linear regression models are often used as empirical models or approximating functions. That is, the true functional relationship between y and $x_1, x_2, \ldots, x_k$ is unknown, but utilizing the complex forms of independent variables, the multiple linear regression model adequately approximates the true unknown functions.

OPTIMAL NONPARAMETRIC TRANSFORMATIONS

Optimal transformations for nonparametric regression techniques have been developed to explore the underlying relationship between the dependent variable and independent variables using statistical and optimization theory when there is no observed functional form for the independent variables. In the following discussion, we use the lower case y and $x_1, \ldots, x_k$ as a realization of the random dependent variable Y and random independent variables $X_1, \ldots, X_k$.

Introduction of Optimal Transformation

A general nonparametric regression model for continuous dependent variable Y and multiple independent variables $X_1,\ldots, X_k$ can be expressed as

$$\theta(Y) = \sum_{l=1}^{k} \phi_l(X_l) + \varepsilon \qquad \text{(III-11)}$$

where θ and $\phi_1,\ldots, \phi_k$ denote the transformations for Y and $X_1,\ldots, X_k$, respectively, and ε is random error.

Breiman and Friedman (1985) developed a general and computationally efficient algorithm called ACE (*alternating conditional expectations*) for deriving optimal nonparametric transformations that minimize the variance of a linear relationship between the transformed dependent variable and the sum of transformed independent variables. For a given set of dependent variable Y and independent variables $X_1,\ldots, X_k$, let $E[\theta^2(Y)]=1$, and assume that all functions have expectation zero. The error (e^2) is not explained by a regression of $\theta(Y)$ on $\sum_{l=1}^{k} \phi_l(X_l)$

$$e^2(\theta,\phi_1,\ldots,\phi_k) = E\{[\theta(Y) - \sum_{l=1}^{k} \phi_l(X_l)]\}^2 \qquad \text{(III-12)}$$

Define optimal transformations $\theta^*(Y)$, $\phi_1^*(X_1),\ldots,\phi_k^*(X_k)$ if they satisfy the following

$$e^{*2}(\theta^*,\phi_1^*,\ldots,\phi_k^*) = \min_{\theta,\phi_1,\ldots\phi_k} e^2(\theta,\phi_1,\ldots,\phi_k) \qquad \text{(III-13)}$$

The maximal correlation between Y and $X_1,\ldots, X_k$ can be defined as follows if $E\{\theta^{**2}(Y)\} = 1$ and $E\{\phi_s^{**2}(X)\} = 1$

$$\rho^* = \max_{\theta,\phi_1,\ldots\phi_k} \rho(\theta(Y),\phi_s(X)) = E[\theta^{**}(Y)\phi_s^{**}(X)] \quad \text{(III-14)}$$

where $\phi_s(X) = \sum_{l=1}^{k} \phi_l(X_l)$ (III-15)

If $\theta^{**}(Y)$, $\phi_1^{**}(X_1),\ldots,\ \phi_k^{**}(X_k)$ are optimal for correlation, then $\theta^*(Y) = \theta^{**}(Y)$, $\phi_1^*(X_1) = \rho^*\phi_1^{**}(X_1)\ ,\ldots,\ \phi_k^*(X_k) = \rho^*\phi_k^{**}(X_k)$ are optimal for regression, and vice versa. The minimum regression error and maximum correlation coefficient are related by $e^{*2} = 1\text{-}\rho^{*2}$. Proof of the existence of optimal transformations can be found in the paper by Breiman and Friedman (1985).

ACE Algorithm

The derivation of optimal transformations $\theta^*,\ \phi_1^*,\ldots,\ \phi_k^*$ is accomplished by minimizing the error e^2 with respect to $\phi_1(X_1),\ldots,\ \phi_k(X_k)$, and $\theta(Y)$. It is performed through a series of minimizations, resulting in the following equations (Breiman and Friedman, 1985):

$$\phi_l(X_l) = E\left[\theta(Y) - \sum_{j\neq l}\phi_j(X_j)\middle|X_l\right] \quad \text{(III-16)}$$

$$\theta(Y) = E\left[\sum_{l=1}^{k}\phi_l(X_l)\middle|Y\right] \Big/ \left\| E\left[\sum_{l=1}^{k}\phi_l(X_l)\middle|Y\right]\right\| \quad \text{(III-17)}$$

where E[.|.] denotes conditional expectation and $\|\cdot\| = [E(\cdot)^2]^{1/2}$ is a measure of length.

The mathematical operations involved in Equations III-16 and III-17 are iterative conditional expectations, hence the name *alternating conditional expectations* (ACE). The procedure involves iterating on Equations III-16 and III-17 until the difference in error as defined by Equation III-12 from two consecutive iterations is within an acceptable tolerance. The resulting transformations are optimal transformations $\phi_1^*(X_l)$, *l*

= 1,..., k and $\theta^*(Y)$. In the transformed space, the dependent and independent variables will be related as follows:

$$\theta^*(y) = \sum_{l=1}^{k} \phi_l^*(x_l) + \varepsilon \qquad \text{(III-18)}$$

where y and $x_1,..., x_k$ are realizations of random variables Y and $X_1,..., X_k$, and ε is random error.

The procedure for ACE can be summarized as follows:

Set $\theta(Y) = Y/\|Y\|$, and $\phi_1(X_1),\ldots, \phi_k(X_k) = 0$;

Iterate until $e^2(\theta,\phi_1,...,\phi_k)$ fails to decrease;

Iterate until $e^2(\theta,\phi_1,...,\phi_k)$ fails to decrease;

For l = 1 to k Do:

$$\phi_{l,1}(X_l) = E\left[\theta(Y) - \sum_{i\neq l}\phi_i(X_i)\middle| X_l\right]$$

replace $\phi_l(X_l)$ with $\phi_{l,1}(X_l)$;

End For Loop;

End Inner Iteration Loop;

$$\theta_1(Y) = E\left[\sum_{i=1}\phi_i(X_i)\middle|Y\right] \Bigg/ \left\| E\left[\sum_{i=1}^{k}\phi_i(X_i)\middle|Y\right]\right\|;$$

replace $\theta(Y)$ with $\theta_1(Y)$;

End Outer Iteration Loop;

$\theta, \phi_1,\ldots, \phi_k$ are the solutions to $\theta^*, \phi_1^*,\ldots, \phi_k^*$;

End ACE Algorithm.

Because the data distribution is rarely known, calculation of conditional expectations in the ACE algorithm is replaced by data-smoothing techniques. Thus, the

transformations derived by ACE, $\{\theta^*(y_i), \phi_1^*(x_{1i}), ..., \phi_k^*(x_{ki}),\ 1 \le i \le n\}$ are estimates of the optimal transformations.

ACE for Estimation

After the relationship between the transformed dependent variable and the sum of transformed independent variables is determined by ACE, the prediction of dependent variable y_j^{pre} given independent variables $\{x_{1j}, ..., x_{kj}\}$ can be estimated as

$$y_j^{pre} = \theta^{*-1}\left[\sum_{l=1}^{k} \phi_l^*(x_{lj})\right] \qquad \text{(III-19)}$$

y_j^{pre} can also be obtained by smoothing the data values of y on the data values of $\sum_{j=1}^{k} \phi_j^*(x_j)$ in the ACE program.

Synthetic Example

A synthetic example with multiple independent variables is used to demonstrate the ability of ACE to identify the functional relationship between the dependent and independent variables. In contrast, a conventional regression (parametric) is usually inadequate due to the assumed functional form for each independent variable. A plot of the function versus the corresponding data values provides the simplest way to understand the shape of the transformations.

The example is similar to that given by Xue (1997). The 200 observations are generated from the following model:

$$y_i = x_{1i}^2 + x_{2i} - x_{3i}^2 + x_{4i}^3 + \varepsilon_i \qquad \text{(III-20)}$$

where x_{1i}, x_{2i}, x_{3i}, and x_{4i} are independently and randomly drawn from a uniform distribution U (-1, 1), and ε_i is drawn from a normal distribution N (0,1). Figures III-2 through III-5 show the plots of y_i versus x_{1i}, x_{2i}, x_{3i}, and x_{4i}, respectively. It is obvious that except for y_i versus x_{2i}, the functional relationships between y_i and x_{1i}, x_{3i}, and x_{4i} cannot be indentified from the scatter plots.

The optimal transformations for y_i, x_{1i}, x_{2i}, x_{3i}, and x_{4i} derived from ACE are shown in Figures III-6 through III-10. The shapes of the transformations for both y_i and x_{2i} are linear, the plots of transformation for x_{1i} and x_{3i} suggest a quadratic function and the transformation for x_{4i} reveals a cubic function. Thus, ACE can identify the following optimal transformation

$$\theta^*(y_i) = y_i$$

$$\phi_1^*(x_{1i}) = x_{1i}^2, \quad \phi_2^*(x_{2i}) = x_{2i}, \quad \phi_3^*(x_{3i}) = -x_{3i}^2, \quad \phi_4^*(x_{4i}) = x_{4i}^3 \qquad \text{(III-21)}$$

whereas the individual scatter plots hardly reveal any such relationship.

Figure III-11 shows a plot of the transformed y_i versus the sum of transformed x_{1i}, x_{2i}, x_{3i}, and x_{4i}. The relationship can be fitted approximately by

$$\theta^*(y_i) = \phi_1^*(x_{1i}) + \phi_2^*(x_{2i}) + \phi_3^*(x_{3i}) + \phi_4^*(x_{4i}) \qquad \text{(III-22)}$$

The linear relationship indicates that these transformations are the optimal ones.

Knowledge of optimal transformations helps explore the relationship between the dependent and independent variables solely based on data measurements with minimal assumptions of data distribution. ACE provides the method for estimating optimal transformations in multiple regression and graphical output to indicate a need for transformations.

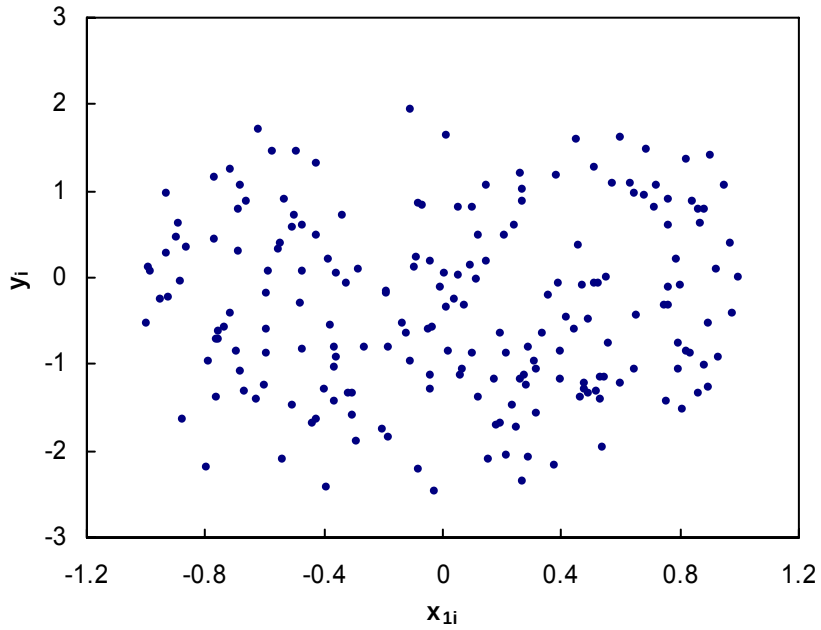

Figure III-2. Scatter plot of y_i versus x_{1i} simulated from the multivariate model $y_i = x_{1i}^{\ 2} + x_{2i} - x_{3i}^{\ 2} + x_{4i}^{\ 3} + \varepsilon_i$.

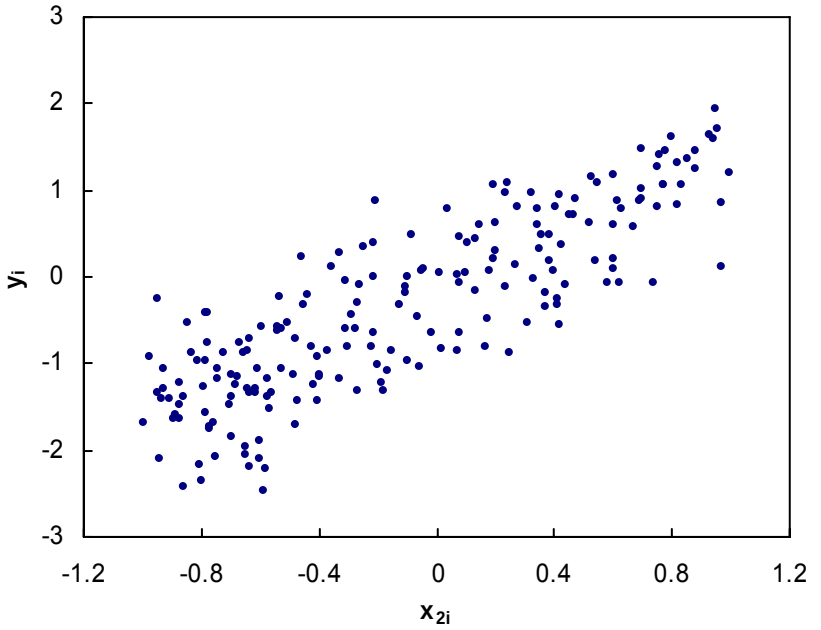

Figure III-3. Scatter plot of y_i versus x_{2i} simulated from the multivariate model $y_i = x_{1i}^{\ 2} + x_{2i} - x_{3i}^{\ 2} + x_{4i}^{\ 3} + \varepsilon_i$.

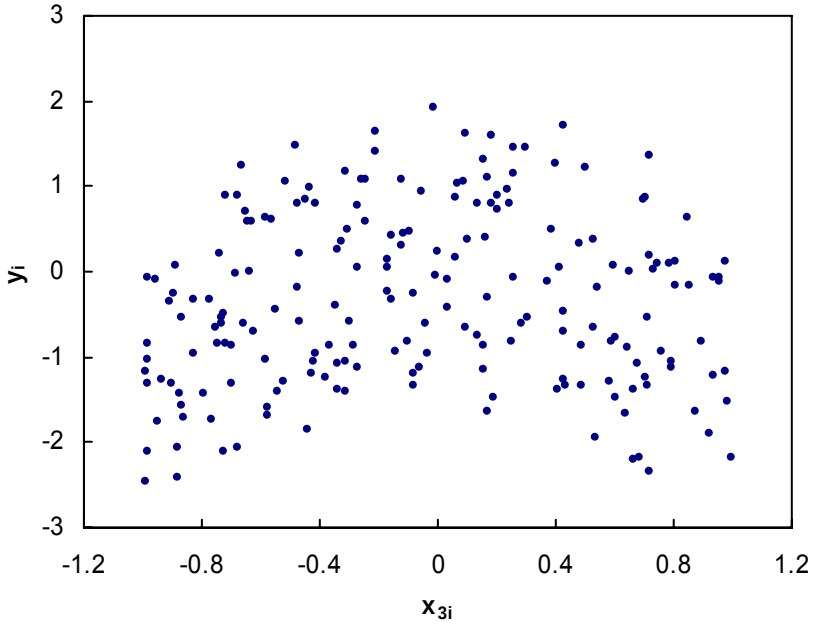

Figure III-4. Scatter plot of y_i versus x_{3i} simulated from the multivariate model $y_i = x_{1i}^{\ 2} + x_{2i} - x_{3i}^{\ 2} + x_{4i}^{\ 3} + \varepsilon_i$.

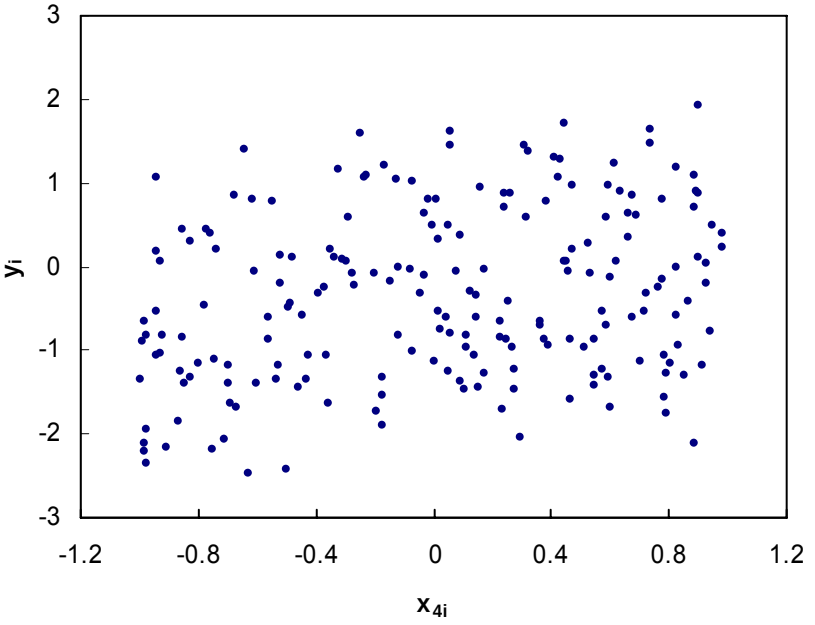

Figure III-5. Scatter plot of y_i versus x_{4i} simulated from the multivariate model $y_i = x_{1i}^{\ 2} + x_{2i} - x_{3i}^{\ 2} + x_{4i}^{\ 3} + \varepsilon_i$.

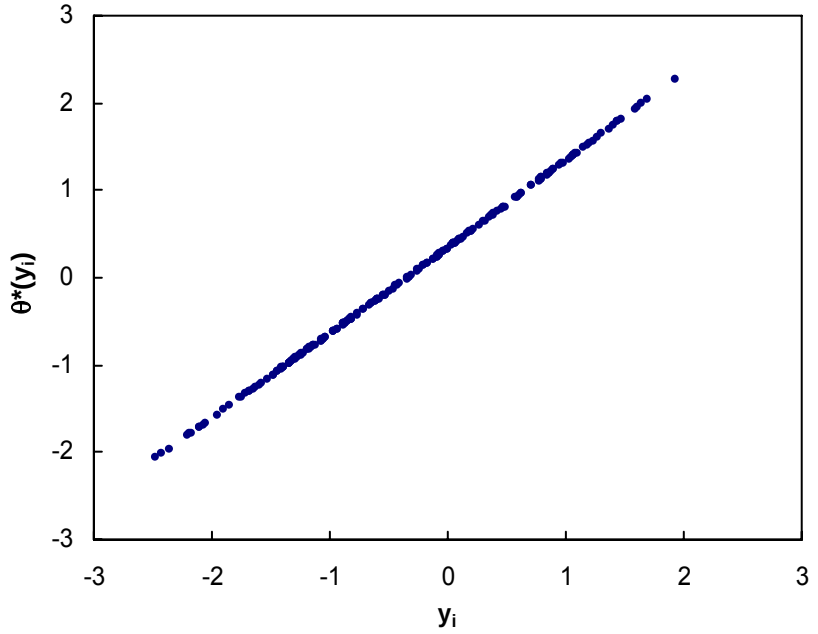

Figure III-6. Optimal transformation of y_i by ACE.

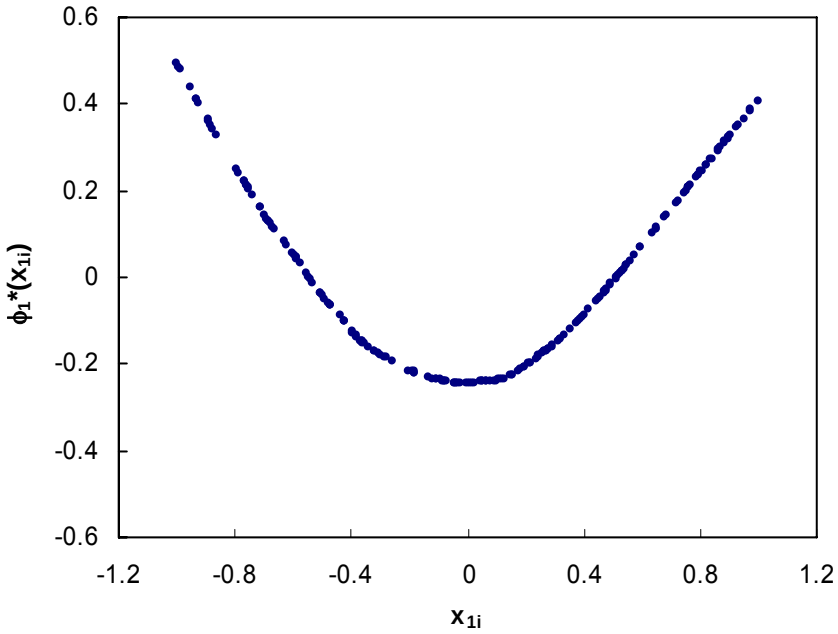

Figure III-7. Optimal transformation of x_{1i} by ACE.

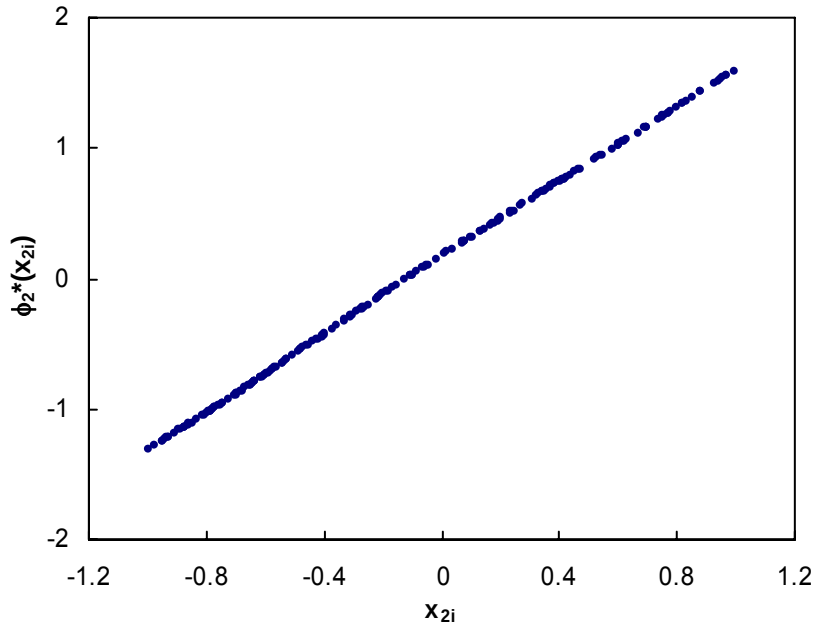

Figure III-8. Optimal transformation of x_{2i} by ACE.

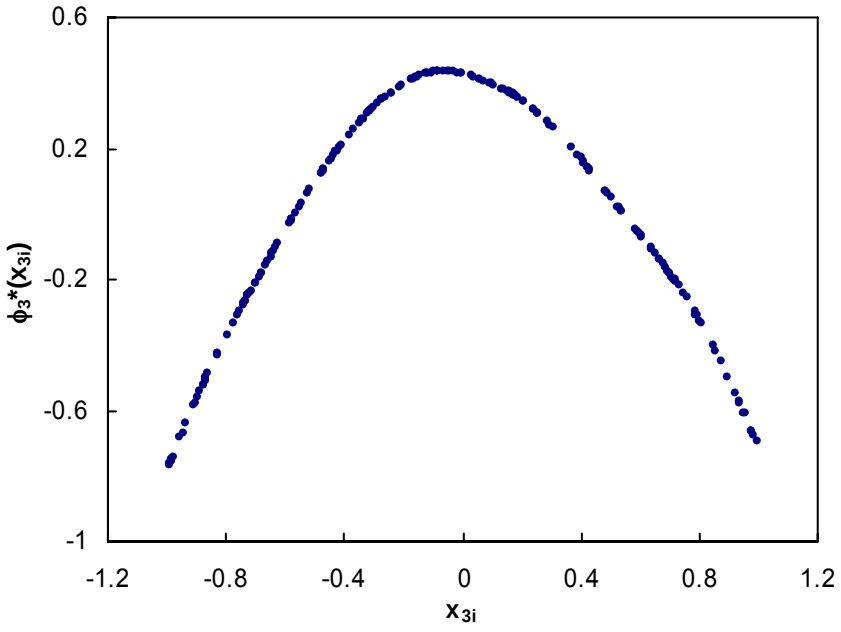

Figure III-9. Optimal transformation of x_{3i} by ACE.

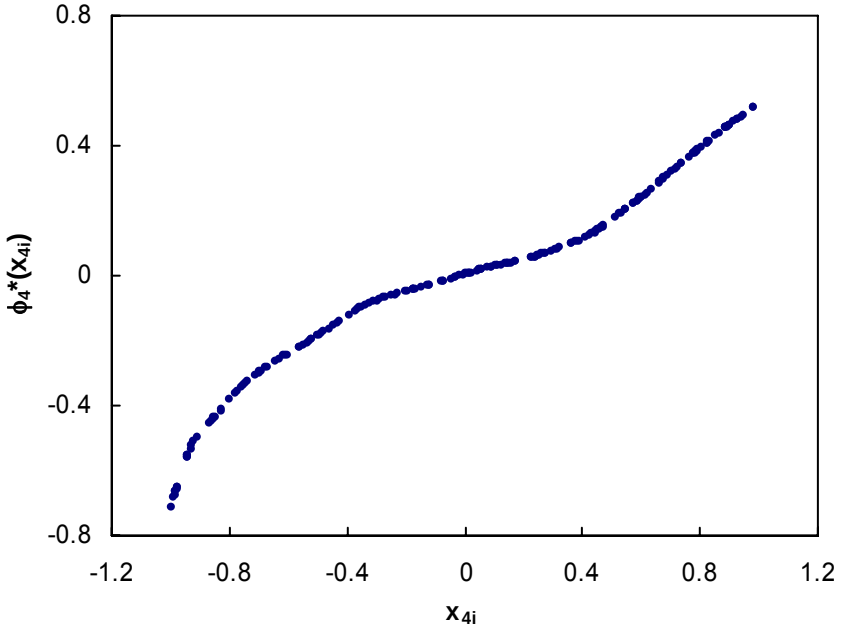

Figure III-10. Optimal transformation of x_{4i} by ACE.

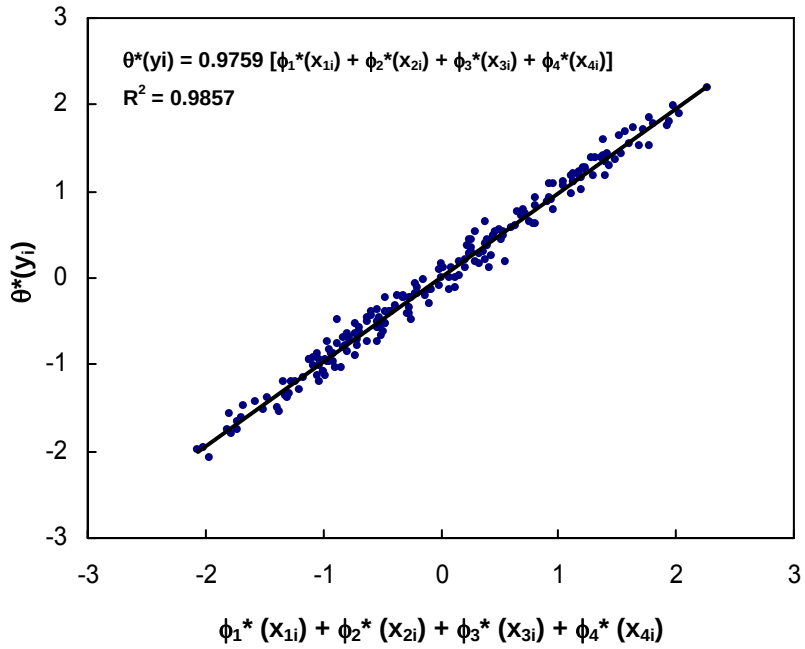

Figure III-11. Optimal transformation of y_i versus the sum of optimal transformations of x_{1i}, x_{2i}, x_{3i}, x_{4i}. The straight line represents a linear regression of the data.

CHAPTER IV

ENZYMATIC HYDROLYSIS

Enzymatic hydrolysis is an ideal approach for converting lignocelluloses into sugars because high sugar yields can be achieved with negligible by-products. However, the enzymatic hydrolysis of lignocelluloses is affected by many factors, such as hydrolysis temperature, time, pH, enzyme loading, substrate concentration, product concentration, and biomass structural features. In this chapter, the effects of structural features, substrate concentration, end-product inhibition, and enzyme loading on digestibility were investigated; the enzymatic hydrolysis conditions employed for model development (Chapter V) were optimized.

SUBSTRATE CONCENTRATION AND END-PRODUCT INHIBITION

Introduction

Substrate concentration is an important factor in the enzymatic hydrolysis of lignocellulosic biomass, because it influences the rate and extent of hydrolysis, and thus significantly influences the economic potential of the overall process. It has been widely reported that there is an inverse relationship between substrate concentration and hydrolysis yield (Breuil et al., 1991; Huang and Penner, 1991; Ortega et al., 2001; Tengborg et al., 2001). In these studies, two types of enzyme concentration were employed: (1) enzyme concentration in the hydrolysis slurry (i.e., mg/mL) was kept constant at various substrate concentrations (Huang and Penner, 1991; Ortega et al., 2001), and (2) equivalent amounts of enzyme at all substrate concentrations, in terms of units of enzyme per gram of dry biomass were employed (Breuil et al., 1991; Lu et al., 2002, Tengborg et al., 2001); however, all the results were very consistent.

It is well known that cellulolytic enzymes are inhibited by hydrolysis end-products such as cellobiose, glucose, or both. The inhibitory effect of cellobiose can be

alleviated by adding supplemental cellobiase that converts cellobiose into glucose. Substrate concentration and end-product inhibition are coupled due to end-product concentration, i.e., a low substrate concentration decreases end-product concentration, thus reducing inhibitory effect. In this study, the influence of substrate concentration on digestibility and the inhibitory effects of cellobiose and glucose were investigated.

Materials and Methods

Corn stover was treated at 100°C for 2 h in the presence of 0.1 g lime/g dry biomass and 10 mL water/g dry biomass. The step-by-step pretreatment procedure is described in Appendix A. Enzymatic hydrolysis was performed in 50-mL Erlenmeyer flasks containing 10, 20, 50, or 100 g dry pretreated corn stover/L, 1.0 mL of 1-M citrate buffer, and 0.6 mL of 0.01-g/mL sodium azide. Distilled water and 0.2–2.0 mL of appropriately diluted enzyme mix was added to bring the total volume to 20 mL. Table IV-1 shows the amounts of biomass, distilled water, and diluted enzyme in the Erlenmeyer flasks containing various substrate concentrations. The flasks were placed in a shaking air bath agitated at 100 rpm and preheated for 1 h prior to enzyme addition. To avoid taking samples from the heterogeneous system of enzymatic hydrolysis, Erlenmeyer flasks containing various substrate concentrations were removed from the shaking air bath after certain incubation periods (1, 6, 24, 48, and 72 h) and boiled for 15 min to denature enzymes. Enzymatic hydrolysis was performed at a cellulase loading of 5 FPU/g dry biomass (Spezyme CP, lot 301-00348-257) and cellobiase loading of 0, 28.4, or 81.2 CBU/g dry biomass (Sigma, G-0395). Glucose and xylose concentrations were measured using HPLC. Detailed procedures for enzymatic hydrolysis and sugar analysis using HPLC are described in Appendices B and E, respectively. Glucose, xylose, and total sugar conversions were calculated using Equations II-4 to II-6.

Results and Discussion

Table IV-1 summarizes enzymatic hydrolysis condition for studying the effects of substrate concentration and end-product inhibition on digestibility. Equivalent

amounts of enzymes were added at all substrate concentrations, in terms of units of enzyme per gram of dry substrate, thus enzyme concentration (mg/mL) increases with an increase in substrate concentration.

Table IV-1. Summary of enzymatic hydrolysis condition at various substrate concentrations

Substrate concentration (g/L)	10	20	50	100
Weight of dry biomass (g)	0.2	0.4	1.0	2.0
Volume of 1-M citrate buffer (mL)	1.0	1.0	1.0	1.0
Volume of 0.01-mg/mL sodium azide (mL)	0.6	0.6	0.6	0.6
Volume of distilled water (mL)	18	17.6	16.4	14.4
Volume of diluted enzyme (mL)	0.2	0.4	1.0	2.0
Total volume of mixture (mL)	20.0	20.0	20.0	20.0
Cellulase loading (FPU/g dry biomass)	5	5	5	5
Cellobiase loading (CBU/g dry biomass)	0, 28.4, 81.2	0, 28.4, 81.2	0, 28.4, 81.2	0, 28.4, 81.2
Incubation time (h)	1, 6, 12, 24, 72	1, 6, 12, 24, 72	1, 6, 12, 24, 72	1, 6, 12, 24, 72

Enzymatic Hydrolysis with no Supplemental Cellobiase

Figure IV-1 illustrates the effects of substrate concentration and hydrolysis time on cellobiose, glucose, and xylose concentrations with no supplemental cellobiase. The broad range of initial substrate concentrations resulted in a wide range of end-product concentrations. Cellobiose concentration increased steeply at shorter hydrolysis times and decreased gradually, and then became almost zero at 72 h regardless of substrate concentration, whereas glucose and xylose concentrations increased considerably as hydrolysis proceeded. High cellobiose concentration at 1 h indicates that supplemental cellobiase is needed to convert cellobiose into glucose.

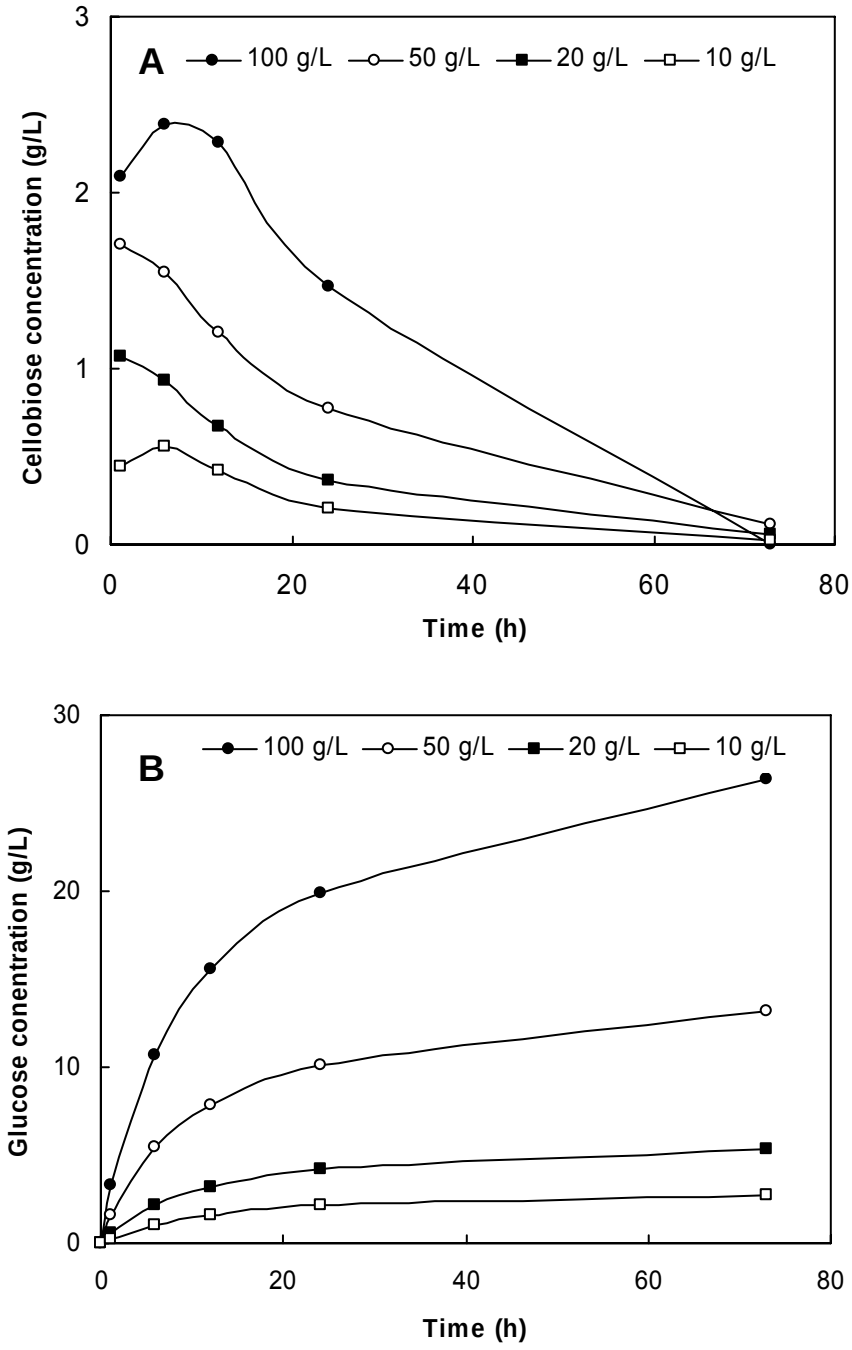

Figure IV-1. Effects of time and substrate concentration on sugar concentrations with no supplemental cellobiase: (A) cellobiose; (B) glucose; (C) xylose. Hydrolysis conditions: 5 FPU/g dry biomass, 0 CBU/g dry biomass.

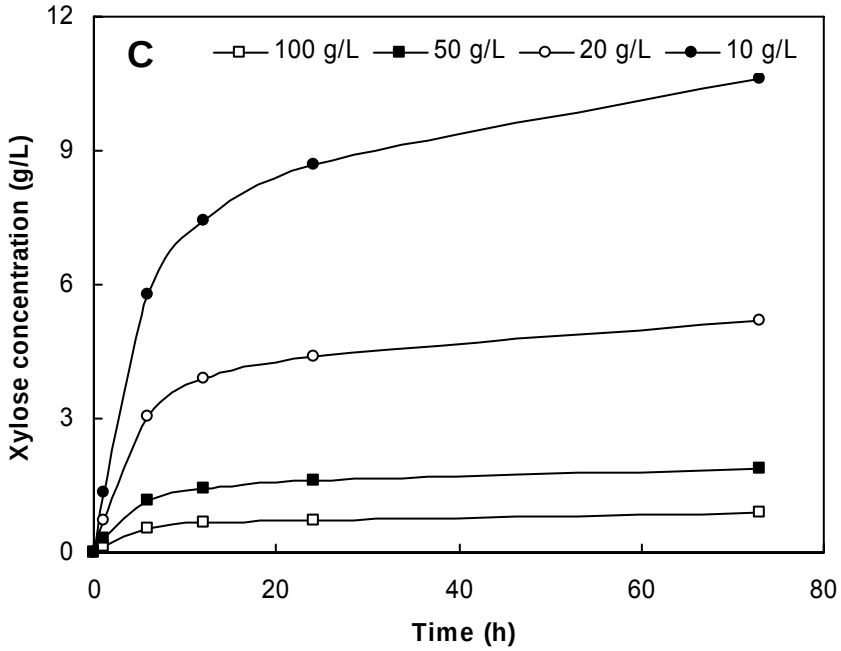

Figure IV-1. Continued.

Figure IV-2 illustrates the effect of substrate concentration on glucan and xylan hydrolyses at various hydrolysis times. Glucan conversion was determined as glucose equivalents (1 mol of cellobiose is converted into 2 mol of glucose). The effect of substrate concentration on glucan hydrolysis changed as hydrolysis proceeded. The highest and lowest initial rates of glucan hydrolysis (i.e., 1-h glucan conversion) were observed at 20- and 100-g/L substrate concentrations, respectively. Glucan conversions (i.e., 6, 12, and 24 h) decreased with increasing substrate concentration, whereas the extents of glucan hydrolysis (i.e., 72-h glucan conversion) at the four substrate concentrations were virtually identical. Actually, increasing substrate concentration has a dual effect on glucan hydrolysis: (1) increasing substrate and enzyme concentrations enhances formation of substrate-enzyme complexes that accelerate the hydrolysis rate, especially the initial hydrolysis rate, and (2) increasing substrate concentrations also cause higher end-product concentrations that inhibit enzymes. Therefore, the effect of substrate concentration on glucan hydrolysis depends on the predominance of these two effects as hydrolysis proceeds.

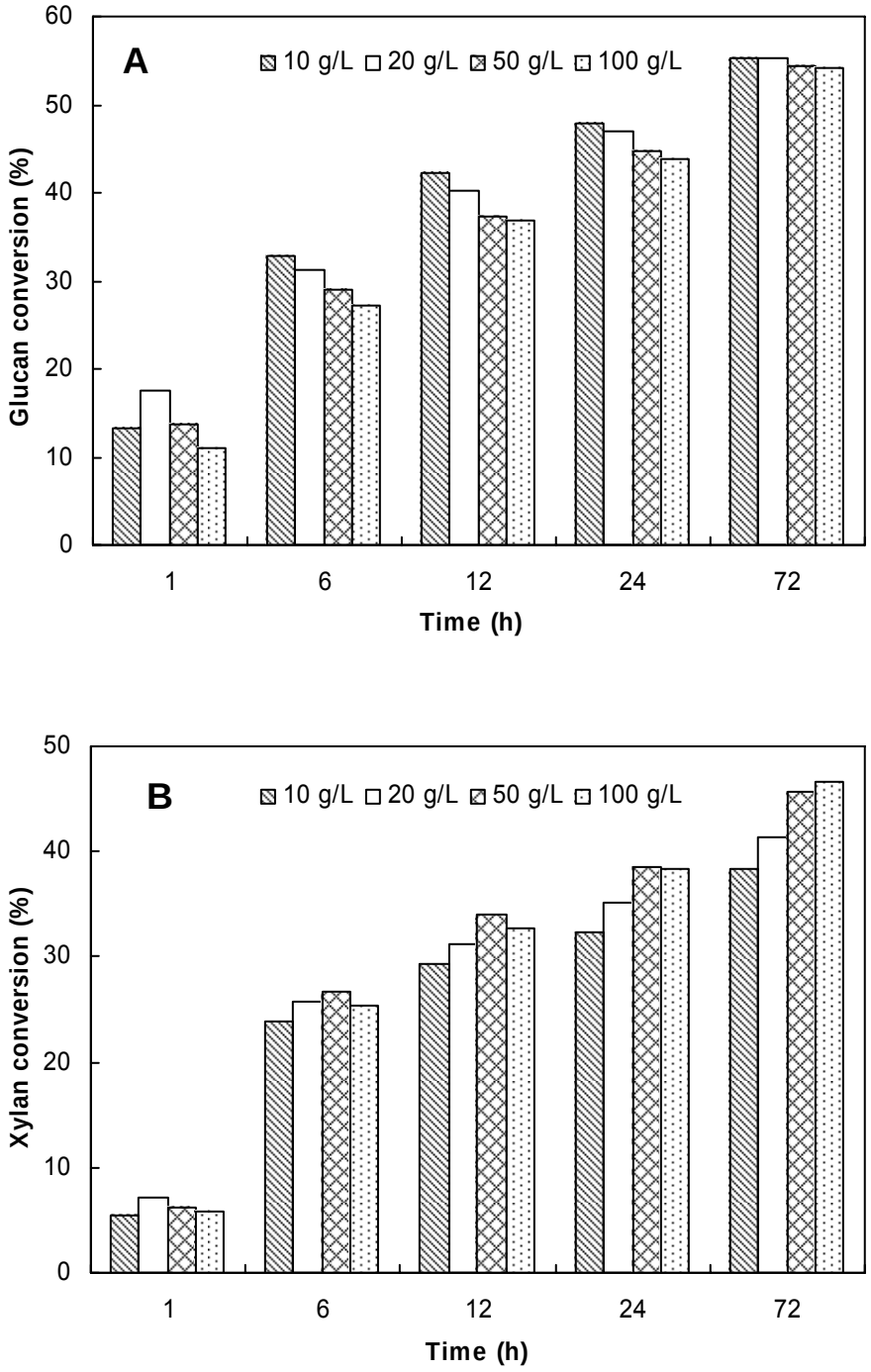

Figure IV-2. Effect of substrate concentration on biomass digestibility with no supplemental cellobiase: (A) glucose; (B) xylose. Hydrolysis conditions: 5 FPU/g dry biomass, 0 CBU/g dry biomass.

Similar to glucan hydrolysis, the highest initial rate of xylan hydrolysis (i.e., 1-h xylan conversion) was observed at 20-g/L substrate concentration. The xylan conversion at 50-g/L substrate concentration outperformed others at 6, 12, and 24 h. The extent of xylan hydrolysis (i.e., 72-h xylan conversion) at 50- and 100-g/L substrate concentrations were comparable and were higher than at 10- and 20-g/L substrate concentration. High substrate and enzyme concentrations appear to allow intensive contact between substrate and enzyme, which results in enhanced rate and extent of xylan hydrolysis. However, further work is needed to investigate the influence of end-product concentration on xylan hydrolysis and explain why xylan conversion in the 100-g/L substrate system is not as high as expected at shorter hydrolysis times.

Enzymatic Hydrolysis Supplemented with Cellobiase

Figure IV-3 demonstrates the effect of substrate concentration on glucan and xylan hydrolyses at various hydrolysis times with the addition of supplemental cellobiase (28.4 CBU/g dry biomass). There was no cellobiose detected at any substrate concentration during the whole hydrolysis process, and the concentration profiles of glucose and xylose (not shown) were similar to those in Figure IV-1 (B) and (C). With the addition of supplemental cellobiase, the initial hydrolysis rate at 10-g/L substrate concentration was lower than at 20-, 50-, and 100- g/L substrate concentrations, whereas the glucan conversions at 6, 12, 24, and 72 h were virtually identical regardless of substrate concentration. It seemed that the decrease in glucan conversion with increasing substrate concentrations (Figure IV-2) could be attributed to end-product inhibition when there is no cellobiase supplemented. Figure IV-3 (A) illustrates that the inhibitory effect of cellobiose on glucan hydrolysis is eliminated by adding cellobiase.

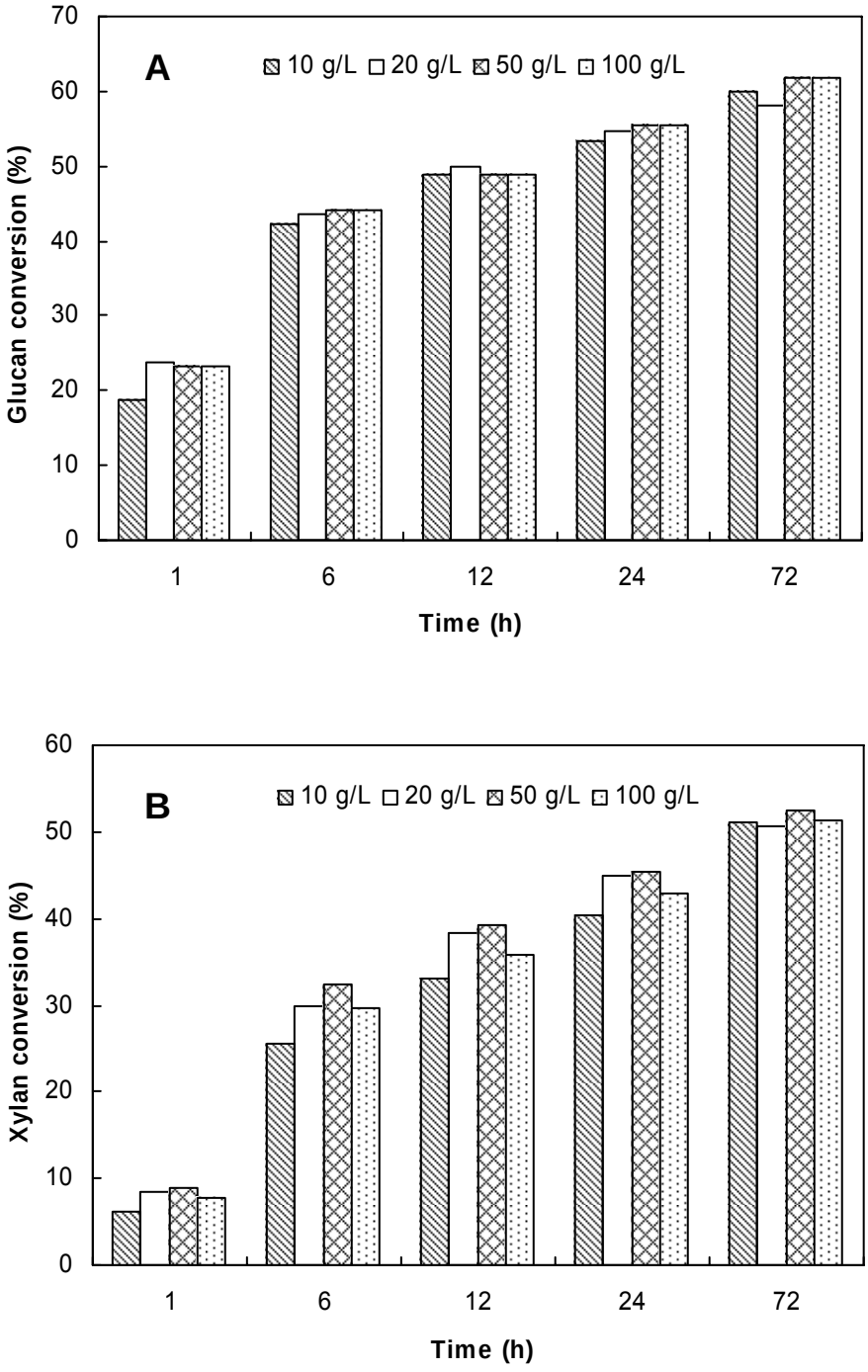

Figure IV-3. Effect of substrate concentration on biomass digestibility with supplemental cellobiase: (A) glucose; (B) xylose. Hydrolysis conditions: 5 FPU/g dry biomass, 28.4 CBU/g dry biomass.

In the studies of enzymatic hydrolysis with no supplemental cellobiase, the inhibitory effect of cellobiose was more pronounced at shorter hydrolysis times (i.e., high cellobiose concentration), and inhibition was still apparent at low cellobiose concentration (i.e., 0.3 g/L). Compared with cellobiose, the inhibitory effect of glucose on the rate and extent of glucan hydrolysis was insignificant, because high glucose concentrations in the 100-g/L substrate concentration system at 72 h (i.e., 26.4 g/L) did not decrease the extent of glucan hydrolysis. The insignificant inhibition of glucose was also verified in the enzymatic hydrolysis with supplemental cellobiase. This observation agrees with other researchers who conclude that cellobiase can alleviate end-product inhibition of cellulase by hydrolyzing cellobiose to glucose, which is less inhibitory than cellobiose (Holtzapple et al., 1990).

Most studies show that there is an inverse relationship between substrate concentration and hydrolysis yield (Breuil et al., 1991; Huang and Penner, 1991; Ortega et al., 2001; Tengborg et al., 2001). Some of them (Huang and Penner, 1991; Ortega et al., 2001) conducted enzymatic hydrolysis at various substrate concentrations with the same enzyme concentration in the hydrolysis slurry (i.e., mg/mL), thus enzyme loading per gram of dry biomass decreased with increasing substrate concentration. Therefore, the amount of enzyme was insufficient to convert cellulose to glucose at high substrate concentrations. Although enzyme loading per gram of dry biomass was equivalent at all substrate concentrations, our results contradicted those reported by others (Schewald et al., 1989; Tengborg et al., 2001). The discrepancy could be attributed to the amount of cellobiase added and the extent of hydrolysis, which highly depends on structural features and cellulase loading. Breuil and his colleague (1991) reported that cellobiose was present in all of the hydrolyzates at 100-g/L substrate concentration, and its concentration decreased with increasing the amounts of supplemental cellobiase, which was inhibited by high glucose concentration. In this study, there was no detectable cellobiose in the hydrolyzate at all substrate concentrations when the cellobiase loading was 28.4 CBU/g dry biomass. In addition, it was also reported that the influence of substrate concentration on the extent of biomass hydrolysis may be different at varied

enzyme loadings (Manonmani and Sreekantiah, 1987). Another factor that cannot be neglected was that the extent of glucan hydrolysis was nearly complete in their studies (Lu et al., 2002; Schwald et al., 1989), thus higher end-product concentration was obtained. In summary, the effect of substrate concentration on digestibility could be attributed to the extent of end-product inhibition, which depends, to some extent, on cellulase and cellobiase loadings, and biomass structural features that influence the initial hydrolysis rate and extent.

By adding supplemental cellobiase, both the highest initial rate and extent of xylan hydrolysis were obtained at 50-g/L substrate concentration. The extent of xylan hydrolysis reached the same level regardless of substrate concentration, indicating that end-product inhibition is not pronounced for xylan hydrolysis.

Influence of Cellobiase Loading on Digestibility and Cellulase Activity

Figure IV-4 illustrates the effect of cellobiase loading on glucan and xylan hydrolyses at 1, 6, and 72 h. The addition of cellobiase greatly increased glucan and xylan conversions at all substrate concentrations (only 50-g/L susbstrate concentration was shown), as cellobiase loading increased from 0 to 28.4 CBU/g dry biomass. However, further increasing cellobiase loading from 28.4 to 81.2 CBU/g dry biomass did not markedly enhance digestibility. It was interesting to note that the improvement in glucan and xylan conversions resulting from supplemental cellobiase may be different during hydrolysis. The addition of cellobiase had more influence on the initial glucan hydrolysis rate than on the hydrolysis extent, because the inhibition from cellobiose in the initial hydrolysis was eliminated by converting cellobiose to glucose with cellobiase. In contrast, the addition of cellobiase had more influence on the extent of xylan hydrolysis than on the initial hydrolysis rate, because xylanase concentration also increased by adding cellobiase that contains xylanase (Lu et al., 2002). An increase in enzyme concentration usually showed more influence on the hydrolysis time required to attain a certain yield than on the initial rate (Sattler et al., 1989). To reduce enzyme cost, it is desirable to utilize as little cellobiase as possible to eliminate end-product inhibition.

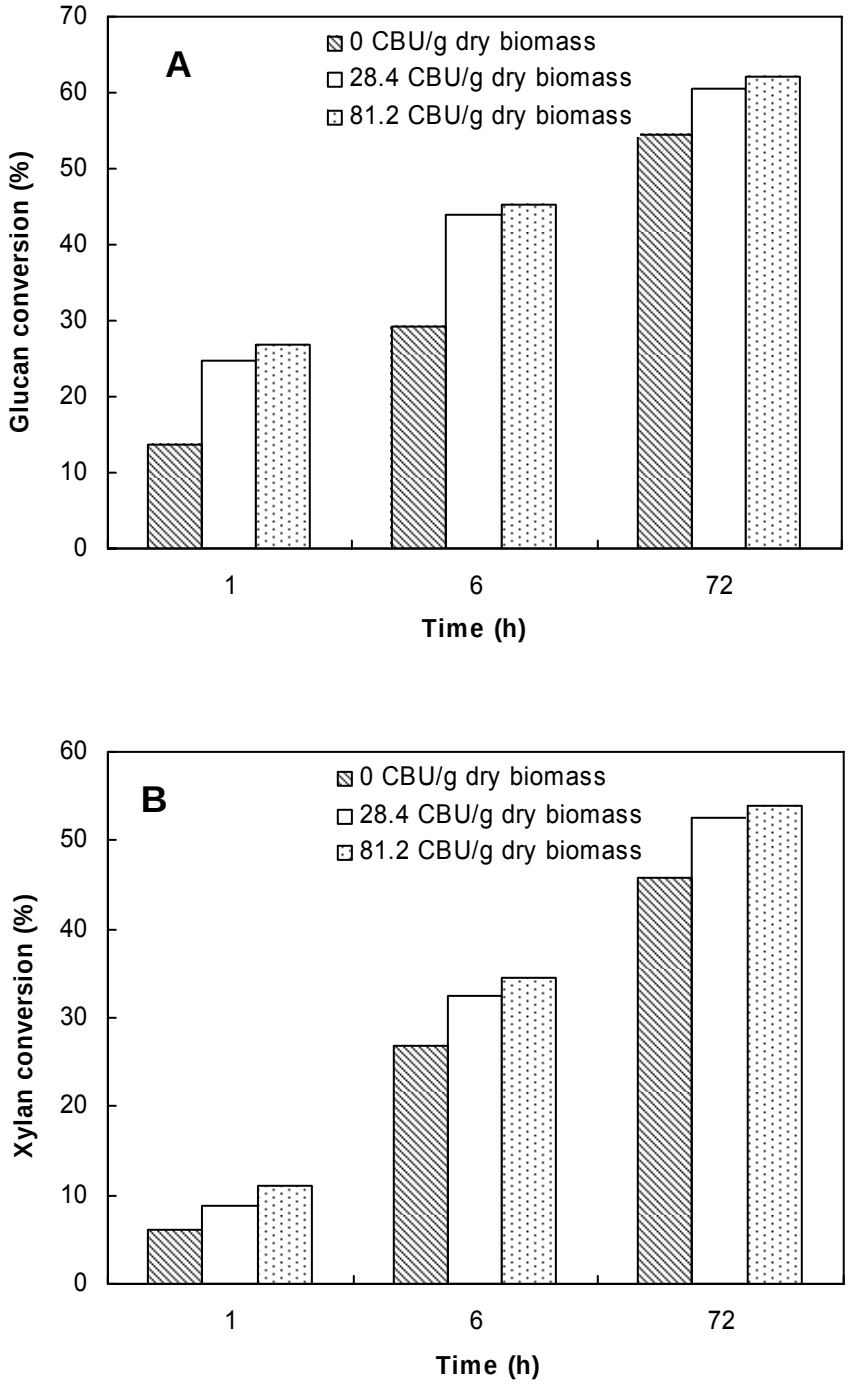

Figure IV-4. Effect of cellobiase loading on biomass digestibility: (A) glucose; (B) xylose. Hydrolysis conditions: 5 FPU/g dry biomass, substrate concentration: 50 g/L.

Some researchers have suggested that the filter paper activity (FPA) of the enzyme complex is enhanced by adding supplemental cellobiase (Coward-Kelly et al., 2003; Joglekar et al., 1983). Figure IV-5 demonstrates the effect of supplemental cellobiase on the FPA of the enzyme complex determined according to NREL standard procedure No. 006 (2004). At low cellobiase levels, the cellulase activity increased linearly (i.e., from 64.8 to 85.3 FPU/mL) as the ratio of cellobiase to cellulase increased from 0 to 0.5 (v/v), whereas further addition of cellobiase did not obviously increase the filter paper activity. This result fits well with other's conclusion (Coward-Kelly et al., 2003; Joglekar et al., 1983). In the diluted enzyme taken for the FPA assay, the enzyme complex is deficient in cellobiase actvity. Cellobiose formed in the initial hydrolysis powerfully inhibits enzyme. In contrast, in the presence of cellobiase, cellobiose is rapidly converted to glucose, which has a signifcantly lower inhibition.

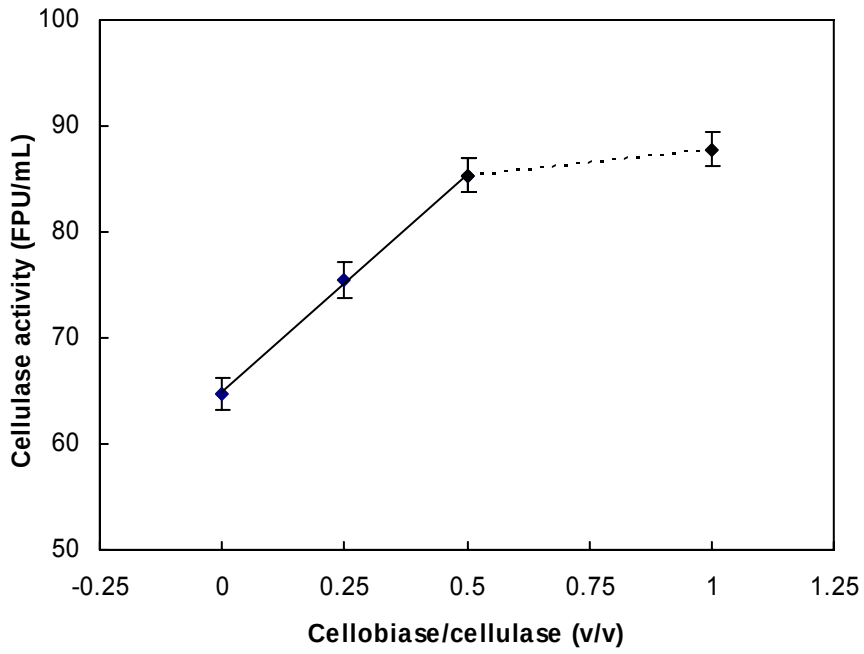

Figure IV-5. Effect of supplemental cellobiase on filter paper activity of the enzyme complex. Each point run in triplicate, bar symbol represents standard deviation. Cellulase activity: 65 FPU/mL; cellobiase activity: 321 CBU/mL.

From a practical viewpoint, the FPA of enzyme complexes determined with supplemental cellobiase is very useful when sugar yields from biomass hydrolyzed by different sources of enzyme supplemented with cellobiase are compared. Commercial enzyme sources may differ widely in resident cellobiase. Even adding the same amount of cellobiase to different enzyme complexes can show different influences on the FPA. Crude enzymes with high cellobiase activity are less affected by supplemental cellobiase. Granda (2004) compared the sugar yield of bagasse hydrolyzed by enzymes from Genenor and Iogen with cellulase loading of 5 FPU/g dry biomass, based on the activities determined by the conventional method without cellobiase supplementation. Sugar yields obtained with the Iogen enzyme were 20% lower than those obtained with the Genenor enzymes; the difference can be attributed to different cellobiase activities in the original enzyme mixtures. Compared with the enzyme from Iogen, the enzyme from Genenor had relatively lower cellobiase activity; therefore, its activity was enhanced more when cellobiase was supplemented. To overcome the lower cellobiase activity in the most widely used cellulase source, *Trichoderma reesi*, cellobiase is supplemented to ensure complete hydrolysis of biomass.

Based on the enzyme activity reported in Chapter II, a cellobiase activity of 321 CBU/mL and cellulase activity of 65 FPU/mL, the ratios of cellobiase to cellulase (v/v) of 0.25, 0.5, and 1.0 in Figure IV-5 indicate cellobiase loadings of 6.2, 12.3, and 24.7 CBU/g dry biomass, respectively, if a cellulase loading of 5 FPU/g dry biomass is assumed. The cellobiase loading of 24.7 CBU/g dry biomass is comparable to the one we normally employed, 28.4 CBU/g dry biomass. Both Figures IV-4 and IV-5 indicate that cellobiase loading of 28.4 CBU/g dry biomass is sufficient to enhance digestibility and alleviate end-product inhibition. Further addition of cellobiase did not increase sugar yields from biomass.

Conclusions

End-product inhibition was more pronounced for short-term hydrolysis, and became negligible for long-term hydrolysis when there was no cellobiase

supplementation to the enzyme complex. By converting the strong inhibitor, cellobiose, to glucose, the addition of supplemental cellobiase to the enzyme complex can significantly increase the initial rate and extent of biomass hydrolysis. It also improved the FPA of the enzyme complex. Above a certain level, further addition of cellobiase did not increase digestibility or the filter paper activity. By adding cellobiase, the extents of glucan and xylan hydrolyses were virtually identical regardless of substrate concentration. Although a 50–100 g/L substrate concentration is more practical from an industrial viewpoint, lower substrate concentrations such as 10–20 g/L are often used in laboratory investigations to prevent end-product inhibitions of cellulase by cellobiose and glucose when the cellobiase activity in the enzyme complex is low.

EFFECTS OF STRUCTURAL FEATURES ON BIOMASS DIGESTIBILITY

Introduction

Among all of the factors influencing enzymatic hydrolysis of lignocellulosic biomass, structural features are the most complicated factors, because they are interrelated and coupled with the extent of pretreatment. It is broadly accepted that accessible surface area and lignin content play significant roles in influencing the rate and extent of biomass hydrolysis. Biomass digestibility is enhanced with an increase in accessible surface area and removal of lignin (Fan et al*.,* 1981; Grethlein, 1985; Thompson and Chen, 1992; Sinitsyn et al*.,* 1991); however, accessible surface area is not considered as a dependent factor because it may correlate with other structural features (Sinitsyn et al., 1991). Based on the previous studies (Chang and Holtzapple, 2000), lignin content, acetyl content, and crystallinity are chosen as key structural features that determine digestibility because these three features are independently controllable in pretreatment processes and are easy to measure. To eliminate cross effect between structural features, selective delignification, deacetylation, and decrystallization were employed to prepare a total of 147 model lignocelluloses; thus, the effect of each structural feature on biomass digestibility could be investigated.

Materials and Methods

Substrate Preparation

A total of 147 model samples of poplar wood with a variety of lignin contents, acetyl contents, and crystallinities were prepared via selective delignification with peracetic acid, selective deacetylation with potassium hydroxide, and selective decrystallization with ball milling (Chang and Holtzapple, 2000). Corn stover was pretreated at 100°C for 2 h in the presence of 0.1 g lime/g dry biomass and 10 mL water/g dry biomass. The dried corn stover was ground to pass through a 40-mesh sieve. The step-by-step pretreatment procedure is described in Appendix A. Chemically pretreated corn stover and poplar wood were ball milled for 72 h to decrease crystallinity. The procedures for lime pretreatment and ball milling are given in Appendices A and C, respectively. Lignin content, acetyl content, biomass crystallinity, and carbohydrate content of pretreated biomass were measured using the methods described in Chapter II. It was reasonable to assume that decrystallization did not change the chemical composition of biomass.

Enzymatic Hydrolysis

Enzymatic hydrolysis was performed at two conditions. The first enzymatic hydrolysis condition described in Chapter II was employed to develop mathematical models that correlate structural features and digestibility. The second one was used to study the effects of three structural features on biomass digestibility at various hydrolysis times, and is briefly introduced as follows:

A small amount (ca., 1.0 g dry biomass) of pretreated poplar wood or corn stover, 45 mL of distilled water, 2.5 mL of 1-M citrate buffer, and 1.5 mL of 0.01-g/mL sodium azide were placed in 125-mL Erlenmeyer flasks. The flasks were placed in a shaking air bath agitated at 100 rpm and preheated for 1 h. The hydrolysis was initiated by adding 1.0 mL of appropriately diluted cellulase and cellobiase. The hydrolysis conditions were performed at the following conditions: temperature = 50°C, pH = 4.8, substrate concentration = 20 g/L, dry weight of biomass = 0.2 g, slurry volume = 50 mL, cellulase

loading = 5 FPU/g dry biomass, cellobiase loading = 28.4 CBU/g dry biomass. To monitor the course of hydrolysis, 2 mL of samples were withdrawn as functions of time (i.e., 0, 1, 3, 6, 12, 24, 48, and 72 h) and centrifuged to separate liquid and solid, and the supernatants were used for sugar analysis. Glucose and xylose concentrations were measured using HPLC. Detailed procedure for sugar analysis using HPLC is given in Appendix E. Glucose, xylose, and total sugar conversions were calculated using Equations II-4 to II-6.

Results and Discussion

Distribution of Structural Features

Table IV-2 summarizes the three structural features and carbohydrate contents of the 147 model lignocelluloses. The samples are named based on the pretreatment conditions by which they were prepared. For example, the treatment conditions for preparing Sample DL01-DA015-DC3 were: delignification (DL) using 0.1 g/g dry biomass of peracetic acid, deacetylation (DA) using 0.15 mmol/g dry biomass of KOH, and decrystallization (DC) using 3-d ball milling. Lignin content, acetyl content, and biomass crystallinity ranged from 0.7% to 26.3%, 0.1% to 3.1%, and 5.4% to 68.8%, respectively. The increases in glucan content (i.e., from 44.4% to 76.5%) and crystallinity (i.e., from 55.4% to 68.8%) were observed with increasing the extent of delignification and deacetylation because amorphous materials, such as lignin and acetyl groups were removed, whereas xylan content fluctuated in a narrow range from 13.8% to 17.6%, indicating that xylan removal occurred during chemical pretreatment. Slight cross effect was observed during severe deacetylation, i.e., some lignin was removed with the removal of 90% acetyl groups by high KOH loading.

Figure IV-6 illustrates the distributions of the three structural features for the model samples. The plots show that data of structural features fall in the every region of the space, except for the region of biomass crystallinity from 35% to 53% and acetyl content from 0.7% to 1.5 %.

Table IV-2. Structural features and carbohydrate contents of model lignocelluloses

Sample	Pretreatment condition			Structural features (%)			Carbohydrate content (%)		Removal[b] (%)	
	Peracetic acid loading (g/g dry biomass)	KOH loading (mmol/g dry biomass)	Ball milling time (d)	Lignin content	Acetyl content	CrI_B[c]	Glucan	Xylan	Lignin	Acetyl
DL00-DA000-DC0[a]	0	0	0	26.3	2.9	55.4	44.4	13.9	---	---
DL00-DA000-DC3	0	0	3	26.3	2.9	29.4	44.4	13.9	---	---
DL00-DA000-DC6	0	0	6	26.3	2.9	14.9	44.4	13.9	---	---
DL00-DA007-DC0	0	0.07	0	25.5	2.8	57.3	46.6	14.5	4.7	6.2
DL00-DA007-DC3	0	0.07	3	25.5	2.8	32.1	46.6	14.5	4.7	6.2
DL00-DA007-DC6	0	0.07	6	25.5	2.8	20.3	46.6	14.5	4.7	6.2
DL00-DA015-DC0	0	0.15	0	25.6	2.5	57.8	46	14.2	4.9	15.8
DL00-DA015-DC3	0	0.15	3	25.6	2.5	27.5	46	14.2	4.9	15.8
DL00-DA015-DC6	0	0.15	6	25.6	2.5	18.9	46	14.2	4.9	15.8
DL00-DA035-DC0	0	0.35	0	25.5	1.9	56.3	47	14.7	5.7	36.8
DL00-DA035-DC3	0	0.35	3	25.5	1.9	25.2	47	14.7	5.7	36.8
DL00-DA035-DC6	0	0.35	6	25.5	1.9	20.4	47	14.7	5.7	36.8
DL00-DA055-DC0	0	0.55	0	26.0	1.3	56	46.4	14.4	4.1	57.3
DL00-DA055-DC3	0	0.55	3	26.0	1.3	22.5	46.4	14.4	4.1	57.3
DL00-DA055-DC6	0	0.55	6	26.0	1.3	12.5	46.4	14.4	4.1	57.3

Table IV-2. Continued

Sample	Pretreatment condition			Structural features (%)			Carbohydrate content (%)		Removal[②] (%)	
	Peracetic acid loading (g/g dry biomass)	KOH loading (mmol/g dry biomass)	Ball milling time (d)	Lignin content	Acetyl content	CrI_B	Glucan	Xylan	Lignin	Acetyl
DL00-DA075-DC0	0	0.75	0	26.0	0.9	60	47.5	14.8	5.3	71.2
DL00-DA075-DC3	0	0.75	3	26.0	0.9	21.6	47.5	14.8	5.3	71.2
DL00-DA075-DC6	0	0.75	6	26.0	0.9	9.9	47.5	14.8	5.3	71.2
DL00-DA150-DC0	0	1.50	0	24.5	0.4	66.2	49.2	13.8	14.5	89.0
DL00-DA150-DC3	0	1.50	3	24.5	0.4	31.2	49.2	13.8	14.5	89.0
DL00-DA150-DC6	0	1.50	6	24.5	0.4	27.3	49.2	13.8	14.5	89.0
DL01-DA000-DC0	0.1	0	0	23.9	2.8	60.2	47.3	14.8	12.7	8.2
DL01-DA000-DC3	0.1	0	3	23.9	2.8	25.9	47.3	14.8	12.7	8.2
DL01-DA000-DC6	0.1	0	6	23.9	2.8	8.2	47.3	14.8	12.7	8.2
DL01-DA007-DC0	0.1	0.07	0	23.1	2.9	60.4	46.4	14.6	16.9	7.8
DL01-DA007-DC3	0.1	0.07	3	23.1	2.9	16.4	46.4	14.6	16.9	7.8
DL01-DA007-DC6	0.1	0.07	6	23.1	2.9	13.9	46.4	14.6	16.9	7.8
DL01-DA015-DC0	0.1	0.15	0	22.8	2.8	59.8	47.2	15	18.4	10.5
DL01-DA015-DC3	0.1	0.15	3	22.8	2.8	22.7	47.2	15	18.4	10.5
DL01-DA015-DC6	0.1	0.15	6	22.8	2.8	14	47.2	15	18.4	10.5

Table IV-2. Continued

Sample	Pretreatment condition			Structural features (%)			Carbohydrate content (%)		Removal[②] (%)	
	Peracetic acid loading (g/g dry biomass)	KOH loading (mmol/g dry biomass)	Ball milling time (d)	Lignin content	Acetyl content	CrI_B	Glucan	Xylan	Lignin	Acetyl
DL01-DA035-DC0	0.1	0.35	0	22.4	2.9	60	47.8	14.8	20.3	7.9
DL01-DA035-DC3	0.1	0.35	3	22.4	2.9	27	47.8	14.8	20.3	7.9
DL01-DA035-DC6	0.1	0.35	6	22.4	2.9	22	47.8	14.8	20.3	7.9
DL01-DA055-DC0	0.1	0.55	0	21.8	2.2	55.7	48.6	15.2	23.3	29.2
DL01-DA055-DC3	0.1	0.55	3	21.8	2.2	24.8	48.6	15.2	23.3	29.2
DL01-DA055-DC6	0.1	0.55	6	21.8	2.2	14.8	48.6	15.2	23.3	29.2
DL01-DA075-DC0	0.1	0.75	0	21.3	1.7	60.8	48.9	15	26.4	47.7
DL01-DA075-DC3	0.1	0.75	3	21.3	1.7	21.1	48.9	15	26.4	47.7
DL01-DA075-DC6	0.1	0.75	6	21.3	1.7	17.3	48.9	15	26.4	47.7
DL01-DA150-DC0	0.1	1.50	0	17.8	0.4	68.8	54.9	15.3	44.2	90.2
DL01-DA150-DC3	0.1	1.50	3	17.8	0.4	28.3	54.9	15.3	44.2	90.2
DL01-DA150-DC6	0.1	1.50	6	17.8	0.4	18.8	54.9	15.3	44.2	90.2
DL02-DA000-DC0	0.2	0	0	21.5	2.9	59.3	47.5	14.8	22.6	5.9
DL02-DA000-DC3	0.2	0	3	21.5	2.9	19	47.5	14.8	22.6	5.9
DL02-DA000-DC6	0.2	0	6	21.5	2.9	16	47.5	14.8	22.6	5.9

Table IV-2. Continued

Sample	Pretreatment condition			Structural features (%)			Carbohydrate content (%)		Removal② (%)	
	Peracetic acid loading (g/g dry biomass)	KOH loading (mmol/g dry biomass)	Ball milling time (d)	Lignin content	Acetyl content	CrI_B	Glucan	Xylan	Lignin	Acetyl
DL02-DA007-DC0	0.2	0.07	0	21.1	3.1	58.9	48.4	15.2	24.6	2.3
DL02-DA007-DC3	0.2	0.07	3	21.1	3.1	23.3	48.4	15.2	24.6	2.3
DL02-DA007-DC6	0.2	0.07	6	21.1	3.1	12.8	48.4	15.2	24.6	2.3
DL02-DA015-DC0	0.2	0.15	0	20.9	3.0	59	48	15.2	25.7	3.6
DL02-DA015-DC3	0.2	0.15	3	20.9	3.0	27.4	48	15.2	25.7	3.6
DL02-DA015-DC6	0.2	0.15	6	20.9	3.0	27.4	48	15.2	25.7	3.6
DL02-DA035-DC0	0.2	0.35	0	19.5	2.9	59.4	48.7	15.3	31.1	7.7
DL02-DA035-DC3	0.2	0.35	3	19.5	2.9	26.5	48.7	15.3	31.1	7.7
DL02-DA035-DC6	0.2	0.35	6	19.5	2.9	22	48.7	15.3	31.1	7.7
DL02-DA055-DC0	0.2	0.55	0	19.5	2.5	61.8	49.2	15.4	31.8	21.0
DL02-DA055-DC3	0.2	0.55	3	19.5	2.5	25.2	49.2	15.4	31.8	21.0
DL02-DA055-DC6	0.2	0.55	6	19.5	2.5	23	49.2	15.4	31.8	21.0
DL02-DA075-DC0	0.2	0.75	0	18.4	1.7	61.4	50.1	15.6	36.8	47.2
DL02-DA075-DC3	0.2	0.75	3	18.4	1.7	28.5	50.1	15.6	36.8	47.2
DL02-DA075-DC6	0.2	0.75	6	18.4	1.7	9.2	50.1	15.6	36.8	47.2

Table IV-2. Continued

Sample	Pretreatment condition			Structural features (%)			Carbohydrate content (%)		Removal② (%)	
	Peracetic acid loading (g/g dry biomass)	KOH loading (mmol/g dry biomass)	Ball milling time (d)	Lignin content	Acetyl content	CrI_B	Glucan	Xylan	Lignin	Acetyl
DL02-DA150-DC0	0.2	1.50	0	14.8	0.3	66.4	55.8	15.5	54.7	92.8
DL02-DA150-DC3	0.2	1.50	3	14.8	0.3	30.1	55.8	15.5	54.7	92.8
DL02-DA150-DC6	0.2	1.50	6	14.8	0.3	9.8	55.8	15.5	54.7	92.8
DL03-DA000-DC0	0.3	0	0	18.7	2.9	61.2	49.3	15.5	35.2	9.3
DL03-DA000-DC3	0.3	0	3	18.7	2.9	23.5	49.3	15.5	35.2	9.3
DL03-DA000-DC6	0.3	0	6	18.7	2.9	9.8	49.3	15.5	35.2	9.3
DL03-DA007-DC0	0.3	0.07	0	17.8	2.9	62.5	50.1	15.8	39.4	11.8
DL03-DA007-DC3	0.3	0.07	3	17.8	2.9	30.8	50.1	15.8	39.4	11.8
DL03-DA007-DC6	0.3	0.07	6	17.8	2.9	10.5	50.1	15.8	39.4	11.8
DL03-DA015-DC0	0.3	0.15	0	17.1	2.5	61.9	50	15.9	42.3	23.8
DL03-DA015-DC3	0.3	0.15	3	17.1	2.5	23.5	50	15.9	42.3	23.8
DL03-DA015-DC6	0.3	0.15	6	17.1	2.5	10.4	50	15.9	42.3	23.8
DL03-DA035-DC0	0.3	0.35	0	16.3	2.8	61.9	50.5	16	45.3	16.0
DL03-DA035-DC3	0.3	0.35	3	16.3	2.8	24.6	50.5	16	45.3	16.0
DL03-DA035-DC6	0.3	0.35	6	16.3	2.8	14.2	50.5	16	45.3	16.0

Table IV-2. Continued

Sample	Pretreatment condition			Structural features (%)			Carbohydrate content (%)		Removal[②] (%)	
	Peracetic acid loading (g/g dry biomass)	KOH loading (mmol/g dry biomass)	Ball milling time (d)	Lignin content	Acetyl content	CrI_B	Glucan	Xylan	Lignin	Acetyl
DL03-DA055-DC0	0.3	0.55	0	16.2	2.6	62.9	51.2	16	46.0	22.2
DL03-DA055-DC3	0.3	0.55	3	16.2	2.6	22.6	51.2	16	46.0	22.2
DL03-DA055-DC6	0.3	0.55	6	16.2	2.6	12	51.2	16	46.0	22.2
DL03-DA075-DC0	0.3	0.75	0	14.7	2.3	63	53.1	16.5	52.0	31.9
DL03-DA075-DC3	0.3	0.75	3	14.7	2.3	23.7	53.1	16.5	52.0	31.9
DL03-DA075-DC6	0.3	0.75	6	14.7	2.3	20.4	53.1	16.5	52.0	31.9
DL03-DA150-DC0	0.3	1.50	0	10.6	0.4	67.2	59.6	16	69.6	88.7
DL03-DA150-DC3	0.3	1.50	3	10.6	0.4	34.2	59.6	16	69.6	88.7
DL03-DA150-DC6	0.3	1.50	6	10.6	0.4	26	59.6	16	69.6	88.7
DL05-DA000-DC0	0.5	0	0	13.9	2.9	57.4	51.8	16.4	54.5	13.2
DL05-DA000-DC3	0.5	0	3	13.9	2.9	19	51.8	16.4	54.5	13.2
DL05-DA000-DC6	0.5	0	6	13.9	2.9	9.5	51.8	16.4	54.5	13.2
DL05-DA007-DC0	0.5	0.07	0	13.4	2.8	60.5	53.5	16.6	57.3	20.6
DL05-DA007-DC3	0.5	0.07	3	13.4	2.8	25.3	53.5	16.6	57.3	20.6
DL05-DA007-DC6	0.5	0.07	6	13.4	2.8	24	53.5	16.6	57.3	20.6

Table IV-2. Continued

Sample	Pretreatment condition			Structural features (%)			Carbohydrate content (%)		Removal[②] (%)	
	Peracetic acid loading (g/g dry biomass)	KOH loading (mmol/g dry biomass)	Ball milling time (d)	Lignin content	Acetyl content	CrI_B	Glucan	Xylan	Lignin	Acetyl
DL05-DA015-DC0	0.5	0.15	0	13.3	2.7	62.1	52.7	16.5	57.9	22.2
DL05-DA015-DC3	0.5	0.15	3	13.3	2.7	24.1	52.7	16.5	57.9	22.2
DL05-DA015-DC6	0.5	0.15	6	13.3	2.7	11.9	52.7	16.5	57.9	22.2
DL05-DA035-DC0	0.5	0.35	0	12.5	2.6	61.7	53.7	16.8	60.6	26.5
DL05-DA035-DC3	0.5	0.35	3	12.5	2.6	25.9	53.7	16.8	60.6	26.5
DL05-DA035-DC6	0.5	0.35	6	12.5	2.6	12.7	53.7	16.8	60.6	26.5
DL05-DA055-DC0	0.5	0.55	0	11.8	2.3	65.6	54.2	16.7	63.2	37.1
DL05-DA055-DC3	0.5	0.55	3	11.8	2.3	25.6	54.2	16.7	63.2	37.1
DL05-DA055-DC6	0.5	0.55	6	11.8	2.3	25.6	54.2	16.7	63.2	37.1
DL05-DA075-DC0	0.5	0.75	0	10.9	2.4	65.9	56	17	66.8	35.1
DL05-DA075-DC3	0.5	0.75	3	10.9	2.4	23.9	56	17	66.8	35.1
DL05-DA075-DC6	0.5	0.75	6	10.9	2.4	21	56	17	66.8	35.1
DL05-DA150-DC0	0.5	1.50	0	6.8	0.6	67.7	63.6	16.3	81.9	85.6
DL05-DA150-DC3	0.5	1.50	3	6.8	0.6	22.4	63.6	16.3	81.9	85.6
DL05-DA150-DC6	0.5	1.50	6	6.8	0.6	24.6	63.6	16.3	81.9	85.6

Table IV-2. Continued

Sample	Pretreatment condition			Structural features (%)			Carbohydrate content (%)		Removal② (%)	
	Peracetic acid loading (g/g dry biomass)	KOH loading (mmol/g dry biomass)	Ball milling time (d)	Lignin content	Acetyl content	CrI_B	Glucan	Xylan	Lignin	Acetyl
DL10-DA000-DC0	1.0	0	0	6.1	2.7	66.1	57	17.6	81.7	27.2
DL10-DA000-DC3	1.0	0	3	6.1	2.7	21.1	57	17.6	81.7	27.2
DL10-DA000-DC6	1.0	0	6	6.1	2.7	17.5	57	17.6	81.7	27.2
DL10-DA007-DC0	1.0	0.07	0	6.0	3.0	65.3	58.7	17.4	82.5	22.1
DL10-DA007-DC3	1.0	0.07	3	6.0	3.0	28.9	58.7	17.4	82.5	22.1
DL10-DA007-DC6	1.0	0.07	6	6.0	3.0	14.7	58.7	17.4	82.5	22.1
DL10-DA015-DC0	1.0	0.15	0	5.9	2.7	66	59.2	17.2	83.1	29.6
DL10-DA015-DC3	1.0	0.15	3	5.9	2.7	32	59.2	17.2	83.1	29.6
DL10-DA015-DC6	1.0	0.15	6	5.9	2.7	17	59.2	17.2	83.1	29.6
DL10-DA035-DC0	1.0	0.35	0	5.6	2.7	66.3	58.7	16.6	84.3	32.0
DL10-DA035-DC3	1.0	0.35	3	5.6	2.7	32.1	58.7	16.6	84.3	32.0
DL10-DA035-DC6	1.0	0.35	6	5.6	2.7	15.1	58.7	16.6	84.3	32.0
DL10-DA055-DC0	1.0	0.55	0	4.5	2.5	68.3	60.9	16.7	87.4	37.8
DL10-DA055-DC3	1.0	0.55	3	4.5	2.5	32.1	60.9	16.7	87.4	37.8
DL10-DA055-DC6	1.0	0.55	6	4.5	2.5	27.9	60.9	16.7	87.4	37.8

Table IV-2. Continued

Sample	Pretreatment condition			Structural features (%)			Carbohydrate content (%)		Removal[②] (%)	
	Peracetic acid loading (g/g dry biomass)	KOH loading (mmol/g dry biomass)	Ball milling time (d)	Lignin content	Acetyl content	CrI_B	Glucan	Xylan	Lignin	Acetyl
DL10-DA075-DC0	1.0	0.75	0	4.1	2.1	67.5	61	16.6	89.0	49.6
DL10-DA075-DC3	1.0	0.75	3	4.1	2.1	26	61	16.6	89.0	49.6
DL10-DA075-DC6	1.0	0.75	6	4.1	2.1	21.2	61	16.6	89.0	49.6
DL10-DA150-DC0	1.0	1.50	0	2.5	0.4	62.7	70.4	16.2	94.0	90.7
DL10-DA150-DC3	1.0	1.50	3	2.5	0.4	22.4	70.4	16.2	94.0	90.7
DL10-DA150-DC6	1.0	1.50	6	2.5	0.4	19.5	70.4	16.2	94.0	90.7
DL50-DA000-DC0	5.0	0	0	1.8	2.7	68.8	67	16.8	95.4	37.1
DL50-DA000-DC3	5.0	0	3	1.8	2.7	37	67	16.8	95.4	37.1
DL50-DA000-DC6	5.0	0	6	1.8	2.7	5.4	67	16.8	95.4	37.1
DL50-DA007-DC0	5.0	0.07	0	1.6	2.6	68.2	70.2	15.4	96.0	42.8
DL50-DA007-DC3	5.0	0.07	3	1.6	2.6	46.9	70.2	15.4	96.0	42.8
DL50-DA007-DC6	5.0	0.07	6	1.6	2.6	21.5	70.2	15.4	96.0	42.8
DL50-DA015-DC0	5.0	0.15	0	1.6	2.3	65.7	70.9	15	96.1	42.8
DL50-DA015-DC3	5.0	0.15	3	1.6	2.3	50.6	70.9	15	96.1	42.8
DL50-DA015-DC6	5.0	0.15	6	1.6	2.3	19.2	70.9	15	96.1	42.8

Table IV-2. Continued

Sample	Pretreatment condition			Structural features (%)			Carbohydrate content (%)		Removal[②] (%)	
	Peracetic acid loading (g/g dry biomass)	KOH loading (mmol/g dry biomass)	Ball milling time (d)	Lignin content	Acetyl content	CrI_B	Glucan	Xylan	Lignin	Acetyl
DL50-DA035-DC0	5.0	0.35	0	1.5	2.2	64.6	71.7	14.4	96.5	53.0
DL50-DA035-DC3	5.0	0.35	3	1.5	2.2	48	71.7	14.4	96.5	53.0
DL50-DA035-DC6	5.0	0.35	6	1.5	2.2	14.9	71.7	14.4	96.5	53.0
DL50-DA055-DC0	5.0	0.55	0	1.3	1.8	65.4	72.7	14.1	97.0	61.5
DL50-DA055-DC3	5.0	0.55	3	1.3	1.8	47.1	72.7	14.1	97.0	61.5
DL50-DA055-DC6	5.0	0.55	6	1.3	1.8	7.3	72.7	14.1	97.0	61.5
DL50-DA075-DC0	5.0	0.75	0	1.1	1.6	62.3	73.2	14.4	97.4	67.0
DL50-DA075-DC3	5.0	0.75	3	1.1	1.6	44.8	73.2	14.4	97.4	67.0
DL50-DA075-DC6	5.0	0.75	6	1.1	1.6	10.8	73.2	14.4	97.4	67.0
DL50-DA150-DC0	5.0	1.50	0	0.7	0.1	66	76.5	15.1	98.4	97.4
DL50-DA150-DC3	5.0	1.50	3	0.7	0.1	50.9	76.5	15.1	98.4	97.4
DL50-DA150-DC6	5.0	1.50	6	0.7	0.1	33	76.5	15.1	98.4	97.4

[a] Based on the initial weight of component before treatment and wash.

[b] Raw poplar wood.

[c] Biomass crystallinity.

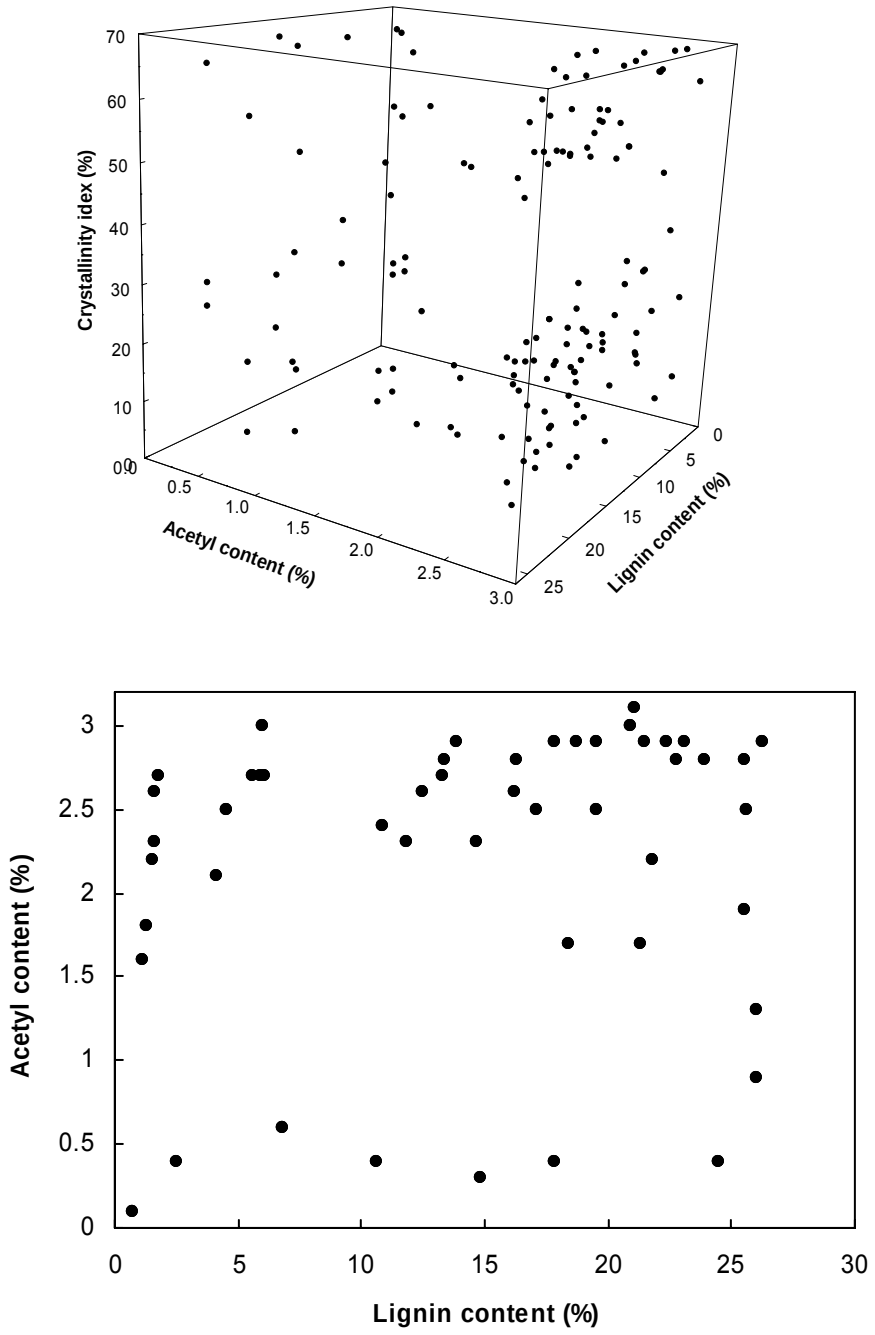

Figure IV-6. Distributions of structural features of model lignocelluloses.

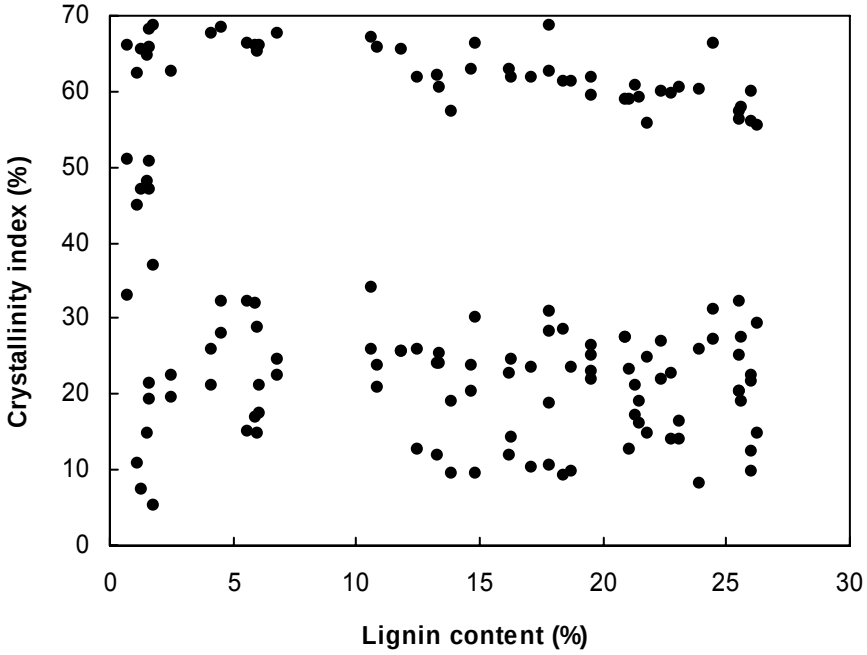

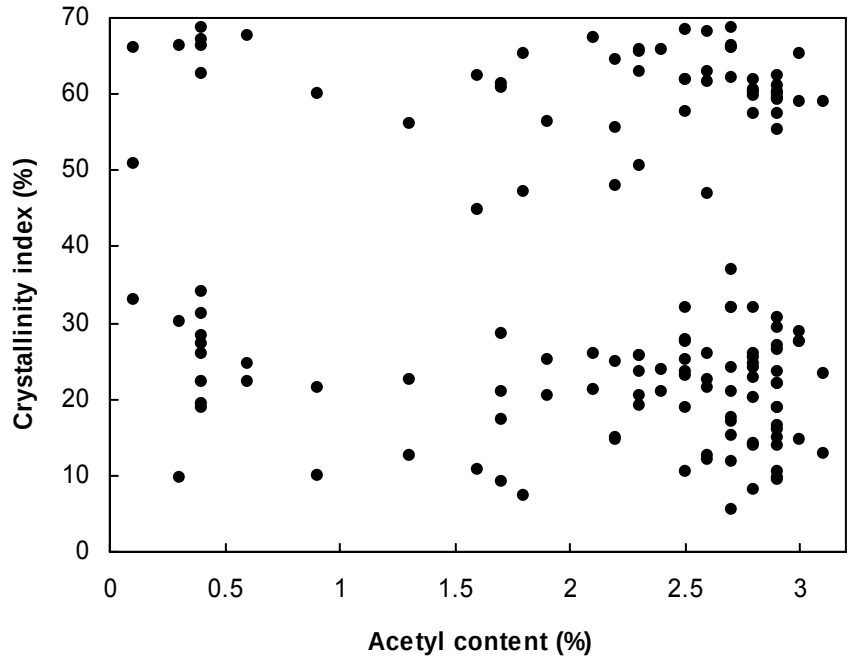

Figure IV-6. Continued.

Effect of Lignin Content

Based on the structural features of the model lignocelluloses shown in Table IV-2, nine samples were selected to investigate the effect of lignin content on digestibility. These samples were categorized into three groups; samples in each group had the same acetyl contents and biomass crystallinity, but different lignin contents. Table IV-3 summarizes structural features and carbohydrate contents of these samples.

Samples (Category I) with low acetyl content (i.e., 0.4%) and high biomass crystallinity (i.e., 66.2%–68.8%) were used to study the effect of lignin content on the hydrolysis profiles of glucan and xylan. Figure IV-7 illustrates that decreased lignin content significantly enhances digestibility. As lignin content decreased from 24.5% to 17.8%, the initial glucan hydrolysis rate increased about 2 times (i.e., from 4.7% to 8.3%), whereas there was no observable increase in the initial xylan hydrolysis rate. The ultimate extent of glucan and xylan hydrolyses increased about 3.5 times (i.e., from 21.5% to 70.2%) and 2 times (i. e., from 40.0% to 86.1%), respectively. For the sample with 10.6% lignin content, the initial rate and ultimate extent of glucan hydrolysis were 12.8% and 92.6%, respectively; the initial rate and ultimate extent of xylan hydrolysis were 12.4% and 99.0%, respectively. Digestibility increased tremendously with the decrease of lignin content from 24.5% to 17.8%, whereas further delignification only moderately improved digestibility.

Figure IV-8 presents the effect of lignin content on the digestibility of low-crystallinity lignocellulose (Category II). For the samples with low crystallinity (i.e., 26.0%–31.2%) and high lignin content (i.e., 24.5%), the initial hydrolysis rate and extent were 26.2% and 64.6% (glucan) and 18.8% and 85.7% (xylan), respectively. Delignification greatly increased the 6-h glucan conversion. As lignin content reduced from 24.5% to 14.8%, the initial glucan hydrolysis rate enhanced from 26.2% to 35.9%, and the ultimate extent of glucan hydrolysis increased from 64.6% to 85.8%, whereas further delignification from 14.8% to 10.9% showed less effect on the initial rate and ultimate extent of glucan hydrolysis. The reduction of lignin content for low-crystalline biomass samples did not show significant influence on xylan digestibility at 1, 6, and 72 h. It seemed that the effect of

delignification on the digestibility of low-crystalline biomass samples was not as significant as high-crystalline biomass samples.

Table IV-3. Structural features and carbohydrate contents of model lignocelluloses for studying the effect of lignin content on digestibility

Category	Sample	Structural features (%)			Carbohydrate content (%)	
		Lignin content	Acetyl content	CrI_B[c]	Glucan	Xylan
I[a]	DL00-DA150-DC0	24.5	0.4	66.2	49.2	13.8
	DL01-DA150-DC0	17.8	0.4	68.8	54.9	15.3
	DL03-DA150-DC0	10.6	0.4	67.2	59.6	16
II[b]	DL00-DA150-DC3	24.5	0.4	31.2	49.2	13.8
	DL02-DA150-DC3	14.8	0.3	30.1	55.8	15.5
	DL03-DA150-DC6	10.6	0.4	26.0	59.6	16
III[b]	DL05-DA075-DC0	10.9	2.4	65.9	56	17
	DL10-DA055-DC0	4.5	2.5	68.3	60.9	16.7
	DL50-DA035-DC0	1.5	2.2	64.6	71.7	14.4

[a] Hydrolysis conditions: 20 g/L substrate concentration, 5 FPU/g dry biomass, 28.4 CBU/g dry biomass.

[b] Hydrolysis conditions: 10 g/L substrate concentration, 5 FPU/g dry biomass, 81.2 CBU/g dry biomass.

[c] Biomass crystallinity.

Figure IV-9 illustrates that lignin contents lower than 10% have insignificant influence on glucan and xylan hydrolyses at 1, 6, and 72 h. The ultimate extents of glucan and xylan hydrolyses were almost complete for the samples with 10% lignin content. Lignin content as low as 10% allows enough enzyme to access biomass. It is obvious that extensive delignification is sufficient to achieve nearly complete hydrolysis regardless of acetyl content and biomass crystallinity. The effect of lignin content on biomass digestibility may be explained as follows: (1) delignification increases the amount of enzyme absorbed on polysaccharides by reducing the nonspecific adsorption of enzyme on lignin (Ooshima et al., 1990; Sewalt et al., 1997), and (2) delignification alleviates steric hindrance (Mooney et al., 1998; Meunier-Goddik et al., 1999). Regardless of the mechanism, removing lignin enhances digestibility to a great extent.

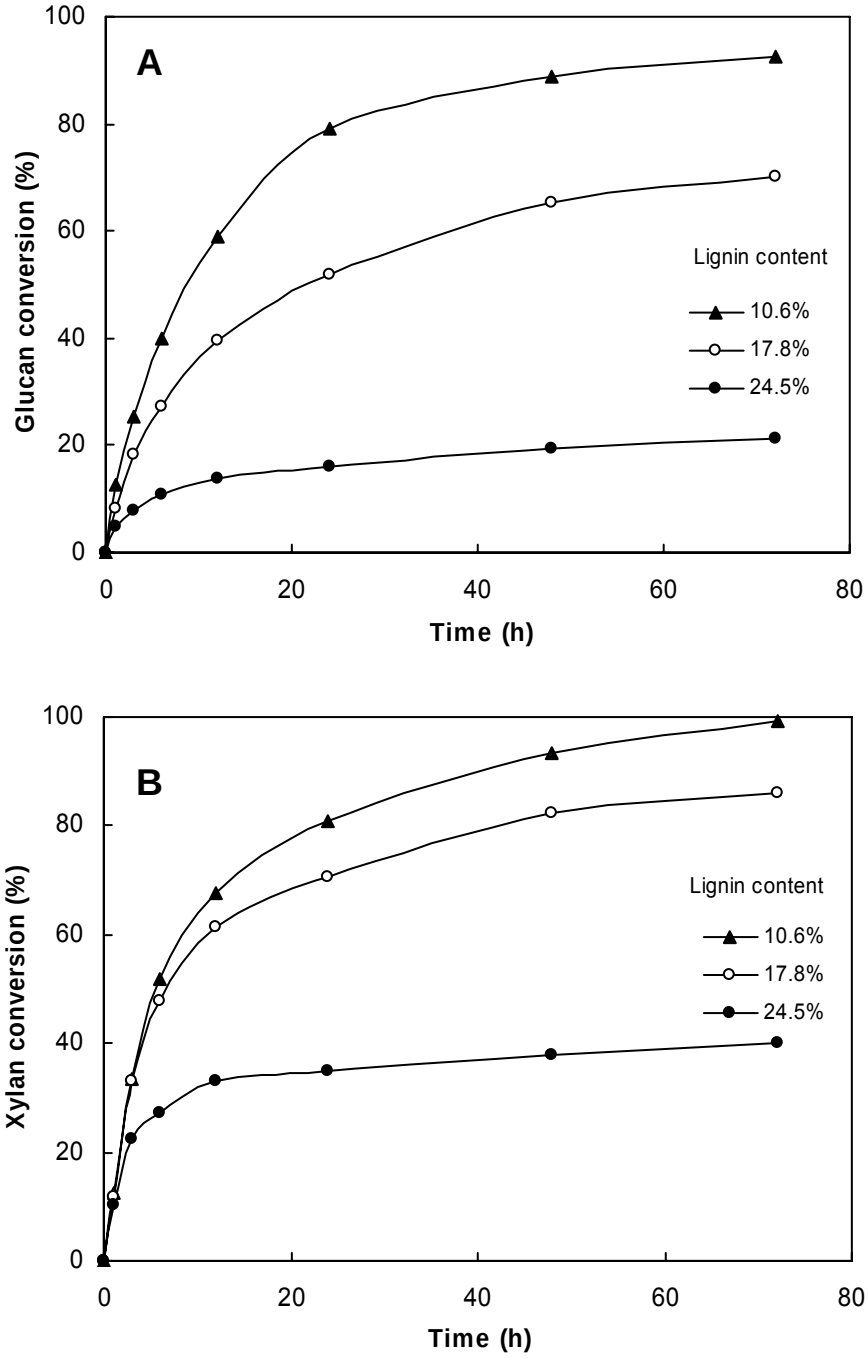

Figure IV-7. Hydrolysis profiles of poplar wood with various lignin contents: (A) glucose; (B) xylose. Hydrolysis condition: 5 FPU/g dry biomass, 28.4 CBU/g dry biomass. Category I: acetyl content: 0.4%, biomass crystallinity: ~67%.

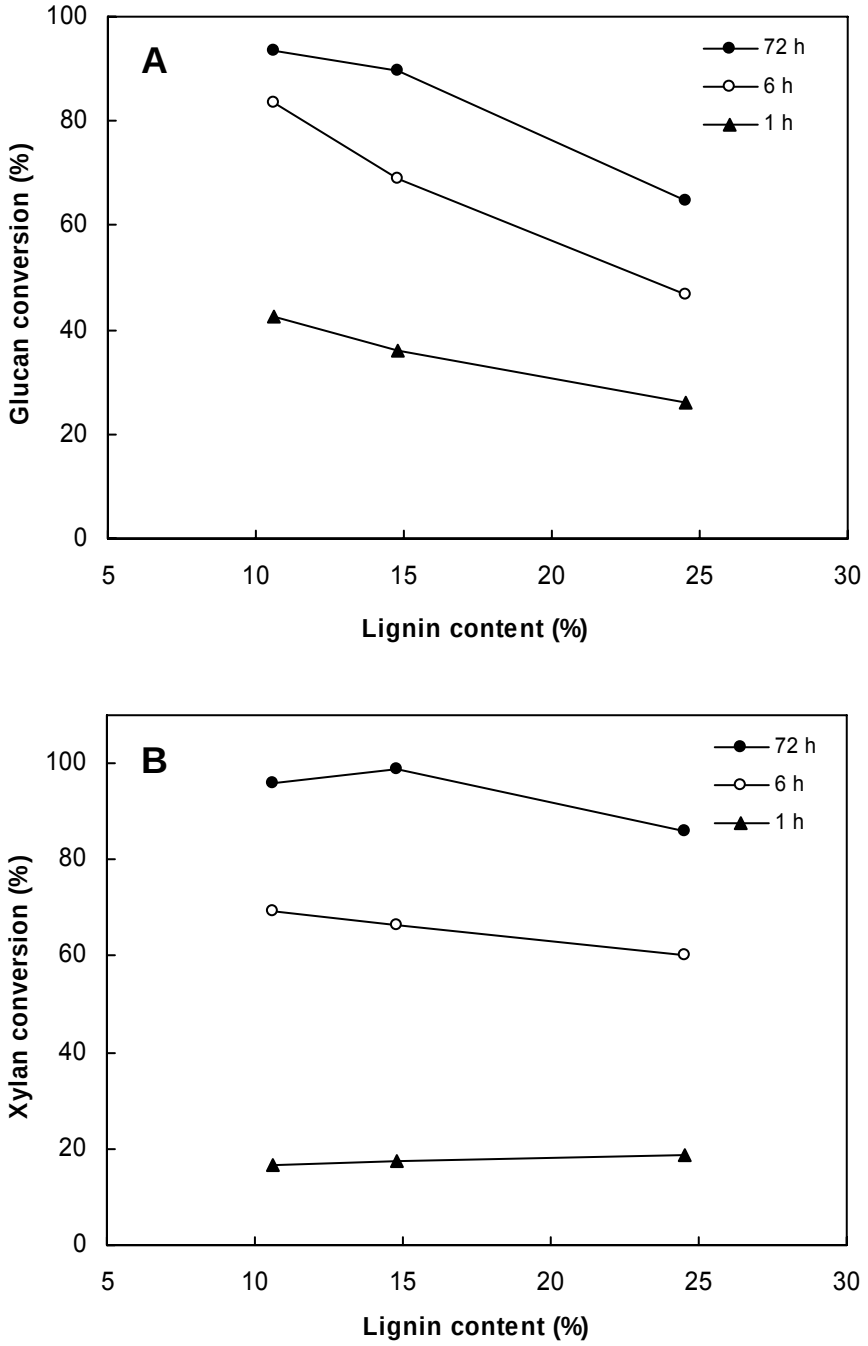

Figure IV-8. Effect of lignin content on digestibility of low-crystallinity biomass: (A) glucose; (B) xylose. Hydrolysis condition: 5 FPU/g dry biomass, 81.2 CBU/g dry biomass. Category II: acetyl content: ~0.4%, biomass crystallinity: ~30%.

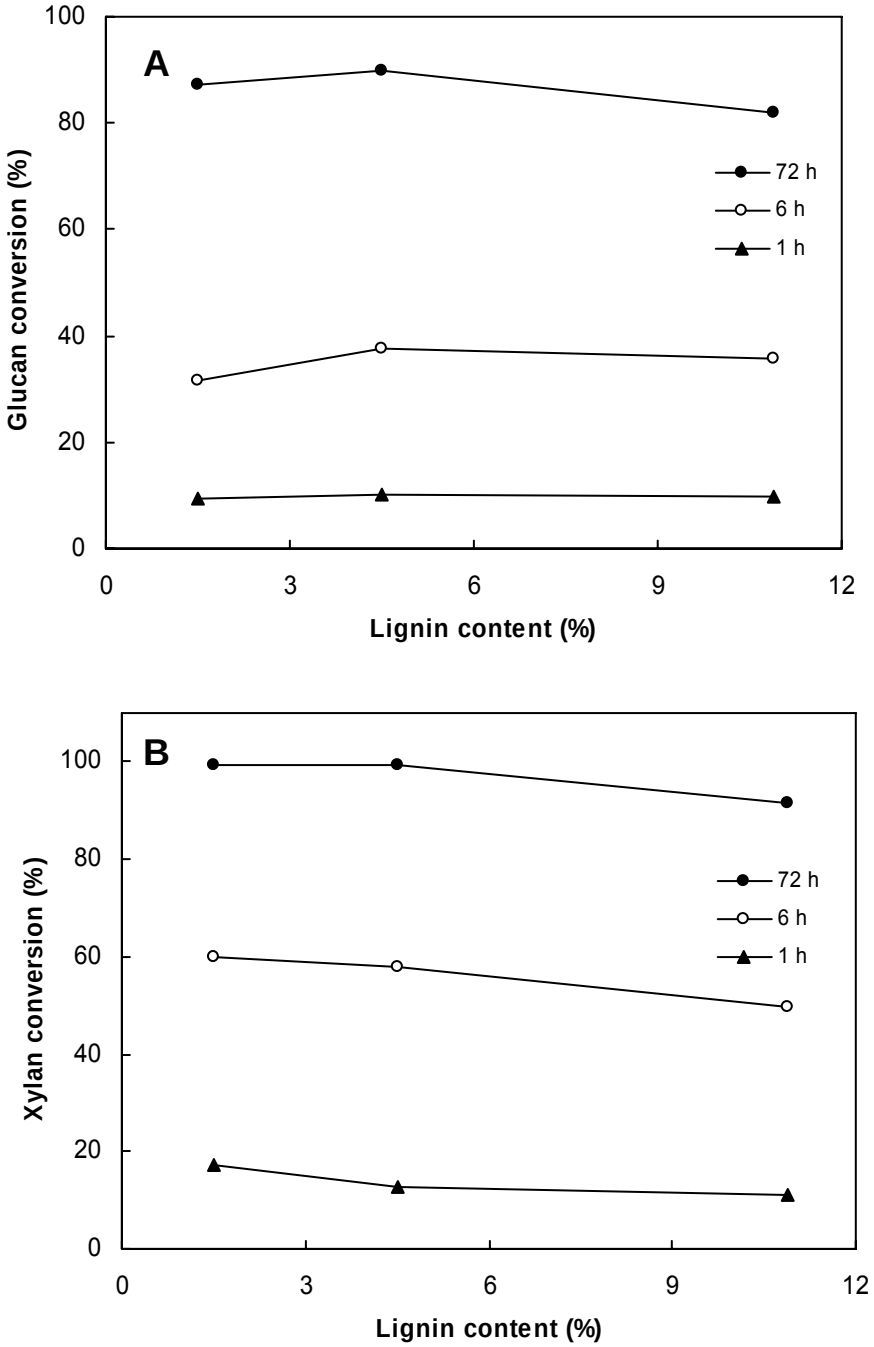

Figure IV-9. Effect of lignin content lower than 10% on biomass digestibility: (A) glucose; (B) xylose. Hydrolysis condition: 5 FPU/g dry biomass, 81.2 CBU/g dry biomass. Category III: acetyl content: ~2.4%, biomass crystallinity: ~66%.

Effect of Acetyl Content

Table IV-4 summarizes the structural features and carbohydrate contents of eight samples used to investigate the effect of acetyl content on digestibility. Figure IV-10 illustrates the effect of acetyl content on the hydrolysis profiles of poplar wood samples (Category I) with medium lignin content (18.4%) and high biomass crystallinity (~60%). As acetyl content decreased from 2.9% (no acetyl group removal) to 1.7%, the initial glucan hydrolysis rate increased from 4.0% to 6.7%, the ultimate extent of glucan hydrolysis increased from 35.8% to 47.0%, the initial xylan hydrolysis rate increased from 6.2% to 7.8%, and the ultimate extent of xylan hydrolysis increased from 40.8% to 49.4%. The removal of acetyl groups enhances sugar conversion, but its effect on digestibility is not as significant as lignin removal, especially for the delignified samples. The small effect of acetyl content on biomass digestibility could also result from the low acetyl content in biomass before pretreatment (ca. 3%).

Figure IV-11 demonstrates the influence of acetyl content on the digestibility of poplar wood (Category II) with higher lignin content (ca. 26%) and high biomass crystallinity (ca. 60%). As acetyl content reduced from 1.9% to 0.4%, the 1-, 6-, and 72-h glucan conversions increased 2 times, the 1-, 6-, and 72-h xylan conversions increased at least 4 times, but glucan and xylan conversions were still low even for the samples with 0.4% acetyl content (i.e., 22% for glucan and 43% for xylan). Figure IV-12 shows the effect of acetyl content on the digestibility of poplar wood (Category III) with high lignin content (ca. 26%) and low biomass crystallinity (ca. 30%). As acetyl content decreased from 2.9% to 1.9%, there was no observable improvement in glucan and xylan conversions. With further decrease of acetyl content to 0.4%, the 1-, 6-, and 72-h glucan conversions increased ~1.5 times, the 1-, 6-, and 72-h xylan conversions increased at least ~2.5 times. Therefore, deactylation had a greater effect on xylan digestibility than on glucan digestibility. This observation agrees well with results from Grohmann (1989) and Kong (1992). For the samples with 90% acetyl removal without the combination of delignification and decrystallization, the ultimate extents of glucan and xylan hydrolyses increased to 22.3% and 43.2%, respectively. The removal of acetyl groups alleviates the

steric hindrance of enzymes and greatly enhanced glucan and xylan digestibility (Grohmann et al., 1989; Kong et al., 1992; Mitchell et al., 1990). Compared to delignification, deacetylation has less effect on digestibility.

Table IV-4. Structural features and carbohydrate contents of model lignocelluloses for studying the effect of acetyl content on digestibility

Category	Sample	Structural features (%)			Carbohydrate content (%)	
		Lignin content	Acetyl content	CrI_B[c]	Glucan	Xylan
I[a]	DL02-DA075-DC0	18.4	1.7	61.4	50.1	15.6
	DL03-DA000-DC0	18.7	2.9	62.5	49.3	15.5
II[b]	DL00-DA035-DC0	25.5	1.9	56.3	47	14.7
	DL00-DA075-DC0	26	0.9	60	47.5	14.8
	DL00-DA150-DC0	24.5	0.4	66.2	49.2	13.8
III[b]	DL00-DA000-DC3	26.3	2.9	29.4	44.4	13.9
	DL00-DA015-DC3	25.6	2.5	27.5	46	14.2
	DL00-DA150-DC3	24.5	0.4	31.2	49.2	13.8

[a] Hydrolysis conditions: 20 g/L substrate concentration, 5 FPU/g dry biomass, 28.4 CBU/g dry biomass.

[b] Hydrolysis conditions: 10 g/L substrate concentration, 5 FPU/g dry biomass, 81.2 CBU/g dry biomass.

[c] Biomass crystallinity.

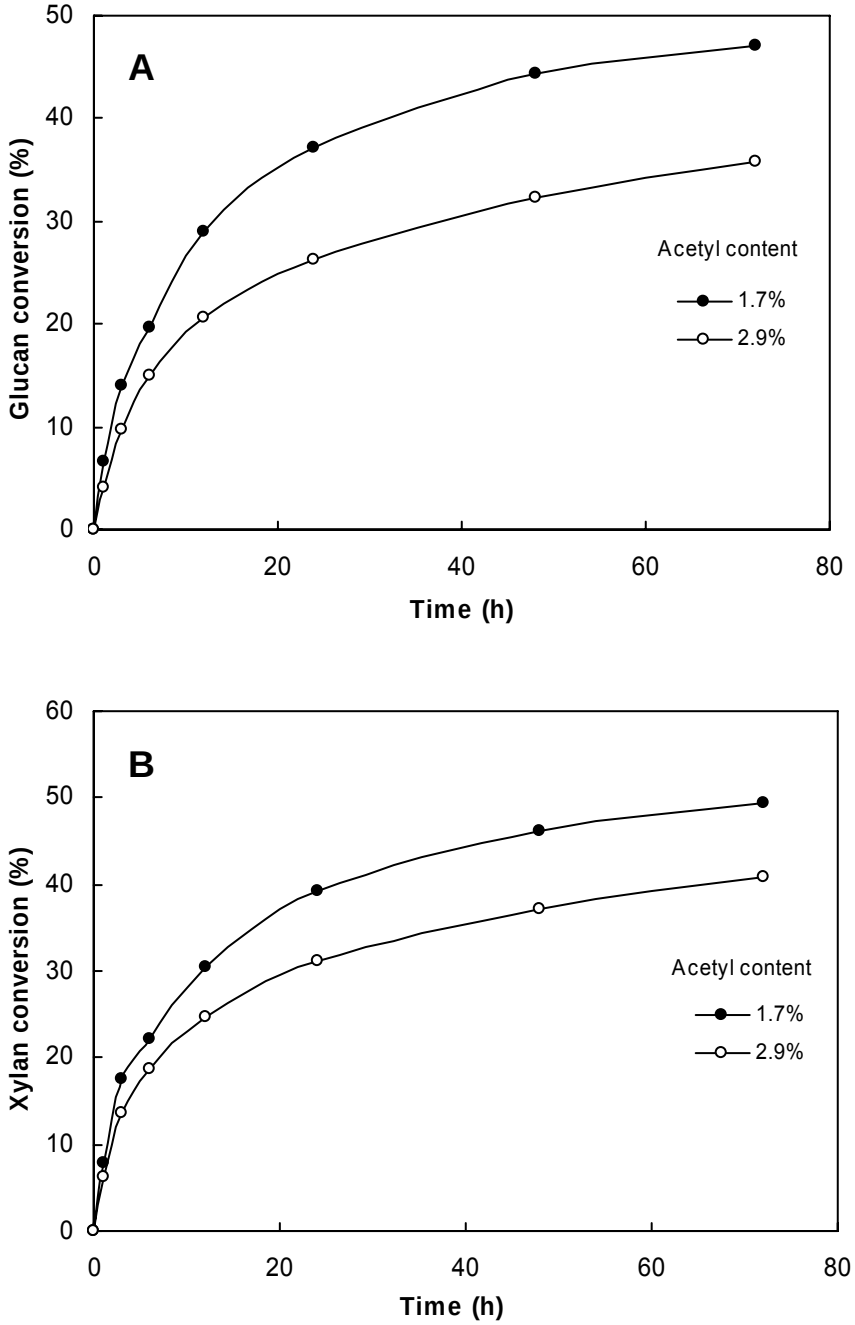

Figure IV-10. Hydrolysis profiles of poplar wood with various acetyl contents: (A) glucose; (B) xylose. Hydrolysis condition: 5 FPU/g dry biomass, 28.4 CBU/g dry biomass. Category I: lignin content: ~18%, biomass crystallinity: ~62%.

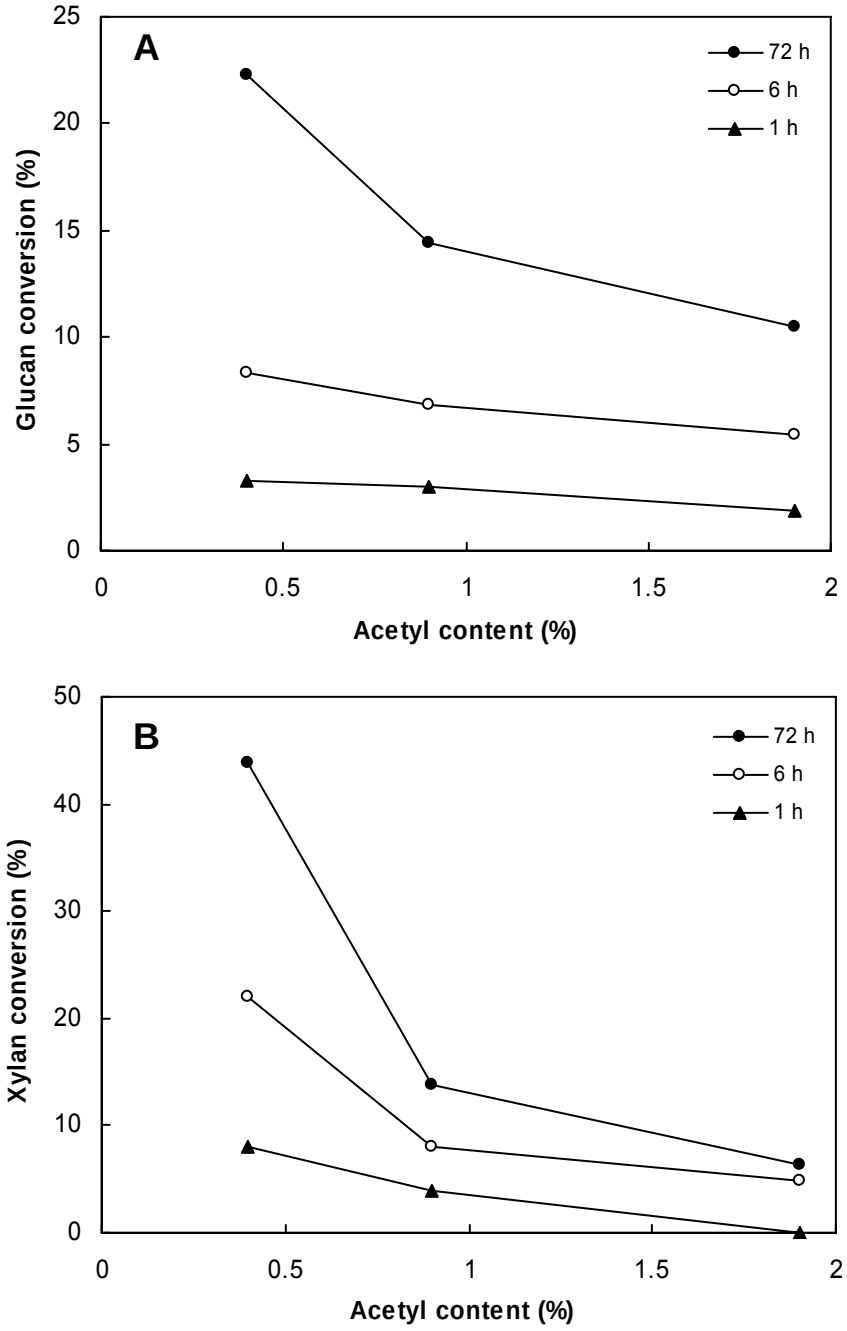

Figure IV-11. Effect of acetyl content on digestibility of high-lignin biomass: (A) glucose; (B) xylose. Hydrolysis condition: 5FPU/g dry biomass, 81.2 CBU/g dry biomass. Category II: lignin content: ~25%, biomass crystallinity: ~60%.

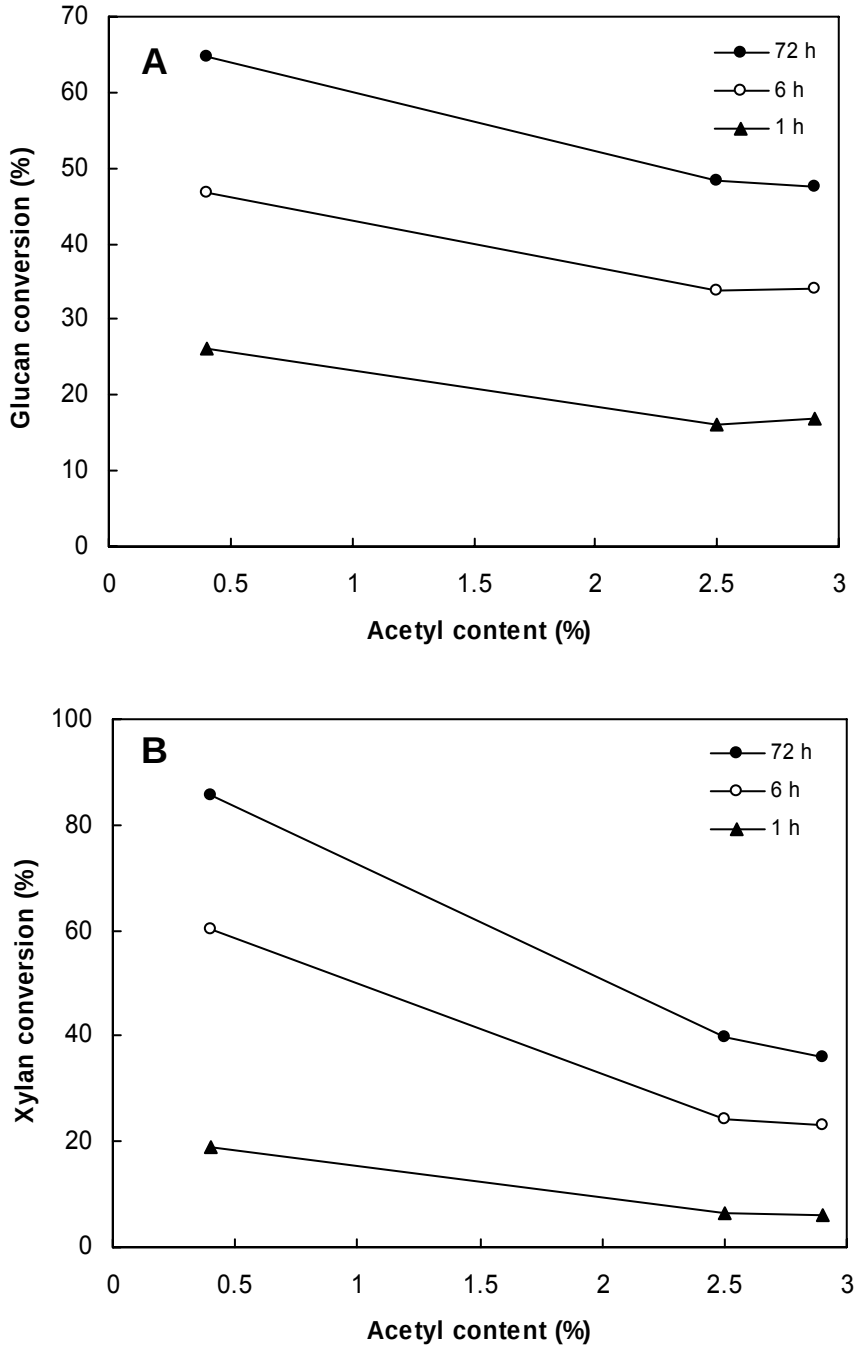

Figure IV-12. Effect of acetyl content on digestibility of low-crystallinity biomass: (A) glucose; (B) xylose. Hydrolysis condition: 5FPU/g dry biomass, 81.2 CBU/g dry biomass. Category III: lignin content: ~25%, biomass crystallinity: ~30%.

Effect of Crystallinity

Table IV-5 summarizes the structural features and carbohydrate contents of five samples used to investigate the effect of biomass crystallinity on digestibility. Figure IV-13 illustrates the influence of crystallinity on the hydrolysis profiles of corn stover (Category I) with medium lignin content (ca. 18.1%) and low acetyl content (ca. 0.3%). As crystallinity decreased from 55.8% to 19.1%, the initial rate and ultimate extent of glucan hydrolysis increased 2 times (i.e., from 12.3% to 22.2%) and 1.5 times (i.e., from 60.5% to 90.0%), respectively. The initial xylan hydrolysis rate increased from 4.9% to 6.2%, the ultimate extent of xylan hydrolysis increased from 50.7% to 79.7%. As shown in Figure IV-13, hydrolysis of decrystallized samples did not continue significantly after 24 h.

Figure IV-14 shows the influence of biomass crystallinity on the digestibility of poplar wood (Category II) with 22.8% lignin content and 2.8% acetyl content, thus the interference from lignin and acetyl contents can be alleviated. The ultimate extents of glucan and xylan hydrolyses increased linearly with decreasing crystallinity. As crystallinity decreased from 59.8% to 22.7%, the 1- and 6-h glucan conversions increased 6 times; the 1 and 6-h xylan conversions increased 5–6 times. Further decreasing crystallinity to 14%, the enhancement was still significant for the initial rate of glucan and xylan hydrolyses, the ultimate extents of glucan and xylan hydrolyses were about 80%. The effect of biomass crystallinity on digestibility was more significant for high-lignin biomass sample.

Figure IV-13 shows that, for low-acetyl biomass sample, the initial xylan hydrolysis rate is not affected by decrystallization whereas the initial glucan hydrolysis rate increases significantly. This observation indicates that decrystallization greatly enhances initial hydrolysis rate and carbohydrate conversion at shorter incubation times (i.e., 6 h) regardless of lignin content. Compared to delignification, decrystallization had less effect on the ultimate extent of hydrolysis. Ball-milling reduces biomass crystallinity by destroying the crystal lattice structure of cellulose fiber, thus increasing the amorphous cellulose and accessible surface area of biomass. Decrystallization makes

biomass more accessible to cellulase, so the initial hydrolysis rate is increased because more substrate-enzyme complex is formed.

Table IV-5. Structural features and carbohydrate contents of model lignocelluloses for studying the effect of biomass crystallinity on digestibility

Group	Sample	Structural features (%)			Carbohydrate content (%)	
		Lignin content	Acetyl content	CrI_B[c]	Glucan	Xylan
I[a]	Corn stover-0	18.14	0.03	55.8	45.77	20.83
	Corn stover-3	18.14	0.03	19.1	45.77	20.83
II[b]	DL01-DA015-DC0	22.8	2.8	59.8	47.2	15
	DL01-DA015-DC3	22.8	2.8	22.7	47.2	15
	DL01-DA015-DC6	22.8	2.8	14	47.2	15

[a] Hydrolysis conditions: 20 g/L substrate concentration, 5 FPU/g dry biomass, 28.4 CBU/g dry biomass.

[b] Hydrolysis conditions: 10 g/L substrate concentration, 5 FPU/g dry biomass, 81.2 CBU/g dry biomass.

[c] Biomass crystallinity.

It has been proposed that delignification and deacetylation increase the amount of absorbed enzyme whereas decrystallization enhances the effectiveness of absorbed enzyme (Chang and Holtzapple, 2000; Lee and Fan, 1982). Based on the above discussion, Figure IV-15 illustrates a schematic diagram to explain the effects of lignin content, acetyl content, and crystallinity on enzyme adsorption and enzymatic hydrolysis at 1, 6, and 72 h. Compared to lignin content, acetyl content has less effect on increasing the amount of absorbed enzyme, thinner and thicker lines indicate the relative effect. The initial hydrolysis rate is reported to be proportional to the amount of enzyme-substrate complex formed (Holtzapple et al., 1984). Although delignification and deacetylation increase the amount of aborbed enzyme, the initial hydrolysis rate does not considerably increase because of the slow hydrolysis rate of crystalline cellulose; however, a relatively high ultimate extent of hydrolysis could be achieved. Compared to crystalline cellulose, amorphous cellulose resulting from decrystallization degrades very fast. Enzyme absorbs on amorphous cellulose and forms an enzyme-substrate complex that

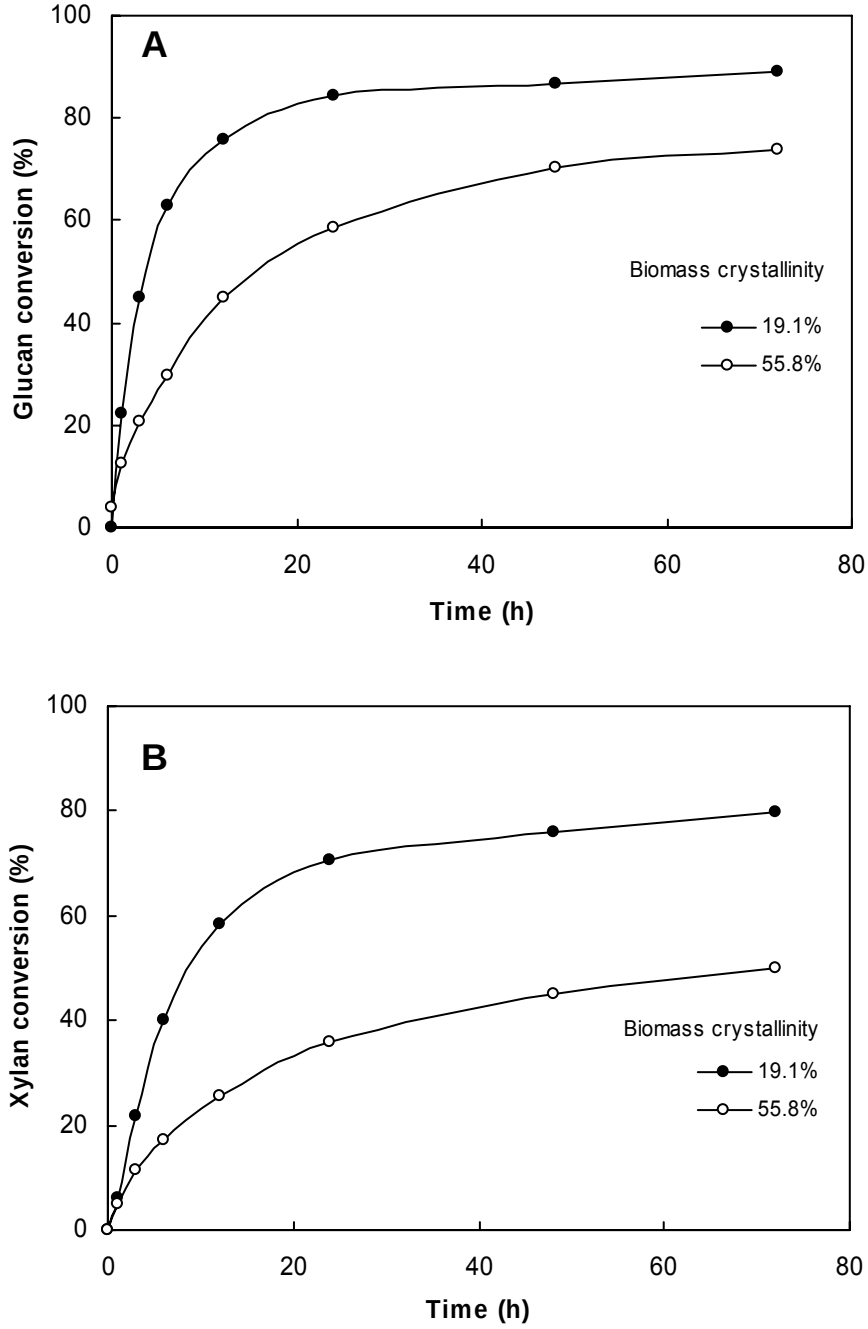

Figure IV-13. Hydrolysis profiles of poplar wood with various biomass crystallinities: (A) glucose; (B) xylose. Hydrolysis conditions: 5 FPU/g dry biomass, 28.4 CBU/g dry biomass. Category I: lignin content: ~18%, acetyl content: ~0.03%.

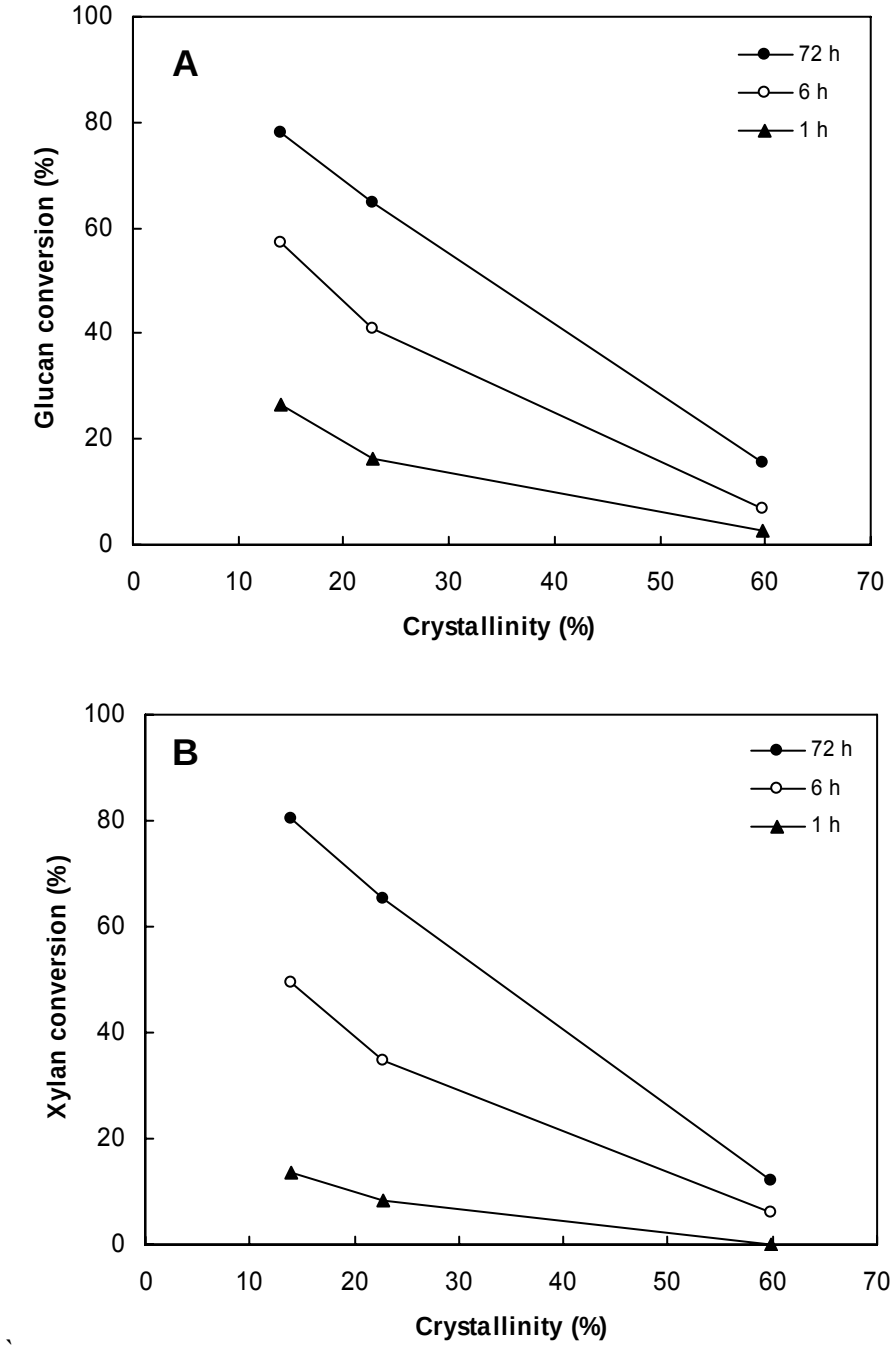

Figure IV-14. Effect of biomass crystallinity on digestibility of high-lignin biomass: (A) glucose; (B) xylose. Hydrolysis condition: 5FPU/g dry biomass, 81.2 CBU/g dry biomass. Category II: lignin content: ~23%, acetyl content: ~2.8%.

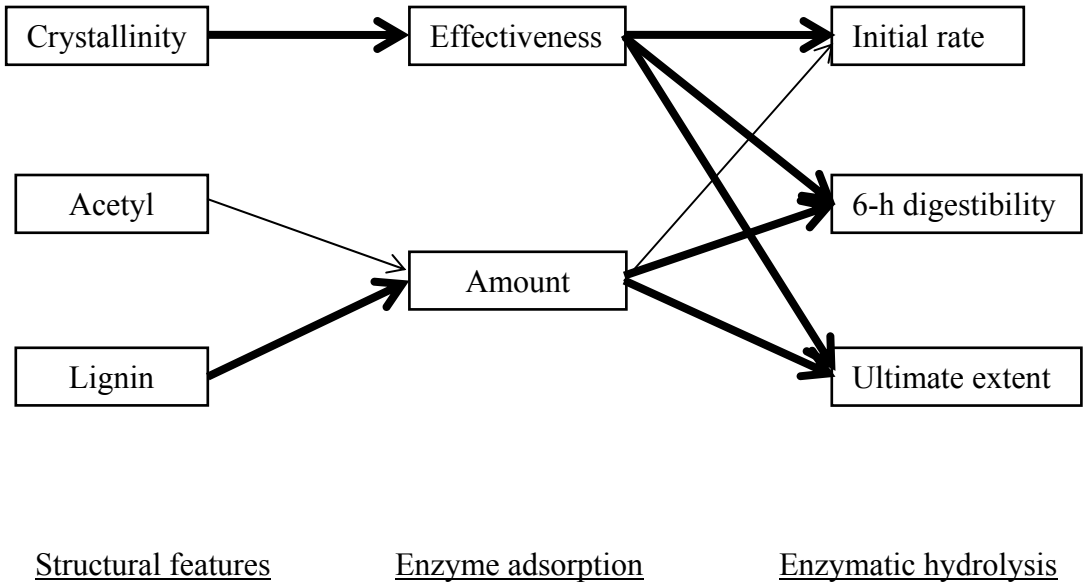

Figure IV-15. A schematic diagram for the effects of lignin, acetyl groups, and crystallinity on enzyme adsorption and enzymatic hydrolysis of biomass. (Note: Thicker lines indicate a more significant effect.)

enhances the initial rate and ultimate extent of biomass hydrolysis. Both the enzyme effectiveness and the amount of absorbed enzyme significantly influence the 6- and 72-h biomass digestibilities.

Conclusions

Based on the above discussion, lignin content and crystallinity play more significant roles on digestibility than acetyl content. Decrystallization tremendously increased digestibility during shorter hydrolysis times whereas delignification greatly enhanced digestibility with longer hydrolysis times. Extensive delignification or decrystallization incurs an extra cost with no significant improvement in degstibility. Decrystallization has a greater effect on cellulose degradation whereas deacteylation has a greater effect on hemicellulose degradation.

The effects of lignin content, acetyl content, and crystallinity on digestibility, to some extent, are interrelated. Delignification shows less effect on the digestibility of low-crystalline biomass samples than it does on the digestibility of highly-crystalline biomass samples. Deacetylation has an insignificant influence on the digestibility of low-lignin or low-crystalline biomass samples.

ENZYME LOADING STUDIES

Introduction

Enzyme loading and biomass structural features are closely interrelated during enzymatic hydrolysis of lignocellulosic biomass, i.e., biomass with structural features more accessible to enzyme requires less enzyme to achieve high sugar yields, whereas digestibility of biomass with structural features recalcitrant to enzyme accessibility can be improved, to some extent, with higher enzyme loading. Due to high enzyme cost, reducing the quantity of enzyme required to achieve high sugar yields from biomass becomes one of the targets in biomass bioconversion technology. In this study, the effect of enzyme loading on the digestibility of biomass with various structural features was investigated.

Materials and Methods

Poplar wood with a variety of lignin contents, acetyl contents, and crystallinities were prepared via selective delignification with peracetic acid, selective deacetylation with potassium hydroxide, and selective decrystallization with ball milling. The pretreatment conditions are described in Chapter II (Chang and Holtzapple, 2000). Enzymatic hydrolysis was performed at the following conditions: temperature = 50^{o}C, pH = 4.8, substrate concentration = 10 g/L, dry weight of biomass = 0.2 g, slurry volume = 20 mL, cellulase loading = 0.1~150 FPU/g dry biomass, cellobiase loading = 81.2 CBU/g dry biomass, rotating speed = 100 rpm, incubation period = 1, 6, and 72 h. Glucose and xylose concentrations were measured using HPLC. Glucose, xylose, and

total sugar conversions were calculated using Equations II-4 to II-6. The detailed procedures for enzymatic hydrolysis and sugar analysis using HPLC are described in Appendices B and E, respectively.

Results and Discussion

The 147 model lignocellulose samples were categorized into three main groups on the basis of structural features and the preliminary studies of the effects of structural features on digestibility. Only lignin content and crystallinity are considered as dominant factors because of the less effect of acetyl content on digestibility. Table IV-6 shows the effect of delignification combined with decrystallization on 72-h digestibility. One sample was chosen from each category to investigate the effect of enzyme loading on the digestibilities of biomass with various structural features. Table IV-7 shows the structural features and carbohydrate contents of the three samples.

Table IV-6. Effects of lignin content and biomass crystallinity on 72-h digestibility

Lignin content (%)			CrI_B[a] (%)			72-h digestibility
<10	10–17	17–26	<20	20–50	>50	
Low	Medium	High	Low	Medium	High	
		×			×	Low
		×		×		Medium
		×	×			High
	×				×	Medium
	×			×		High
	×		×			High
×					×	Medium
×				×		High
×			×			High

[a] Biomass crystallinity.

Table IV-7. Structural features and carbohydrate contents of selected model lignocelluloses

Digestibility	Sample	Structural features (%)			Carbohydrate contents (%)	
		Lignin content	Acetyl content	CrI_B[a]	Glucan	Xylan
Low	DL02-DA035-DC0	19.5	2.9	59.4	48.7	15.3
Medium	DL50-DA035-DC0	1.5	2.2	64.6	57	17.6
High	DL10-DA000-DC6	6.1	2.7	17.5	71.7	14.4

[a] Biomass crystallinity.

Effect of Enzyme Loading

Figure IV-16 illustrates the effect of enzyme loading on the initial hydrolysis rate of biomass samples with different digestibilities. Increasing the enzyme loading from 1 to 12 FPU/g dry biomass tremendously accelerated the initial glucan hydrolysis rate (i.e., from 11.1% to 58.3%) of high-digestibility biomass with low lignin content (i.e., 6.1%) and low biomass crystallinity (i.e., 17.5%). When the enzyme loading was raised from 1 to 30 FPU/g dry biomass, the initial glucan hydrolysis rate only increased to 30% and 10% for the medium- and low-digestibility biomass, respectively. An increase in enzyme loading did not accelerate the initial xylan hydrolysis rate (i.e., from 8.2% to 27.0%) of high-digestibility biomass as much as glucan; however, the initial xylan hydrolysis rate of medium-digestibility biomass reached 37.2% with an enzyme loading of 30 FPU/g dry biomass. The initial xylan hydrolysis rate of low-digestibility biomass was not detected for enzyme loadings lower than 5 FPU/g dry biomass. Similar to glucan hydrolysis, the initial xylan hydrolysis rate of low-digestibility biomass was about 10% with an enzyme loading of 30 FPU/g dry biomass. This observation agrees well with Chang's (2000) conclusion that crystallinity had a more significant influence on the initial hydrolysis rate of glucan than on that of xylan.

Figure IV-17 demonstrates the effect of enzyme loading on the 6-h hydrolysis of biomass samples with different digestibilities. The glucan hydrolysis of high-digestibility biomass was nearly complete (i.e., 90%) at 12 FPU/g dry biomass. The glucan conversion of medium-digestibility biomass was increased 10 times (i. e., from

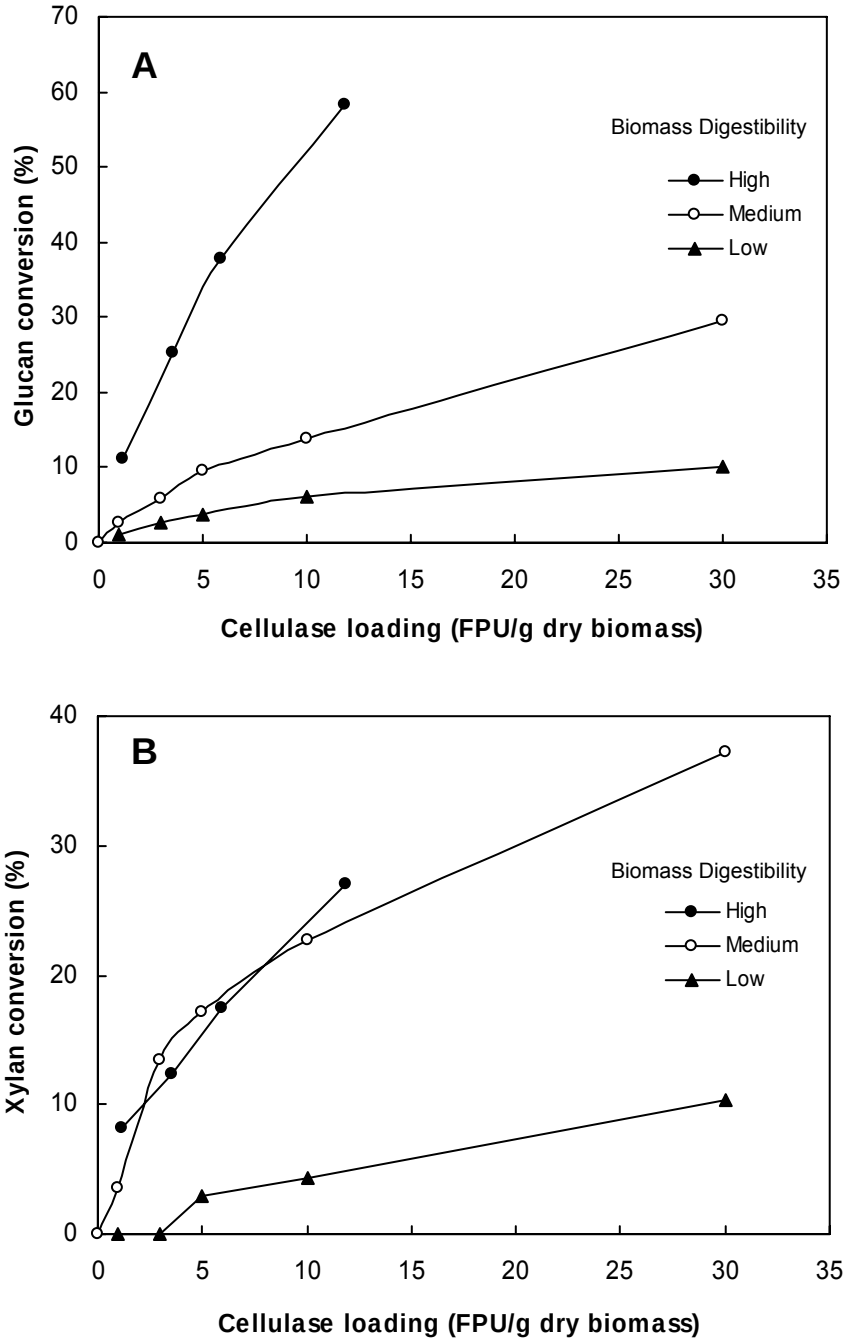

Figure IV-16. Enzyme loading studies at 1-h hydrolysis for poplar wood with various digestibilities: (A) glucose; (B) xylose. Hydrolysis conditions: 81.2 CBU/g dry biomass, substrate concentration: 10 g/L.

8.5% to 84.6%) by increasing enzyme loading from 1 to 60 FPU/g dry biomass. The glucan conversion of low-digestibility biomass was only 26% even with an enzyme loading of 50 FPU/g dry biomass. An increase of enzyme loading from 1 to 12 FPU/g dry biomass enhanced the 6-h xylan conversion of high-digestibility biomass from 46.6% to 82.8%. The xylan hydrolysis of medium-digestibility biomass with low lignin content (i.e., 1.5%) and high crystallinity (i.e., 64.6%) was nearly complete (i.e., 94%) with an enzyme loading of 60 FPU/g dry biomass, whereas xylan conversion was high even at low enzyme loading (i.e., 33.2% at 1 FPU/g dry biomass). Similar to glucan hydrolysis, the 6-h xylan conversion of low-digestibility biomass was 26% even at an enzyme loading of 50 FPU/g dry biomass.

Comparing the 6-h xylan conversion of medium-digestibility biomass to that of glucan, xylan conversion was much higher, especially at low enzyme loadings, i.e., glucan and xylan conversions were 8.5% and 33.2% at 1 FPU/ g dry biomass, respectively. The difference in xylan and glucan conversions became less significant as enzyme loading increased.

Because enzymatic degradation of biomass is relatively slow, the extent of biomass hydrolysis at longer incubation times (i.e., 72 h) is the target in most studies. Figure IV-18 presents the quantity of enzyme required for biomass samples with different digestibilities to attain complete hydrolysis at 72 h. An enzyme loading of 2 FPU/g dry biomass was sufficient for high-digestibility biomass to achieve nearly complete hydrolysis (i.e., 91.4% for glucan, 95.3% for xylan). An enzyme loading of 5 FPU/g dry biomass was required for medium-digestibility biomass to achieve nearly complete hydrolysis (i.e., 87.0% for glucan, 94% for xylan), further increasing enzyme loading to 30 FPU/g dry biomass did not notably improve glucan and xylan conversions (i.e., 88.8% for glucan, 95.5% for xylan). For the hydrolysis of low-digestibility biomass at 72 h, both glucan and xylan conversions were only around 50% with an enzyme loading of 50 FPU/g dry biomass. Figure IV-19 indicates that further increase in enzyme loading to 180 FPU/g dry biomass only enhanced the extents of glucan and xylan hydrolysis to 60%. Therefore, it is difficult to digest biomass with recalcitrant structural features by simply increasing enzyme loading.

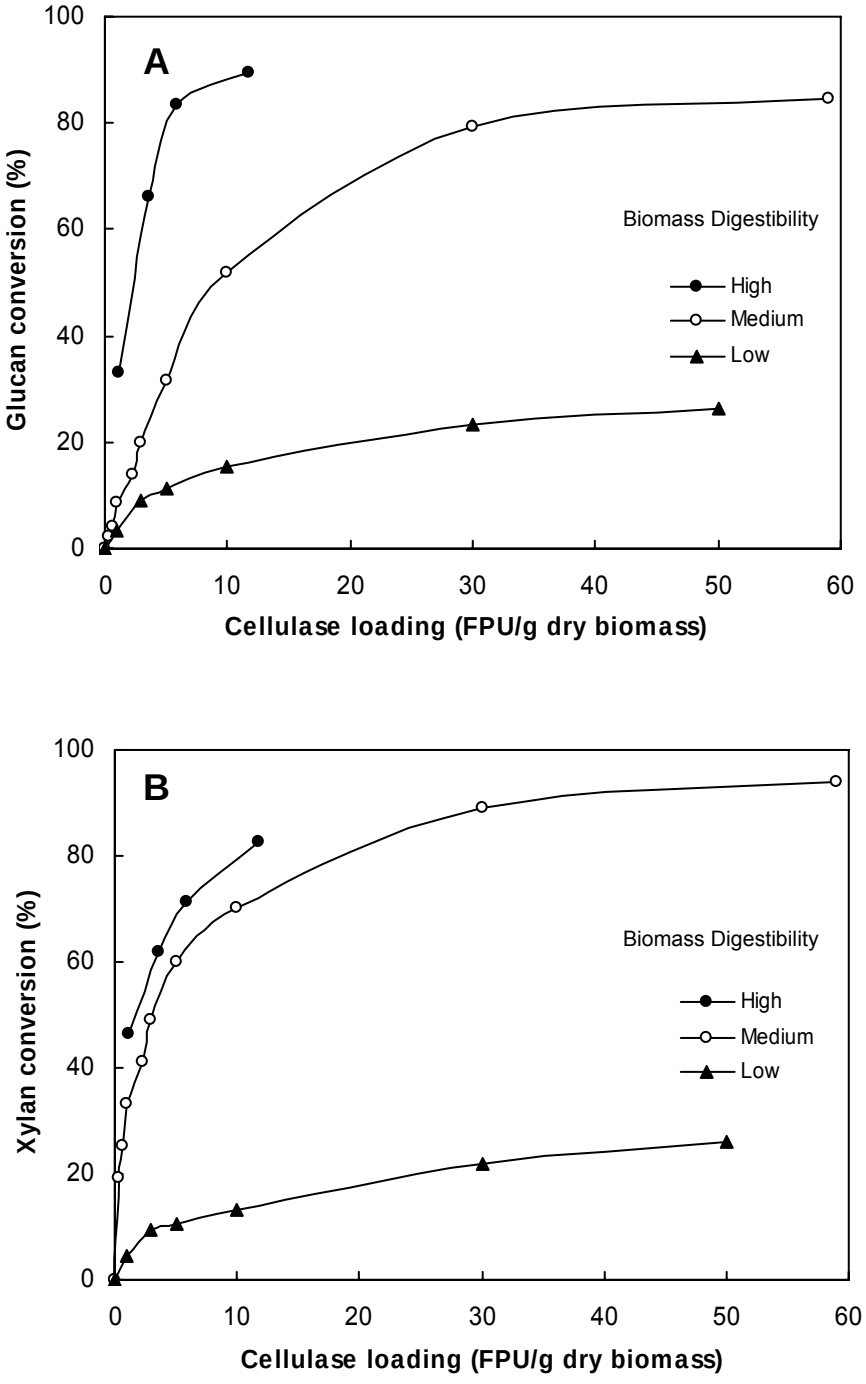

Figure IV-17. Enzyme loading studies at 6-h hydrolysis for poplar wood with various digestibilities: (A) glucose; (B) xylose. Hydrolysis conditions: 81.2 CBU/g dry biomass, substrate concentration: 10 g/L.

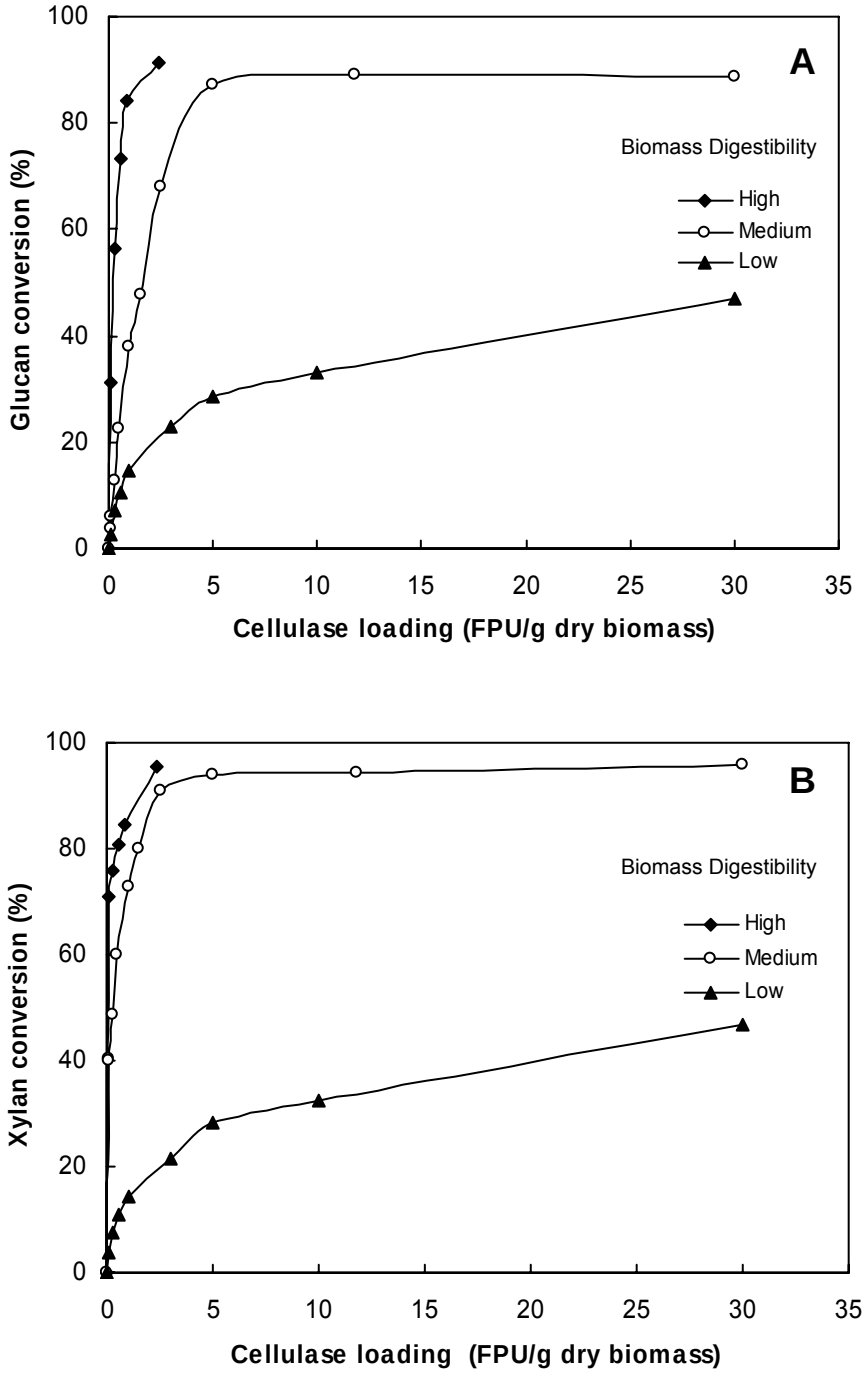

Figure IV-18. Enzyme loading studies at 72-h hydrolysis for poplar wood with various digestibilities: (A) glucose; (B) xylose. Hydrolysis conditions: 81.2 CBU/g dry biomass, substrate concentration: 10 g/L.

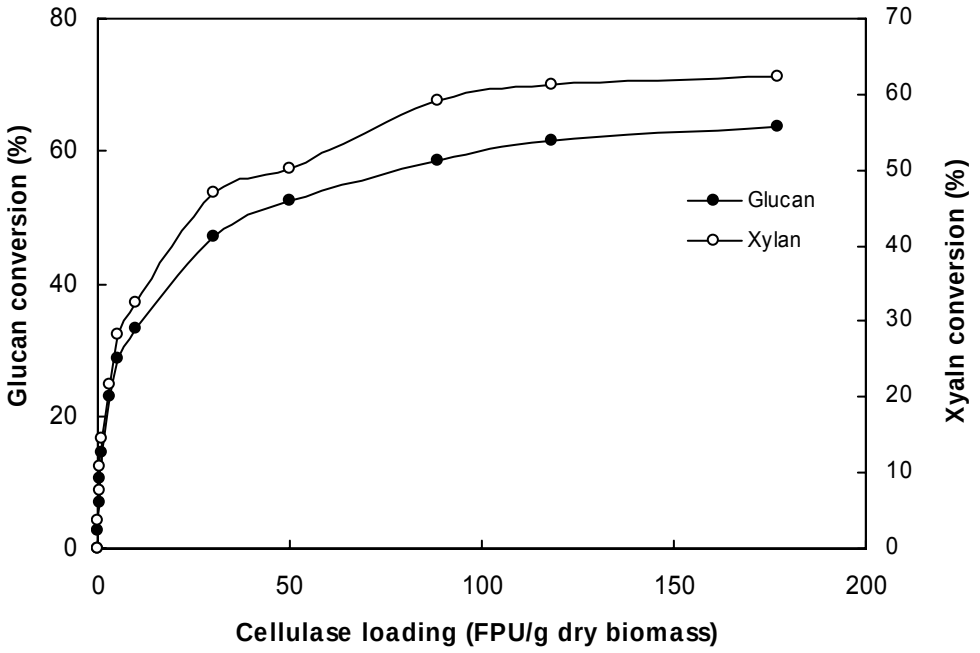

Figure IV-19. Enzyme loading studies at 72-h hydrolysis for low-digestibility poplar wood. Hydrolysis conditions: 81.2 CBU/g dry biomass, substrate concentration: 10 g/L.

For medium-digestibility biomass samples with low lignin content and high crystallinity, a remarkable difference in the ultimate extents of glucan and xylan hydrolyses at low enzyme loading was also observed. Xylan conversion reached 40% with an enzyme loading of 0.1 FPU/g dry biomass whereas glucan conversion was only 6%. The difference was insignificant at high enzyme loading (5 FPU/g dry biomass). It was interesting to note that 72-h xylan conversion of high-digestibility biomass sample attained 71% with an enzyme loading of 0.1 FPU/g dry biomass, whereas glucan conversion was only 31%. The ultimate extent of glucan and xylan hydrolyses were comparable as enzyme loading increased above 0.75 FPU/g dry biomass. Therefore, delignification shows a greater effect on xylan hydrolysis than on glucan hydrolysis at longer hydrolysis periods. The difference in xylan and glucan conversions can be overcome by increasing enzyme loading. Another reason to explain high xylan conversion with low enzyme loading is the xylanase activity present in cellobiase employed in hydrolysis (Lu et al.,

2002). Because the quantity of cellobiase added in each cellulase loading was constant, the xylanase activity in cellobiase may become dominant at low cellulase loading.

Validity of Simplified HCH-1 Model

To verify the simplified HCH-1 model (Equation I-3), the 1-, 6-, and 72-h sugar conversions (glucose, xylose, or total sugar) were plotted against the natural logarithm of cellulase loadings. The medium-digestibility biomass was hydrolyzed with a wide range of cellulase loadings and was employed to determine the range of sugar conversion valid for the simplified HCH-1 model. Figure IV-20 illustrates that the 1-, 6-, and 72-h glucan, xylan, and total sugar conversions are proportional to the natural logarithm of cellulase loadings from 10–15% to about 90% sugar conversion. For glucan hydrolysis at 6 and 72 h, the plots of conversion lower than 10% or higher than 90% versus the natural logarithm of cellulase loadings also gave nearly straight lines. However, the slopes of these two "straight" lines were small, indicating that the change in cellulase loading does not significantly influence digestibility. Figure IV-20 (D) is divided into three linear regions; the valid region for the simplified HCH-1 model is more attractive, because the large slope indicated that increasing enzyme loading greatly enhanced biomass digestibility. In contrast, the other two regions are not interesting due to low sugar conversions and inefficient enzyme utilization.

Figure IV-21 shows the linear relationships between the 1-, 6-, and 72-h glucan, xylan, and total sugar conversions and the natural logarithm of cellulase loadings in the range of 30% to 90% sugar conversion, indicating that the simplified HCH-1 model is also valid for high-digestibility biomass sample. The region of low conversion shown in Figure IV-20 (D) was not observed due to the high biomass digestibility. Extremely low enzyme loadings were required for high-digestibility biomass to attain 72-h sugar conversion below 10%. The relatively narrow linear range of 72-h xylan conversions (i.e., 40–90% for medium-digestibility biomass, 70–90% for high-digestibility biomass) that was valid for the simplified HCH-1 model could be attributed to the significant effect of delignification on xylan hydrolysis at long hydrolysis periods.

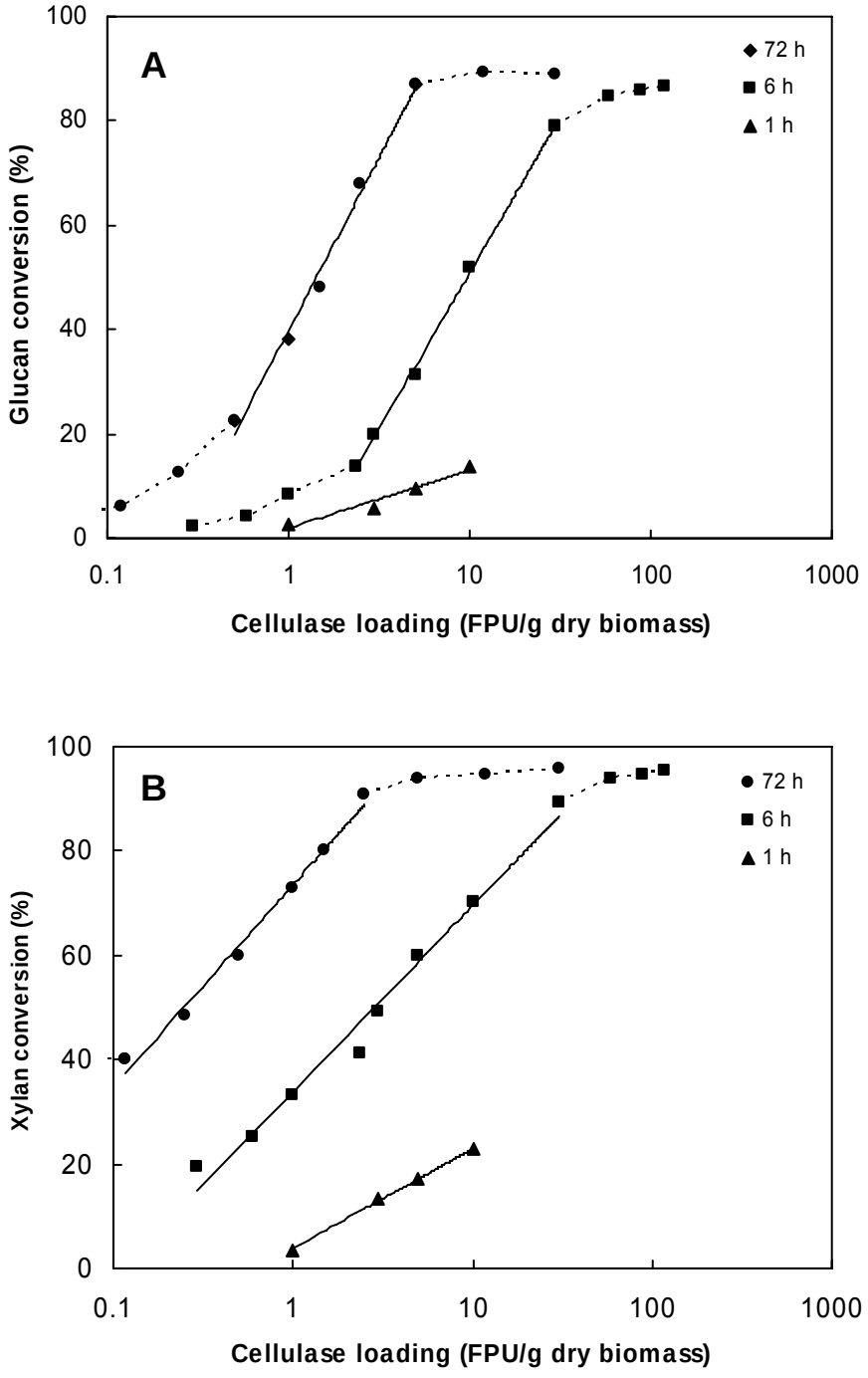

Figure IV-20. Sugar yields of medium-digestibility poplar wood: (A) glucose; (B) xylose; (C) total sugar; (D) Glucose at 72 h**.** Hydrolysis conditions: 81.2 CBU/g dry biomass, substrate concentration: 10 g/L.

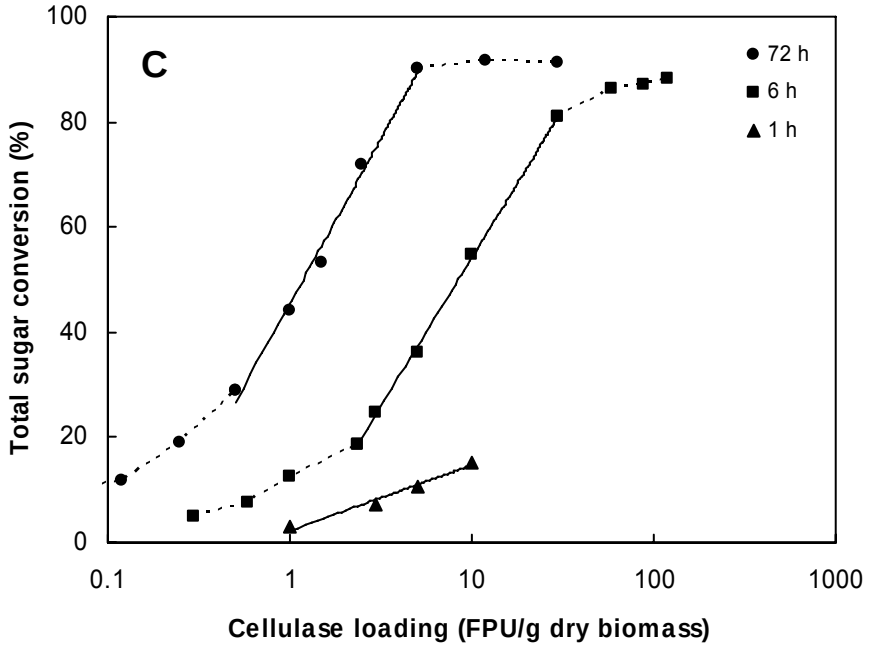

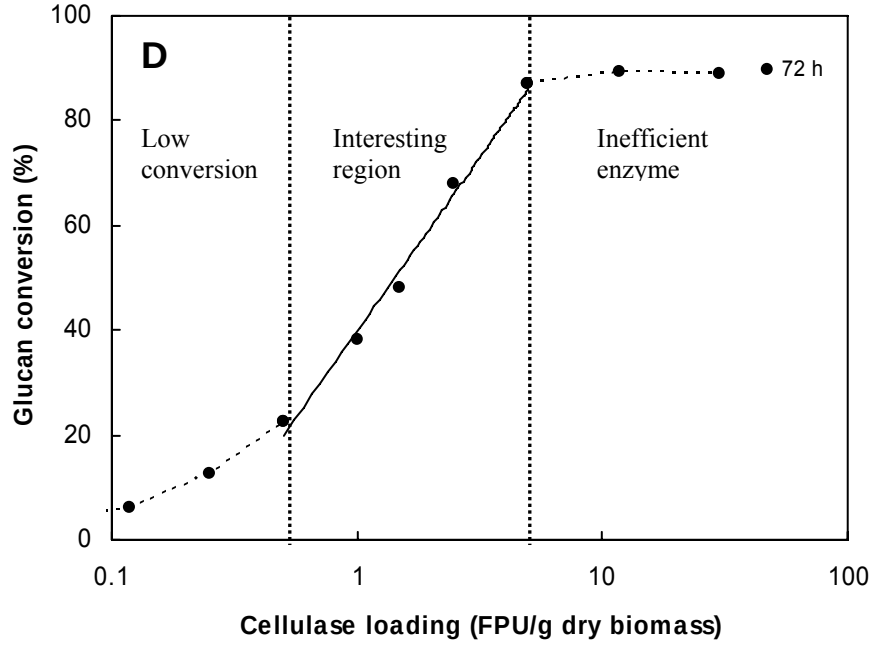

Figure IV-20. Continued.

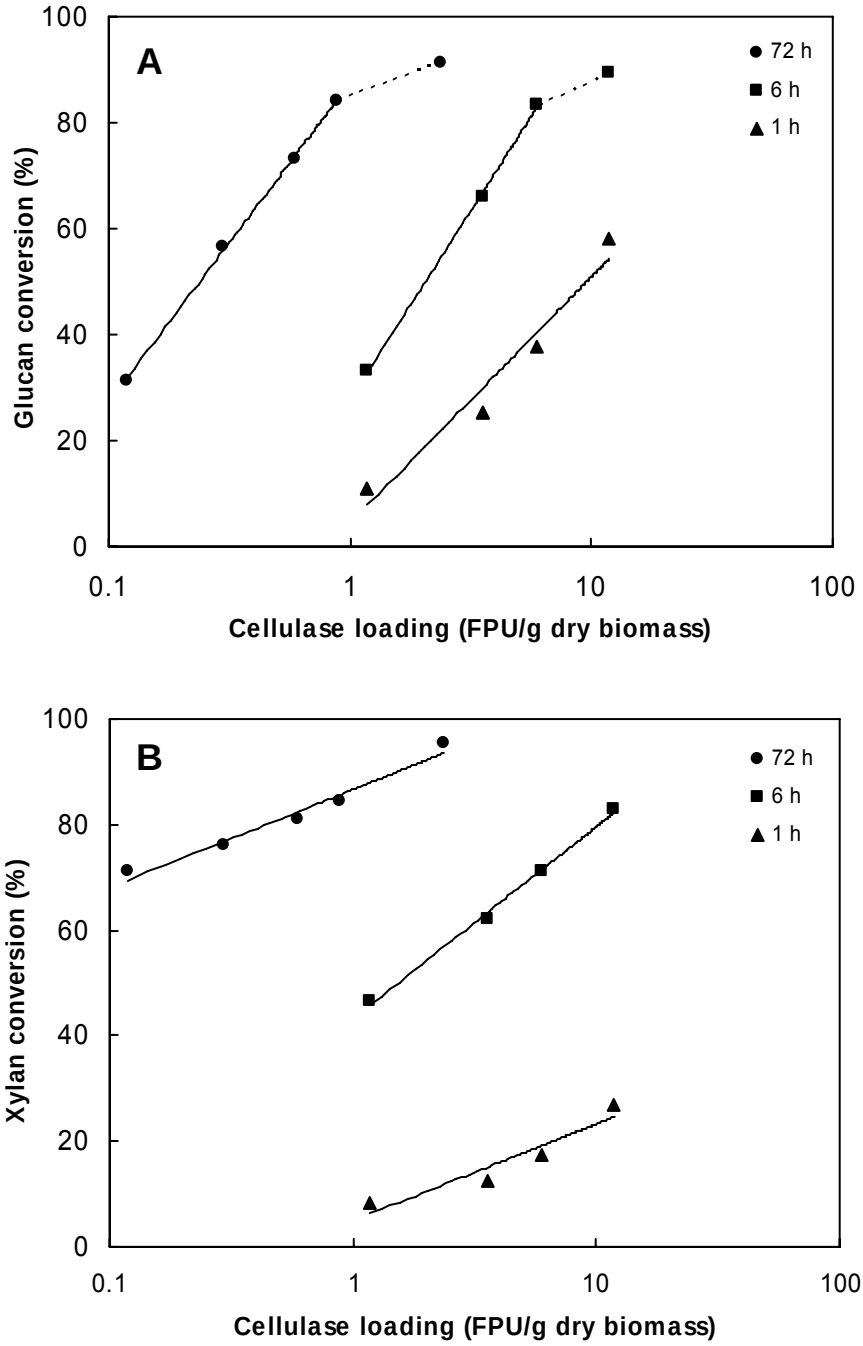

Figure IV-21. Sugar yields of high-digestibility poplar wood: (A) glucose; (B) xylose; (C) total sugar. Hydrolysis conditions: 81.2 CBU/g dry biomass, substrate concentration: 10 g/L.

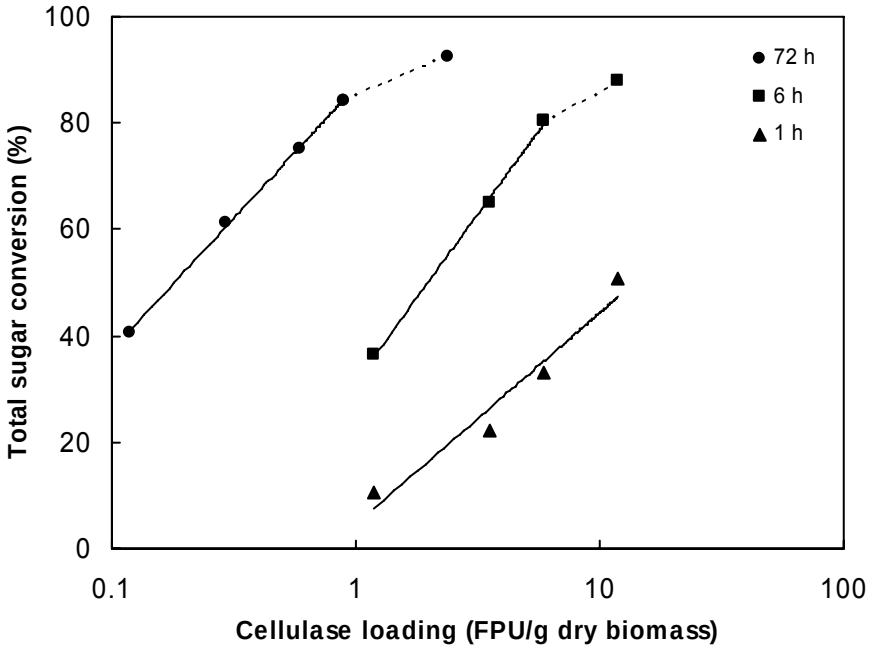

Figure IV-21. Continued

Figure IV-22 indicates that the simplified HCH-1 model is valid for the 1-, 6-, and 72-h sugar conversions of low-digestibility biomass samples. In contrast to high-digestibility biomass samples, the so called "inefficient region" in Figure IV-20 (D) was not observed due to the recalcitrant structural features; however, the enzyme utilization was really inefficient because sugar conversion was only 60% with an enzyme loading of 180 FPU/g dry biomass. It seemed impossible to achieve sugar conversion of 90% for low-digestibility biomass samples, because increasing enzyme loading from 88 to 180 FPU/g dry biomass only slightly improved sugar conversions (i.e., from 58.6 to 68.3%).

It should be noted that the correlation of 1-h sugar conversions with the natural logarithm of cellulase loadings were not as good as those at 6 and 72 h regardless of biomass digestibility. The enzyme loading required for the 1-h sugar conversions in the range of 10–90% was pretty high and negative intercepts were obtained.

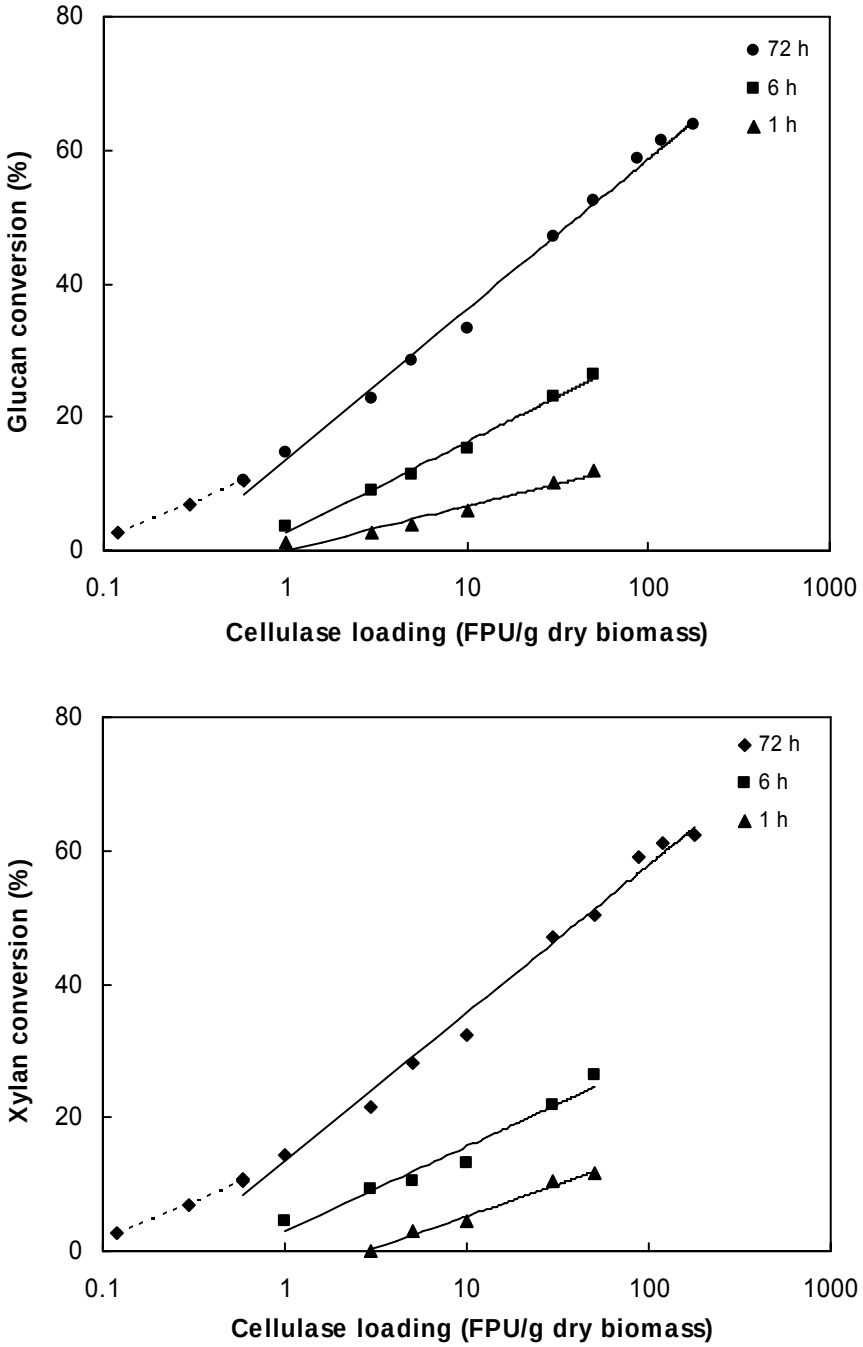

Figure IV-22. Sugar yields of low-digestibility poplar wood: (A) glucose; (B) xylose; (C) total sugar. Hydrolysis conditions: 81.2 CBU/g dry biomass, substrate concentration: 10 g/L.

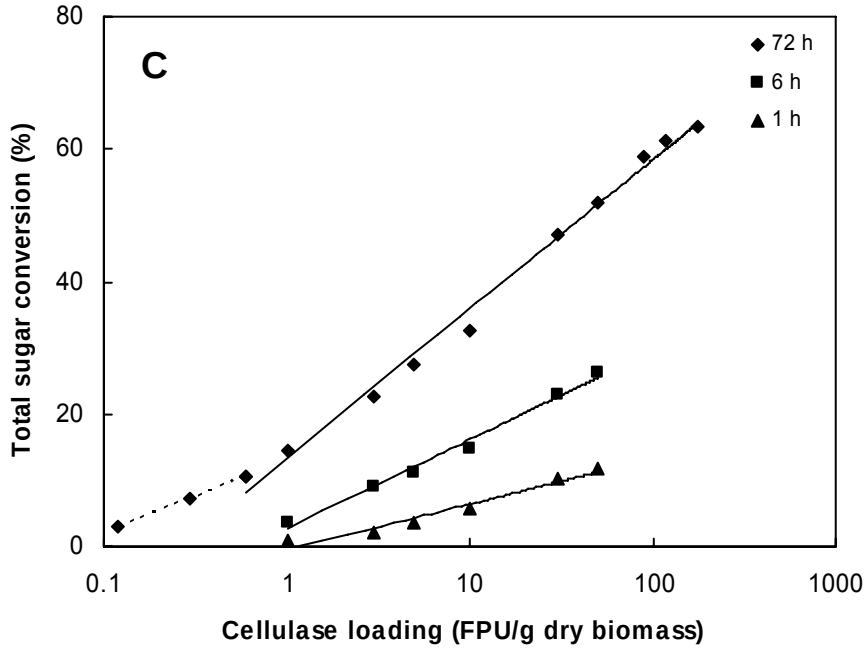

Figure IV-22. Continued.

Based on enzyme loading studies, Table IV-8 summarizes enzyme loadings employed at 1-, 6-, and 72-h hydrolysis for biomass samples with various digestibilities. Sugar conversions at the suggested enzyme loading were normally in the range of 15% to 90%, where the simplified HCH-1 model should be valid for describing the relationship of enzyme loading and digestibility. Therefore, carbohydrate conversions at a given time versus the natural logarithm of cellulase loadings were plotted to obtain the slopes and intercepts of the straight line. Mathematical models can be developed to correlate the slopes and intercepts with lignin content, acetyl content, and crystallinity.

Table IV-8. Summary of enyzme loading for biomass samples with various digestibilities

Digestibility	Enzyme loading for various incubation periods (FPU/g dry biomass)		
	1 h	6 h	72 h
High	1, 3, 10	1, 3, 10	0.25, 0.75, 2
Medium	1, 3, 10	1, 3, 10	0.5, 1.5, 5
Low	1, 5, 30	1, 5, 30	1, 5, 30

Reproducibility of Enzymatic Hydrolysis

The reproducibility of enzymatic hydrolysis is very important to develop a reliable mathematical model based on sugar yields produced from biomass during enzymatic hydrolysis. Figure IV-23 shows sugar yields in enzymatic hydrolysis performed five times. Data are expressed as the mean value and 2 standard deviations are presented as the error bar. It can be concluded that the reproducibility of enzymatic hydrolysis was good.

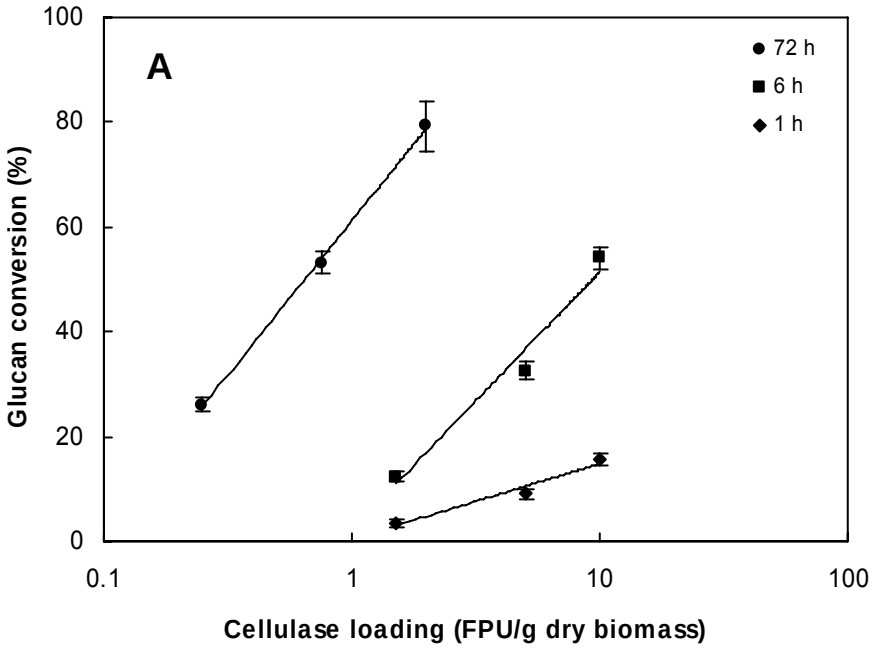

Figure IV-23. Sugar yields of poplar wood. (A) glucose; (B) xylose; (C) total sugar. Each point run five times, bar symbol represents 2 standard deviations. Hydrolysis conditions: 81.2 CBU/g dry biomass, substrate concentration: 10 g/L.

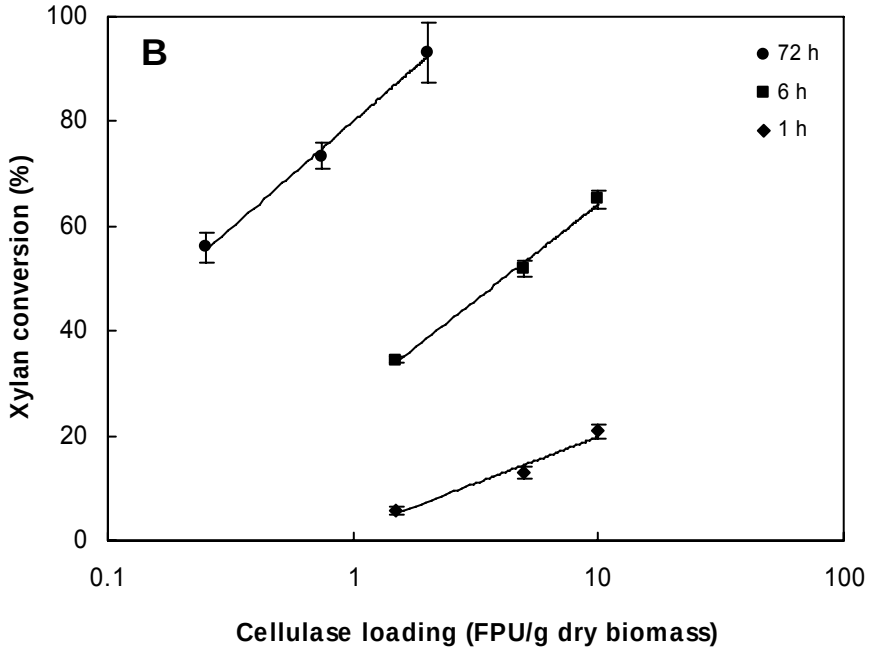

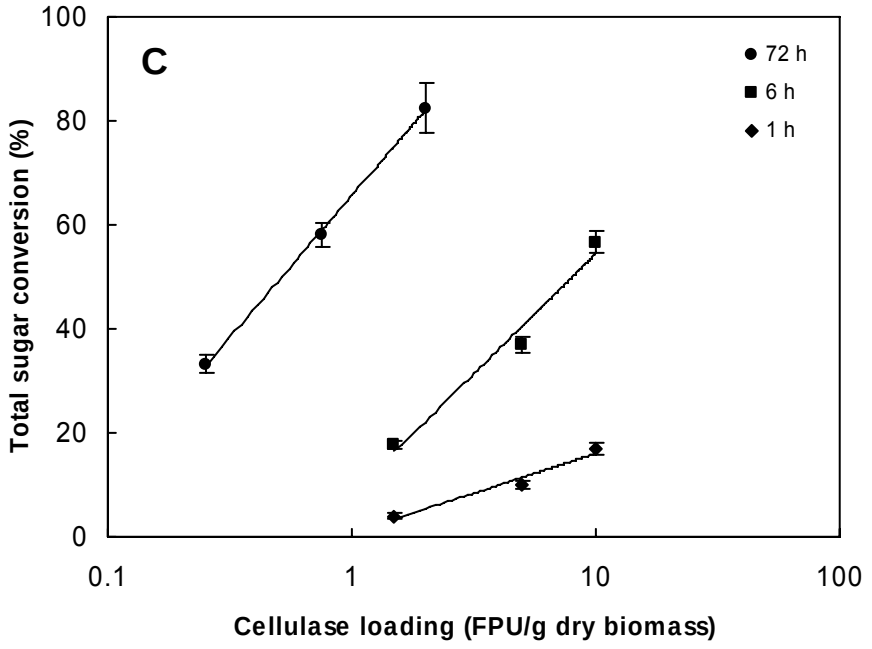

Figure IV-23. Continued.

Conclusions

The influence of increasing enzyme loading on biomass digestibility highly depends on structural features resulting from pretreatment. Decrystallization had a more significant influence on the initial rate of glucan hydrolysis than that of xylan hydrolysis. The benefit of delignification on xylan hydrolysis was more pronounced for long-term hydrolysis. Low enzyme loadings (i.e., 2 FPU/g dry biomass) are sufficient for high-digestibility biomass samples to achieve nearly complete hydrolysis at 72 h. The poor effect of pretreatment resulting in structural features recalcitrant to enzymatic hydrolysis, to some extent, can be overcome by increasing enzyme loading. The 1-, 6-, and 72-h glucan, xylan, and total sugar conversions were proportional to the natural logarithm of cellulase loadings from 10–15% to about 90% conversion, indicating the simplified HCH-1 model is valid for predicting enzymatic hydrolysis of lignocelluloses with various structural features. Sugar yields during enzymatic hydrolysis were consistent for developing a reliable mathematical model.

EFFECTS OF STRUCTURAL FEATURES ON SLOPES AND INTERCEPTS

It has been shown that structural features, such as, lignin content, acetyl content, and crystallinity have different extents of influence on the 1-, 6-, and 72-h digestibility. A simple version of the HCH-1 model describes the linear relationship between carbohydrate conversion and the natural logarithm of cellulase loading. The simplified HCH-1 model has been proven to be valid for determining 1-, 6-, and 72-h digestibilities of biomass samples with various structural features if the enzyme loading at a given hydrolysis time is properly chosen. In this study, the effect of structural features on the slopes and intercepts of the straight lines obtained by plotting sugar conversions versus the natural logarithm of cellulase loadings were investigated.

Materials and Methods

Poplar wood with a variety of lignin contents, acetyl contents, and crystallinities were prepared via selective delignification, selective deacetylation, and selective decrystallization. The pretreatment conditions are described in Chapter II. The hydrolysis conditions were as follows: temperature = 50°C, pH = 4.8, substrate concentration = 10 g/L, dry weight of biomass = 0.2 g, slurry volume = 20 mL, cellulase loading = 0.25–30 FPU/g dry biomass, cellobiase loading = 81.2 CBU/g dry biomass, rotating speed = 100 rpm, incubation period = 1, 6, and 72 h. Glucose and xylose concentrations were measured using HPLC. Glucose, xylose, and total sugar conversions were calculated using Equations II-4 to II-6. Detailed procedures for enzymatic hydrolysis and sugar analysis using HPLC are described in Appendices B and E, respectively. Glucan, xylan, and total sugar conversions at 1, 6, and 72 h versus the natural logarithm of cellulase loadings were plotted to obtain the slopes and intercepts of the resulting straight lines.

Results and Discussion

Tables IV-9 to IV-11 summarize the slopes, intercepts, and R^2 values of glucan, xylan, and total sugar hydrolysis of model lignocelluloses at 1, 6, and 72 h, respectively. In these tables, cellulose crystallinity (CrI_C) is employed in the correlations of slopes and intercepts with structural features. Cellulose crystallinity can be obtained by correlating biomass crystallinity (CrI_B) and hemicellulose content (O'Dwyer, 2005) as follows:

$$CrI_C = 1.097 \times CrI_B + 0.939 \times HC - 11.433 \quad \text{(IV-1)}$$

where CrI_C = cellulose crystallinity (%)

CrI_B = biomass crystallinity (%)

HC = hemicellulose content (%)

Biomass crystallinity was used in other studies. Slopes and intercepts of glucan, xylan, and total sugar hydrolyses vary with the changes in hydrolysis times and structural features. The slopes and intercepts provide insight on enzymatic hydrolysis, i.e., larger intercepts indicate that a relatively small amount of enzyme is required to achieve the desired sugar yields and larger slopes indicate that increasing enzyme loading is effective in enhancing digestibility. Similar to the study of the influences of structural features on digestibility, samples from the model lignocelluloses were divided into several groups due to the wide range and interrelation of structural features. Table IV-12 shows the range of structural features in each group. To eliminate interference from the other two structural features, samples in each group have various values of one structural feature but the other two structural features are kept constant, for example, samples in L1 group have contant acetyl content and biomass crystallinity, but a variety of lignin contents.

Effect of Lignin Content

Figures IV-24 and IV-25 illustrate the effect of lignin content on the 1-, 6-, and 72-h slopes and intercepts of total sugar hydrolysis. Because the 72-h intercept was relatively large compared to the other regression parameters, two y-axes with different scales were used to demonstrate the change in slopes and intercepts as the lignin content changed. Model samples in the L1 group have low acetyl content (i.e., 0.4–0.6%) and high biomass crystallinity (i.e., 66.2–68.8%). Decreasing lignin content from 24.5% to 14.8% substantially increased the 72-h intercept (i.e., from 9.7 to 52.2) and, to some extent, increased the 1-, 6-, and 72-h slopes and 1- and 6-h intercepts. Further decreasing the lignin content from 14.8% to 6.8%, there was no obvious increase in the 1-, 6- and 72-h slopes and intercepts. Model samples in the L2 group have high acetyl content (i.e., 2.4–2.6%) and low biomass crystallinity (i.e., 25–30%). Because the 72-h intercept of the high-lignin sample (i.e., 24%) was large (i.e., 46), the increase in 72-h intercept resulting from delignification was not as significant as that of model samples with high biomass crystallinity in the L1 group. Delignification from 23.9% to 13.4% fairly increased the 1-, 6-, and 72-h slopes and 6-h intercept. Further decreasing the lignin

Table IV-9. Regression parameters of glucan hydrolysis of model lignocelluloses determined by equation I-3

Sample	Lignin×0.1 (%)	Acetyl (%)	CrI_C[a]×0.1 (%)	Glucan×0.1 (%)	1 h			6 h			72 h		
					Slope	Intercept	R^2	Slope	Intercept	R^2	Slope	Intercept	R^2
DL00-DA000-DC0[L]	2.63	2.9	6.24	4.44	1.06	0.00	0.99	1.88	1.82	1.00	2.19	5.85	0.98
DL00-DA000-DC3[L]	2.63	2.9	3.39	4.44	8.85	3.25	0.99	9.41	15.47	0.99	6.45	35.74	0.99
DL00-DA000-DC6[L]	2.63	2.9	1.80	4.44	12.02	2.88	0.97	14.25	19.62	0.99	7.01	53.50	0.96
DL00-DA007-DC0[L]	2.55	2.8	6.51	4.66	0.93	0.44	1.00	1.77	1.46	0.99	2.75	5.21	0.99
DL00-DA007-DC3[L]	2.55	2.8	3.74	4.66	7.95	2.51	0.97	10.30	12.71	0.99	7.29	35.04	0.96
DL00-DA007-DC6[L]	2.55	2.8	2.45	4.66	11.00	2.67	0.98	12.53	16.50	0.99	6.20	45.50	0.98
DL00-DA015-DC0[L]	2.56	2.5	6.53	4.6	0.98	0.00	0.99	1.90	0.81	0.99	2.25	5.79	1.00
DL00-DA015-DC3[L]	2.56	2.5	3.21	4.6	8.88	2.76	0.98	9.79	14.90	0.99	5.70	36.74	0.99
DL00-DA015-DC6[M]	2.56	2.5	2.26	4.6	7.81	4.97	0.96	15.66	16.06	1.00	10.35	45.42	0.99
DL00-DA035-DC0[L]	2.55	1.9	6.41	4.7	1.06	0.57	0.96	1.74	2.44	0.99	2.78	6.29	0.99
DL00-DA035-DC3[L]	2.55	1.9	3.00	4.7	8.28	2.67	0.98	9.47	14.10	0.99	6.88	33.64	0.99
DL00-DA035-DC6[M]	2.55	1.9	2.48	4.7	10.06	3.56	0.97	13.30	16.02	0.99	10.65	40.97	0.99
DL00-DA055-DC0[L]	2.6	1.3	6.35	4.64	1.24	0.07	0.98	1.75	2.94	1.00	2.98	6.79	0.99
DL00-DA055-DC3[L]	2.6	1.3	2.68	4.64	13.45	3.21	0.98	13.37	21.08	0.97	6.43	52.03	0.98
DL00-DA055-DC6[M]	2.6	1.3	1.58	4.64	12.92	4.29	0.98	17.36	21.26	1.00	12.28	54.18	0.94
DL00-DA075-DC0[L]	2.6	0.9	6.83	4.75	1.43	0.76	0.99	2.68	2.52	0.99	4.43	7.19	0.99
DL00-DA075-DC3[L]	2.6	0.9	2.62	4.75	15.29	3.47	0.98	15.37	23.39	0.98	7.32	58.11	0.95
DL00-DA075-DC6[M]	2.6	0.9	1.33	4.75	14.30	5.11	0.98	17.91	23.21	0.99	8.72	59.26	0.99

Table IV-9. Continued

Sample	Lignin×0.1 (%)	Acetyl (%)	CrI_C×0.1 (%)	Glucan×0.1 (%)	1 h			6 h			72 h		
					Slope	Intercept	R^2	Slope	Intercept	R^2	Slope	Intercept	R^2
DL00-DA150-DC0 ^{L}	2.45	0.4	7.42	4.92	2.74	0.00	0.97	6.08	0.99	0.96	12.82	6.19	0.97
DL00-DA150-DC3 ^{M}	2.45	0.4	3.58	4.92	12.41	5.64	0.98	15.75	18.63	1.00	13.87	42.59	0.99
DL00-DA150-DC6 ^{M}	2.45	0.4	3.15	4.92	12.34	7.25	0.97	14.66	23.12	1.00	14.09	51.49	1.00
DL01-DA000-DC0 ^{L}	2.39	2.8	6.85	4.73	1.31	0.06	0.97	2.30	1.90	0.99	4.21	6.70	0.99
DL01-DA000-DC3 ^{M}	2.39	2.8	3.09	4.73	9.87	3.39	0.95	14.73	18.46	1.00	12.03	46.24	0.99
DL01-DA000-DC6 ^{H}	2.39	2.8	1.15	4.73	13.97	2.87	0.99	20.44	21.17	0.99	16.40	61.13	0.98
DL01-DA007-DC0 ^{L}	2.31	2.9	6.86	4.64	1.26	0.37	1.00	2.60	2.21	0.99	4.90	6.84	0.99
DL01-DA007-DC3 ^{M}	2.31	2.9	2.03	4.64	13.24	2.61	0.99	14.57	20.24	0.99	11.20	51.88	0.99
DL01-DA007-DC6 ^{M}	2.31	2.9	1.75	4.64	11.40	2.46	0.94	18.81	18.26	1.00	13.17	54.70	0.99
DL01-DA015-DC0 ^{L}	2.28	2.8	6.83	4.72	1.24	1.06	0.96	2.51	2.89	0.99	4.99	7.94	0.99
DL01-DA015-DC3 ^{L}	2.28	2.8	2.76	4.72	11.19	2.58	0.97	13.40	17.74	1.00	8.68	48.02	0.97
DL01-DA015-DC6 ^{M}	2.28	2.8	1.80	4.72	14.18	3.47	0.97	18.78	21.83	0.99	10.70	60.20	0.97
DL01-DA035-DC0 ^{L}	2.24	2.9	6.83	4.78	1.60	0.35	0.99	2.71	2.63	1.00	5.22	8.16	0.99
DL01-DA035-DC3 ^{M}	2.24	2.9	3.21	4.78	11.43	3.50	0.98	15.45	18.81	0.99	11.37	48.44	0.99
DL01-DA035-DC6 ^{M}	2.24	2.9	2.66	4.78	14.38	3.71	0.97	19.06	24.88	1.00	17.14	63.68	0.99
DL01-DA055-DC0 ^{L}	2.18	2.2	6.40	4.86	2.16	0.78	0.96	4.03	3.55	0.99	7.19	10.72	0.99
DL01-DA055-DC3 ^{M}	2.18	2.2	3.01	4.86	12.93	3.88	0.96	17.51	22.14	1.00	11.79	55.74	0.98
DL01-DA055-DC6 ^{H}	2.18	2.2	1.91	4.86	15.05	2.54	0.95	19.90	22.64	0.99	19.33	64.75	0.99

Table IV-9. Continued

Sample	Lignin×0.1 (%)	Acetyl (%)	CrI_C×0.1 (%)	Glucan×0.1 (%)	1 h			6 h			72 h		
					Slope	Intercept	R^2	Slope	Intercept	R^2	Slope	Intercept	R^2
DL01-DA075-DC0 ^{L}	2.13	1.7	6.94	4.89	2.55	1.31	1.00	5.51	5.03	0.98	8.36	15.72	0.99
DL01-DA075-DC3 ^{M}	2.13	1.7	2.58	4.89	13.62	6.09	0.98	18.95	23.43	1.00	13.93	58.08	0.99
DL01-DA075-DC6 ^{M}	2.13	1.7	2.16	4.89	17.02	4.56	0.97	21.28	28.11	1.00	13.81	65.82	0.94
DL01-DA150-DC0 ^{L}	1.78	0.4	7.84	5.49	4.89	0.83	0.96	14.97	4.72	0.97	19.11	32.60	0.99
DL01-DA150-DC3 ^{M}	1.78	0.4	3.40	5.49	19.30	7.15	0.96	20.96	33.75	1.00	19.53	68.95	0.98
DL01-DA150-DC6 ^{H}	1.78	0.4	2.36	5.49	20.80	7.08	0.98	24.26	34.36	0.99	19.95	79.83	0.99
DL02-DA000-DC0 ^{L}	2.15	2.9	6.75	4.75	1.87	0.81	0.98	3.55	3.52	0.99	7.40	10.05	0.98
DL02-DA000-DC3 ^{M}	2.15	2.9	2.33	4.75	13.16	5.65	0.94	20.57	22.29	0.99	13.00	59.72	0.96
DL02-DA000-DC6 ^{M}	2.15	2.9	2.00	4.75	15.64	2.01	0.97	20.83	23.61	1.00	7.80	45.47	0.99
DL02-DA007-DC0 ^{L}	2.11	3.1	6.75	4.84	1.95	0.62	0.96	3.96	3.45	0.98	8.10	7.46	0.99
DL02-DA007-DC3 ^{M}	2.11	3.1	2.84	4.84	7.53	6.27	0.99	19.18	20.05	1.00	12.71	57.01	0.98
DL02-DA007-DC6 ^{H}	2.11	3.1	1.69	4.84	16.88	2.58	0.96	22.94	25.25	0.99	18.44	69.96	0.99
DL02-DA015-DC0 ^{L}	2.09	3	6.76	4.8	2.04	1.65	0.97	4.57	4.11	0.97	8.89	11.92	0.99
DL02-DA015-DC3 ^{M}	2.09	3	3.29	4.8	11.46	4.80	0.98	16.83	20.53	0.99	10.82	55.73	0.99
DL02-DA015-DC6 ^{M}	2.09	3	3.29	4.8	13.25	3.31	0.96	20.60	19.33	1.00	7.64	67.44	0.98
DL02-DA035-DC0 ^{L}	1.95	2.9	6.81	4.87	2.64	0.61	0.96	5.79	3.00	0.99	9.06	15.15	0.98
DL02-DA035-DC3 ^{M}	1.95	2.9	3.20	4.87	14.39	3.00	0.96	20.14	20.96	1.00	16.25	56.49	0.95
DL02-DA035-DC6 ^{H}	1.95	2.9	2.71	4.87	14.28	4.04	0.98	21.68	20.85	0.99	18.99	64.98	0.99

Table IV-9. Continued

Sample	Lignin×0.1 (%)	Acetyl (%)	CrI_C×0.1 (%)	Glucan×0.1 (%)	1 h			6 h			72 h		
					Slope	Intercept	R^2	Slope	Intercept	R^2	Slope	Intercept	R^2
DL02-DA055-DC0 ^{L}	1.95	2.5	7.08	4.92	3.55	1.29	0.96	7.47	6.04	0.99	10.85	20.65	1.00
DL02-DA055-DC3 ^{M}	1.95	2.5	3.07	4.92	12.59	5.53	0.96	19.72	21.74	0.99	12.28	61.57	0.99
DL02-DA055-DC6 ^{M}	1.95	2.5	2.83	4.92	15.63	3.13	0.97	20.99	24.66	1.00	12.54	65.31	0.95
DL02-DA075-DC0 ^{L}	1.84	1.7	7.06	5.01	4.40	0.49	0.95	9.68	4.92	0.98	12.04	24.23	0.99
DL02-DA075-DC3 ^{M}	1.84	1.7	3.45	5.01	17.14	3.49	0.97	21.49	28.36	1.00	13.15	68.37	0.97
DL02-DA075-DC6 ^{H}	1.84	1.7	1.33	5.01	21.15	3.95	0.96	23.92	31.62	0.98	21.97	83.57	0.99
DL02-DA150-DC0 ^{M}	1.48	0.3	7.60	5.58	6.76	2.14	0.95	20.08	8.92	0.97	23.94	46.62	1.00
DL02-DA150-DC3 ^{H}	1.48	0.3	3.61	5.58	18.66	7.96	0.97	24.06	31.34	0.99	19.68	73.75	0.99
DL02-DA150-DC6 ^{H}	1.48	0.3	1.37	5.58	23.25	8.01	0.98	20.44	47.71	0.94	26.46	84.47	0.72
DL03-DA000-DC0 ^{L}	1.87	2.9	7.03	4.93	3.38	0.04	0.93	7.56	3.51	0.97	13.20	16.27	0.99
DL03-DA000-DC3 ^{M}	1.87	2.9	2.89	4.93	18.09	3.41	0.96	23.16	29.77	1.00	20.88	74.61	0.98
DL03-DA000-DC6 ^{H}	1.87	2.9	1.39	4.93	20.16	2.60	0.95	23.22	33.42	0.98	22.62	85.53	0.99
DL03-DA007-DC0 ^{L}	1.78	2.9	7.20	5.01	3.68	1.09	0.95	8.28	4.97	0.98	11.75	26.80	0.98
DL03-DA007-DC3 ^{M}	1.78	2.9	3.72	5.01	13.17	3.43	0.98	22.14	20.34	1.00	14.22	59.90	0.98
DL03-DA007-DC6 ^{M}	1.78	2.9	1.49	5.01	15.45	3.93	0.97	23.31	32.35	0.99	8.68	77.48	0.90
DL03-DA015-DC0 ^{L}	1.71	2.5	7.14	5	3.81	0.30	0.93	8.74	4.16	0.98	13.32	21.30	0.99
DL03-DA015-DC3 ^{M}	1.71	2.5	2.93	5	16.66	2.44	0.96	22.89	25.18	1.00	14.77	67.30	0.93
DL03-DA015-DC6 ^{H}	1.71	2.5	1.49	5	19.43	2.18	0.96	24.13	29.88	0.99	23.12	83.81	0.99

Table IV-9. Continued

Sample	Lignin×0.1 (%)	Acetyl (%)	CrI_C×0.1 (%)	Glucan×0.1 (%)	1 h			6 h			72 h		
					Slope	Intercept	R^2	Slope	Intercept	R^2	Slope	Intercept	R^2
DL03-DA035-DC0 ^{L}	1.63	2.8	7.15	5.05	4.69	0.84	0.96	11.36	5.55	0.99	13.09	30.92	0.99
DL03-DA035-DC3 ^{H}	1.63	2.8	3.06	5.05	13.99	5.82	0.97	24.77	24.06	0.99	18.70	69.96	0.98
DL03-DA035-DC6 ^{M}	1.63	2.8	1.92	5.05	20.66	2.08	0.95	23.63	32.79	0.99	20.65	79.17	0.99
DL03-DA055-DC0 ^{M}	1.62	2.6	7.26	5.12	4.20	1.11	0.99	12.71	5.13	0.99	14.29	32.54	0.99
DL03-DA055-DC3 ^{M}	1.62	2.6	2.84	5.12	18.05	3.26	0.96	23.78	28.43	1.00	20.74	74.62	1.00
DL03-DA055-DC6 ^{H}	1.62	2.6	1.68	5.12	21.80	2.97	0.96	27.86	34.00	0.99	24.37	90.70	0.99
DL03-DA075-DC0 ^{M}	1.47	2.3	7.32	5.31	4.72	1.30	0.94	16.32	6.28	0.97	18.91	40.34	0.99
DL03-DA075-DC3 ^{H}	1.47	2.3	3.01	5.31	15.62	6.24	0.97	25.02	29.64	0.99	21.78	76.95	0.99
DL03-DA075-DC6 ^{M}	1.47	2.3	2.64	5.31	20.28	3.69	0.95	23.31	31.78	0.98	20.11	77.23	1.00
DL03-DA150-DC0 ^{M}	1.06	0.4	7.73	5.96	7.66	1.46	0.94	22.84	8.16	0.97	21.56	50.12	0.99
DL03-DA150-DC3 ^{H}	1.06	0.4	4.11	5.96	20.05	5.80	0.96	22.93	34.92	0.99	21.61	76.96	0.94
DL03-DA150-DC6 ^{H}	1.06	0.4	3.21	5.96	22.01	6.04	0.97	28.35	33.58	0.99	24.33	87.84	0.96
DL05-DA000-DC0 ^{M}	1.39	2.9	6.69	5.18	3.71	1.08	0.95	14.32	4.97	0.97	20.80	36.62	1.00
DL05-DA000-DC3 ^{H}	1.39	2.9	2.48	5.18	18.47	4.05	0.96	26.06	26.01	0.99	16.12	73.23	1.00
DL05-DA000-DC6 ^{M}	1.39	2.9	1.44	5.18	22.14	3.70	0.96	22.67	37.41	0.94	20.23	82.99	0.96
DL05-DA007-DC0 ^{M}	1.34	2.8	7.05	5.35	3.04	1.29	0.96	11.27	5.16	0.96	17.05	32.98	0.99
DL05-DA007-DC3 ^{M}	1.34	2.8	3.19	5.35	17.57	2.56	0.96	24.29	26.89	1.00	22.41	76.43	0.99
DL05-DA007-DC6 ^{H}	1.34	2.8	3.05	5.35	19.62	2.28	0.96	24.95	26.94	0.99	26.37	83.31	0.95

Table IV-9. Continued

Sample	Lignin×0.1 (%)	Acetyl (%)	CrI_C×0.1 (%)	Glucan×0.1 (%)	1 h			6 h			72 h		
					Slope	Intercept	R^2	Slope	Intercept	R^2	Slope	Intercept	R^2
DL05-DA015-DC0 ^{M}	1.33	2.7	7.22	5.27	1.79	1.94	0.98	7.26	7.58	0.96	23.19	37.65	1.00
DL05-DA015-DC3 ^{H}	1.33	2.7	3.05	5.27	15.22	5.07	0.98	22.14	24.51	0.99	21.12	68.26	0.99
DL05-DA015-DC6 ^{H}	1.33	2.7	1.71	5.27	21.96	1.57	0.98	23.47	35.25	0.97	19.32	80.16	0.91
DL05-DA035-DC0 ^{M}	1.25	2.6	7.20	5.37	4.43	0.69	0.96	18.21	5.10	0.92	19.88	40.25	0.99
DL05-DA035-DC3 ^{M}	1.25	2.6	3.28	5.37	17.96	3.07	0.95	24.31	27.46	1.00	21.17	74.51	1.00
DL05-DA035-DC6 ^{H}	1.25	2.6	1.83	5.37	22.50	3.28	0.96	24.94	33.63	0.98	25.62	88.96	0.99
DL05-DA055-DC0 ^{M}	1.18	2.3	7.62	5.42	4.74	1.13	0.96	18.20	5.78	0.95	22.27	43.26	0.99
DL05-DA055-DC3 ^{H}	1.18	2.3	3.23	5.42	17.78	5.62	0.94	25.06	25.77	0.99	25.79	80.32	0.99
DL05-DA055-DC6 ^{H}	1.18	2.3	3.23	5.42	18.33	5.85	0.94	25.29	27.25	0.98	26.14	77.69	0.74
DL05-DA075-DC0 ^{M}	1.09	2.4	7.68	5.6	5.38	2.05	0.98	19.68	5.04	0.95	24.22	43.38	0.99
DL05-DA075-DC3 ^{H}	1.09	2.4	3.08	5.6	19.02	3.85	0.97	24.11	29.15	0.99	25.95	77.60	0.77
DL05-DA075-DC6 ^{H}	1.09	2.4	2.76	5.6	23.00	4.23	0.97	23.60	34.82	0.95	25.39	90.70	0.99
DL05-DA150-DC0 ^{M}	0.68	0.6	7.82	6.36	7.69	1.69	0.95	23.93	8.82	0.97	21.80	53.59	0.95
DL05-DA150-DC3 ^{H}	0.68	0.6	4.67	6.36	17.78	7.69	0.98	26.58	28.82	0.99	27.04	87.86	0.99
DL05-DA150-DC6 ^{H}	0.68	0.6	3.09	6.36	21.26	5.22	0.96	23.54	35.99	0.97	25.22	85.20	0.96
DL10-DA000-DC0 ^{M}	0.61	2.7	7.76	5.7	4.86	0.32	0.97	19.23	2.90	0.92	26.01	43.64	0.99
DL10-DA000-DC3 ^{H}	0.61	2.7	2.82	5.7	19.66	4.32	0.97	23.71	32.46	0.98	25.87	83.03	0.94
DL10-DA000-DC6 ^{H}	0.61	2.7	2.43	5.7	20.60	4.73	0.96	24.43	31.38	0.98	26.20	87.56	0.99

Table IV-9. Continued

Sample	Lignin×0.1 (%)	Acetyl (%)	CrI_C×0.1 (%)	Glucan×0.1 (%)	1 h			6 h			72 h		
					Slope	Intercept	R^2	Slope	Intercept	R^2	Slope	Intercept	R^2
DL10-DA007-DC0 ^{M}	0.6	3	7.66	5.87	4.45	0.99	0.94	21.18	3.75	0.94	24.67	46.43	0.98
DL10-DA007-DC3 ^{H}	0.6	3	3.66	5.87	17.34	4.52	0.95	27.21	22.87	0.99	25.71	76.38	0.98
DL10-DA007-DC6 ^{H}	0.6	3	2.10	5.87	21.11	3.05	0.97	23.71	35.62	0.97	27.74	92.53	1.00
DL10-DA015-DC0 ^{M}	0.59	2.7	7.71	5.92	4.99	1.67	0.99	19.51	6.05	0.96	27.55	45.95	0.99
DL10-DA015-DC3 ^{H}	0.59	2.7	3.98	5.92	17.44	3.01	0.96	24.96	26.01	1.00	22.86	74.35	0.97
DL10-DA015-DC6 ^{H}	0.59	2.7	2.34	5.92	21.93	2.57	0.95	24.20	32.22	0.98	26.68	88.57	0.99
DL10-DA035-DC0 ^{M}	0.56	2.7	7.69	5.87	4.56	1.18	0.93	20.05	5.05	0.94	24.61	47.39	0.99
DL10-DA035-DC3 ^{H}	0.56	2.7	3.94	5.87	16.81	5.81	0.96	26.94	25.59	0.99	23.03	78.56	0.99
DL10-DA035-DC6 ^{H}	0.56	2.7	2.07	5.87	21.04	3.24	0.97	23.74	34.62	0.98	20.62	79.83	0.93
DL10-DA055-DC0 ^{M}	0.45	2.5	7.92	6.09	5.82	0.78	0.92	22.43	5.08	0.93	25.73	49.04	0.99
DL10-DA055-DC3 ^{H}	0.45	2.5	3.95	6.09	17.54	3.69	0.97	24.21	26.26	1.00	33.41	69.30	0.91
DL10-DA055-DC6 ^{H}	0.45	2.5	3.49	6.09	19.32	3.49	0.97	25.30	26.63	0.99	25.75	81.48	0.95
DL10-DA075-DC0 ^{M}	0.41	2.1	7.82	6.1	5.09	1.00	0.94	21.22	5.06	0.94	23.30	47.47	0.98
DL10-DA075-DC3 ^{H}	0.41	2.1	3.27	6.1	18.20	6.20	0.95	26.54	28.45	0.99	24.07	77.75	0.98
DL10-DA075-DC6 ^{H}	0.41	2.1	2.74	6.1	19.42	4.20	0.97	25.30	29.71	0.99	19.74	80.39	0.94
DL10-DA150-DC0 ^{H}	0.25	0.4	7.26	7.04	8.46	3.44	0.97	26.54	10.20	0.95	29.18	65.62	0.99
DL10-DA150-DC3 ^{H}	0.25	0.4	2.84	7.04	18.42	4.13	0.96	25.27	28.30	0.99	27.65	86.88	0.99
DL10-DA150-DC6 ^{H}	0.25	0.4	2.52	7.04	20.81	4.77	0.97	29.95	30.15	0.99	30.32	89.26	0.99

Table IV-9. Continued

Sample	Lignin×0.1 (%)	Acetyl (%)	CrI_C×0.1 (%)	Glucan×0.1 (%)	1 h			6 h			72 h		
					Slope	Intercept	R^2	Slope	Intercept	R^2	Slope	Intercept	R^2
DL50-DA000-DC0 ^{M}	0.18	2.7	7.98	6.7	3.18	0.43	0.92	7.09	6.21	0.99	24.56	38.18	1.00
DL50-DA000-DC3 ^{H}	0.18	2.7	4.49	6.7	14.25	4.55	0.97	26.27	18.66	0.99	21.35	72.71	0.99
DL50-DA000-DC6 ^{H}	0.18	2.7	1.03	6.7	17.31	3.39	0.97	25.76	27.01	0.98	30.24	73.74	0.83
DL50-DA007-DC0 ^{M}	0.16	2.6	7.79	7.02	4.09	0.79	0.92	18.08	2.54	0.93	27.26	40.74	0.99
DL50-DA007-DC3 ^{H}	0.16	2.6	5.45	7.02	12.44	1.47	0.96	25.97	13.18	0.99	33.68	61.39	0.96
DL50-DA007-DC6 ^{H}	0.16	2.6	2.66	7.02	16.34	2.05	0.95	29.39	19.29	0.99	22.28	67.70	0.99
DL50-DA015-DC0 ^{M}	0.16	2.3	7.47	7.09	3.26	0.85	0.93	15.25	4.17	0.98	26.10	36.76	1.00
DL50-DA015-DC3 ^{H}	0.16	2.3	5.82	7.09	10.67	2.57	0.93	22.81	14.72	0.99	23.20	58.77	0.99
DL50-DA015-DC6 ^{H}	0.16	2.3	2.37	7.09	15.47	1.24	0.95	26.21	19.15	1.00	21.36	73.83	0.97
DL50-DA035-DC0 ^{M}	0.15	2.2	7.30	7.17	4.86	2.01	0.95	18.94	5.25	0.94	28.14	40.08	0.99
DL50-DA035-DC3 ^{H}	0.15	2.2	5.48	7.17	12.03	1.11	0.95	24.94	11.69	0.99	25.71	60.89	1.00
DL50-DA035-DC6 ^{H}	0.15	2.2	1.84	7.17	17.94	1.91	0.95	24.94	24.80	0.99	29.61	83.83	0.99
DL50-DA055-DC0 ^{M}	0.13	1.8	7.36	7.27	4.62	1.00	0.91	17.62	4.71	0.95	23.83	42.60	1.00
DL50-DA055-DC3 ^{H}	0.13	1.8	5.35	7.27	12.57	2.49	0.97	25.70	12.86	0.99	24.83	64.77	0.99
DL50-DA055-DC6 ^{H}	0.13	1.8	1.46	7.27	17.36	1.23	0.95	26.36	24.03	0.99	27.38	82.93	0.94
DL50-DA075-DC0 ^{M}	0.11	1.6	7.04	7.32	6.33	2.44	0.95	21.83	5.69	0.95	26.13	48.20	0.99
DL50-DA075-DC3 ^{H}	0.11	1.6	5.12	7.32	12.70	2.34	0.97	26.59	13.62	1.00	27.68	67.79	0.98
DL50-DA075-DC6 ^{H}	0.11	1.6	1.39	7.32	16.35	2.59	0.95	26.13	22.75	0.99	28.96	83.64	0.99

Table IV-9. Continued

Sample	Lignin×0.1 (%)	Acetyl (%)	CrI_C×0.1 (%)	Glucan×0.1 (%)	1 h			6 h			72 h		
					Slope	Intercept	R^2	Slope	Intercept	R^2	Slope	Intercept	R^2
DL50-DA150-DC0 [H]	0.07	0.1	7.52	7.65	8.97	1.95	0.94	25.57	10.82	0.97	27.65	60.39	0.99
DL50-DA150-DC3 [H]	0.07	0.1	5.86	7.65	15.75	2.34	0.97	30.13	12.78	0.98	24.36	71.77	0.99
DL50-DA150-DC6 [H]	0.07	0.1	3.90	7.65	16.45	2.66	0.96	26.24	22.38	1.00	32.01	71.02	0.93

[L] Low-digestibility; enzyme loading: 1, 5, and 30 FPU/g dry biomass for 1-, 6-, and 72-h incubation periods.

[M] Medium-digestibility; enzyme loading: 1, 3, and 10 FPU/g dry biomass for 1- and 6-h incubation periods; 0.5, 1.5, and 5 FPU/g dry biomass for 72-h incubation period.

[H] High-digestibility; enzyme loading: 1, 3, and 10 FPU/g dry biomass for 1- and 6-h incubation periods; 0.25, 0.75, and 2 FPU/g dry biomass for 72-h incubation period.

Table IV-10. Regression parameters of xylan hydrolysis of model lignocelluloses determined by equation I-3

Sample	Lignin×0.1 (%)	Acetyl (%)	CrI_C×0.1 (%)	Xylan×0.1 (%)	1 h			6 h			72 h		
					Slope	Intercept	R^2	Slope	Intercept	R^2	Slope	Intercept	R^2
DL00-DA000-DC0^{L}	2.63	2.9	6.24	1.39	---	---	---	---	---	---	1.49	3.26	0.95
DL00-DA000-DC3^{L}	2.63	2.9	3.39	1.39	5.82	-0.16	0.95	7.78	10.47	0.99	6.91	28.43	0.99
DL00-DA000-DC6^{L}	2.63	2.9	1.80	1.39	8.26	0.00	0.93	11.04	18.46	1.00	8.28	48.92	1.00
DL00-DA007-DC0^{L}	2.55	2.8	6.51	1.45	---	---	---	---	---	---	1.34	2.90	0.95
DL00-DA007-DC3^{L}	2.55	2.8	3.74	1.45	7.953	2.509	0.975	7.79	10.51	1.00	7.22	31.23	0.96
DL00-DA007-DC6^{L}	2.55	2.8	2.45	1.45	7.18	-0.41	0.94	10.26	11.89	0.99	7.52	36.50	1.00
DL00-DA015-DC0^{L}	2.56	2.5	6.53	1.42	---	---	---	---	---	---	---	---	---
DL00-DA015-DC3^{L}	2.56	2.5	3.21	1.42	6.07	-0.08	0.94	8.22	11.10	0.99	6.48	29.48	0.99
DL00-DA015-DC6^{M}	2.56	2.5	2.26	1.42	6.25	2.67	0.99	9.19	24.71	0.98	8.12	45.16	1.00
DL00-DA035-DC0^{L}	2.55	1.9	6.41	1.47	---	---	---	---	---	---	1.26	4.94	0.94
DL00-DA035-DC3^{L}	2.55	1.9	3.00	1.47	5.69	0.88	0.92	8.48	11.11	1.00	6.73	28.59	1.00
DL00-DA035-DC6^{M}	2.55	1.9	2.48	1.47	5.80	1.28	0.94	10.67	13.62	0.99	11.54	34.94	0.99
DL00-DA055-DC0^{L}	2.6	1.3	6.35	1.44	---	---	---	2.04	2.65	1.00	2.63	4.97	1.00
DL00-DA055-DC3^{L}	2.6	1.3	2.68	1.44	10.31	-0.38	0.93	11.80	19.71	0.99	7.71	49.22	0.99
DL00-DA055-DC6^{M}	2.6	1.3	1.58	1.44	8.36	4.14	0.94	10.52	33.17	0.99	13.40	52.15	0.98
DL00-DA075-DC0^{L}	2.6	0.9	6.83	1.48	1.95	0.29	0.98	2.21	4.67	0.99	3.11	8.40	0.99
DL00-DA075-DC3^{L}	2.6	0.9	2.62	1.48	11.96	1.10	0.92	12.82	28.25	1.00	8.45	59.68	0.98
DL00-DA075-DC6^{M}	2.6	0.9	1.33	1.48	8.18	3.28	0.95	15.02	25.38	0.99	9.35	61.39	0.99

Table IV-10. Continued

Sample	Lignin×0.1 (%)	Acetyl (%)	CrI_C×0.1 (%)	Xylan×0.1 (%)	1 h			6 h			72 h		
					Slope	Intercept	R^2	Slope	Intercept	R^2	Slope	Intercept	R^2
DL00-DA150-DC0 ^{L}	2.45	0.4	7.42	1.38	8.86	0.00	0.94	11.71	9.36	0.98	14.31	21.73	0.98
DL00-DA150-DC3 ^{M}	2.45	0.4	3.58	1.38	9.53	6.00	0.93	15.93	34.67	0.99	12.15	66.17	0.99
DL00-DA150-DC6 ^{M}	2.45	0.4	3.15	1.38	9.24	6.74	0.94	8.64	50.19	0.85	8.70	75.10	0.87
DL01-DA000-DC0 ^{L}	2.39	2.8	6.85	1.48	---	---	---	1.53	2.81	0.99	3.36	6.41	0.99
DL01-DA000-DC3 ^{M}	2.39	2.8	3.09	1.48	6.48	2.51	0.84	9.04	27.07	0.80	13.31	45.43	1.00
DL01-DA000-DC6 ^{H}	2.39	2.8	1.15	1.48	7.58	1.43	0.94	17.49	20.24	0.99	13.75	62.62	1.00
DL01-DA007-DC0 ^{L}	2.31	2.9	6.86	1.46	---	---	---	2.62	0.26	0.99	3.57	5.82	0.99
DL01-DA007-DC3 ^{M}	2.31	2.9	2.03	1.46	10.18	-1.58	0.92	13.83	17.50	0.99	10.36	53.26	0.99
DL01-DA007-DC6 ^{M}	2.31	2.9	1.75	1.46	6.97	2.28	0.86	6.97	27.21	0.87	11.63	58.74	0.95
DL01-DA015-DC0 ^{L}	2.28	2.8	6.83	1.5	---	---	---	1.75	3.02	0.99	3.94	5.93	0.99
DL01-DA015-DC3 ^{L}	2.28	2.8	2.76	1.5	8.36	0.27	0.90	12.09	17.11	0.99	9.75	46.47	0.98
DL01-DA015-DC6 ^{M}	2.28	2.8	1.80	1.5	7.69	1.31	0.96	16.37	19.77	0.99	11.69	59.65	0.99
DL01-DA035-DC0 ^{L}	2.24	2.9	6.83	1.48	---	---	---	1.20	2.91	0.98	3.48	7.46	1.00
DL01-DA035-DC3 ^{M}	2.24	2.9	3.21	1.48	6.89	1.01	0.94	14.74	17.18	0.99	11.84	48.27	0.99
DL01-DA035-DC6 ^{M}	2.24	2.9	2.66	1.48	8.68	3.36	0.93	15.19	32.57	0.96	11.19	68.32	0.95
DL01-DA055-DC0 ^{L}	2.18	2.2	6.40	1.52	2.41	-0.17	0.99	3.87	3.74	0.99	6.38	9.48	0.99
DL01-DA055-DC3 ^{M}	2.18	2.2	3.01	1.52	7.52	2.55	0.92	14.92	24.42	1.00	12.82	57.58	1.00
DL01-DA055-DC6 ^{H}	2.18	2.2	1.91	1.52	7.20	1.00	0.93	17.62	20.91	0.99	12.79	62.65	0.99

Table IV-10. Continued

Sample	Lignin×0.1 (%)	Acetyl (%)	CrI_C×0.1 (%)	Xylan×0.1 (%)	1 h			6 h			72 h		
					Slope	Intercept	R^2	Slope	Intercept	R^2	Slope	Intercept	R^2
DL01-DA075-DC0 ^{L}	2.13	1.7	6.94	1.5	2.77	0.13	1.00	5.16	7.10	0.99	7.08	17.53	1.00
DL01-DA075-DC3 ^{M}	2.13	1.7	2.58	1.5	7.51	3.96	0.97	15.34	28.78	0.99	10.74	65.00	0.99
DL01-DA075-DC6 ^{M}	2.13	1.7	2.16	1.5	9.82	3.46	0.94	16.36	39.24	0.95	11.62	76.81	0.99
DL01-DA150-DC0 ^{L}	1.78	0.4	7.84	1.53	6.99	2.38	0.98	17.87	19.00	0.99	15.53	59.41	0.99
DL01-DA150-DC3 ^{M}	1.78	0.4	3.40	1.53	10.20	5.79	0.82	15.43	49.71	0.95	12.91	86.12	1.00
DL01-DA150-DC6 ^{H}	1.78	0.4	2.36	1.53	8.22	5.21	0.94	17.97	40.37	0.99	11.91	86.87	0.99
DL02-DA000-DC0 ^{L}	2.15	2.9	6.75	1.48	1.53	0.13	0.99	2.85	4.19	1.00	6.62	10.96	0.99
DL02-DA000-DC3 ^{M}	2.15	2.9	2.33	1.48	7.73	2.81	0.91	16.51	25.81	0.99	15.48	61.66	0.99
DL02-DA000-DC6 ^{M}	2.15	2.9	2.00	1.48	7.72	3.38	0.97	20.83	23.61	1.00	0.99	52.93	0.90
DL02-DA007-DC0 ^{L}	2.11	3.1	6.75	1.52	1.76	-0.16	0.99	3.42	3.52	0.97	7.84	7.46	0.99
DL02-DA007-DC3 ^{M}	2.11	3.1	2.84	1.52	5.54	1.66	0.99	17.74	21.53	0.99	10.79	64.44	0.96
DL02-DA007-DC6 ^{H}	2.11	3.1	1.69	1.52	8.25	1.04	0.94	19.70	26.53	0.99	14.66	74.78	0.99
DL02-DA015-DC0 ^{L}	2.09	3	6.76	1.52	2.02	0.00	1.00	3.49	4.98	0.92	8.52	10.02	1.00
DL02-DA015-DC3 ^{M}	2.09	3	3.29	1.52	6.50	1.94	0.92	14.46	21.24	0.99	9.52	60.70	0.99
DL02-DA015-DC6 ^{M}	2.09	3	3.29	1.52	7.47	2.26	0.89	15.17	28.02	0.95	12.13	66.27	0.98
DL02-DA035-DC0 ^{L}	1.95	2.9	6.81	1.53	---	---	---	6.50	2.97	0.95	8.84	15.96	0.99
DL02-DA035-DC3 ^{M}	1.95	2.9	3.20	1.53	7.58	2.44	0.87	14.48	29.35	0.93	12.36	67.19	0.99
DL02-DA035-DC6 ^{H}	1.95	2.9	2.71	1.53	8.65	0.83	0.96	18.56	24.35	0.99	11.62	66.96	0.99

Table IV-10. Continued

Sample	Lignin×0.1 (%)	Acetyl (%)	CrI_C×0.1 (%)	Xylan×0.1 (%)	1 h			6 h			72 h		
					Slope	Intercept	R^2	Slope	Intercept	R^2	Slope	Intercept	R^2
DL02-DA055-DC0 ^{L}	1.95	2.5	7.08	1.54	3.97	0.00	0.99	6.54	9.88	0.97	9.93	23.98	0.99
DL02-DA055-DC3 ^{M}	1.95	2.5	3.07	1.54	7.15	3.80	0.96	16.92	28.09	0.99	16.27	66.35	0.99
DL02-DA055-DC6 ^{M}	1.95	2.5	2.83	1.54	8.18	3.16	0.88	15.61	34.37	0.97	10.11	75.32	0.99
DL02-DA075-DC0 ^{L}	1.84	1.7	7.06	1.56	5.72	-1.10	0.97	9.47	9.30	0.98	11.62	29.05	0.99
DL02-DA075-DC3 ^{M}	1.84	1.7	3.45	1.56	7.90	2.69	0.95	18.45	30.39	1.00	13.54	74.00	0.99
DL02-DA075-DC6 ^{H}	1.84	1.7	1.33	1.56	8.89	3.41	0.92	20.78	33.88	0.99	12.49	84.56	0.99
DL02-DA150-DC0 ^{M}	1.48	0.3	7.60	1.55	6.48	4.32	0.96	18.35	27.83	0.99	17.99	71.73	0.99
DL02-DA150-DC3 ^{H}	1.48	0.3	3.61	1.55	8.64	6.69	0.93	15.58	43.70	0.99	13.84	87.25	0.97
DL02-DA150-DC6 ^{H}	1.48	0.3	1.37	1.55	7.72	5.64	0.96	16.57	43.93	1.00	12.43	89.03	0.75
DL03-DA000-DC0 ^{L}	1.87	2.9	7.03	1.55	4.48	-1.10	0.95	7.80	6.73	0.98	14.07	21.22	0.99
DL03-DA000-DC3 ^{M}	1.87	2.9	2.89	1.55	8.37	2.70	0.93	19.69	31.84	1.00	11.26	79.89	1.00
DL03-DA000-DC6 ^{H}	1.87	2.9	1.39	1.55	9.12	2.92	0.92	20.50	35.49	0.99	11.61	85.25	0.99
DL03-DA007-DC0 ^{L}	1.78	2.9	7.20	1.58	3.98	0.00	0.98	8.31	5.99	0.98	11.94	28.85	0.98
DL03-DA007-DC3 ^{M}	1.78	2.9	3.72	1.58	6.47	3.08	0.96	15.40	26.99	0.98	14.93	64.31	0.99
DL03-DA007-DC6 ^{M}	1.78	2.9	1.49	1.58	6.26	2.37	0.95	19.81	29.80	1.00	10.39	81.54	0.99
DL03-DA015-DC0 ^{L}	1.71	2.5	7.14	1.59	4.35	-1.06	0.95	8.78	5.65	0.98	14.42	24.82	0.99
DL03-DA015-DC3 ^{M}	1.71	2.5	2.93	1.59	7.71	1.37	0.94	19.43	26.20	1.00	13.81	74.27	0.98
DL03-DA015-DC6 ^{H}	1.71	2.5	1.49	1.59	8.39	1.88	0.95	20.13	30.87	1.00	11.12	83.44	0.99

Table IV-10. Continued

Sample	Lignin×0.1 (%)	Acetyl (%)	CrI_C×0.1 (%)	Xylan×0.1 (%)	1 h			6 h			72 h		
					Slope	Intercept	R^2	Slope	Intercept	R^2	Slope	Intercept	R^2
DL03-DA035-DC0 ^{L}	1.63	2.8	7.15	1.6	4.82	0.00	0.99	10.49	8.45	0.99	12.95	34.30	1.00
DL03-DA035-DC3 ^{H}	1.63	2.8	3.06	1.6	6.83	2.94	0.93	16.78	30.00	0.99	11.77	75.13	0.99
DL03-DA035-DC6 ^{M}	1.63	2.8	1.92	1.6	7.99	1.88	0.94	19.77	31.40	1.00	10.94	84.05	1.00
DL03-DA055-DC0 ^{M}	1.62	2.6	7.26	1.6	5.29	0.19	0.99	12.39	10.59	0.99	13.25	40.07	0.99
DL03-DA055-DC3 ^{M}	1.62	2.6	2.84	1.6	7.85	2.50	0.94	18.99	32.43	1.00	10.88	83.14	1.00
DL03-DA055-DC6 ^{H}	1.62	2.6	1.68	1.6	8.68	2.56	0.91	18.57	37.96	0.99	10.57	89.35	0.99
DL03-DA075-DC0 ^{M}	1.47	2.3	7.32	1.65	4.85	1.76	0.97	14.22	15.85	1.00	16.10	51.01	0.99
DL03-DA075-DC3 ^{H}	1.47	2.3	3.01	1.65	6.44	5.24	0.92	19.20	37.19	0.99	12.46	83.62	0.99
DL03-DA075-DC6 ^{M}	1.47	2.3	2.64	1.65	7.96	3.62	0.91	18.48	35.33	1.00	9.55	85.03	0.99
DL03-DA150-DC0 ^{M}	1.06	0.4	7.73	1.6	7.86	2.60	0.95	20.61	28.07	0.99	16.93	77.95	0.99
DL03-DA150-DC3 ^{H}	1.06	0.4	4.11	1.6	7.37	5.25	0.91	17.64	41.23	0.98	12.31	86.44	0.98
DL03-DA150-DC6 ^{H}	1.06	0.4	3.21	1.6	8.38	5.23	0.93	16.97	42.06	0.99	10.65	90.12	0.99
DL05-DA000-DC0 ^{M}	1.39	2.9	6.69	1.64	4.13	3.05	0.97	13.45	15.36	1.00	18.45	49.96	1.00
DL05-DA000-DC3 ^{H}	1.39	2.9	2.48	1.64	7.43	5.26	0.96	18.89	32.51	0.99	11.38	77.51	0.99
DL05-DA000-DC6 ^{M}	1.39	2.9	1.44	1.64	8.03	3.61	0.94	17.88	37.73	1.00	8.93	87.50	1.00
DL05-DA007-DC0 ^{M}	1.34	2.8	7.05	1.66	5.10	-0.02	1.00	13.08	9.89	0.99	15.80	44.87	0.99
DL05-DA007-DC3 ^{M}	1.34	2.8	3.19	1.66	7.41	2.70	0.93	18.32	33.86	1.00	11.70	85.96	1.00
DL05-DA007-DC6 ^{H}	1.34	2.8	3.05	1.66	8.76	2.54	0.94	18.98	35.16	0.99	11.84	86.67	0.99

Table IV-10. Continued

Sample	Lignin×0.1 (%)	Acetyl (%)	CrI_C×0.1 (%)	Xylan×0.1 (%)	1 h			6 h			72 h		
					Slope	Intercept	R^2	Slope	Intercept	R^2	Slope	Intercept	R^2
DL05-DA015-DC0 ^{M}	1.33	2.7	7.22	1.65	3.91	0.16	1.00	9.93	12.71	0.99	21.96	47.15	1.00
DL05-DA015-DC3 ^{H}	1.33	2.7	3.05	1.65	5.88	3.36	0.97	13.20	33.40	0.98	15.20	83.18	0.99
DL05-DA015-DC6 ^{H}	1.33	2.7	1.71	1.65	8.01	2.16	0.96	19.22	34.74	1.00	11.04	87.89	1.00
DL05-DA035-DC0 ^{M}	1.25	2.6	7.20	1.68	6.05	-0.36	0.99	13.92	18.40	0.99	16.09	57.19	0.99
DL05-DA035-DC3 ^{M}	1.25	2.6	3.28	1.68	7.88	2.15	0.93	18.96	32.98	1.00	10.50	83.89	1.00
DL05-DA035-DC6 ^{H}	1.25	2.6	1.83	1.68	8.53	2.61	0.93	18.81	37.53	1.00	10.01	88.06	0.99
DL05-DA055-DC0 ^{M}	1.18	2.3	7.62	1.67	4.54	2.41	0.98	12.66	24.28	0.95	17.44	59.22	0.99
DL05-DA055-DC3 ^{H}	1.18	2.3	3.23	1.67	8.40	4.09	0.94	16.88	38.46	0.99	9.84	85.73	0.99
DL05-DA055-DC6 ^{H}	1.18	2.3	3.23	1.67	7.40	3.38	0.91	19.54	32.31	1.00	10.89	84.85	0.73
DL05-DA075-DC0 ^{M}	1.09	2.4	7.68	1.7	6.02	2.80	0.98	16.60	22.61	0.99	16.36	64.89	0.99
DL05-DA075-DC3 ^{H}	1.09	2.4	3.08	1.7	7.85	2.97	0.94	18.16	35.66	1.00	13.85	84.59	0.92
DL05-DA075-DC6 ^{H}	1.09	2.4	2.76	1.7	8.70	4.17	0.94	16.82	41.96	0.99	8.87	89.89	0.99
DL05-DA150-DC0 ^{M}	0.68	0.6	7.82	1.63	5.69	4.40	0.97	19.37	24.96	1.00	15.96	72.33	0.93
DL05-DA150-DC3 ^{H}	0.68	0.6	2.85	1.63	6.73	7.69	0.96	17.53	41.46	0.97	13.32	89.01	0.99
DL05-DA150-DC6 ^{H}	0.68	0.6	3.09	1.63	7.76	4.87	0.92	16.47	41.63	1.00	11.91	86.71	0.98
DL10-DA000-DC0 ^{M}	0.61	2.7	7.76	1.76	6.76	3.68	0.91	16.01	29.71	0.98	12.62	77.33	0.99
DL10-DA000-DC3 ^{H}	0.61	2.7	2.82	1.76	7.76	4.97	0.93	15.75	43.10	1.00	10.14	88.26	1.00
DL10-DA000-DC6 ^{H}	0.61	2.7	2.43	1.76	8.26	5.11	0.92	15.77	43.26	0.99	9.26	86.79	0.99

Table IV-10. Continued

Sample	Lignin×0.1 (%)	Acetyl (%)	CrI_C×0.1 (%)	Xylan×0.1 (%)	1 h			6 h			72 h		
					Slope	Intercept	R^2	Slope	Intercept	R^2	Slope	Intercept	R^2
DL10-DA007-DC0 ^{M}	0.6	3	7.66	1.74	5.41	3.33	0.96	18.38	24.16	1.00	15.19	73.23	0.96
DL10-DA007-DC3 ^{H}	0.6	3	3.66	1.74	7.91	4.71	0.94	17.18	39.47	0.98	16.09	85.88	0.97
DL10-DA007-DC6 ^{H}	0.6	3	2.10	1.74	7.85	3.28	0.94	17.98	37.82	1.00	10.56	90.58	1.00
DL10-DA015-DC0 ^{M}	0.59	2.7	7.71	1.72	6.64	1.65	0.95	17.26	26.21	0.99	17.81	75.08	0.98
DL10-DA015-DC3 ^{H}	0.59	2.7	3.98	1.72	7.84	2.96	0.93	18.19	36.86	1.00	12.53	87.32	1.00
DL10-DA015-DC6 ^{H}	0.59	2.7	2.34	1.72	8.51	3.50	0.92	16.49	41.06	0.99	8.15	86.05	0.99
DL10-DA035-DC0 ^{M}	0.56	2.7	7.69	1.66	5.50	3.30	0.96	17.16	26.23	0.99	15.73	73.90	0.97
DL10-DA035-DC3 ^{H}	0.56	2.7	3.94	1.66	8.30	5.40	0.94	17.73	42.78	0.99	11.00	91.40	0.99
DL10-DA035-DC6 ^{H}	0.56	2.7	2.07	1.66	8.09	3.10	0.93	18.06	37.92	1.00	15.25	87.24	0.98
DL10-DA055-DC0 ^{M}	0.45	2.5	7.92	1.67	6.90	2.95	0.93	18.06	29.65	0.98	16.46	77.95	0.99
DL10-DA055-DC3 ^{H}	0.45	2.5	3.95	1.67	7.94	3.58	0.95	16.97	38.24	1.00	15.53	85.97	0.96
DL10-DA055-DC6 ^{H}	0.45	2.5	3.49	1.67	8.18	3.85	0.94	16.85	39.66	0.99	11.54	86.98	0.99
DL10-DA075-DC0 ^{M}	0.41	2.1	7.82	1.66	5.85	3.08	0.96	17.53	25.91	0.98	14.48	71.42	0.98
DL10-DA075-DC3 ^{H}	0.41	2.1	3.27	1.66	7.70	6.14	0.93	14.78	45.93	0.99	14.40	87.75	0.99
DL10-DA075-DC6 ^{H}	0.41	2.1	2.74	1.66	7.90	3.82	0.94	16.90	39.46	1.00	9.71	88.24	1.00
DL10-DA150-DC0 ^{H}	0.25	0.4	7.26	1.62	5.85	6.01	0.98	19.48	30.29	0.96	20.17	84.22	0.99
DL10-DA150-DC3 ^{H}	0.25	0.4	2.84	1.62	7.18	5.26	0.93	16.44	38.87	1.00	12.79	87.13	1.00
DL10-DA150-DC6 ^{H}	0.25	0.4	2.52	1.62	7.82	6.45	0.94	14.45	43.11	0.99	11.48	85.34	0.99

Table IV-10. Continued

Sample	Lignin×0.1 (%)	Acetyl (%)	CrI_C×0.1 (%)	Xylan×0.1 (%)	1 h			6 h			72 h		
					Slope	Intercept	R^2	Slope	Intercept	R^2	Slope	Intercept	R^2
DL50-DA000-DC0 ^{M}	0.18	2.7	7.98	1.68	5.92	4.06	0.94	10.90	30.05	1.00	14.73	69.00	1.00
DL50-DA000-DC3 ^{H}	0.18	2.7	4.49	1.68	7.67	7.73	0.92	14.58	42.32	0.99	11.96	89.32	0.99
DL50-DA000-DC6 ^{H}	0.18	2.7	1.03	1.68	8.62	4.80	0.95	15.58	44.32	1.00	13.95	82.12	0.98
DL50-DA007-DC0 ^{M}	0.16	2.6	7.79	1.54	7.15	3.60	0.94	17.13	28.65	0.98	17.36	74.81	0.99
DL50-DA007-DC3 ^{H}	0.16	2.6	5.45	1.54	9.20	3.59	0.95	17.82	38.99	1.00	15.78	81.23	0.98
DL50-DA007-DC6 ^{H}	0.16	2.6	2.66	1.54	8.72	4.56	0.94	17.02	39.18	0.99	11.42	82.55	0.99
DL50-DA015-DC0 ^{M}	0.16	2.3	7.47	1.5	5.97	3.61	0.96	16.30	26.28	0.99	17.70	68.11	1.00
DL50-DA015-DC3 ^{H}	0.16	2.3	5.82	1.5	8.26	5.38	0.92	16.87	41.24	0.97	11.09	80.45	0.99
DL50-DA015-DC6 ^{H}	0.16	2.3	2.37	1.5	9.27	3.32	0.95	18.49	37.23	1.00	14.16	87.22	1.00
DL50-DA035-DC0 ^{M}	0.15	2.2	7.30	1.44	8.31	3.80	0.99	18.15	31.84	0.99	19.20	72.92	0.99
DL50-DA035-DC3 ^{H}	0.15	2.2	5.48	1.44	11.35	3.20	0.89	16.14	42.49	1.00	10.14	81.89	0.96
DL50-DA035-DC6 ^{H}	0.15	2.2	1.84	1.44	9.28	5.56	0.94	16.16	42.76	0.99	10.16	86.84	0.99
DL50-DA055-DC0 ^{M}	0.13	1.8	7.36	1.41	6.35	4.37	0.92	17.78	26.79	0.99	16.06	72.67	0.96
DL50-DA055-DC3 ^{H}	0.13	1.8	5.35	1.41	9.30	5.74	0.94	17.25	40.77	0.99	12.82	84.56	0.99
DL50-DA055-DC6 ^{H}	0.13	1.8	0.98	1.41	9.53	4.93	0.95	16.18	44.69	1.00	15.08	88.94	0.99
DL50-DA075-DC0 ^{M}	0.11	1.6	7.04	1.44	8.46	3.23	0.97	20.18	27.31	0.99	18.42	75.44	0.99
DL50-DA075-DC3 ^{H}	0.11	1.6	5.12	1.44	10.26	4.27	0.92	17.00	41.08	0.99	15.25	84.27	1.00
DL50-DA075-DC6 ^{H}	0.11	1.6	1.39	1.44	8.42	6.44	0.92	16.35	42.68	0.99	11.36	85.81	0.98

Table IV-10. Continued

Sample	Lignin×0.1 (%)	Acetyl (%)	CrI_C×0.1 (%)	Xylan×0.1 (%)	1 h			6 h			72 h		
					Slope	Intercept	R^2	Slope	Intercept	R^2	Slope	Intercept	R^2
DL50-DA150-DC0 [H]	0.07	0.1	7.52	1.51	6.56	4.53	0.95	20.40	26.97	0.98	21.81	76.14	0.99
DL50-DA150-DC3 [H]	0.07	0.1	5.86	1.51	8.07	4.96	0.93	20.93	28.88	0.99	15.25	80.04	0.99
DL50-DA150-DC6 [H]	0.07	0.1	3.90	1.51	8.04	4.78	0.93	17.37	35.07	0.99	20.17	81.51	1.00

[L] Low-digestibility; enzyme loading: 1, 5, and 30 FPU/g dry biomass for 1-, 6-, and 72-h incubation periods.

[M] Medium-digestibility; enzyme loading: 1, 3, and 10 FPU/g dry biomass for 1- and 6-h incubation periods; 0.5, 1.5, and 5 FPU/g dry biomass for 72-h incubation period.

[H] High-digestibility; enzyme loading: 1, 3, and 10 FPU/g dry biomass for 1- and 6-h incubation periods; 0.25, 0.75, and 2 FPU/g dry biomass for 72-h incubation period.

Table IV-11. Regression parameters of total sugar hydrolysis of model lignocelluloses determined by equation I-3

Sample	Lignin×0.1 (%)	Acetyl (%)	CrI_C×0.1 (%)	TS×0.1 (%)	1 h			6 h			72 h		
					Slope	Intercept	R^2	Slope	Intercept	R^2	Slope	Intercept	R^2
DL00-DA000-DC0^{L}	2.63	2.9	6.24	5.83	0.80	0.00	0.99	1.78	1.18	1.00	2.02	5.22	0.97
DL00-DA000-DC3^{L}	2.63	2.9	3.39	5.83	8.12	2.42	0.98	9.02	14.26	0.99	6.56	33.96	0.99
DL00-DA000-DC6^{L}	2.63	2.9	1.80	5.83	11.11	2.10	0.97	13.47	19.34	0.99	7.32	52.39	0.98
DL00-DA007-DC0^{L}	2.55	2.8	6.51	6.11	0.71	0.33	1.00	1.68	0.92	0.98	2.41	4.66	0.99
DL00-DA007-DC3^{L}	2.55	2.8	3.74	6.11	7.22	2.12	0.97	9.69	12.18	1.00	7.27	34.12	0.96
DL00-DA007-DC6^{L}	2.55	2.8	2.45	6.11	10.08	1.93	0.98	11.98	15.39	0.99	6.52	43.33	0.99
DL00-DA015-DC0^{L}	2.56	2.5	6.53	6.02	0.74	0.00	0.99	1.75	0.71	1.00	1.94	5.28	1.00
DL00-DA015-DC3^{L}	2.56	2.5	3.21	6.02	8.20	2.08	0.98	9.41	13.99	0.99	5.88	35.00	0.99
DL00-DA015-DC6^{M}	2.56	2.5	2.26	6.02	7.44	4.42	0.97	14.11	18.13	0.99	9.81	45.36	0.99
DL00-DA035-DC0^{L}	2.55	1.9	6.41	6.17	1.00	0.32	0.93	1.73	2.04	0.98	2.41	5.96	0.99
DL00-DA035-DC3^{L}	2.55	1.9	3.00	6.17	7.65	2.24	0.97	9.23	13.37	1.00	6.84	32.42	0.99
DL00-DA035-DC6^{M}	2.55	1.9	2.48	6.17	9.03	3.01	0.97	12.66	15.44	0.99	10.86	39.51	0.99
DL00-DA055-DC0^{L}	2.6	1.3	6.35	6.08	1.27	0.00	0.94	1.82	2.87	1.00	2.89	6.35	1.00
DL00-DA055-DC3^{L}	2.6	1.3	2.68	6.08	12.69	2.34	0.97	12.99	20.75	0.98	6.74	51.35	0.98
DL00-DA055-DC6^{M}	2.6	1.3	1.58	6.08	11.82	4.25	0.97	15.71	24.13	1.00	12.55	53.69	0.95
DL00-DA075-DC0^{L}	2.6	0.9	6.83	6.23	1.56	0.64	0.99	2.57	3.04	1.00	4.11	7.48	0.99
DL00-DA075-DC3^{L}	2.6	0.9	2.62	6.23	14.48	2.90	0.97	14.75	24.56	0.98	7.59	58.49	0.96
DL00-DA075-DC6^{M}	2.6	0.9	1.33	6.23	12.82	4.67	0.97	17.21	23.73	0.99	8.88	59.78	0.99

Table IV-11. Continued

Sample	Lignin×0.1 (%)	Acetyl (%)	CrI_C×0.1 (%)	TS×0.1 (%)	1 h			6 h			72 h		
					Slope	Intercept	R^2	Slope	Intercept	R^2	Slope	Intercept	R^2
DL00-DA150-DC0 ^{L}	2.45	0.4	7.42	6.3	4.11	0.00	0.96	7.34	2.86	0.97	13.15	9.67	0.97
DL00-DA150-DC3 ^{M}	2.45	0.4	3.58	6.3	11.77	5.72	0.97	15.79	22.23	0.99	13.48	47.87	0.99
DL00-DA150-DC6 ^{M}	2.45	0.4	3.15	6.3	11.65	7.13	0.96	13.31	29.19	1.00	12.88	56.78	1.00
DL01-DA000-DC0 ^{L}	2.39	2.8	6.85	6.21	1.25	-0.10	0.94	2.12	2.17	1.00	4.00	6.63	0.99
DL01-DA000-DC3 ^{M}	2.39	2.8	3.09	6.21	9.05	3.18	0.93	13.35	20.55	0.99	12.34	46.04	0.99
DL01-DA000-DC6 ^{H}	2.39	2.8	1.15	6.21	12.42	2.52	0.96	19.72	20.94	0.99	15.76	61.49	0.99
DL01-DA007-DC0 ^{L}	2.31	2.9	6.86	6.1	1.21	0.14	0.98	2.60	1.73	1.00	4.57	6.59	0.99
DL01-DA007-DC3 ^{M}	2.31	2.9	2.03	6.1	12.50	1.59	0.97	14.39	19.57	0.99	11.00	52.22	0.99
DL01-DA007-DC6 ^{M}	2.31	2.9	1.75	6.1	10.32	2.42	0.93	17.22	20.44	0.99	12.80	55.68	1.00
DL01-DA015-DC0 ^{L}	2.28	2.8	6.83	6.22	1.22	0.64	0.93	2.32	2.92	0.99	4.73	7.45	0.99
DL01-DA015-DC3 ^{L}	2.28	2.8	2.76	6.22	10.49	2.02	0.96	13.08	17.58	1.00	8.94	47.64	0.97
DL01-DA015-DC6 ^{M}	2.28	2.8	1.80	6.22	12.59	2.94	0.97	18.19	21.32	0.99	10.94	60.06	0.98
DL01-DA035-DC0 ^{L}	2.24	2.9	6.83	6.26	1.53	0.09	0.97	2.35	2.70	1.00	4.81	7.99	0.99
DL01-DA035-DC3 ^{M}	2.24	2.9	3.21	6.26	10.34	2.90	0.98	15.28	18.42	0.99	11.48	48.40	0.99
DL01-DA035-DC6 ^{M}	2.24	2.9	2.66	6.26	13.01	3.63	0.96	18.13	26.73	1.00	15.71	64.80	0.99
DL01-DA055-DC0 ^{L}	2.18	2.2	6.40	6.38	2.22	0.55	0.97	3.99	3.60	0.99	7.00	10.42	0.99
DL01-DA055-DC3 ^{M}	2.18	2.2	3.01	6.38	11.62	3.56	0.95	16.89	22.69	1.00	12.04	56.18	0.99
DL01-DA055-DC6 ^{H}	2.18	2.2	1.91	6.38	13.15	2.16	0.95	19.34	22.23	0.99	17.74	64.24	0.99

Table IV-11. Continued

Sample	Lignin×0.1 (%)	Acetyl (%)	CrI_C×0.1 (%)	TS×0.1 (%)	1 h			6 h			72 h		
					Slope	Intercept	R^2	Slope	Intercept	R^2	Slope	Intercept	R^2
DL01-DA075-DC0 ^{L}	2.13	1.7	6.94	6.39	2.60	1.03	1.00	5.43	5.53	0.98	8.06	16.15	1.00
DL01-DA075-DC3 ^{M}	2.13	1.7	2.58	6.39	12.16	5.58	0.98	18.09	24.71	0.99	13.17	59.74	0.99
DL01-DA075-DC6 ^{M}	2.13	1.7	2.16	6.39	15.30	4.30	0.96	20.11	30.76	1.00	13.29	68.44	0.97
DL01-DA150-DC0 ^{L}	1.78	0.4	7.84	7.02	5.36	1.17	0.97	15.61	7.89	0.99	18.32	38.55	0.99
DL01-DA150-DC3 ^{M}	1.78	0.4	3.40	7.02	17.28	6.85	0.95	19.73	37.29	1.00	18.06	72.76	0.98
DL01-DA150-DC6 ^{H}	1.78	0.4	2.36	7.02	18.01	6.67	0.98	22.78	35.75	0.99	18.16	81.39	0.99
DL02-DA000-DC0 ^{L}	2.15	2.9	6.75	6.23	1.79	0.64	0.99	3.38	3.67	0.99	7.21	10.27	0.98
DL02-DA000-DC3 ^{M}	2.15	2.9	2.33	6.23	11.85	4.96	0.94	19.59	23.14	0.99	13.60	60.19	0.98
DL02-DA000-DC6 ^{M}	2.15	2.9	2.00	6.23	13.72	2.34	0.97	19.19	26.04	1.00	6.15	47.27	0.99
DL02-DA007-DC0 ^{L}	2.11	3.1	6.75	6.36	1.90	0.43	0.97	3.83	3.46	0.97	8.03	7.46	0.99
DL02-DA007-DC3 ^{M}	2.11	3.1	2.84	6.36	7.05	5.15	1.00	18.83	20.41	1.00	12.24	58.81	0.99
DL02-DA007-DC6 ^{H}	2.11	3.1	1.69	6.36	14.78	2.20	0.96	22.16	25.56	0.99	17.57	71.19	0.99
DL02-DA015-DC0 ^{L}	2.09	3	6.76	6.32	2.04	1.25	0.98	4.31	4.32	0.97	8.80	11.45	0.99
DL02-DA015-DC3 ^{M}	2.09	3	3.29	6.32	10.24	4.10	0.96	16.25	20.71	0.99	10.50	56.94	0.99
DL02-DA015-DC6 ^{M}	2.09	3	3.29	6.32	11.83	3.05	0.95	19.27	21.46	1.00	8.74	67.15	0.98
DL02-DA035-DC0 ^{L}	1.95	2.9	6.81	6.4	2.74	0.30	0.96	5.96	3.00	0.98	9.00	15.35	0.98
DL02-DA035-DC3 ^{M}	1.95	2.9	3.20	6.4	12.73	2.86	0.95	18.76	23.00	1.00	15.31	59.09	0.98
DL02-DA035-DC6 ^{H}	1.95	2.9	2.71	6.4	12.91	3.26	0.97	20.92	21.70	0.99	17.19	65.46	0.99

Table IV-11. Continued

Sample	Lignin×0.1 (%)	Acetyl (%)	CrI_C×0.1 (%)	TS×0.1 (%)	1 h			6 h			72 h		
					Slope	Intercept	R^2	Slope	Intercept	R^2	Slope	Intercept	R^2
DL02-DA055-DC0 ^{L}	1.95	2.5	7.08	6.46	3.65	0.90	0.97	7.25	6.97	0.99	10.63	21.46	1.00
DL02-DA055-DC3 ^{M}	1.95	2.5	3.07	6.46	11.27	5.11	0.96	19.04	23.28	0.99	13.24	62.73	0.99
DL02-DA055-DC6 ^{M}	1.95	2.5	2.83	6.46	13.82	3.13	0.96	19.68	27.02	1.00	11.95	67.74	0.98
DL02-DA075-DC0 ^{L}	1.84	1.7	7.06	6.57	4.72	0.10	0.96	9.63	5.98	0.98	11.94	25.39	0.99
DL02-DA075-DC3 ^{M}	1.84	1.7	3.45	6.57	14.90	3.30	0.97	20.75	28.85	1.00	13.25	69.73	0.97
DL02-DA075-DC6 ^{H}	1.84	1.7	1.33	6.57	18.19	3.82	0.95	23.16	32.17	0.99	19.66	83.80	0.99
DL02-DA150-DC0 ^{M}	1.48	0.3	7.60	7.13	6.70	2.62	0.95	19.70	13.10	0.97	22.62	52.18	1.00
DL02-DA150-DC3 ^{H}	1.48	0.3	3.61	7.13	16.44	7.68	0.97	22.19	34.07	0.99	18.38	76.73	0.99
DL02-DA150-DC6 ^{H}	1.48	0.3	1.37	7.13	19.81	7.49	0.98	19.58	46.87	0.96	23.35	85.48	0.72
DL03-DA000-DC0 ^{L}	1.87	2.9	7.03	6.48	3.65	-0.23	0.93	7.62	4.30	0.98	13.41	17.48	0.99
DL03-DA000-DC3 ^{M}	1.87	2.9	2.89	6.48	15.72	3.24	0.95	22.32	30.27	1.00	18.54	75.89	0.99
DL03-DA000-DC6 ^{H}	1.87	2.9	1.39	6.48	17.48	2.68	0.95	22.56	33.92	0.99	19.94	85.46	0.99
DL03-DA007-DC0 ^{L}	1.78	2.9	7.20	6.59	3.75	0.69	0.96	8.29	5.22	0.98	11.79	27.30	0.98
DL03-DA007-DC3 ^{M}	1.78	2.9	3.72	6.59	11.54	3.35	0.98	20.49	21.96	1.00	14.39	60.98	0.99
DL03-DA007-DC6 ^{M}	1.78	2.9	1.49	6.59	13.21	3.55	0.97	22.45	31.73	1.00	9.10	78.47	0.93
DL03-DA015-DC0 ^{L}	1.71	2.5	7.14	6.59	3.94	-0.04	0.94	8.75	4.53	0.98	13.59	22.17	0.99
DL03-DA015-DC3 ^{M}	1.71	2.5	2.93	6.59	14.46	2.18	0.95	22.04	25.43	1.00	14.53	69.01	0.94
DL03-DA015-DC6 ^{H}	1.71	2.5	1.49	6.59	16.72	2.11	0.96	23.15	30.12	0.99	20.18	83.72	0.99

Table IV-11. Continued

Sample	Lignin×0.1 (%)	Acetyl (%)	CrI_C×0.1 (%)	TS×0.1 (%)	1 h			6 h			72 h		
					Slope	Intercept	R^2	Slope	Intercept	R^2	Slope	Intercept	R^2
DL03-DA035-DC0 ^{L}	1.63	2.8	7.15	6.65	4.72	0.51	0.97	11.15	6.26	0.99	13.06	31.75	0.99
DL03-DA035-DC3 ^{H}	1.63	2.8	3.06	6.65	12.24	5.12	0.96	22.82	25.50	1.00	17.15	71.22	0.99
DL03-DA035-DC6 ^{M}	1.63	2.8	1.92	6.65	17.56	2.03	0.95	22.68	32.45	0.99	18.27	80.37	0.99
DL03-DA055-DC0 ^{M}	1.62	2.6	7.26	6.72	4.46	0.88	0.99	12.63	6.45	0.99	14.04	34.36	0.99
DL03-DA055-DC3 ^{M}	1.62	2.6	2.84	6.72	15.58	3.07	0.96	22.62	29.40	1.00	18.35	76.69	1.00
DL03-DA055-DC6 ^{H}	1.62	2.6	1.68	6.72	18.62	2.87	0.95	25.61	34.96	0.98	21.62	90.83	0.99
DL03-DA075-DC0 ^{M}	1.47	2.3	7.32	6.96	4.75	1.41	0.95	15.81	8.59	0.98	18.23	42.91	0.99
DL03-DA075-DC3 ^{H}	1.47	2.3	3.01	6.96	13.40	6.00	0.97	23.26	31.46	0.99	19.54	78.56	0.99
DL03-DA075-DC6 ^{M}	1.47	2.3	2.64	6.96	17.31	3.67	0.95	22.14	32.63	0.99	17.56	79.11	1.00
DL03-DA150-DC0 ^{M}	1.06	0.4	7.73	7.56	7.70	1.71	0.94	22.36	12.45	0.98	20.56	56.12	0.99
DL03-DA150-DC3 ^{H}	1.06	0.4	4.11	7.56	17.32	5.68	0.96	21.79	36.28	0.99	19.60	79.00	0.95
DL03-DA150-DC6 ^{H}	1.06	0.4	3.21	7.56	19.08	5.87	0.97	25.72	35.52	0.99	21.45	88.43	0.99
DL05-DA000-DC0 ^{M}	1.39	2.9	6.69	6.82	3.81	1.56	0.95	14.11	7.51	0.98	20.23	39.88	1.00
DL05-DA000-DC3 ^{H}	1.39	2.9	2.48	6.82	15.78	4.34	0.96	24.30	27.60	1.00	14.96	74.27	1.00
DL05-DA000-DC6 ^{M}	1.39	2.9	1.44	6.82	18.69	3.68	0.96	21.50	37.49	0.96	17.47	84.09	0.97
DL05-DA007-DC0 ^{M}	1.34	2.8	7.05	7.01	3.54	0.98	0.98	11.70	6.30	0.97	16.75	35.85	0.99
DL05-DA007-DC3 ^{M}	1.34	2.8	3.19	7.01	15.12	2.59	0.96	22.85	28.57	1.00	19.83	78.73	1.00
DL05-DA007-DC6 ^{H}	1.34	2.8	3.05	7.01	17.00	2.34	0.96	23.51	28.92	0.99	22.87	84.11	0.99

Table IV-11. Continued

Sample	Lignin×0.1 (%)	Acetyl (%)	CrI_C×0.1 (%)	TS×0.1 (%)	1 h			6 h			72 h		
					Slope	Intercept	R^2	Slope	Intercept	R^2	Slope	Intercept	R^2
DL05-DA015-DC0 ^{M}	1.33	2.7	7.22	6.92	2.31	1.51	0.99	7.91	8.82	0.97	22.89	39.96	1.00
DL05-DA015-DC3 ^{H}	1.33	2.7	3.05	6.92	12.96	4.66	0.98	19.97	26.67	0.99	19.69	71.88	0.99
DL05-DA015-DC6 ^{H}	1.33	2.7	1.71	6.92	18.58	1.71	0.97	22.44	35.13	0.98	17.31	82.03	0.94
DL05-DA035-DC0 ^{M}	1.25	2.6	7.20	7.05	4.83	0.43	0.97	17.17	8.32	0.95	18.96	44.36	0.99
DL05-DA035-DC3 ^{M}	1.25	2.6	3.28	7.05	15.52	2.84	0.95	23.01	28.80	1.00	18.58	76.78	1.00
DL05-DA035-DC6 ^{H}	1.25	2.6	1.83	7.05	19.11	3.11	0.96	23.46	34.58	0.98	21.83	88.74	0.99
DL05-DA055-DC0 ^{M}	1.18	2.3	7.62	7.09	4.69	1.44	0.96	16.87	10.21	0.95	21.11	47.08	0.99
DL05-DA055-DC3 ^{H}	1.18	2.3	3.23	7.09	15.55	5.25	0.94	23.10	28.81	0.99	22.24	81.63	0.99
DL05-DA055-DC6 ^{H}	1.18	2.3	3.23	7.09	15.71	5.25	0.94	23.91	28.46	0.98	22.49	79.41	0.74
DL05-DA075-DC0 ^{M}	1.09	2.4	7.68	7.3	5.53	2.23	0.98	18.95	9.18	0.96	22.36	48.45	0.99
DL05-DA075-DC3 ^{H}	1.09	2.4	3.08	7.3	16.39	3.64	0.97	22.71	30.68	0.99	22.48	79.58	0.77
DL05-DA075-DC6 ^{H}	1.09	2.4	2.76	7.3	19.63	4.22	0.97	22.00	36.51	0.97	21.50	90.51	0.99
DL05-DA150-DC0 ^{M}	0.68	0.6	7.82	7.99	7.27	2.26	0.95	22.98	12.17	0.97	20.58	57.48	0.95
DL05-DA150-DC3 ^{H}	0.68	0.6	2.85	7.99	15.49	7.69	0.98	24.70	31.44	0.99	23.81	87.94	0.99
DL05-DA150-DC6 ^{H}	0.68	0.6	3.09	7.99	18.45	5.15	0.96	22.07	37.16	0.98	22.20	85.61	0.96
DL10-DA000-DC0 ^{M}	0.61	2.7	7.76	7.46	5.31	1.12	0.96	18.46	9.31	0.94	22.81	51.69	0.99
DL10-DA000-DC3 ^{H}	0.61	2.7	2.82	7.46	16.81	4.47	0.96	21.81	35.00	0.99	21.58	84.12	0.94
DL10-DA000-DC6 ^{H}	0.61	2.7	2.43	7.46	17.66	4.82	0.96	22.36	34.07	0.99	21.52	86.89	0.99

Table IV-11. Continued

Sample	Lignin×0.1 (%)	Acetyl (%)	CrI_C×0.1 (%)	TS×0.1 (%)	1 h			6 h			72 h		
					Slope	Intercept	R^2	Slope	Intercept	R^2	Slope	Intercept	R^2
DL10-DA007-DC0 ^{M}	0.6	3	7.66	7.61	4.67	1.53	0.95	20.53	8.47	0.96	22.48	52.64	0.98
DL10-DA007-DC3 ^{H}	0.6	3	3.66	7.61	15.16	4.56	0.95	24.89	26.71	0.99	23.48	78.58	0.98
DL10-DA007-DC6 ^{H}	0.6	3	2.10	7.61	18.04	3.10	0.96	22.39	36.13	0.98	23.76	92.08	1.00
DL10-DA015-DC0 ^{M}	0.59	2.7	7.71	7.64	5.49	0.98	0.92	19.78	8.71	0.94	25.32	52.62	0.99
DL10-DA015-DC3 ^{H}	0.59	2.7	3.98	7.64	15.24	3.00	0.96	23.41	28.50	1.00	20.49	77.33	0.98
DL10-DA015-DC6 ^{H}	0.59	2.7	2.34	7.64	18.86	2.79	0.95	22.44	34.29	0.99	22.44	88.00	0.99
DL10-DA035-DC0 ^{M}	0.56	2.7	7.69	7.53	4.77	1.66	0.94	19.40	9.80	0.96	22.62	53.34	0.99
DL10-DA035-DC3 ^{H}	0.56	2.7	3.94	7.53	14.90	5.72	0.96	24.87	29.45	0.99	20.33	81.44	0.99
DL10-DA035-DC6 ^{H}	0.56	2.7	2.07	7.53	18.14	3.21	0.97	22.46	35.36	0.99	19.41	81.49	0.94
DL10-DA055-DC0 ^{M}	0.45	2.5	7.92	7.76	6.06	1.26	0.92	21.48	10.46	0.94	23.70	55.37	0.99
DL10-DA055-DC3 ^{H}	0.45	2.5	3.95	7.76	15.44	3.66	0.97	22.62	28.88	1.00	29.49	72.95	0.92
DL10-DA055-DC6 ^{H}	0.45	2.5	3.49	7.76	16.88	3.57	0.96	23.45	29.48	0.99	18.68	76.12	0.99
DL10-DA075-DC0 ^{M}	0.41	2.1	7.82	7.76	5.26	1.45	0.95	20.42	9.60	0.95	21.38	52.68	0.98
DL10-DA075-DC3 ^{H}	0.41	2.1	3.27	7.76	15.91	6.18	0.95	23.98	32.26	1.00	21.96	79.93	0.99
DL10-DA075-DC6 ^{H}	0.41	2.1	2.74	7.76	16.91	4.11	0.96	23.47	31.83	0.99	17.56	82.10	0.95
DL10-DA150-DC0 ^{H}	0.25	0.4	7.26	8.66	7.96	3.93	0.97	25.19	14.03	0.95	27.46	69.17	0.99
DL10-DA150-DC3 ^{H}	0.25	0.4	2.84	8.66	16.29	4.35	0.96	23.59	30.31	0.99	24.83	86.93	0.99
DL10-DA150-DC6 ^{H}	0.25	0.4	2.52	8.66	18.34	5.09	0.97	26.98	32.64	0.99	26.73	88.52	0.99

Table IV-11. Continued

Sample	Lignin×0.1 (%)	Acetyl (%)	CrI_C×0.1 (%)	TS×0.1 (%)	1 h			6 h			72 h		
					Slope	Intercept	R^2	Slope	Intercept	R^2	Slope	Intercept	R^2
DL50-DA000-DC0 ^{M}	0.18	2.7	7.98	8.38	3.74	1.17	0.93	7.87	11.07	0.99	22.55	44.47	1.00
DL50-DA000-DC3 ^{H}	0.18	2.7	4.49	8.38	12.91	5.20	0.96	23.88	23.49	0.99	19.44	76.10	0.99
DL50-DA000-DC6 ^{H}	0.18	2.7	1.03	8.38	15.54	3.68	0.97	23.68	30.54	0.99	26.92	75.45	0.85
DL50-DA007-DC0 ^{M}	0.16	2.6	7.79	8.56	4.65	1.31	0.92	17.90	7.32	0.94	25.44	46.98	0.99
DL50-DA007-DC3 ^{H}	0.16	2.6	5.45	8.56	11.85	1.86	0.96	24.48	17.91	0.99	30.40	65.02	0.96
DL50-DA007-DC6 ^{H}	0.16	2.6	2.66	8.56	14.95	2.51	0.95	27.12	22.93	0.99	20.18	69.83	0.99
DL50-DA015-DC0 ^{M}	0.16	2.3	7.47	8.59	3.74	1.34	0.94	15.44	8.10	0.98	24.61	42.33	1.00
DL50-DA015-DC3 ^{H}	0.16	2.3	5.82	8.59	10.24	3.07	0.93	21.75	19.43	0.99	21.05	62.63	0.99
DL50-DA015-DC6 ^{H}	0.16	2.3	2.37	8.59	14.37	1.61	0.95	26.41	25.89	1.00	20.08	76.22	0.98
DL50-DA035-DC0 ^{M}	0.15	2.2	7.30	8.61	5.45	2.31	0.98	18.81	9.78	0.95	26.62	45.68	0.99
DL50-DA035-DC3 ^{H}	0.15	2.2	5.48	8.61	11.91	1.46	0.95	23.45	16.91	0.99	23.07	64.45	1.00
DL50-DA035-DC6 ^{H}	0.15	2.2	1.84	8.61	16.47	2.56	0.95	23.45	27.86	0.99	26.86	84.50	0.99
DL50-DA055-DC0 ^{M}	0.13	1.8	7.36	8.68	4.91	1.56	0.92	17.65	8.36	0.96	22.54	47.58	0.99
DL50-DA055-DC3 ^{H}	0.13	1.8	5.35	8.68	12.03	3.03	0.96	24.30	17.48	0.99	22.85	68.04	0.99
DL50-DA055-DC6 ^{H}	0.13	1.8	0.98	8.68	16.06	1.84	0.95	24.67	27.45	0.99	24.74	83.82	0.94
DL50-DA075-DC0 ^{M}	0.11	1.6	7.04	8.76	6.69	2.57	0.96	21.55	9.31	0.96	24.84	52.76	0.99
DL50-DA075-DC3 ^{H}	0.11	1.6	5.12	8.76	12.29	2.66	0.96	24.98	18.23	0.99	25.59	70.55	0.98
DL50-DA075-DC6 ^{H}	0.11	1.6	1.39	8.76	15.02	3.23	0.95	24.49	26.09	0.99	26.24	84.35	0.99

Table IV-11. Continued

Sample	Lignin×0.1 (%)	Acetyl (%)	CrI_C×0.1 (%)	TS×0.1 (%)	1 h			6 h			72 h		
					Slope	Intercept	R^2	Slope	Intercept	R^2	Slope	Intercept	R^2
DL50-DA150-DC0 [H]	0.07	0.1	7.52	9.16	8.57	2.38	0.94	24.70	13.54	0.97	26.67	63.04	0.99
DL50-DA150-DC3 [H]	0.07	0.1	5.86	9.16	14.46	2.78	0.96	28.59	15.48	0.99	22.83	73.16	0.99
DL50-DA150-DC6 [H]	0.07	0.1	3.90	9.16	15.03	3.02	0.96	24.75	24.51	1.00	30.02	72.78	0.94

[L] Low-digestibility; enzyme loading: 1, 5, and 30 FPU/g dry biomass for 1-, 6-, and 72-h incubation periods.

[M] Medium-digestibility; enzyme loading: 1, 3, and 10 FPU/g dry biomass for 1- and 6-h incubation periods; 0.5, 1.5, and 5 FPU/g dry biomass for 72-h incubation period.

[H] High-digestibility; enzyme loading: 1, 3, and 10 FPU/g dry biomass for 1- and 6-h incubation periods; 0.25, 0.75, and 2 FPU/g dry biomass for 72-h incubation period.

content from 13.4% to 6.1%, there was no obvious increase in the 1-h slope and 1-, 6-, and 72-h intercepts whereas 6- and 72-h intercepts increased moderately. It was obvious that the influence of lignin content on the 1-h intercept was not conclusive because of the small value.

Table IV-12. Division of structural features for studying their influences on slopes and intercepts

Structural features	Group	Lignin content	Acetyl content	CrI_B[a]
Lignin	L1	Various	Low (<0.9%)	High (unmilled)
	L2	Various	High (>2.4%)	Low (<30%)
Acetyl	A1	High (>17%)	Various	High (unmilled)
	A2	High (>17%)	Various	Low (<30%)
CrI_B[a]	C1	High (>17%)	High (>2.4%)	Various
	C2	Medium (10–17%)	High (>2.4%)	Various

[a] Biomass crystallinity.

Effect of Acetyl Content

Figures IV-26 to IV-28 illustrate the effect of acetyl content on the 1-, 6-, and 72-h slopes and intercepts of total sugar hydrolysis. Figure IV-26 shows that decreasing the acetyl content from 2.8% to 0.9% only slightly increases the 1-, 6-, and 72-h slopes and intercepts; only severe deacetylation (i.e., 0.4%) considerably increased the 1-, 6-, and 72-h slopes and 72-h intercept for high-lignin and high-crystallinity poplar wood, but the increase in each parameter was not as significant as that resulting from delignification. Figures IV-27 and IV-28 demonstrate that severe deacetylation moderately increases the 1-, 6-, and 72-h slopes and intercepts for low-crystallinity poplar wood, whereas the effect of severe deacetylation on the 1-, 6-, and 72-h slopes and 6- and 72-h intercepts are less pronounced for low-lignin poplar wood. Similar to delignification, the effect of deacetylation on the 1-h intercept was not conclusive.

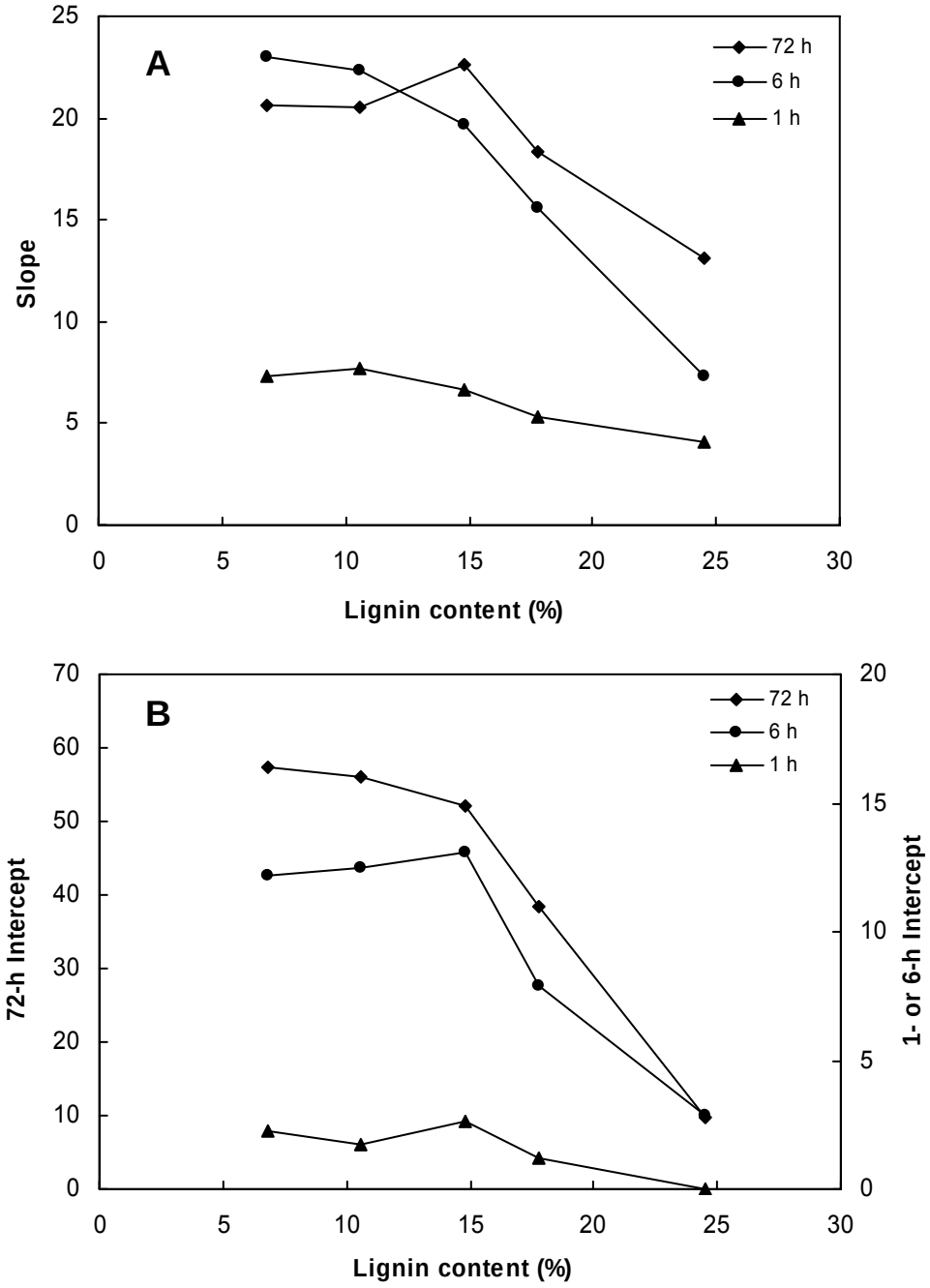

Figure IV-24. Effect of lignin content on 1-, 6-, and 72-h slopes and intercepts of total sugar hydrolysis: (A) slope; (B) intercept. Category L1: high-biomass crystallinity and low-acetyl biomass samples.

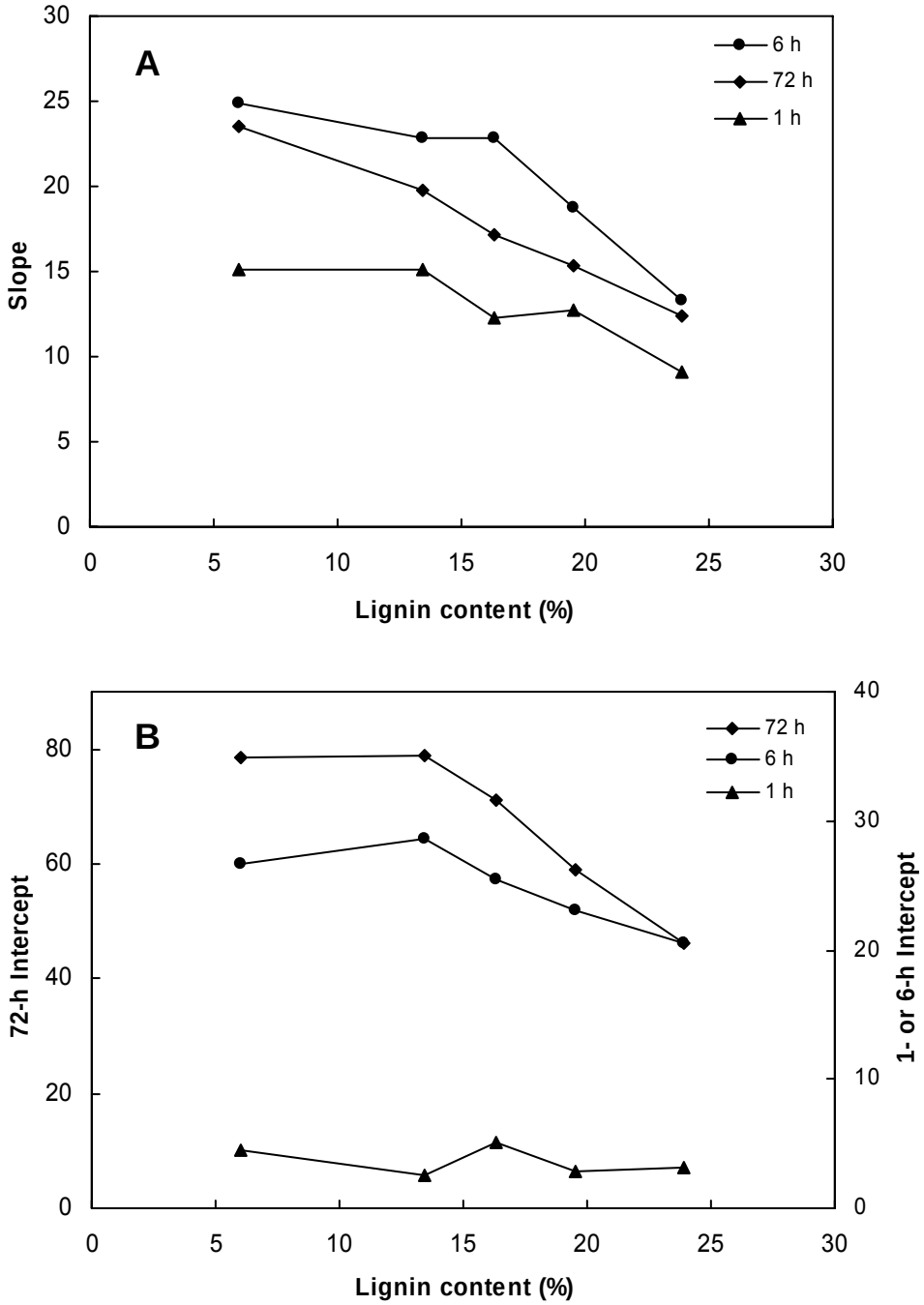

Figure IV-25. Effect of lignin content on 1-, 6-, and 72-h slopes and intercepts of total sugar hydrolysis: (A) slope; (B) intercept. Category L2: low-biomass crystallinity and high-acetyl biomass samples.

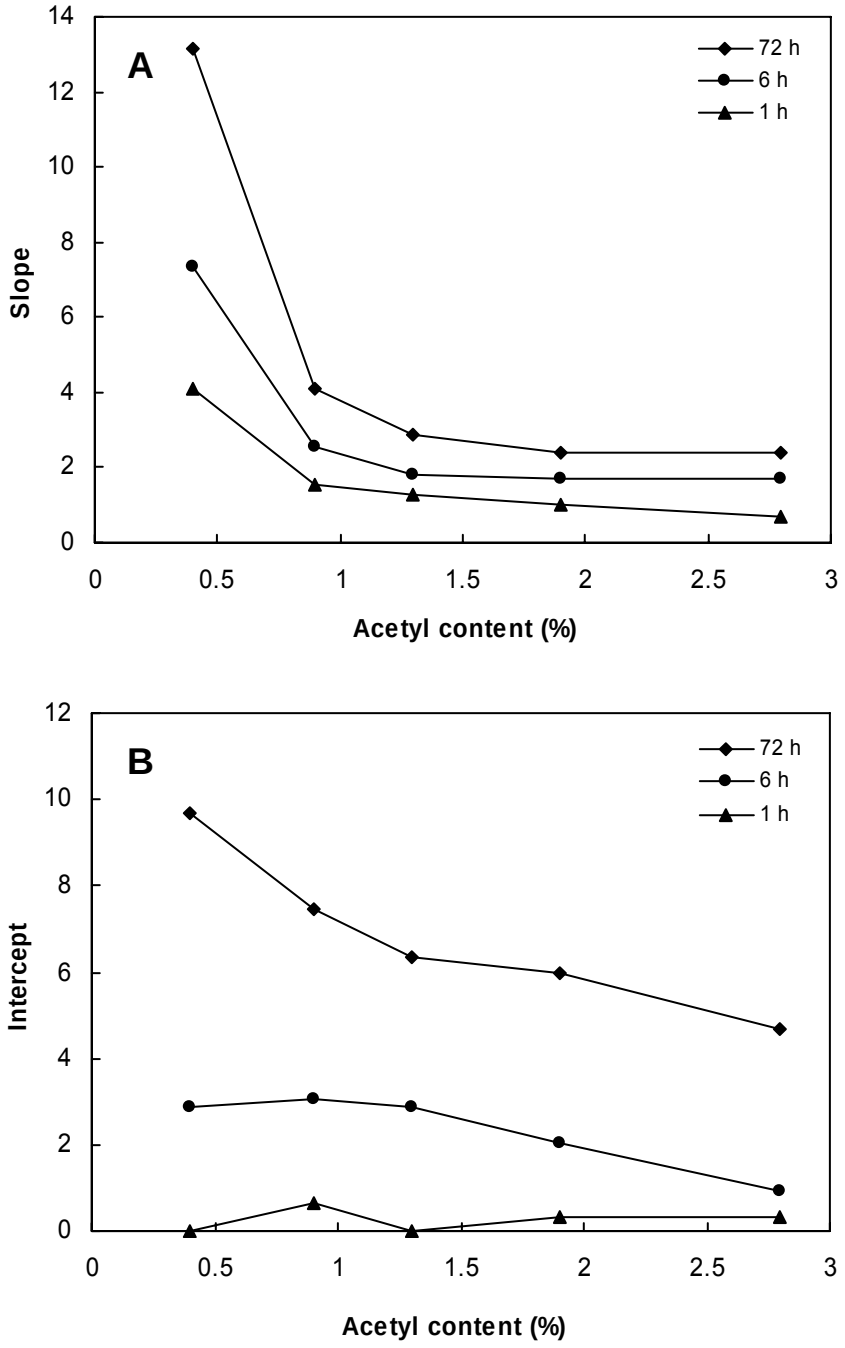

Figure IV-26. Effect of acetyl content on 1-, 6-, and 72-h slopes and intercepts of total sugar hydrolysis: (A) slope; (B) intercept. Category A1: high-biomass crystallinity and high-lignin biomass samples.

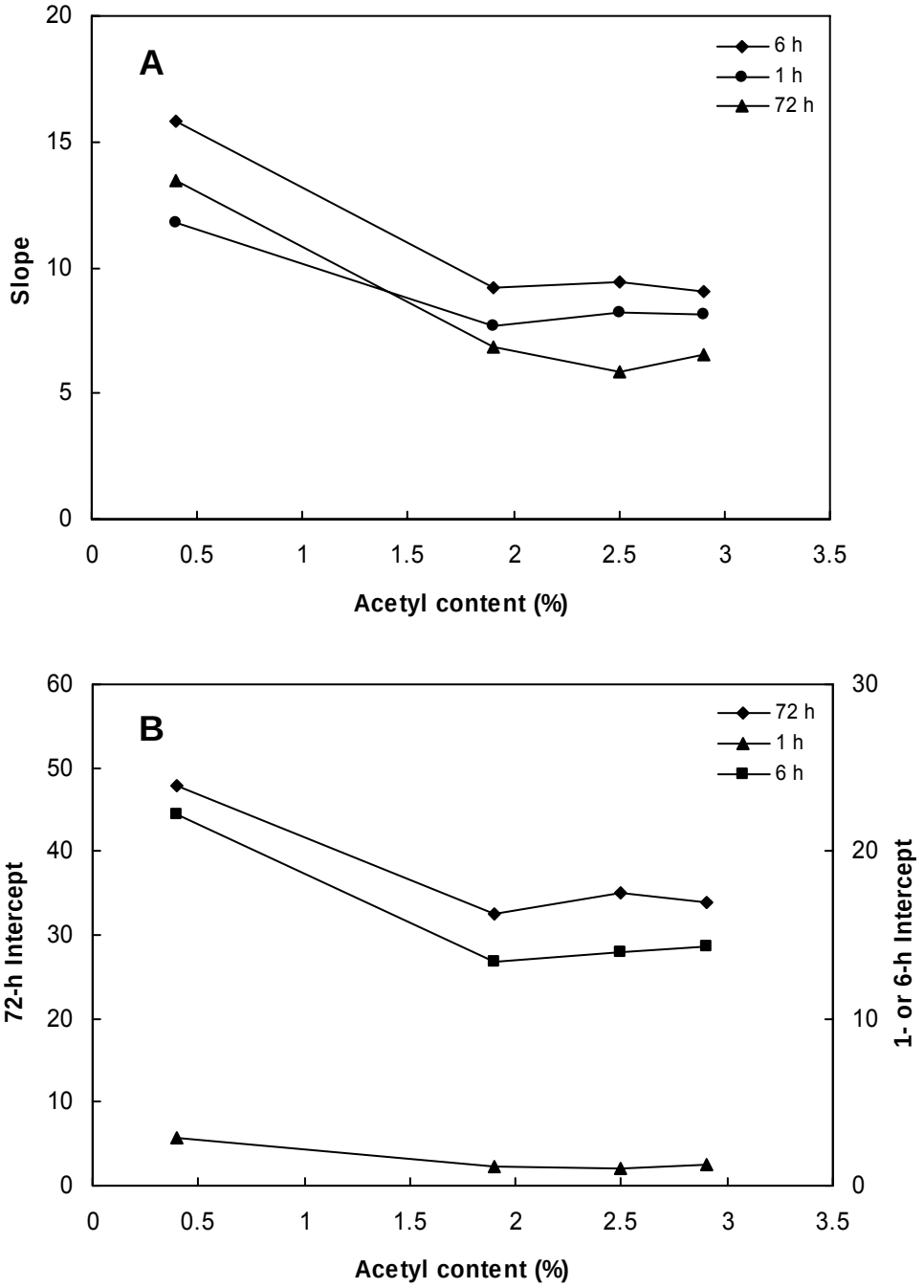

Figure IV-27. Effect of acetyl content on 1-, 6-, and 72-h slopes and intercepts of total sugar hydrolysis: (A) slope; (B) intercept. Category A2: low-biomass crystallinity and high-lignin biomass samples.

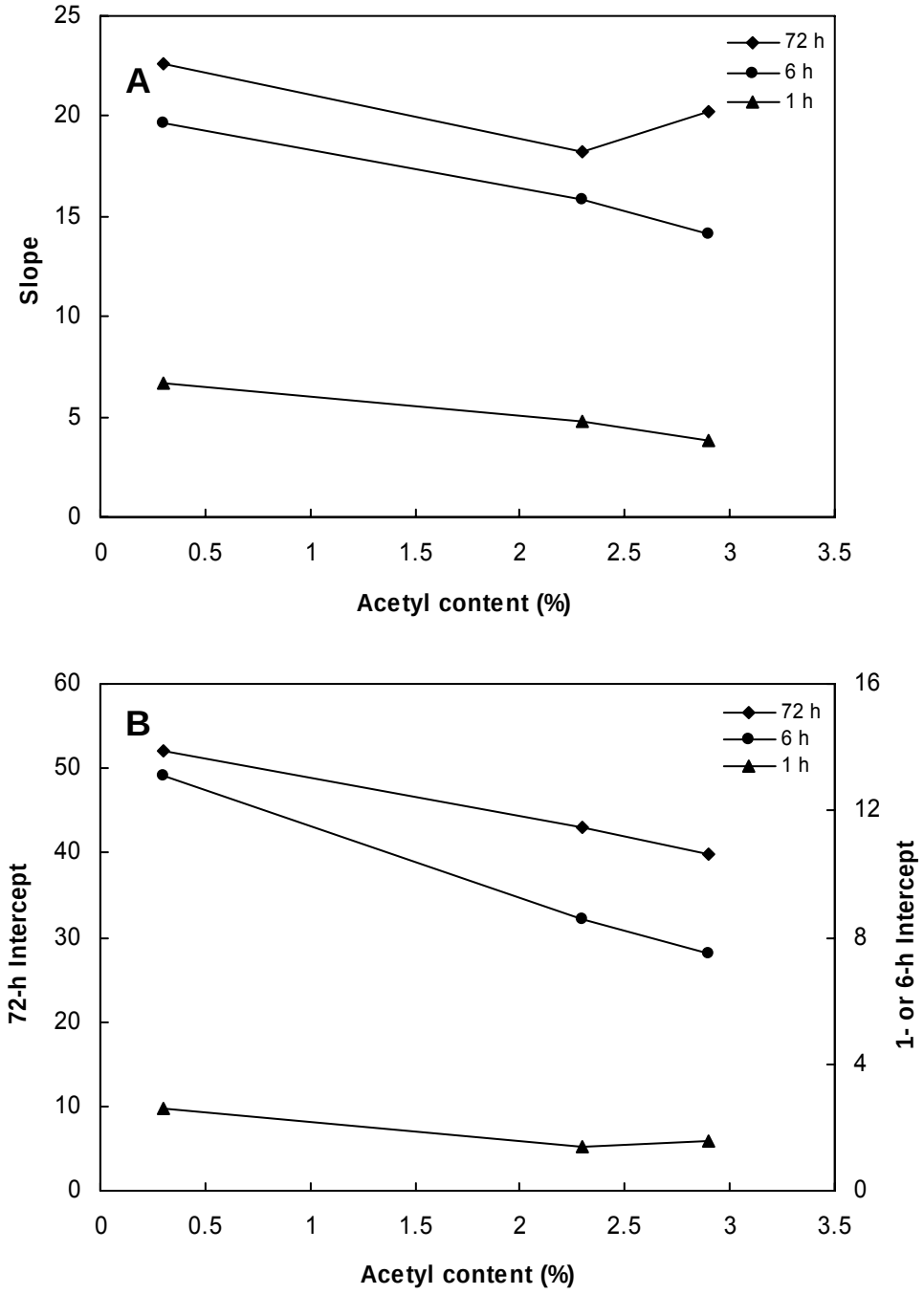

Figure IV-28. Effect of acetyl content on 1-, 6-, and 72-h slopes and intercepts of total sugar hydrolysis: (A) slope; (B) intercept. Category A3: high-biomass crystalinity and low-lignin biomass samples.

Effect of Crystallinity

Figures IV-29 and IV-30 illustrate the effect of biomass crystallinity on the 1-, 6-, and 72-h slopes and intercepts for total sugar hydrolysis. The 6- and 72-h intercepts and 1-h slope were inversely proportional to crystallinity regardless of lignin content. For the high-lignin samples, reducing crystallinity from 59.8% to 22.7% drastically increased all the correlation parameters except for the 1-h intercept because of the small value resulting from high lignin content (C1). Reducing biomass crystallinity from 61.7% to 25.9% significantly increased the 6- and 72-h intercepts and the 1-h slope for low-lignin poplar wood (C2), and had less effect on the 6- and 72-h slopes. Decrystallization increased the 1-h intercept of total sugar hydrolysis slightly.

Conclusions

Both delignification and decrystallization showed more significant effect on the 1-, 6-, and 72-h slopes and intercepts of total sugar hydrolysis than deacetylation. The large 72-h intercept and relatively small slope for the decrystallized samples indicate that small amounts of enzyme are required to achieve the desired carbohydrate conversion; the large 72-h slope for the delignified samples signifies that the ultimate extent of biomass hydrolysis could be virtually complete at higher enzyme loadings. Decrystallization greatly accelerated the initial hydrolysis rate because of the large 1-h slope. Both delignification and decrystrallization had significant influences on the 6-h slope and intercept of total sugar hydrolysis.

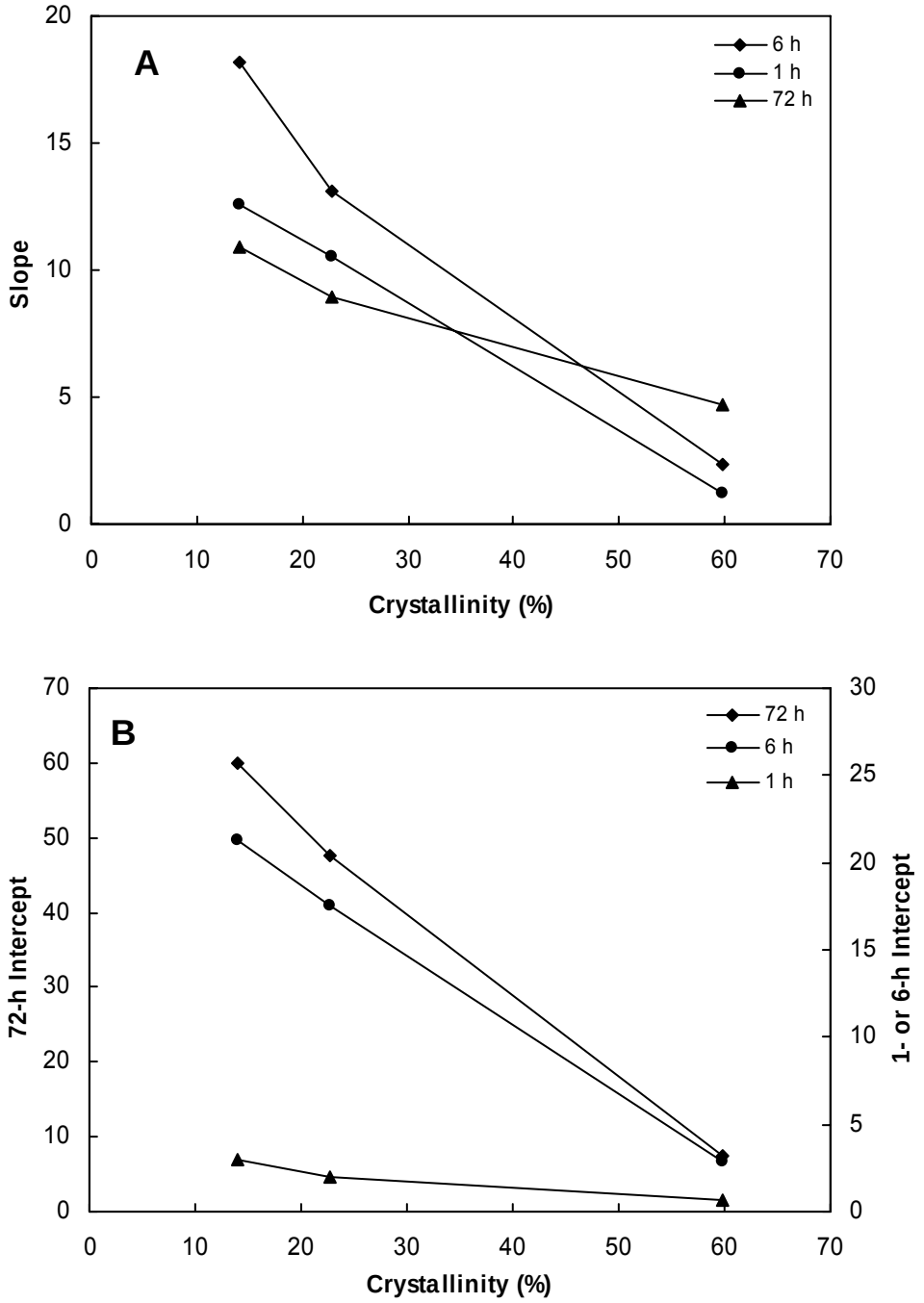

Figure IV-29. Effect of biomass crystallinity on 1-, 6-, and 72-h slopes and intercepts of total sugar hydrolysis: (A) slope; (B) intercept. Category C1: high-lignin and high-acetyl biomass samples.

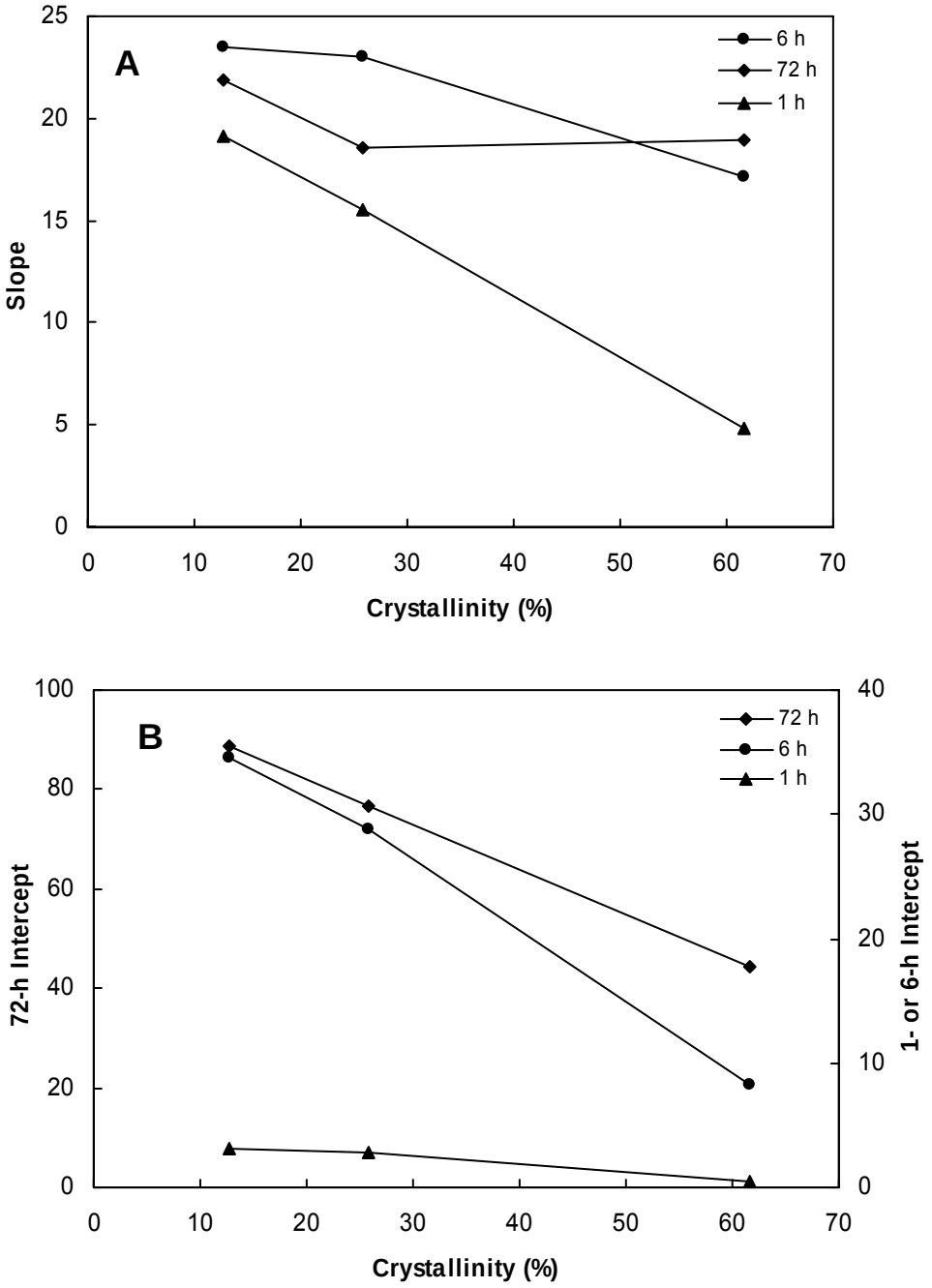

Figure IV-30. Effect of biomass crystallinity on 1-, 6-, and 72-h slopes and intercepts of total sugar hydrolysis: (A) slope; (B) intercept. Category C2: low-lignin and high-acetyl biomass samples.

CONCLUSIONS

The addition of supplemental cellobiase to the enzyme complex can signifcantly increase biomass digestiblity and the filter paper activity of the enzyme complex by converting the strong inhibitor, cellobiose, to glucose. Excessively high cellobiase loadings only slightly improved digestibility and the filter paper activity. By adding cellobiase, the extent of biomass hydrolysis was essentially identical regardless of substrate concentration. Low substrate concentrations such as 10–20 g/L are often used in laboratory investigations to prevent end-product inhibition of cellulase by cellobiose and glucose when the cellobiase activity in the enzyme complex is low.

The infuence of increasing enzyme loading on biomass digestibility highly depends on structural features resulting from pretreatment. A low enzyme loading (i.e., 2 FPU/g dry biomass) is sufficient for high-digestibility biomass to achieve nearly complete hydrolysis at 72 h. To some extent, the digestibility of biomass with structural features recalcitrant to enzymatic hydrolysis can be improved by increasing enzyme loadings. Severe delignification and decrystallization are not necessary to achieve high digestibility. The 1-, 6-, and 72-h glucan, xylan, and total sugar conversions were proportional to the natural logarithm of cellulase loadings from 10–15% to 90% conversions, indicating that the simplified HCH-1 model is valid for describing the enzymatic hydrolysis of lignocelluloses with various structural features.

The effects of lignin content, acetyl content, and biomass crystallinity on digestibility are, to some extent, interrelated. Lignin content and crystallinity play more significant roles on biomass digestibility than acetyl content. Decrystallization has a greater effect on the initial glucan hydrolysis rate whereas delignification has a greater effect on xylan hydrolysis. Delignification shows more influence on the ultimate extent of biomass hydrolysis than decrystallization. Both delignification and decrystallization showed more significant effect on the 1-, 6-, and 72-h slopes and intercepts of total sugar hydrolysis than deacetylation. The large 72-h intercept and relatively small value of 72-h slope for the decrystallized samples indicate that small amounts of enzyme are required

to achieve the desired carbohydrate conversion. The large 72-h slope for the delignified sample signifies that the ultimate extent of carbohydrate hydrolysis could be virtually complete at higher enzyme loadings. Decrystallization greatly accelerated the initial hydrolysis rate because the 1-h slope and intercept increased as crystallinity decreased. Both delignification and decrystrallization had significant influences on the 6-h slope and intercept of total sugar hydrolysis.

CHAPTER V

MATHEMATICAL MODELS CORRELATING STRUCTURAL FEATURES AND DIGESTIBILITY

INTRODUCTION

Lignocellulose digestibility is greatly affected by structural features resulting from pretreatment. Literature describes the effects of structural features including lignin content, acetyl content, crystallinity, and accessible surface area on digestibility. Some empirical models have been derived to correlate structural features with digestibility. However, the validity of these models is questionable due to the small number of tested samples (Fan et al., 1981), the narrow spectrum of investigated structural features (Grarpuray et al., 1983; Thompson and Chen, 1992) and the neglected interactions of structural features (Koullas et al., 1992).

In the previous studies by Chang and Holtzapple (2000), 147 model lignocellulose samples with a variety of structural features were prepared to study the influences of structural features, such as the extent of lignification, acetylation, and crystallization on digestibility. Mathematical models were developed to correlate structural features with 1- and 72-h digestibility with a cellulase loading of 5 FPU/g dry biomass. The mathematical model could predict the initial hydrolysis rate and ultimate conversion of α-cellulose and lime-treated switch grass, poplar wood, and bagasse.

The mathematical model derived by Chang and Holtzapple (2000) could only predict biomass digestibility with one cellulase loading (5 FPU/g biomass), which was excessive for biomass with low lignin content and low crystallinity. It is desirable to develop a mathematical model that can predict digestibility over a wide range of cellulase loadings, thus lower enzyme costs and higher hydrolysis conversions may be achieved. It has been known that the relationship between carbohydrate conversion and cellulase loading fit well the simplified HCH-1 model (Equation I-3) (Holtzapple et al.,

1994) and the linearity was valid over a wide range (i.e., 10–90%) of carbohydrate conversions (Mandels et al., 1981; Reese and Mandels., 1971). In Chapter IV, it has been shown that the simplified HCH-1 model is suitable for describing the linear relationship between the natural logarithm of cellulase loadings and the digestibility of biomass with various structural features during specified incubation periods.

As discussed in the previous chapter, model lignocelluloses with various structural features were hydrolyzed for 1, 6, and 72 h with a variety of cellulase loadings recommended in Table IV-8 on the basis of structural features. Carbohydrate conversions at a given time versus the natural logarithm of cellulase loadings were plotted to obtain the slopes and intercepts of the straight lines. In this chapter, mathematical models have been developed by parametric and nonparametric regression approaches to correlate the slope and intercept with lignin content, acetyl content, crystallinity, and carbohydrate content. The validity of these models has been evaluated to predict digestibilities of various biomass types (corn stover, bagasse, and rice straw) treated by the following methods: ammonia fiber explosion (AFEX), aqueous ammonia, oxidative lime, nonoxidative lime, and dilute acid.

CORRELATION FOR MODEL LIGNOCELLULOSES

As it was pointed out, the effects of these three structural features on glucan and xylan digestibility were different (Chang and Holtzapple, 2000), thus two kinds of mathematical models correlating glucan and xylan conversions with structural features were derived. In this study, a total of 18 mathematical models were developed to depict the correlations of structural features with the slopes and intercepts of glucan, xylan, and total sugar hydrolyses at incubation periods of 1, 6, and 72 h. Schematics of the modeling approach are shown in Figure II-2.

Materials and Methods

The preparation of the model lignocelluloses, enzymatic hydrolysis, and analytical methods for determining biomass structural features, carbohydrate contents, and sugar conversions are given in Chapter II. The parametric (multiple linear models) and nonparametric (ACE) approach are introduced in Chapter III.

Results and Discussion

Parametric Regression Model

Equations V-1 and V-2 were proposed to correlate the slopes and intercepts of glucan, xylan, and total sugar hydrolyses at 1, 6, and 72 h with three structural features, respectively using parametric regression models.

$$\text{Slope } (A) = f\,(\text{Lignin, Acetyl, CrI}_C\text{, Carbohydrate}) \quad \text{(V-1)}$$

$$\text{Intercept } (B) = f\,(\text{Lignin, Acetyl, CrI}_C\text{, Carbohydrate}) \quad \text{(V-2)}$$

where CrI_C is cellulose crystallinity and carbohydrate is glucan, xylan, or total sugar. The lignin content is expressed as a percentage of the total biomass rather than as a ratio to glucan or xylan. Because of low glucan or xylan contents in some biomass samples used to evaluate the predictive ability of these models, the lignin/glucan or lignin/xylan ratios are not in the range of the model lignocelluloses. Similarly, acetyl content is expressed as a percentage of the total biomass, rather than as a ratio. Carbohydrate content is considered as an independent variable that directly influences digestibility. Because cellulose crystallinity is the factor that influences biomass digestibility the most and because biomass crystallinity depends on the contents of amorphous lignin and hemicellulose, cellulose crystallinity is used instead of biomass crystallinity as one of the structural features by correlating cellulose crystallinity with biomass crystallinity and hemicellulose content (Equation IV-1). To make the correlation parameters fall in a reasonable range, the values of some independent variables were scaled. The dependent variable and scaled independent variables are shown in Tables IV-9 to IV-11. To obtain

reliable mathematical models, model lignocelluloses with coefficients of determinations (R^2) smaller than 0.93 were not used for model development.

Multiple linear regression models are often used as empirical models or approximating functions when more than one independent variable is involved. That is, the true functional relationship between the dependent variable and independent variables is unknown, but by utilizing complex forms of independent variables, the multiple linear regression model adequately approximates the true unknown functions. In this study, mathematical models that include the quadratic terms of each independent variable and the interaction terms between the three structural features may take the following form:

$$y = \beta_0 + \beta_1 L + \beta_2 A + \beta_3 CrI_C + \beta_4 C + \beta_{11} L^2 + \beta_{22} A^2 + \beta_{33} CrI_C{}^2 + \beta_{44} C^2 + \beta_{12} L * A + \beta_{13} L * CrI_C + \beta_{23} A * CrI_C + \varepsilon \quad \text{(V-3)}$$

where y = slope or intercept

L = lignin content (%) × 0.1

A = acetyl content (%)

CrI_C = cellulose crystallinity (%) × 0.1

C = carbohydrate content (%) × 0.1

β_0–β_{44} are correlation parameters, ε is random errors.

Equation V-3 is valid in the region

$$0.7\% < L < 26.3\% \quad \text{(V-4)}$$

$$0.1\% < A < 3.0\% \quad \text{(V-5)}$$

$$13.9\% < CrI_C < 79.8\% \quad \text{(V-6)}$$

$$44.4\% < \text{Glucan} < 76.5\% \quad \text{(V-7)}$$

$$13.8\% < \text{Xylan} < 17.6\% \quad \text{(V-8)}$$

$$58.3\% < \text{Total sugar} < 91.6\% \quad \text{(V-9)}$$

Although Equation V-3 includes all the influential factors, not all of these variables may be significant factors for the 18 different dependent variables. An appropriate subset of variables for each model should be determined. Building a regression model that includes a subset of available variables involves two conflicting objectives: (1) It is desirable to include as many variables as possible in the model so that the information content in these factors can influence the predicted value of y. (2) The variance of the prediction y increases as the number of variables increases. The process of finding a model is a compromise between these two objectives. Various criteria for selecting variables and evaluating regression models are employed. In this study, Mallow's C_P value, which is related to the mean square error of a fitted value, is used as the criterion. Generally, small values of C_P are desirable, indicating low total error. The computational techniques for variable selection on the basis of Mallow's C_P value can be accomplished using the SAS PROC REG stepwise regression algorithm. It is also recommended that the predictive ability of a model be assessed by observing its performance on new data not used to build the model. In this study, the criteria for variable selection are the combination of the Mallow's C_P value and the predictive ability of a model.

After variables in each model are determined, correlation parameters are obtained using the SAS PROC REG. Tables V-1 to V-3 summarize the correlation parameters for the slopes and intercepts of glucan, xylan, and total sugar hydrolyses, respectively. It is evident that 5–8 variables are selected to predict the slopes and intercepts. Based on the observations of correlation parameters, lignin content (β_1 and β_{11}) showed significant influence on all the slopes and intercepts of glucan, xylan, and total sugar hydrolyses except for the 1-h intercept; cellulose crystallinity (β_3 and β_{33}) had more influence on the slopes and intercepts of glucan hydrolysis than on those of xylan hydrolyses. Compared to lignin content and cellulose crystallinity, acetyl content (β_2 and β_{22}) had less effect on

the slopes and intercepts of glucan, xylan, and total sugar hydrolyses. It is conclusive that lignin content and crystallinity have more significant effect on biomass digestibility than acetyl content, which agrees well with Chang's conclusion (Chang and Holtzapple, 2000). It is apparent that the quadratic terms of glucan or xylan and interaction terms between three structural features are selected to correlate with the slopes and intercepts.

Table V-1. Correlation parameters for slopes and intercepts of glucan hydrolysis

Parameters	1 h		6 h		72 h	
	Slope	Intercept	Slope	Intercept	Slope	Intercept
β_0	34.87	9.16	22.55	59.9	33.68	116
β_1	-----	-----	7.65	3.96	3.88	12.2
β_2	-1.12	-1.52	-----	-3.46	-3.73	-----
β_3	-----	1.50	2.05	-1.53	-2.44	-----
β_4	-----	-----	-----	-----	-----	-----
β_{11}	-2.09	-----	-3.5	-4.39	-3.2	-10
β_{22}	-----	-----	-----	-----	1.04	-----
β_{33}	-0.24	-0.20	-0.19	-0.33	0.25	-0.4
β_{44}	-0.23	-0.13	-----	-0.44	-----	-0.59
β_{12}	-----	-----	-----	-----	-0.57	-0.17
β_{13}	-----	-0.33	-1.1	-----	-0.54	-2
β_{23}	-0.18	0.11	-0.33	-----	-----	-1.1
R^2	0.95	0.72	0.93	0.95	0.90	0.96
MSE	2.5	1.0	4.3	7.1	6.9	22
No. of variables	5	6	6	6	8	7

Lignin content (%) × 0.1.

Acetyl content (%).

Cellulose crystallinity (%) × 0.1.

Glucan content (%) × 0.1.

Table V-2. Correlation parameters for slopes and intercepts of xylan hydrolysis

Parameters	1 h		6 h		72 h	
	Slope	Intercept	Slope	Intercept	Slope	Intercept
β_0	9.15	4.18	16.2	43.2	16.7	82.6
β_1	1.69	0.42	12.66	12.2	9.08	43.2
β_2	1.19	-----	-----	-----	-----	3.85
β_3	-----	0.79	1.21	-----	-----	-----
β_4	-----	-----	-----	-----	-----	-----
β_{11}	-----	-----	-4.20	-4.67	-3.09	-15.3
β_{22}	-----	-----	-----	-----	-----	-----
β_{33}	-----	-0.1	-----	-0.24	0.17	-----
β_{44}	-0.84	-----	-1.52	-----	-2.83	-1.55
β_{12}	-0.79	-0.62	-----	-2.74	-----	-4.15
β_{13}	-0.25	-0.21	-1.22	-1.17	-0.86	-3.9
β_{23}	-0.13	-----	-0.29	-----	-0.14	-0.76
R^2	0.69	0.71	0.86	0.9	0.63	0.95
MSE	1.1	1.3	3.4	15	6.3	35
No. of variables	6	5	6	5	6	7

Lignin content (%) × 0.1.

Acetyl content (%).

Cellulose crystallinity × 0.1.

Xylan content (%) × 0.1.

Table V-3. Correlation parameters for slopes and intercepts of total sugar hydrolysis

Parameters	1 h		6 h		72 h	
	Slope	Intercept	Slope	Intercept	Slope	Intercept
β_0	23.8	13.2	21.1	-16.9	25.6	160
β_1	2.5	-0.28	7.84	-----	3.45	-----
β_2	-----	-1.55	-----	-3.61	-----	-----
β_3	-----	1.2	1.69	-----	-1.1	-----
β_4	-----	-----	-----	22.6	-----	-----
β_{11}	-2.13	-0.34	-3.37	-3.36	-2.87	-8.4
β_{22}	-----	-----	-----	-----	-----	-----
β_{33}	-0.15	-0.17	-0.13	-0.47	0.2	-0.27
β_{44}	-0.07	-0.13	-----	-1.86	-----	-0.96
β_{12}	-----	-----	-----	-----	-----	-----
β_{13}	-0.13	-0.25	-1.1	-----	-0.62	-2.16
β_{23}	-0.29	0.1	-0.33	-----	-0.22	-1.35
R^2	0.94	0.74	0.93	0.95	0.88	0.96
MSE	1.9	0.9	3.6	5.9	5.6	25
No. of variables	6	8	6	5	6	5

Lignin content (%) × 0.1.

Acetyl content (%).

Cellulose crystallinity × 0.1.

Total sugar content (%) × 0.1.

Using Equation V-3 and the parameters in Table V-1, the slopes and intercepts of glucan hydrolysis were calculated and compared with the measured data in Table IV-9, as shown in Figures V-1 to V-3 for 1-, 6-, and 72-h hydrolysis, respectively. The R^2 values were in the range of 0.9 to 0.96 for the slopes and intercepts of glucan hydrolysis except for the 1-h intercept (i.e., 0.72), indicating that Equation V-3 describes the 1-, 6-, and 72-h slopes and intercepts of glucan hydrolysis satisfactorily. Almost all of the data points are in the region of the 95% prediction interval. Except for the 1-h intercept, the 95% prediction intervals of the slopes and intercepts were relatively narrow, indicating small errors of prediction. The large value of 72-h intercept caused the large MSE value in Table V-1 can. The small R^2 value of the 1-h intercept can be explained: the R^2 values for the regression of 1-h glucan and xylan conversions versus the natural logarithm of cellulase loadings (shown in Tables IV-9 and IV-10) were not as good as those of 6 and 72 h. Moreover, it was indicated in Chapter IV that the effects of structural features on the 1-h intercept were not conclusive.

Similarly, the 1-, 6-, and 72-h slopes and intercepts of xylan hydrolysis were calculated using Equation V-3 and the parameters in Table V-2. The plots of the calculated slopes and intercepts vs the measured data in Table IV-10 are shown in Figures V-4 to V-6 for 1-, 6-, and 72-h hydrolysis, respectively. Although most of the data points are in the range of the 95% prediction interval, the wider range of the interval indicates less predictive ability. The R^2 values for the regressions of the 1-h slope and intercept, and 72-h slope (0.69, 0.70, and 0.63, respectively) were much lower than those of the 6-h slope and intercept, and 72-h intercept (0.84, 0.9, and 0.95, respectively), indicating that Equation V-3 predicts the 1-h slope and intercept, 72-h slope of xylan hydrolysis less satisfactorily than it does for the 6-h slope and intercept, and 72-h intercept. The regressions of 72-h xylan conversions versus the natural logarithm of cellulase loadings were as good as those of glucan (Table IV-10); however, the correlation of 72-h slope with structural features was worse than that of glucan. Because the 72-h slopes of xylan hydrolysis for low-crystallinity poplar wood were small, the correlation of the 72-h xylan slopes for highly-crystalline poplar wood with structural

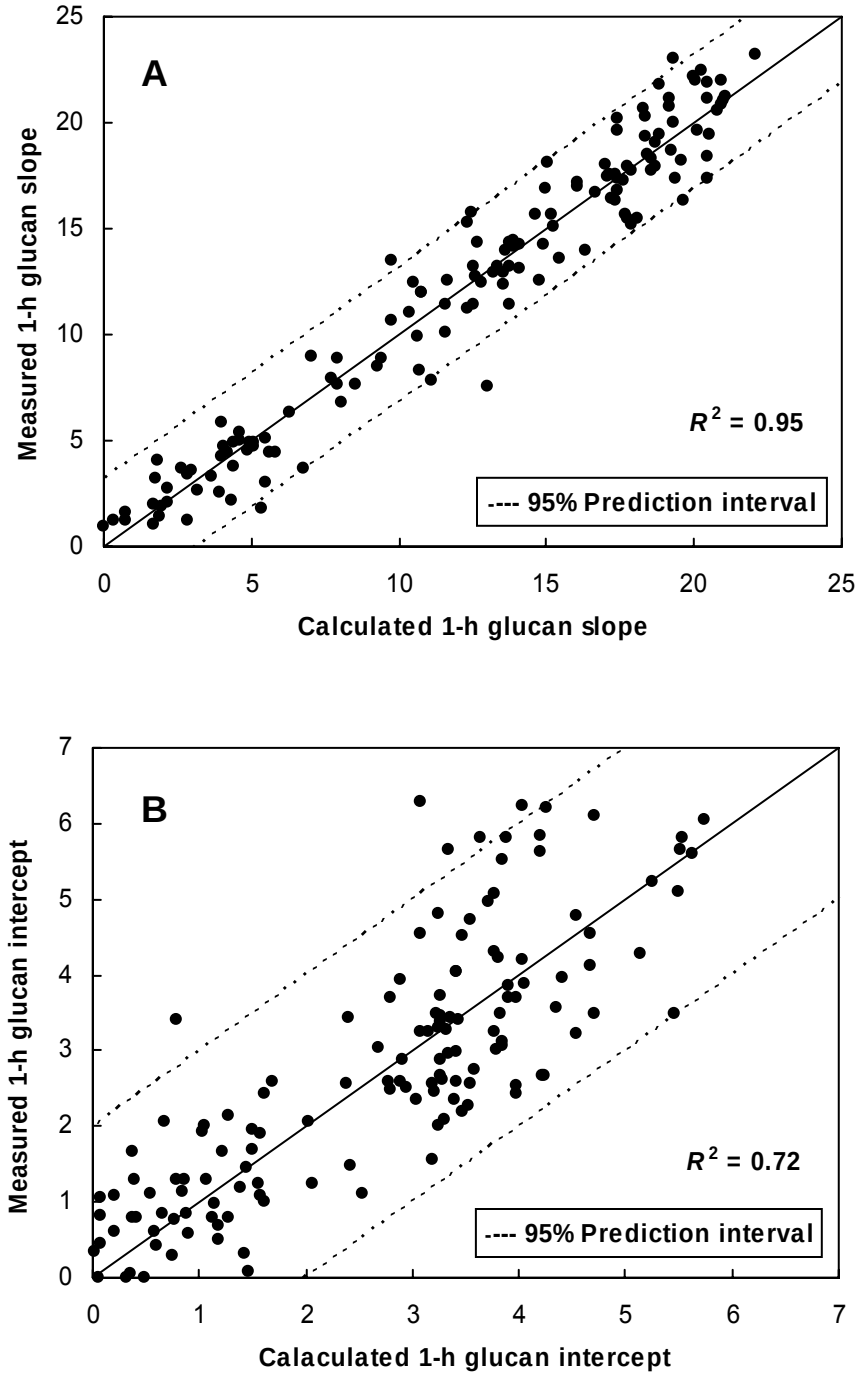

Figure V-1. Correlation between 1-h slope and intercept of glucan hydrolysis with *L*, *A*, CrI_C, and *G* for model lignocelluloses: (A) slope; (B) intercept. Calculated slope and intercept were obtained using Equation V-3.

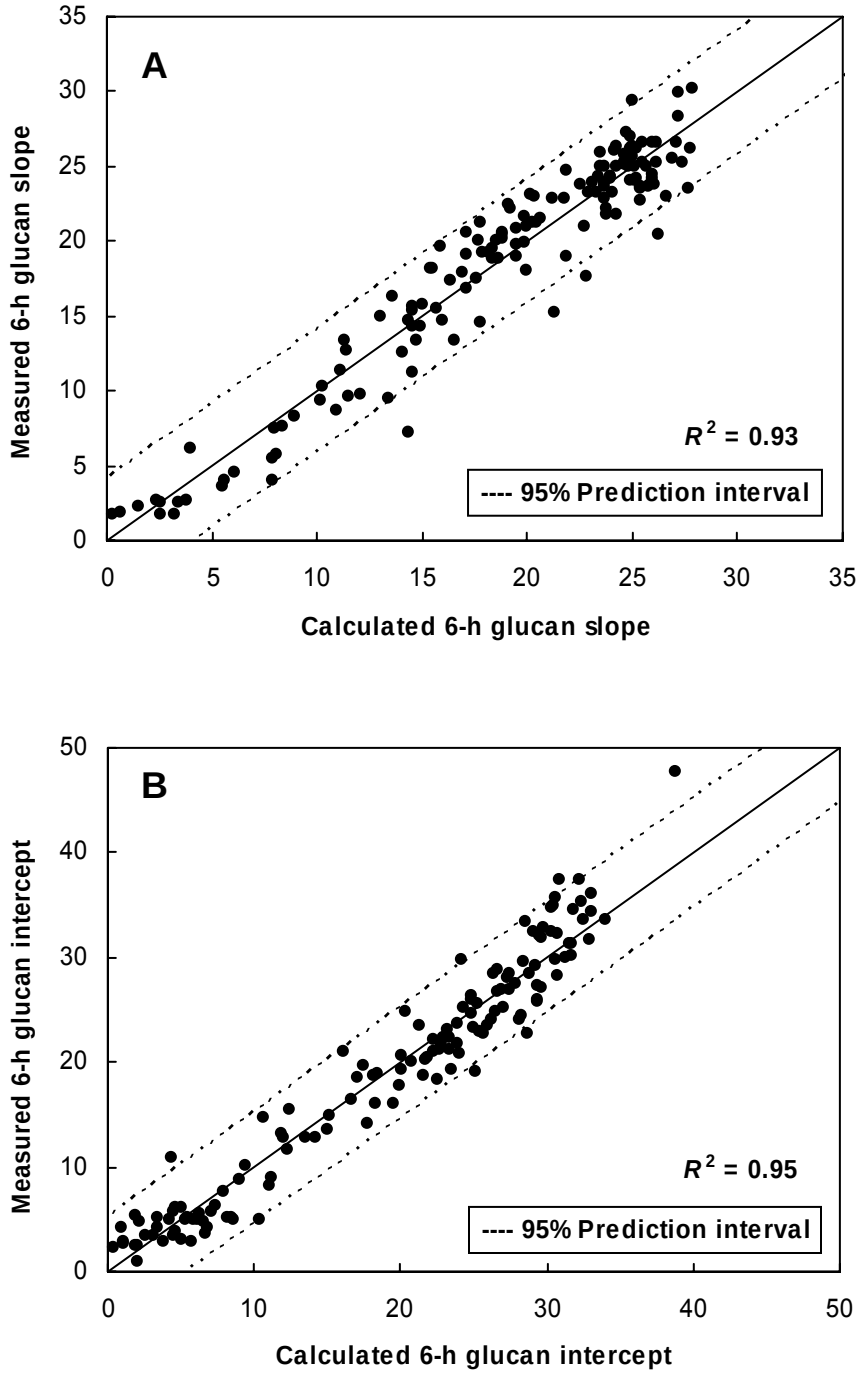

Figure V-2. Correlation between 6-h slope and intercept of glucan hydrolysis with *L*, *A*, CrI_C, and *G* for model lignocelluloses: (A) slope; (B) intercept. Calculated slope and intercept were obtained using Equation V-3.

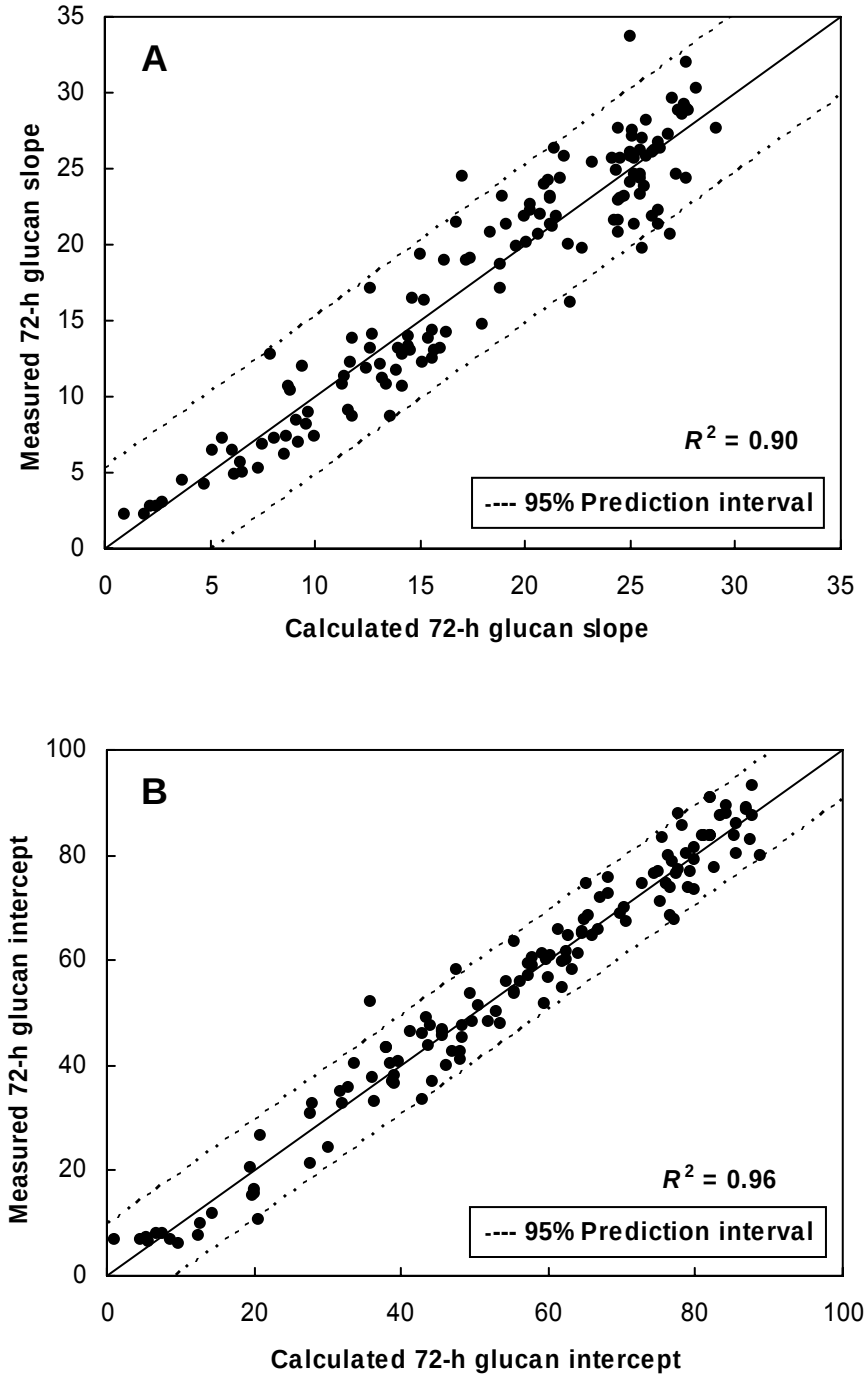

Figure V-3. Correlation between 72-h slope and intercept of glucan hydrolysis with *L*, *A*, CrI_C, and *G* for model lignocelluloses: (A) slope; (B) intercept. Calculated slope and intercept were obtained using Equation V-3.

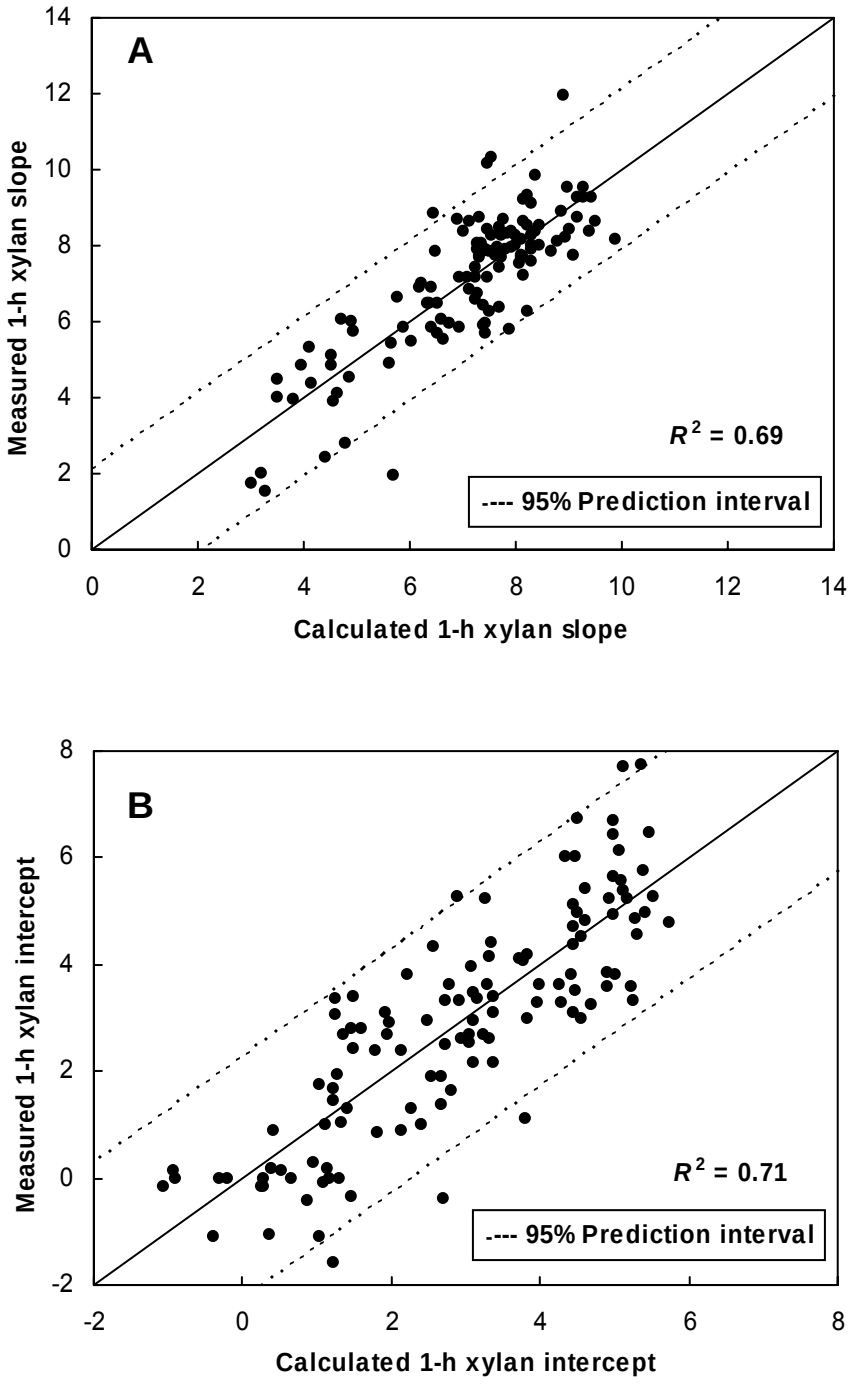

Figure V-4. Correlation between 1-h slope and intercept of xylan hydrolysis with *L*, *A*, CrI_C, and *X* for model lignocelluloses: (A) slope; (B) intercept. Calculated slope and intercept were obtained using Equation V-3.

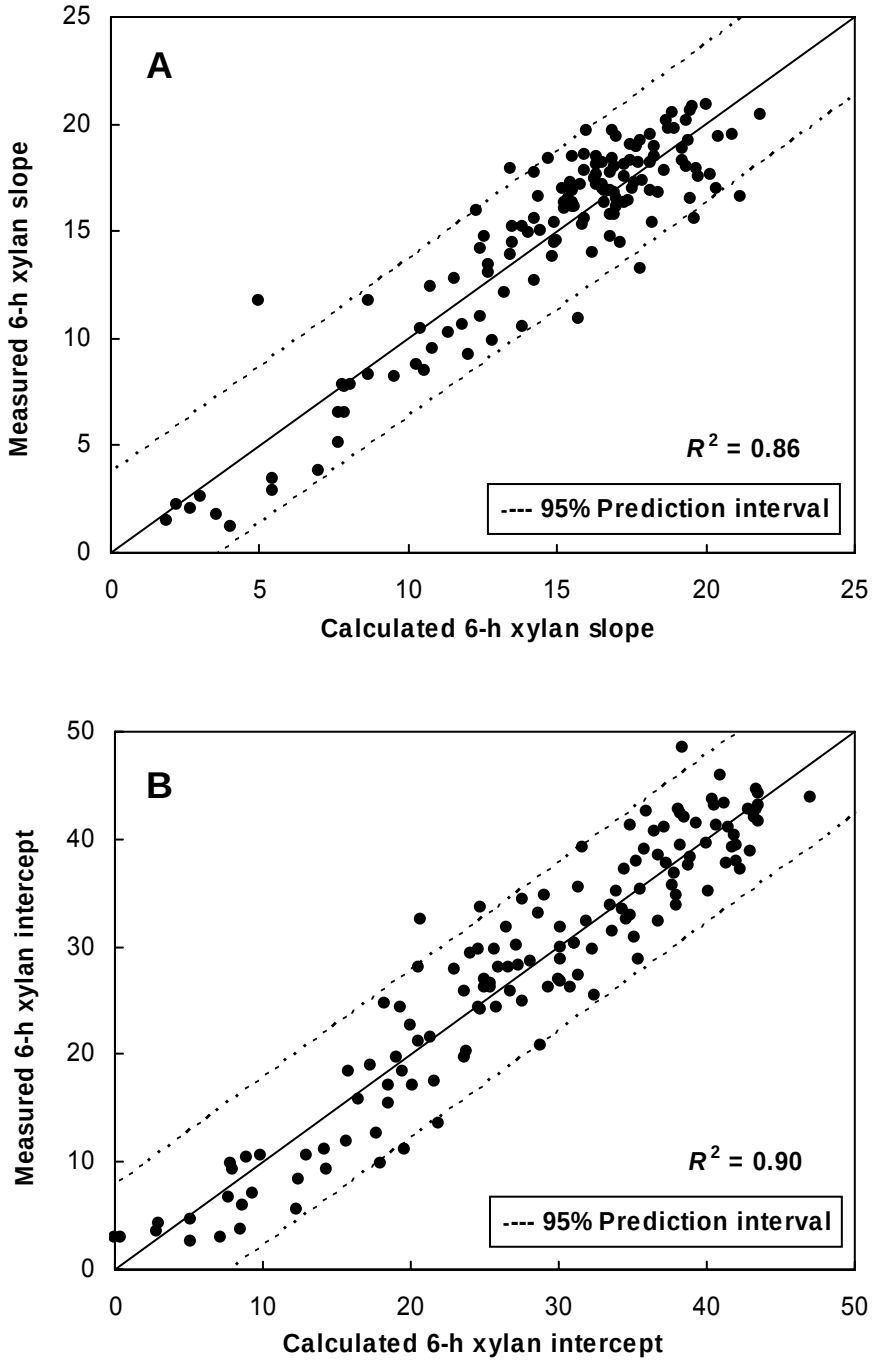

Figure V-5. Correlation between 6-h slope and intercept of xylan hydrolysis with *L*, *A*, CrI_C, and *X* for model lignocelluloses: (A) slope; (B) intercept. Calculated slope and intercept were obtained using Equation V-3.

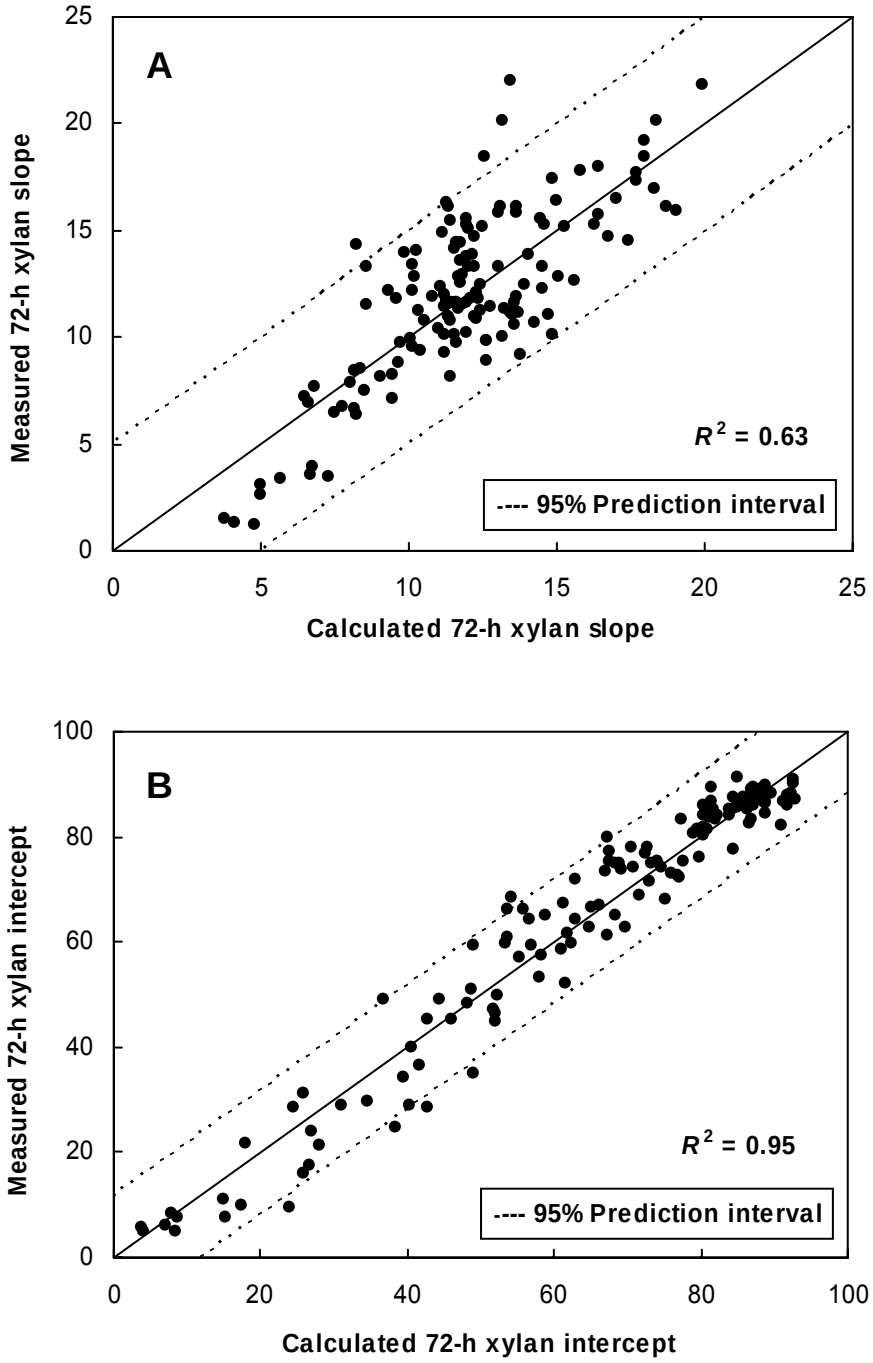

Figure V-6. Correlation between 72-h slope and intercept of xylan hydrolysis with *L*, *A*, CrI_C, and *X* for model lignocelluloses: (A) slope; (B) intercept. Calculated slope and intercept were obtained using Equation V-3.

features was fairly good (i.e., 0.88 not shown). Apparently, the regressions for the slopes and intercepts of glucan hydrolysis were much better than those of xylan hydrolysis by comparing the corresponding R^2 values. This may result from three possible causes:

1. In the model lignocelluloses, the xylan content is only 1/3 to 1/5 of the glucan content. It is difficult to determine an accurate xylose concentration in the enzymatic hydrolyzate at 10-g/L substrate concentration, low enzyme loadings, and short incubation periods.
2. The enzyme loading is expressed as cellulase, not xylanase. Furthermore, the xylanase activity in the supplemental cellobiase should be quantified if a large amount of cellobiase is supplemented (Lu et al., 2002). The method of measuring xylanase activity in the enzyme complex is given in Appendix G.
3. Because glucan is closely associated with xylan in lignocellulosic biomass and because cellulase and xylanase in the enzyme complex need to adsorb on glucan and xylan, respectively, the hydrolyses of glucan and xylan may interfere with each other due to steric hindrance.

The 1-, 6-, and 72-h slopes and intercepts of total sugar hydrolysis were calculated using Equation V-3 and the parameters in Table V-3. Figures V-7 to V-9 show the plots of the calculated slopes and intercepts vs the measured data in Table IV-11 for 1-, 6-, and 72-h hydrolysis, respectively. The R^2 values were in the range of 0.88 to 0.95 for the slopes and intercepts of total sugar, except for the 1-h intercept (i.e., 0.74), indicating that Equation V-3 describes the 1-, 6-, and 72-h slopes and intercepts of total sugar hydrolysis satisfactorily. Compared to the correlations of glucan hydrolysis, the correlations of total sugar hydrolysis had smaller MSE values; therefore, the 95% prediction intervals were narrower than those of glucan.

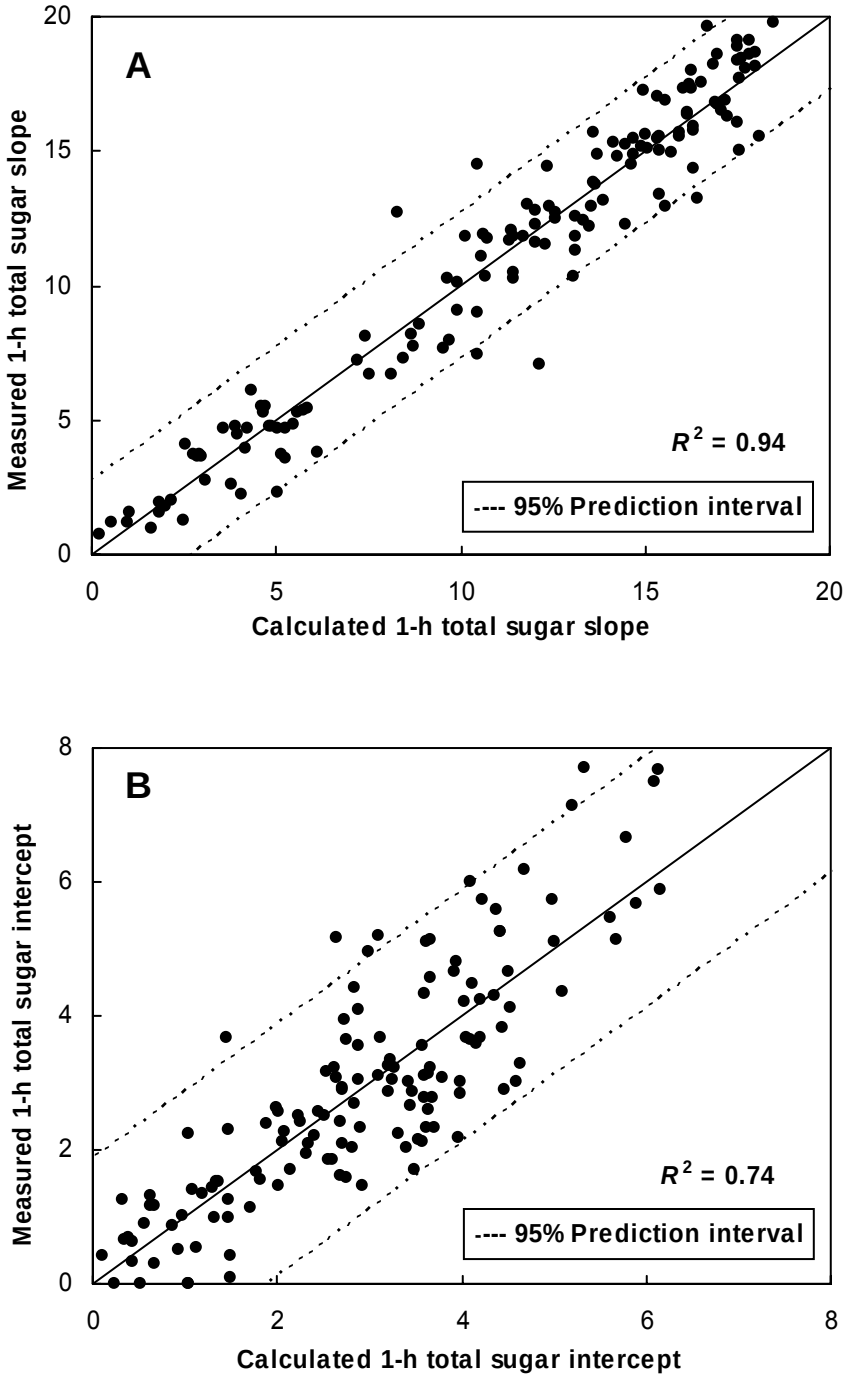

Figure V-7. Correlation between 1-h slope and intercept of total sugar hydrolysis with *L*, *A*, CrI_C, and *TS* for model lignocelluloses: (A) slope; (B) intercept. Calculated slope and intercept were obtained using Equation V-3.

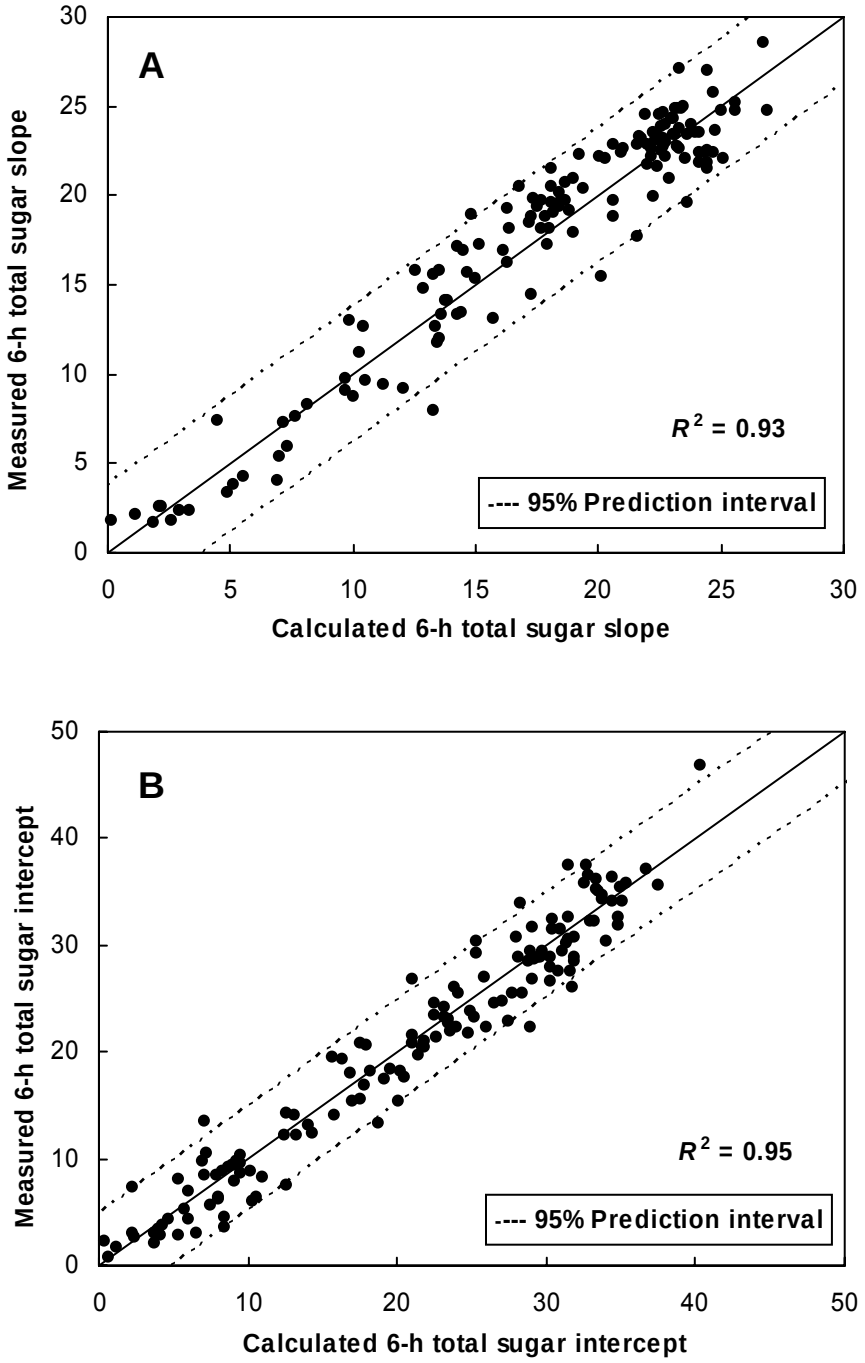

Figure V-8. Correlation between 6-h slope and intercept of total sugar hydrolysis with *L*, *A*, CrI_C, and *TS* for model lignocelluloses: (A) slope; (B) intercept. Calculated slope and intercept were obtained using Equation V-3.

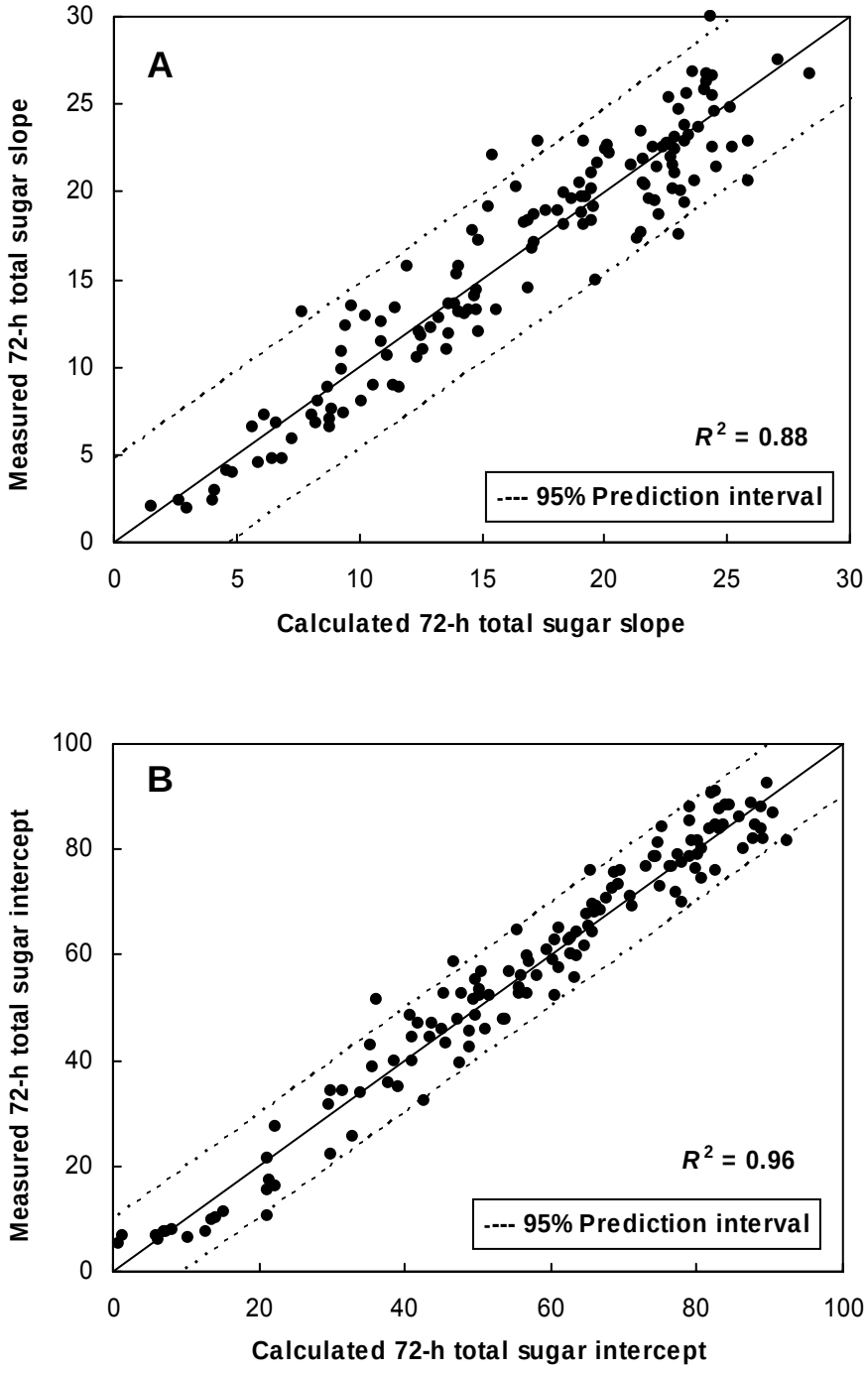

Figure V-9. Correlation between 72-h slope and intercept of total sugar hydrolysis with *L*, *A*, CrI_C, and *TS* for model lignocelluloses: (A) slope; (B) intercept. Calculated slope and intercept were obtained using Equation V-3.

Nonparametric Regression Model

Nonparametric regression requires no assumed functional form between the dependent and independent variables; the correlation is derived solely based on the data set. The ACE (*alternating conditional expectations*) algorithm provides an optimal correlation between a dependent variable and multiple independent variables through nonparametric transformations of dependent and independent variables. The final correlation is given by plotting the transformed dependent variable against the sum of the transformed independent variables. Furthermore, ACE also has been shown to identify the dominant and the optimum number of independent variables when more independent variables are involved (Wu et al., 2000). Insight into the relationship between the dependent and independent variables gained in ACE can be employed to develop effective models by other approaches, such as neural networks and multiple linear models.

The GRACE program (Graph of ACE), which was developed on the basis of the ACE algorithm (Breiman and Friedman, 1985), has been used successfully to correlate 3-D seismic data with well data (Xue, 1997). This software was kindly provided by Dr. Datta-Gupta (Petroleum Engineering, Texas A&M University). The program generates a transformed value corresponding to each data point for the dependent and independent variables. These data can be used to obtain plots of optimal transformations for the dependent and each independent variable, transformed dependent variable vs. sum of transformed independent variables, and observed vs. predicted values of the dependent variable based on the optimal correlation developed. To obtain the predicted dependent variable given a set of independent variables, the transformation of the dependent variable is monotonic and the transformations of the independent variables are orderable.

To predict the dependent variable, it is desirable to generate the functional form of each transformation. The GRACE program generates an EXCEL file that summarizes the results used for generating functional forms, which is accomplished using the EXCEL macro. The GRACE program provides two kinds of coefficients of determination (R^2): (1) the maximal R^2 for the correlation between the transformed

dependent variables and the sum of transformed independent variable, which is based only on the data set; and (2) the fitted R^2 for the correlation between the measured values of dependent variable and the calculated values obtained through a series of functional forms that transform the dependent and independent variables. The latter R^2 is usually smaller than the prior one and highly depends on the functional forms chosen for each transformation. The more appropriate the functional forms for transformation are, the smaller the difference between these two kinds of R^2.

Using the nonparametric regression approach, Equations V-10 and V-11 were proposed to correlate the 1-, 6-, and 72-h slopes and intercepts of glucan, xylan, and total sugar hydrolyses with three structural features, respectively.

$$\text{Slope } (A) = f\,(\text{Lignin, Acetyl, CrI}_C) \tag{V-10}$$

$$\text{Intercept } (B) = f\,(\text{Lignin, Acetyl, CrI}_C) \tag{V-11}$$

Equations V-10 and V-11 are valid in the region

$$0.7\% < \text{Lignin} < 26.3\% \tag{V-12}$$

$$0.1\% < \text{Acetyl} < 3.0\% \tag{V-13}$$

$$13.9\% < \text{CrI}_C < 79.8\% \tag{V-14}$$

The correlation data in Table V-4 indicate that considering glucan or xylan content as one of the independent variables, – just like the lignin content (L), acetyl content (A), cellulose crystallinity (CrI_C) – does not improve the correlations of the slopes or intercepts. The maximal R^2, fitted R^2, and MSE values in the models developed with four independent variables were comparable to those models developed with three independent variables. Therefore, in the nonparametric models, the slopes and intercepts are correlated with just the three structural features. The correlation parameters in the

parametric models correlating the slopes and intercepts with the three structural features are shown in APPENDIX J.

Table V-4. Comparison of correlation parameters determined with four and three independent variables using the nonparametric approach

Dependent variable		Four independent variables			Three independent variables		
		L[a], A[b], CrI_C[c], carbohydrate content[d]			L[a], A[b], CrI_C[c]		
		Maxi R^2	Fitted R^2	MSE	Maxi R^2	Fitted R^2	MSE
Glucan	1-h slope	0.97	0.93	3.3	0.98	0.94	2.9
	1-h intercept	0.88	0.68	1.1	0.91	0.72	1
	6-h slope	0.96	0.83	9.9	0.96	0.84	9.3
	6-h intercept	0.98	0.91	11	0.99	0.94	7.8
	72-h slope	0.95	0.81	12	0.95	0.86	9
	72-h intercept	0.98	0.94	37	0.98	0.94	41
Xylan	1-h slope	0.86	0.51	1.8	0.84	0.51	1.7
	1-h intercept	0.87	0.67	1.4	0.86	0.69	1.4
	6-h slope	0.91	0.51	11	0.9	0.52	11
	6-h intercept	0.94	0.84	24	0.94	0.83	26
	72-h slope	0.87	0.36	10	0.88	0.33	11
	72-h intercept	0.97	0.86	105	0.97	0.86	105
Total Sugar	1-h slope	0.97	0.93	2.1	0.97	0.94	2.1
	1-h intercept	0.88	0.66	1.1	0.90	0.61	1.3
	6-h slope	0.95	0.86	6.7	0.95	0.83	8.8
	6-h intercept	0.98	0.94	8	0.98	0.93	8.9
	72-h slope	0.95	0.79	9.8	0.95	0.84	7.6
	72-h intercept	0.98	0.92	48	0.98	0.92	49

[a] Lignin content.

[b] Acetyl content.

[c] Cellulose crystallinity.

[d] Carbohydrate content: glucan, xylan, and total sugar. Total sugar = glucan + xylan.

Table V-5 compares the fitted R^2 values and MSE determined by the nonparametric and parametric regression models. The R^2 values determined by nonparametric models are usually smaller, and the MSE values are larger, indicating that nonparametric models predict the slopes and intercepts of glucan, xylan, and total sugar hydrolysis less satisfactorily than the parametric models. Because the appropriate functional forms for the transformation of each variable are not easily assumed, the summation of these transformations results in larger errors of the predicted slopes and intercepts.

Although ACE could provide the optimal correlation between the transformed dependent variable and the sum of transformed independent variables, it is highly sensitive to outliers (Breiman and Friedman, 1985; Tibshirani, 1988). ACE results depend on the order in which the independent variables are entered into analysis (Wang and Murphy, 2004), i.e., the order they are in the X matrix. ACE will not generally perform well with empirical data due to the following reasons which include: (1) some unobservable independent variables are omitted; (2) some superfluous variables may be included in the regression model; (3) the dependent variable has a lower correlation with independent variables; (4) correlation exists in some independent variables; (5) outliers tend to exist. The correlation between the transformed dependent variable and the sum of transformed independent variables can be improved as above reasons are considered.

It is noticeable that the MSE values of 6- and 72-h slopes and intercepts of xylan hydrolysis in the nonparametric models are much larger than those in the parametric models. Considering the influence of glucan on xylan hydrolysis, the corresponding predicted slope or intercept of glucan hydrolysis was considered as one of the independent variables, i.e., the 6-h glucan slope predicted by the nonparametric model was assumed as one of the independent variables for the correlation of the 6-h slope of xylan hydrolysis. Table V-6 shows that the R^2 and MSE values of 6- and 72-h slopes and intercepts of xylan hydrolysis are improved significantly whereas the correlations of 1-h slope and intercept of xylan hydrolysis do not improve when the predicted 1-h slope and intercept of glucan hydrolysis are involved, respectively. The plots (not shown)

comparing the measured slopes and intercepts and the values calculated by the nonparametric models were similar to those determined by the parametric models and the larger MSE values in the nonparametric models led to wider 95% prediction interval in the plots.

Table V-5. Comparison of correlation parameters determined by the parametric and nonparametric models

Dependent variables		Parametric model		Nonparametric model	
		R^2	MSE	R^2	MSE
Glucan	1-h slope	0.95	2.5	0.94	2.9
	1-h intercept	0.72	1.0	0.72	1
	6-h slope	0.93	4.3	0.84	9.3
	6-h intercept	0.95	7.1	0.94	7.8
	72-h slope	0.9	6.9	0.86	9
	72-h intercept	0.96	22	0.94	41
Xylan	1-h slope	0.69	1.1	0.51	1.7
	1-h intercept	0.71	1.3	0.69	1.4
	6-h slope	0.86	3.4	0.52	11
	6-h intercept	0.9	15	0.83	26
	72-h slope	0.63	6.3	0.33	11
	72-h intercept	0.95	35	0.86	105
Total Sugar	1-h slope	0.94	1.9	0.94	2.1
	1-h intercept	0.74	0.9	0.61	1.3
	6-h slope	0.93	3.6	0.83	8.8
	6-h intercept	0.95	5.9	0.93	8.9
	72-h slope	0.88	5.6	0.84	7.6
	72-h intercept	0.96	25	0.92	49

Table V-6. Summary of correlation parameters for slopes and intercepts of xylan hydrolysis determined by the nonparametric models

Independent variables	Correlation coefficients	1 h		6 h		72 h	
		Slope	Intercept	Slope	Intercept	Slope	Intercept
L^a, A^b, CrI_C^c	R^2	0.51	0.69	0.52	0.83	0.33	0.86
	MSE	1.7	1.4	11	26	11	105
L^a, A^b, CrI_C^c, predicted data of glucan	R^2	0.55	0.69	0.8	0.87	0.58	0.94
	MSE	1.6	1.4	4.4	21	7.2	42

[a] Lignin content.

[b] Acetyl content.

[c] Cellulose crystallinity.

Conclusions

In summary, both the parametric and nonparametric models correlated well the 1-, 6-, and 72-h slopes and intercepts of glucan, xylan, and total sugar hydrolyses with lignin content, acetyl content, cellulose crystallinity, and carbohydrate content (only for the parametric models). From the observations of variables selected for each model by the parametric approach, lignin content and cellulose crystallinity have more effect on the slopes and intercepts of glucan, xylan, and total sugar hydrolyses than acetyl content. Based on the R^2 and MSE values, the parametric models – which include the quadratic and interaction terms of three structural features – provided more satisfactory correlations than the nonparametric models.

PREDICTIVE ABILITY OF MODELS

A satisfactory model correlating digestibility with structural features should be able to predict the digestibility of a variety of biomass types other than those used to derive the models. The predictive ability of these models was evaluated by predicting the digestibility of corn stover, bagasse, and rice straw treated by the following methods: AFEX, aqueous ammonia, oxidative lime, nonoxidative lime, and dilute acid.

Materials and Methods

Substrate Preparation

Our group members provided oxidative and nonoxidative lime-treated corn stover (Kim, 2004), lime-treated bagasse, and lime-treated rice straw. Dr. Dale's research group at Michigan State University kindly provided AFEX-treated corn stover. The treatment conditions are described by Teymouri et al. (2004). Bagasse and rice straw were treated with 1% (w/w) H_2SO_4 at 121°C for 2 h; the liquid loading was 20 mL/g dry biomass. Bagasse was treated with 15% (w/w) aqueous ammonia at 60°C for 12 h; the liquid loading was 6–8 mL/g dry biomass. The pretreated bagasse and rice straw were washed and centrifuged to remove the acid- or base-soluble biomass until the pH of the biomass slurry was neutral. The pretreated biomass was dried at 45°C and ground through a 40-mesh sieve. In many cases, the pretreated biomass was ball milled for 2–6 d to decrease crystallinity. The detailed procedures of various chemical pretreatments and ball milling are described in Appendices A and C, respectively. Lignin content, acetyl content, cellulose crystallinity, and carbohydrate content of pretreated biomass samples were measured using the methods described in Chapters II and IV.

Enzymatic Hydrolysis

The hydrolysis conditions were temperature = 50°C, pH = 4.8, substrate concentration = 10 g/L, cellobiase loading = 81.25 CBU/g dry biomass, dry weight of biomass = 0.2 g, slurry volume = 20 mL, rotating speed = 100 rpm, incubation period = 1, 6, and 72 h. The cellulase loading for each sample was employed on the basis of structural features (shown in Table IV-8). The detailed procedure for enzymatic hydrolysis is given in Appendix B. Glucose and xylose concentrations were measured using HPLC. Glucose, xylose, and total sugar conversions were calculated using Equations II-4 to II-6. The detailed procedure for sugar analysis using HPLC is described in Appendix E.

Verification of Mathematical Models

Carbohydrate conversions at a given time versus the natural logarithm of cellulase loadings were plotted to obtain the measured slopes and intercepts of the straight lines. The predicted slopes and intercepts were obtained from structural features using the parametric and nonparametric models. Model verification was accomplished comparing the measured and predicted slopes and intercepts, and the measured and predicted sugar conversions calculated from the predicted slopes and intercepts.

Results and Discussion

Table V-7 summarizes the pretreatment conditions, carbohydrate contents, and structural features of pretreated biomass used to evaluate the predictive ability of the models. Figure V-10 illustrates the distributions of the three structural features and carbohydrate contents of the biomass samples used for model verification. The boxes indicate the range of structural features or carbohydrate contents in the model lignocelluloses. The plots show that all the data of cellulose crystallinity fall in the region of model samples; all the data of lignin content are in the range of model samples except for dilute acid-treated biomass. Acetyl contents in lime-treated corn stover and aqueous ammonia-treated baggase are not in the range of model samples. Due to the narrow range of xylan content of model samples, most data of xylan content fall outside the region. Only half glucan content data are in the range of model samples.

Table V-7. Pretreatment condition, structural features, and carbohydrate contents of biomass samples for model verification

Sample	Pretreatment condition						Structural features (%)			Carbohydrate content (%)		Category of reactivity
	Biomass	Reagent loading (g/g dry biomass)	Liquid/ solid (mL/g)	Time (h)	Temp (°C)	Ball milling time (d)	Lignin content	Acetyl content	CrI_B[a]	Glucan	Xylan	
Lime ($Ca(OH)_2$)												
C1[b]	Corn stover	0.5	10	2688	45	0	9.94	0.03	61.6	44.3	14.37	High
C2[c]	Corn stover	0.5	10	2016	45	0	14.35	0.11	58.8	48.14	21.81	High
C3	Corn stover	0.1	10	2	100	3	18.14	0.03	19.1	45.77	20.83	High
C4	Corn stover	0.1	10	2	100	6	18.07	0.03	11.8	47.43	21.47	High
B1	Bagasse	0.1	10	1	100	0	27.16	0.50	60.1	33.49	13.46	Low
B2	Bagasse	0.1	10	1	100	4	27.16	0.50	18.5	33.49	13.46	High
R1	Rice straw	0.1	10	1	100	0	31.19	0.80	50.0	30.12	14.07	Low
R2	Rice straw	0.1	10	1	100	2	30.75	0.80	33.9	29.77	14.01	Medium
Dilute acid (H_2SO_4)												
B3	Bagasse	1[d]	20	2	121	0	31.68	0.25	58.1	61.71	6.31	Low
B4	Bagasse	1	20	2	121	3	31.68	0.25	24.7	61.71	6.31	High
R3	Rice straw	1	20	2	121	0	29.58	0.23	55.8	55.07	5.08	Low
R4	Rice straw	1	20	2	121	2	29.58	0.23	41.6	55.07	5.08	Medium

Table V-7. Continued

Sample	Pretreatment condition						Structural features (%)			Carbohydrate content (%)		Category of reactivity
	Biomass	Reagent loading (g/g dry biomass)	Liquid/ solid (mL/g)	Time (h)	Temp (°C)	Ball milling time (d)	Lignin content	Acetyl content	CrI_B	Glucan	Xylan	
AFEX (NH_3)												
C5	Corn stover	1	0.4[f]	1/12	90	0	18.63	1.95	44.7	37.32	21.20	Medium
C6	Corn stover	1	0.4	1/12	90	6	18.63	1.95	11.0	37.32	21.20	High
C7	Corn stover	1	0.6	1/12	90	0	18.09	1.88	50.7	37.94	21.29	Medium
C8	Corn stover	1	0.6	1/12	90	2	18.09	1.88	28.6	37.94	21.29	High
C9	Corn stover	1	0.6	1/12	100	0	18.14	1.82	44.1	36.26	20.90	Medium
C10	Corn stover	1	0.6	1/12	100	4	18.14	1.82	16.3	36.26	20.90	High
Aqueous ammonia (NH_3)												
B5	Bagasse	15[e]	6	12	60	0	22.94	0.04	56.9	49.23	18.73	Low
B6	Bagasse	15	6	12	60	2	22.94	0.04	19.5	49.23	18.73	High
B7	Bagasse	15	8	12	60	0	22.96	0.05	55.9	48.67	18.72	Low
B8	Bagasse	15	8	12	60	2	22.96	0.05	25.1	48.67	18.72	High

[a] Biomass crystallinity.

[b] Pretreated under air.

[c] Pretreated under nitrogen.

[d e] Acid or base concentration (w/w%).

[f] Moisture content of biomass.

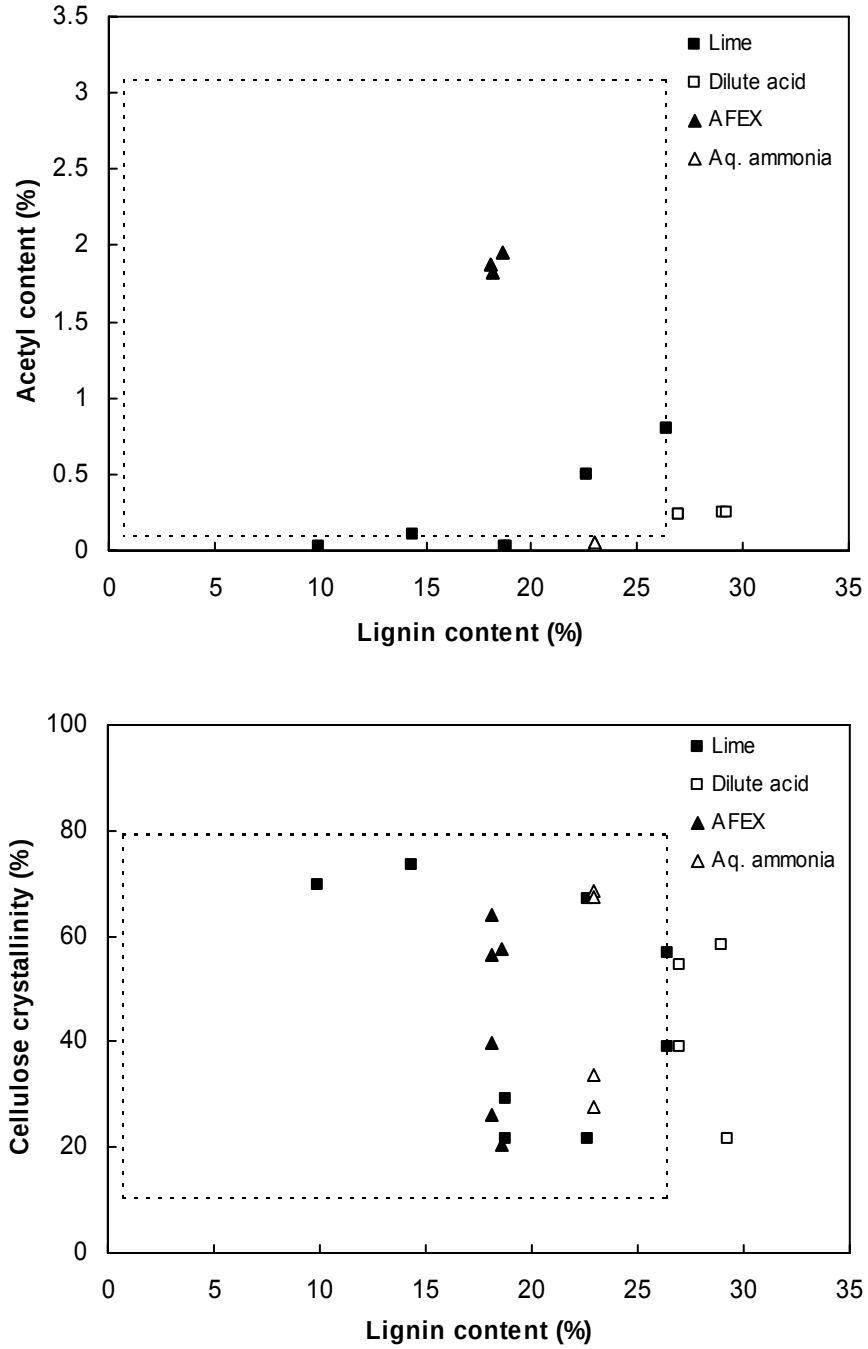

Figure V-10. Distributions of structural features and carbohydrate contents of biomass samples for model verification. The box indicates the range of the 147 model lignocelluloses.

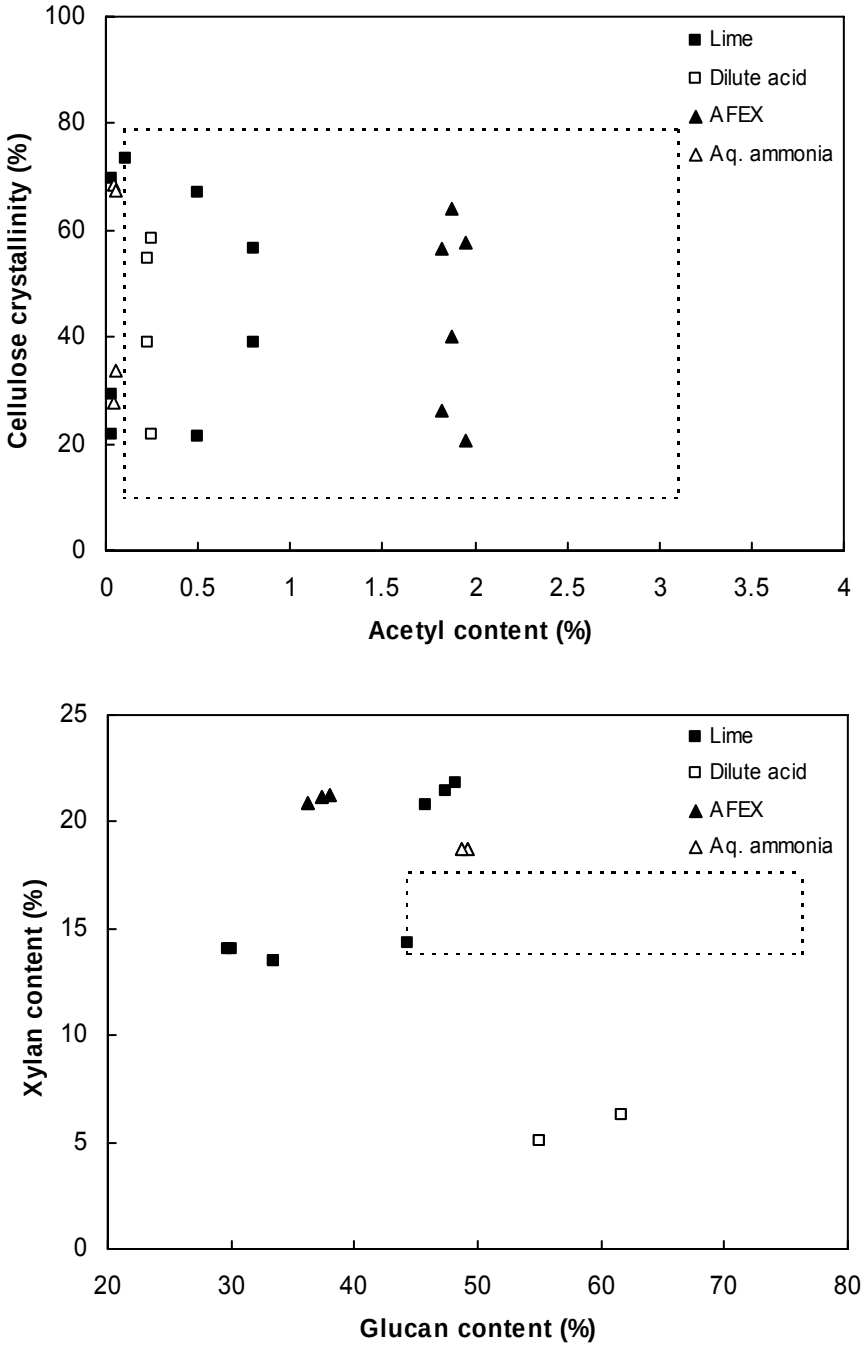

Figure V-10. Continued

Prediction of Slopes and Intercepts

Tables V-8 to V-10 summarize the 1-, 6-, and 72-h slopes, intercepts, and R^2 values of glucan, xylan, and total sugar hydrolyses of the 22 biomass samples for evaluating the predictive ability of the models. Similar to the model lignocelluloses used for model development, biomass samples with R^2 smaller than 0.93 were not used for model verification. Using Equation V-3 and the parameters in Tables V-1 to V-3, the 1-, 6-, and 72-h slopes and intercepts of glucan, xylan, and total sugar hydrolyses were calculated and the MSE values of each model were used to evaluate the predictive ability. The 1-, 6-, and 72-h slopes and intercepts of glucan, xylan, and total sugar hydrolyses and MSE were also calculated using the transformations of the dependent variable and independent variables determined by the ACE program.

Table V-11 summarizes the MSE value of the parametric and nonparametric models. The smaller MSE in the parametric model indicates better predictive ability. The larger MSE in the nonparametric model could be attributed to the large errors resulting from the transformation of the dependent and independent variables. In the parametric models, the prediction errors decreased significantly as biomass crystallinity was replaced by cellulose crystallinity. This observation demonstrates that cellulose crystallinity is the essential factor that influences digestibility.

Figures V-11 to V-13 illustrate the predictions of Equation V-3 on the 1-, 6-, and 72-h slopes and intercepts of glucan hydrolysis for biomass samples treated with lime, dilute acid, AFEX, and aqueous ammonia, identified with different symbols. These figures show that the predictive ability of the 6- and 72-h slopes of glucan hydrolysis are better than others, as shown by the relatively narrow 95% predictive intervals. The predicted slopes and intercepts of lime-treated corn stover agreed satisfactorily with the measured data. The points out of the 95% prediction interval were mainly from lime- and acid-treated rice straw. The predicted 6- and 72-h slopes and intercepts of AFEX-treated corn stover agreed well with the measured data, whereas the predicted 1-h intercepts were outside the 95% prediction interval. For bagasse treated with aqueous ammonia, the predicted slopes fit well with the measured slopes, whereas the intercepts

Table V-8. Regression parameters of glucan hydrolysis of biomass samples determined by equation I-3

Sample	Lignin×0.1 (%)	Acetyl (%)	CrI_C[a]×0.1 (%)	Glucan×0.1 (%)	1 h			6 h			72 h		
					Slope	Intercept	R^2	Slope	Intercept	R^2	Slope	Intercept	R^2
Lime ($Ca(OH)_2$)													
C1	0.99	0.03	6.96	4.43	14.47	4.67	0.97	25.13	22.39	0.99	27.1	73.34	0.99
C2	1.43	0.11	7.36	4.81	11.63	3.64	0.98	18.62	17.19	0.99	15.55	50	0.99
C3	1.81	0.03	2.91	4.58	19.29	6	0.94	25.09	26.38	0.99	22.38	69.82	0.99
C4	1.81	0.03	2.17	4.74	20.82	8.08	0.96	23.32	32.41	0.99	20.25	75.52	0.98
B1	2.26	0.50	6.72	3.35	6.12	0.74	0.98	8.68	9.76	1.00	7.98	27.72	0.94
B2	2.26	0.50	2.15	3.35	19.94	9.51	0.96	21.76	37.30	0.98	19.83	77.25	0.97
R1	2.64	0.80	5.66	3.01	10.74	3.00	0.96	11.81	20.50	0.98	8.49	45.41	1.00
R2	2.64	0.80	3.89	2.98	23.24	8.70	0.96	20.86	41.38	0.95	9.59	77.95	0.96
Dilute acid (H_2SO_4)													
B3	2.90	0.25	5.82	6.17	2.63	1.17	0.99	4.88	4.86	0.99	8.93	10.32	1.00
B4	2.92	0.25	2.16	6.17	4.40	1.60	0.97	11.44	5.33	0.97	10.07	20.88	0.99
R3	2.70	0.23	5.46	5.51	8.90	4.43	1.00	8.94	21.84	0.95	6.23	42.06	0.98
R4	2.70	0.23	3.90	5.51	8.50	2.74	0.99	20.42	13.34	1.00	18.00	46.52	0.96

Table V-8. Continued

Sample	Lignin×0.1 (%)	Acetyl (%)	CrI_C[a]×0.1 (%)	Glucan×0.1 (%)	1 h			6 h			72 h		
					Slope	Intercept	R^2	Slope	Intercept	R^2	Slope	Intercept	R^2
AFEX (NH_3)													
C5	1.86	1.95	5.75	3.73	6.20	3.88	0.94	13.50	15.81	1.00	11.70	42.85	0.94
C6	1.86	1.95	2.05	3.73	19.24	13.96	0.98	17.40	39.48	0.99	13.29	72.48	0.97
C7	1.81	1.88	6.42	3.79	6.44	3.77	0.99	12.45	13.16	0.99	12.62	39.10	1.00
C8	1.81	1.88	3.99	3.79	14.80	11.41	0.98	16.60	28.72	0.99	12.43	59.16	0.99
C9	1.81	1.82	5.66	3.63	6.37	5.20	0.99	13.19	13.64	0.99	13.58	42.07	0.99
C10	1.81	1.82	2.61	3.63	18.24	13.22	0.97	19.40	34.70	0.99	13.95	68.69	0.98
Aqueous ammonia (NH_3)													
B5	2.29	0.04	6.86	4.92	6.10	0.10	0.93	10.17	3.89	0.97	12.21	11.43	0.99
B6	2.29	0.04	2.76	4.92	8.76	3.32	0.94	17.59	10.06	0.98	14.43	37.65	0.99
B7	2.30	0.05	6.75	4.87	6.20	0.13	0.92	10.82	3.81	0.97	12.81	12.19	0.99
B8	2.30	0.05	3.37	4.87	8.7	3.74	0.96	17.65	10.46	0.97	14.43	37.74	0.99

[a] Cellulose crystallinity.

Table V-9. Regression parameters of xylan hydrolysis of biomass samples determined by equation I-3

Sample	Lignin×0.1 (%)	Acetyl (%)	CrI_C[a]×0.1 (%)	Xylan×0.1 (%)	1 h			6 h			72 h		
					Slope	Intercept	R^2	Slope	Intercept	R^2	Slope	Intercept	R^2
Lime ($Ca(OH)_2$)													
C1	0.99	0.03	6.96	1.44	6.18	5.82	0.99	17.7	32.14	0.99	14.92	80.34	0.99
C2	1.43	0.11	7.36	2.18	5.97	2.94	0.96	14.72	21.74	0.97	8.37	59.48	0.99
C3	1.81	0.03	2.91	2.08	4.88	5.57	0.93	13.99	36.84	0.98	10.48	80.22	0.98
C4	1.81	0.03	2.17	2.15	4.81	6.01	0.97	12.93	39.83	0.98	6.75	78.99	0.99
B1	2.26	0.50	6.72	1.35	6.73	1.44	0.94	7.49	18.05	1.00	6.37	37.54	0.99
B2	2.26	0.50	2.15	1.35	3.69	7.77	0.77	13.93	39.85	0.99	11.36	83.77	0.98
R1	2.64	0.80	5.66	1.41	7.49	1.74	0.93	8.20	23.42	1.00	7.03	47.81	0.99
R2	2.64	0.80	3.89	1.40	7.01	5.95	0.92	12.33	44.13	0.99	5.45	80.05	0.94
Dilute acid (H_2SO_4)													
B3	2.90	0.25	5.82	0.63	2.62	0.00	0.96	4.52	4.27	0.97	7.05	13.32	1.00
B4	2.92	0.25	2.16	0.63	9.52	11.58	0.97	9.34	34.74	0.99	7.00	52.20	0.92
R3	2.70	0.23	5.46	0.51	0.39	0.07	0.86	0.48	0.90	1.00	0.80	2.13	0.99
R4	2.70	0.23	3.90	0.51	8.55	6.64	0.99	13.19	22.19	0.99	10.08	49.53	1.00

Table V-9. Continued

Sample	Lignin×0.1 (%)	Acetyl (%)	CrI_C[a]×0.1 (%)	Xylan×0.1 (%)	1 h			6 h			72 h		
					Slope	Intercept	R^2	Slope	Intercept	R^2	Slope	Intercept	R^2
AFEX (NH_3)													
C5	1.86	1.95	5.75	2.12	4.40	3.62	0.92	9.94	21.59	0.99	5.81	45.71	0.99
C6	1.86	1.95	2.05	2.12	5.85	5.35	0.94	11.61	38.41	0.99	5.10	71.24	0.99
C7	1.81	1.88	6.42	2.13	4.75	3.61	0.94	8.89	22.57	0.99	6.03	47.81	0.99
C8	1.81	1.88	3.99	2.13	5.78	5.13	0.96	9.91	35.24	0.99	5.79	63.73	0.99
C9	1.81	1.82	5.66	2.09	4.90	3.19	0.96	8.57	21.75	0.99	6.96	47.77	0.99
C10	1.81	1.82	2.61	2.09	5.67	5.26	0.92	11.93	35.54	0.99	4.52	67.52	0.98
Aqueous ammonia (NH_3)													
B5	2.29	0.04	6.86	1.87	6.18	0.94	0.94	8.36	12.48	0.97	9.37	24.69	0.99
B6	2.29	0.04	2.76	1.87	5.87	3.89	0.94	13.85	24.28	0.99	7.8	55.03	0.99
B7	2.30	0.05	6.75	1.87	6.32	0.87	0.93	8.75	13.13	0.97	10.06	25.74	1.00
B8	2.30	0.05	3.37	1.87	6.34	3.83	0.94	14.56	24.82	0.97	8.06	57.28	0.99

[a] Cellulose crystallinity.

Table V-10. Regression parameters of total sugar hydrolysis of biomass samples determined by equation I-3

Sample	Lignin×0.1 (%)	Acetyl (%)	CrI_C[a]×0.1 (%)	TS×0.1 (%)	1 h			6 h			72 h		
					Slope	Intercept	R^2	Slope	Intercept	R^2	Slope	Intercept	R^2
Lime ($Ca(OH)_2$)													
C1	0.99	0.03	6.96	5.87	12.4	4.96	0.97	23.28	24.82	0.99	24.06	75.08	0.99
C2	1.43	0.11	7.36	7.0	9.84	3.42	0.98	17.38	18.44	0.99	13.28	53	0.99
C3	1.81	0.03	2.91	6.66	15.14	5.86	0.94	21.56	29.71	0.99	18.6	73.12	0.99
C4	1.81	0.03	2.17	6.89	15.75	7.42	0.96	20.03	34.76	0.99	15.98	76.62	0.99
B1	2.26	0.50	6.72	4.70	6.30	0.94	0.97	8.33	12.17	1.00	7.51	30.58	0.96
B2	2.26	0.50	2.15	4.70	15.20	9.00	0.95	19.48	38.05	0.99	17.36	79.15	0.99
R1	2.64	0.80	5.66	4.42	9.69	2.59	0.96	10.64	21.47	0.99	8.02	46.81	1.00
R2	2.64	0.80	3.89	4.38	17.96	7.80	0.95	18.09	42.28	0.97	8.25	78.63	0.96
Dilute acid (H_2SO_4)													
B3	2.90	0.25	5.82	6.80	2.63	1.25	0.99	4.84	5.05	0.99	8.75	10.76	1.00
B4	2.92	0.25	2.16	6.80	4.88	2.55	0.97	11.24	8.11	0.97	9.78	23.84	0.99
R3	2.70	0.23	5.46	6.02	4.60	2.37	0.99	4.66	11.40	0.96	3.48	22.02	0.99
R4	2.70	0.23	3.90	6.02	8.50	3.08	0.99	19.80	14.10	1.00	17.31	46.78	0.96

Table V-10. Continued

Sample	Lignin×0.1 (%)	Acetyl (%)	CrI_C[a]×0.1 (%)	TS×0.1 (%)	1 h			6 h			72 h		
					Slope	Intercept	R^2	Slope	Intercept	R^2	Slope	Intercept	R^2
AFEX (NH_3)													
C5	1.86	1.95	5.75	5.85	5.54	3.79	0.94	12.19	17.93	1.00	9.53	43.90	0.99
C6	1.86	1.95	2.05	5.85	14.32	10.80	0.98	15.27	39.08	0.99	10.28	72.02	0.99
C7	1.81	1.88	6.42	6.92	5.82	3.71	0.98	11.15	16.59	0.99	10.22	42.28	0.99
C8	1.81	1.88	3.99	5.92	11.51	9.12	0.98	14.16	31.09	1.00	10.01	60.83	0.99
C9	1.81	1.82	5.66	5.72	5.83	4.45	0.98	11.47	16.65	0.99	11.13	44.18	0.99
C10	1.81	1.82	2.61	5.72	13.58	10.27	0.96	16.63	35.01	0.99	10.46	68.26	0.99
Aqueous ammonia (NH_3)													
B5	2.29	0.04	6.86	6.80	6.13	0.31	0.93	9.66	6.29	0.97	11.41	15.14	0.99
B6	2.29	0.04	2.76	6.80	7.95	3.48	0.94	16.54	14.04	0.98	12.57	42.51	0.99
B7	2.30	0.05	6.75	6.74	6.24	0.34	0.92	10.23	6.44	0.97	12.03	16.02	1.00
B8	2.30	0.05	3.37	6.74	8.03	3.77	0.96	16.78	14.52	0.97	12.63	43.26	0.99

[a] Cellulose crystallinity.

Table V-11. Comparison of predictive ability of the parametric and nonparametric models on slopes and intercepts of carbohydrate hydrolysis

Dependent variables		MSE		
		L[a], A[b], CrI_C[c], carbohydrate content[d]		Nonparametric model[d]
		CrI_C[b]	CrI_B[c]	
Glucan	1-h slope	17	23	22
	1-h intercept	9.6	10	16
	6-h slope	14	19	16
	6-h intercept	76	97	100
	72-h slope	11	18	15
	72-h intercept	211	310	251
Xylan	1-h slope	4.2	15	3.3
	1-h intercept	5.0	7.5	7.6
	6-h slope	7.3	7.7	12[e]
	6-h intercept	66	65	58[e]
	72-h slope	9.3	8.7	32[e]
	72-h intercept	186	194	250[e]
Total Sugar	1-h slope	8.2	11	11
	1-h intercept	4.5	4.8	8.9
	6-h slope	13	17	11
	6-h intercept	75	88	81
	72-h slope	21	24	14
	72-h intercept	124	176	229

[a] Data obtained from Equation V-3 and parameters in Tables V-1 to V-3.

[b] Cellulose crystallinity.

[c] Biomass crystallinity.

[d] Lignin content, acetyl content, and CrI_C as independent variables.

[e] Lignin content, acetyl content, CrI_C, and corresponding predicted slope or intercept of glucan as independent variables.

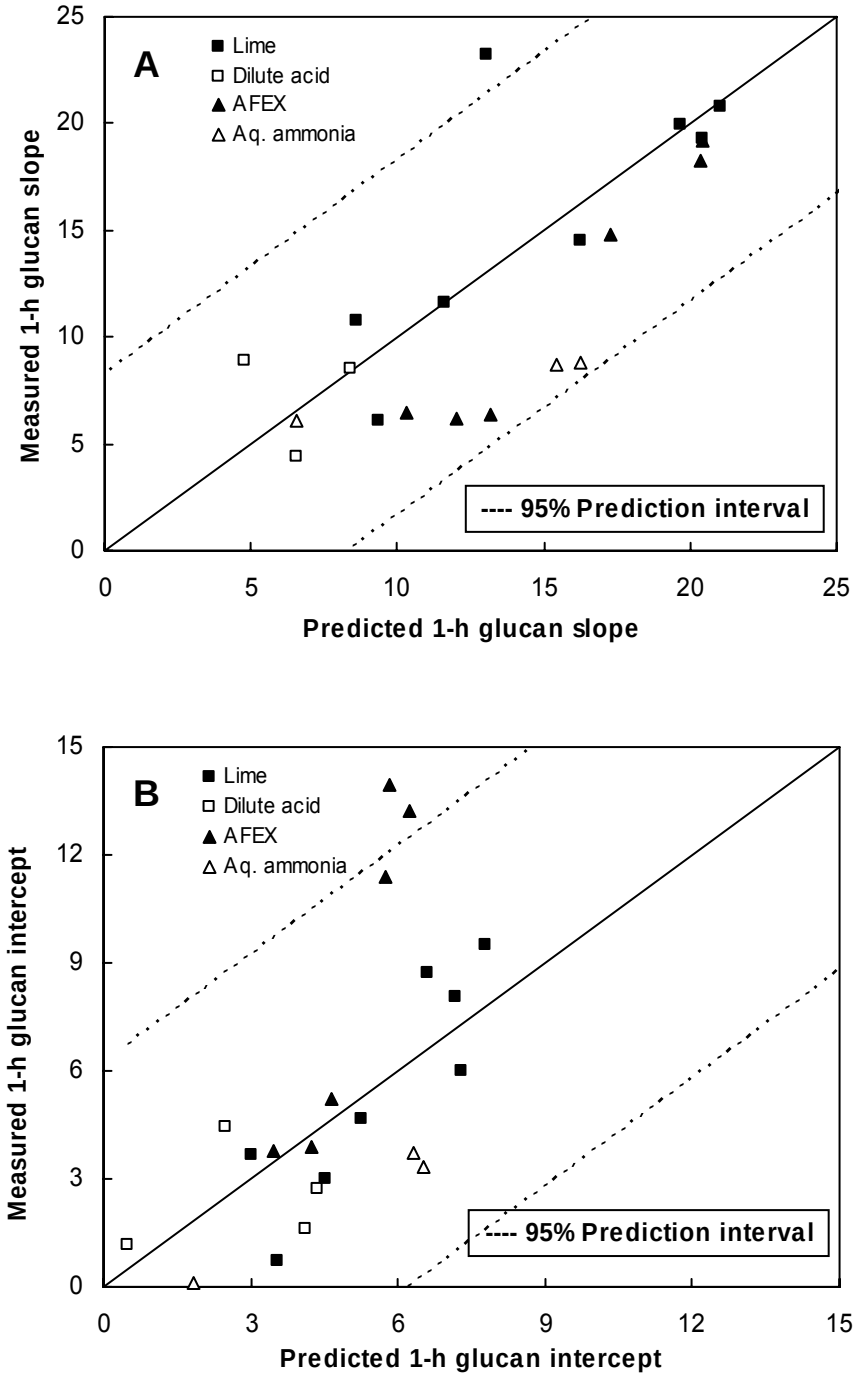

Figure V-11. Prediction of equation V-3 on 1-h slope and intercept of glucan hydrolysis for corn stover, bagasse, and rice straw treated with lime, dilute acid, AFEX, and aqueous ammonia: (A) slope; (B) intercept.

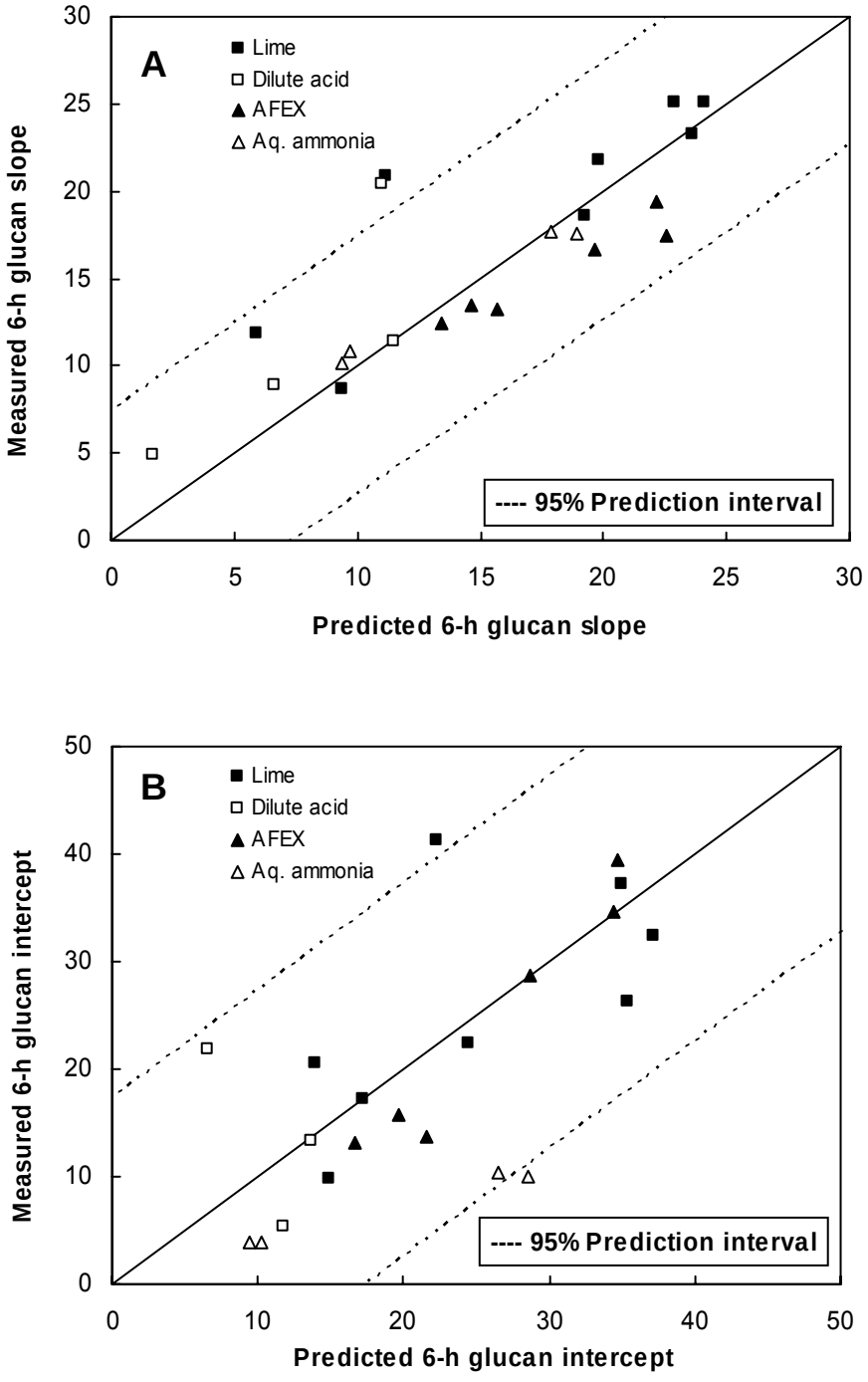

Figure V-12. Prediction of equation V-3 on 6-h slope and intercept of glucan hydrolysis for corn stover, bagasse, and rice straw treated with lime, dilute acid, AFEX, and aqueous ammonia: (A) slope; (B) intercept.

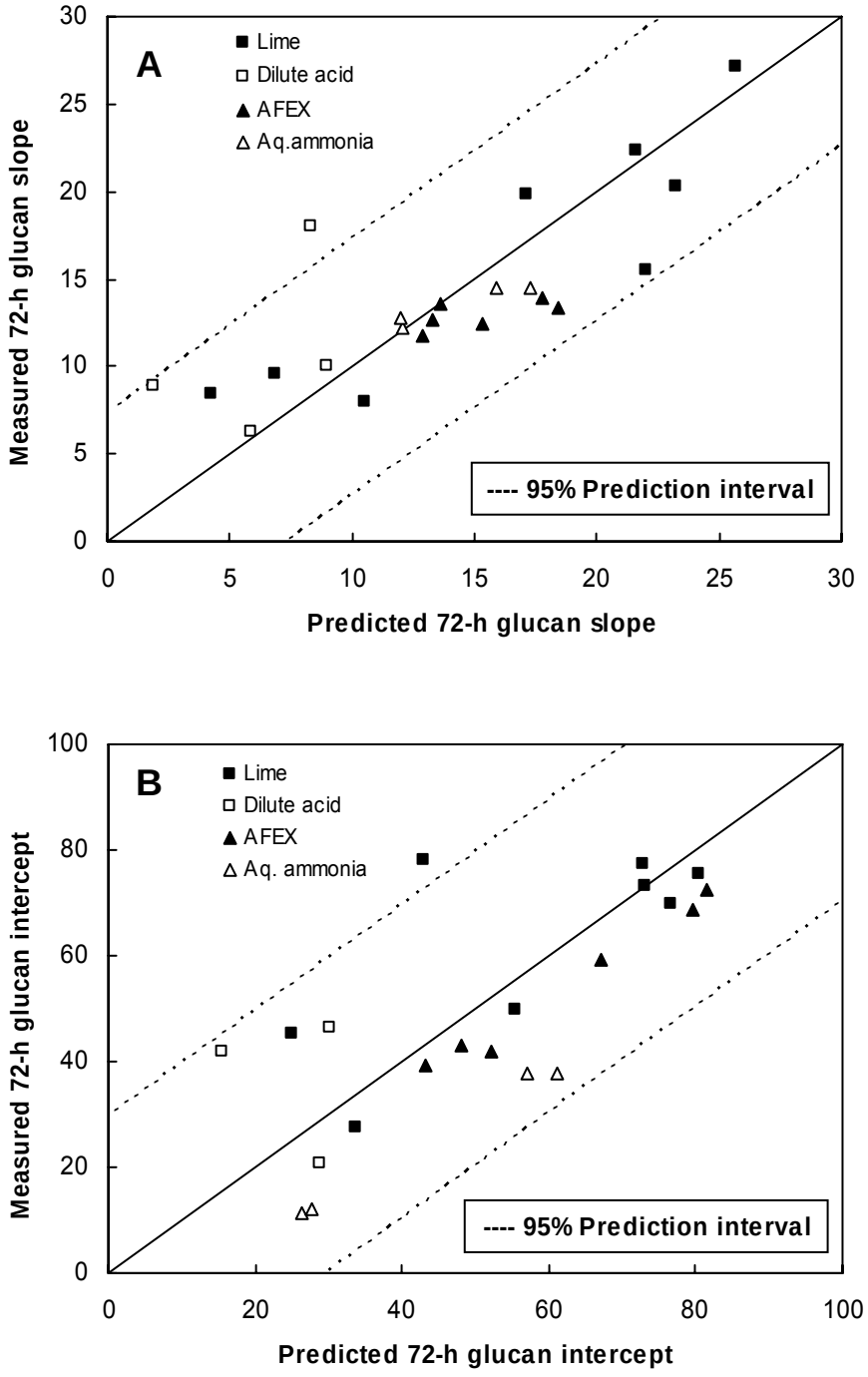

Figure V-13. Prediction of equation V-3 on 72-h slope and intercept of glucan hydrolysis for corn stover, bagasse, and rice straw treated with lime, dilute acid, AFEX, and aqueous ammonia: (A) slope; (B) intercept.

Were overestimated. The unsatisfactory prediction of slopes and intercepts could be explained by the following reasons:

1. Lignin content was not accurately quantified. The lime-treatment procedure for rice straw and bagasse was different from that of corn stover. The pretreated rice straw and bagasse were dried at 105°C directly after neutralization with CO_2 without the washing procedure to remove lime-soluble lignin. Therefore, the lignin content associated with cellulose and hemicellulose was overestimated due to the lime-soluble lignin precipitated on biomass. It has been reported that acid-soluble lignin recondensed and formed an altered lignin polymer during acid hydrolysis (Torget et al., 1991), thus lignin content in the dilute acid-treated biomass needs to be recalculated by multiplying a factor that considers the altered lignin.
2. The glucan contents in the lime-treated bagasse and rice straw and AFEX-treated corn stover were not in the range of the model lignocelluloses (Figure V-10). Glucan contents show more influence on the intercept than on the slope, because the 6- and 72-h slopes of glucan hydrolysis were not correlated with glucan content (shown in Table V-1). The overestimation of the 6- and 72-h intercepts of aqueous ammonia-treated bagasse might be attributed to the low glucan content in biomass samples.
3. Cellulose crystallinity of diluted acid-treated bagasse and rice straw may be underestimated, because the cellulose crystallinity was linearly correlated only with biomass crystallinity and hemicellulose content.

Because the acetyl content in lime-treated corn stover was ~0.03% (out of the range of acetyl content in the model lignocelluloses), the well-predicted slopes and intercepts of lime-treated corn stover indicated that acetyl content had less effect on the slopes and intercepts than lignin content and crystallinity.

Figures V-14 to V-16 compare the predicted 1-, 6-, and 72-h slopes and intercepts of xylan hydrolysis using Equation V-3 and the measured values. Similar to glucan hydrolysis, the predictive abilities of 6- and 72-h slopes of xylan hydrolysis were better

than others. The predicted slopes and intercepts of corn stover treated with lime and AFEX agreed pretty well with the measured data. The predicted slopes of bagasse treated by aqueous ammonia fit with the measured slopes, whereas the intercepts were overestimated. Because dilute acid solubilizes most of the xylan in biomass, the xylan content (5–6%) was not in the range of the model lignocelluloses (Figure V-10) and the predicted slopes and intercepts of dilute acid-treated bagasse and rice straw did not fit well with the measured data.

Using Equation V-3 and the measured data, Figures V-17 to V-19 illustrate the plots of predicted 1-, 6-, and 72-h slopes and intercepts of total sugar hydrolysis. The predictive ability of 1- and 6-h slopes and 1- and 72-h intercepts are satisfactory. The predicted slopes and intercepts of lime-treated corn stover were consistent with the measured data, the predicted slopes of aqueous ammonia- treated bagasse fit with the measured slopes, whereas the intercepts were overestimated. For the reasons discussed above, the predicted slopes and intercepts of lime- and acid-treated bagasse and rice straw fit the measured data less satisfactorily.

The plots of slopes and intercepts predicted by the nonparametric models vs the measured data (not shown) were similar to Figures V-11 to V-19 with wider 95% prediction intervals due to the larger MSE values.

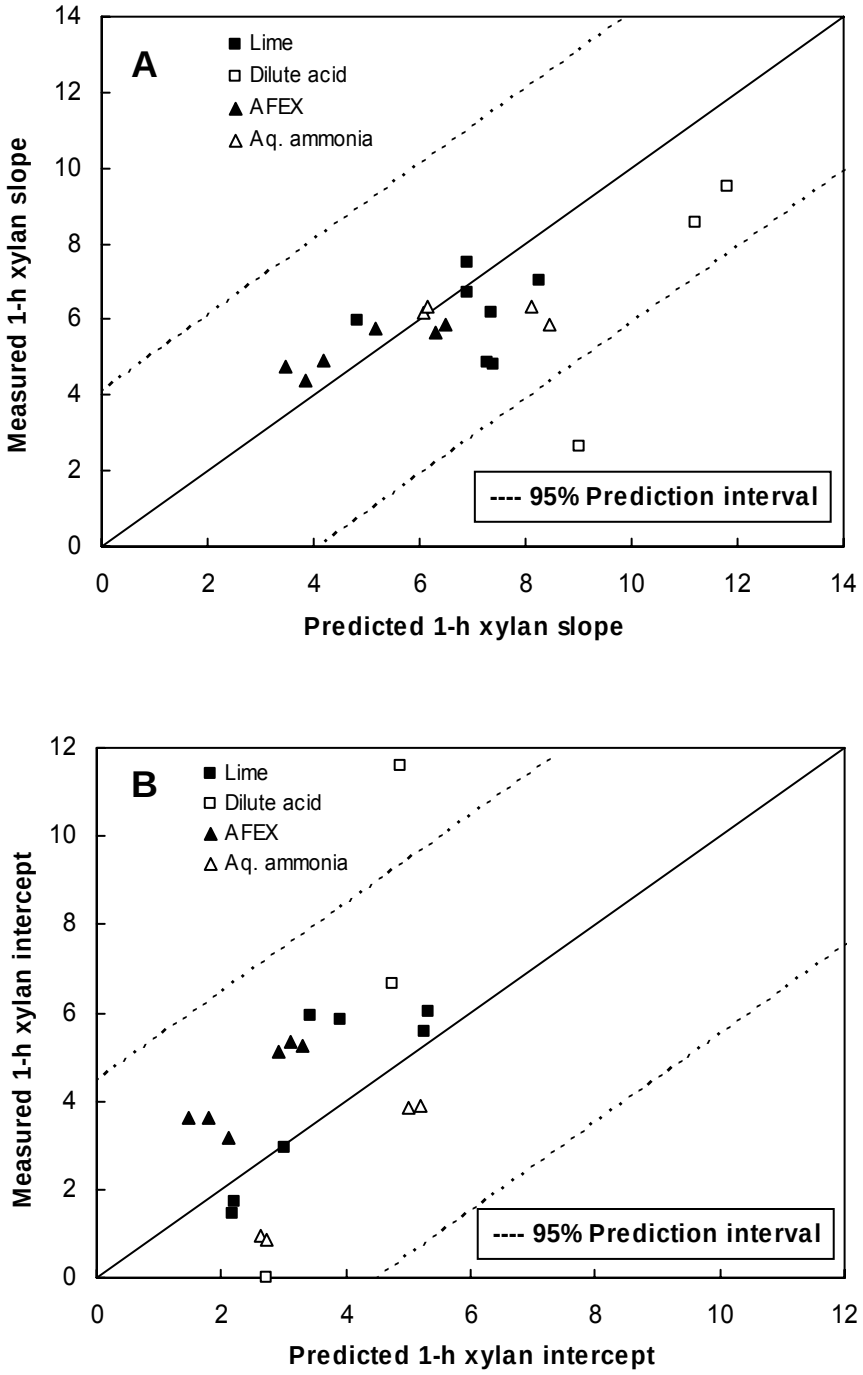

Figure V-14. Prediction of equation V-3 on 1-h slope and intercept of xylan hydrolysis for corn stover, bagasse, and rice straw treated with lime, dilute acid, AFEX, and aqueous ammonia: (A) slope; (B) intercept.

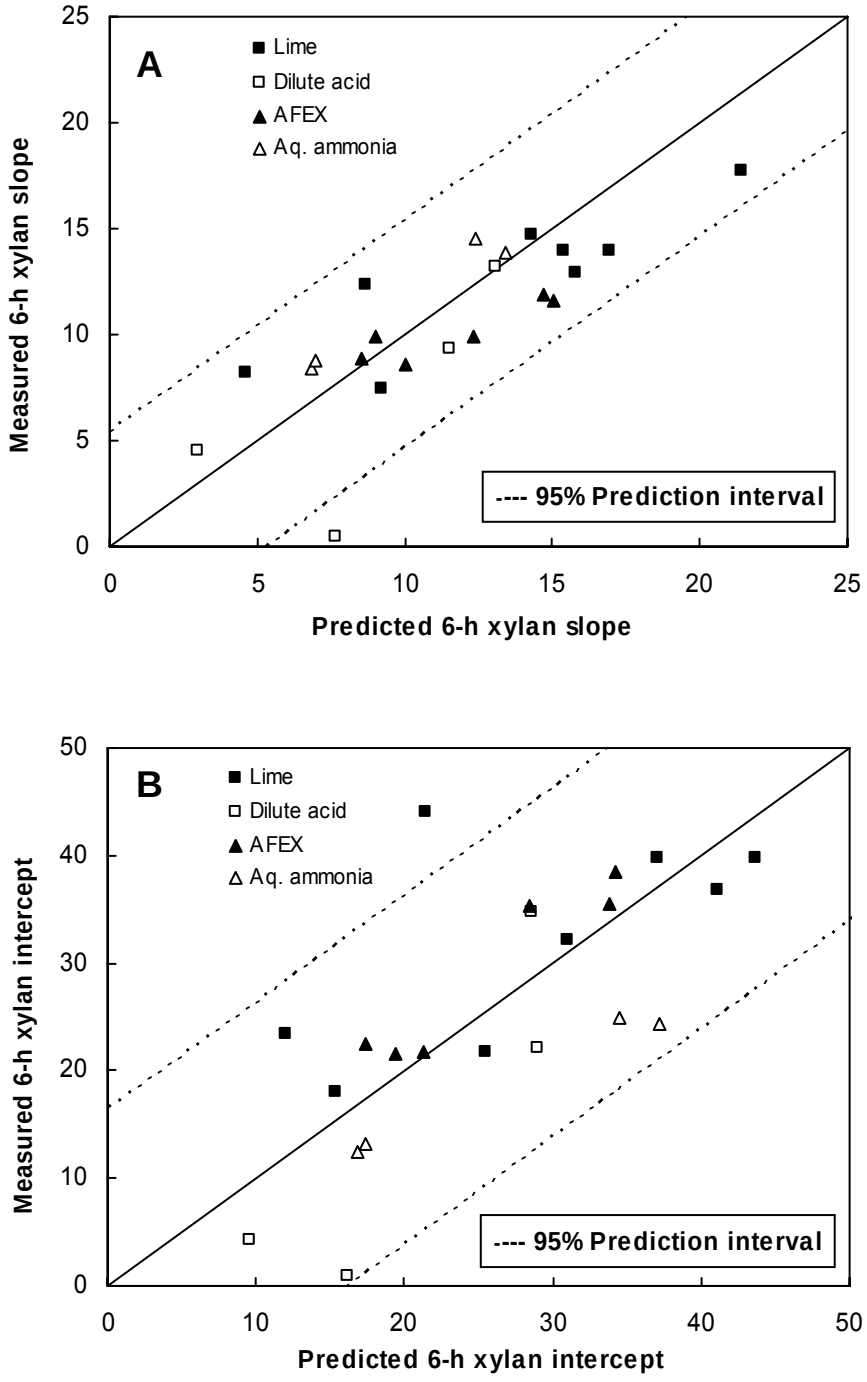

Figure V-15. Prediction of equation V-3 on 6-h slope and intercept of xylan hydrolysis for corn stover, bagasse, and rice straw treated with lime, dilute acid, AFEX, and aqueous ammonia: (A) slope; (B) intercept.

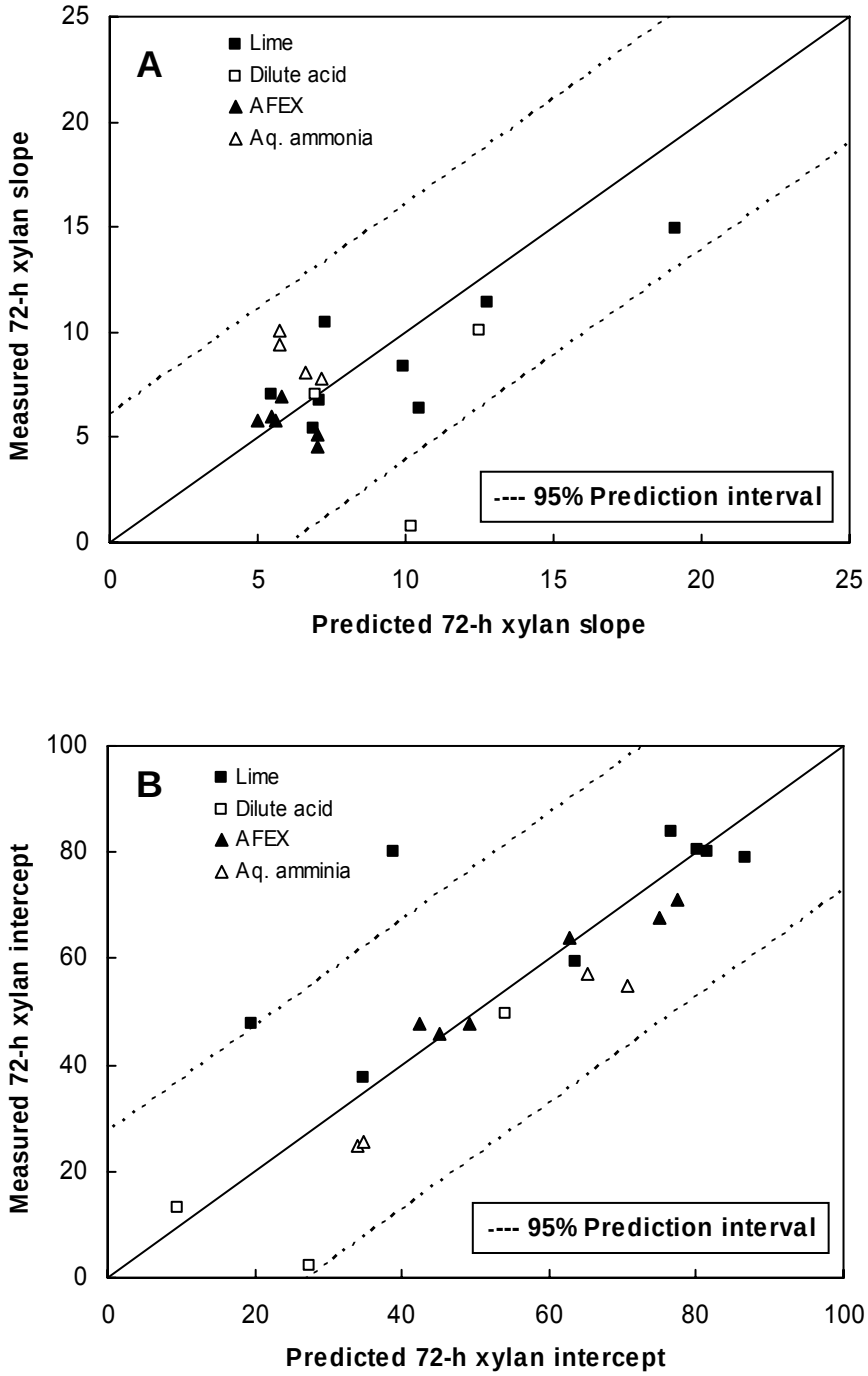

Figure V-16. Prediction of equation V-3 on 72-h slope and intercept of xylan hydrolysis for corn stover, bagasse, and rice straw treated with lime, dilute acid, AFEX, and aqueous ammonia: (A) slope; (B) intercept.

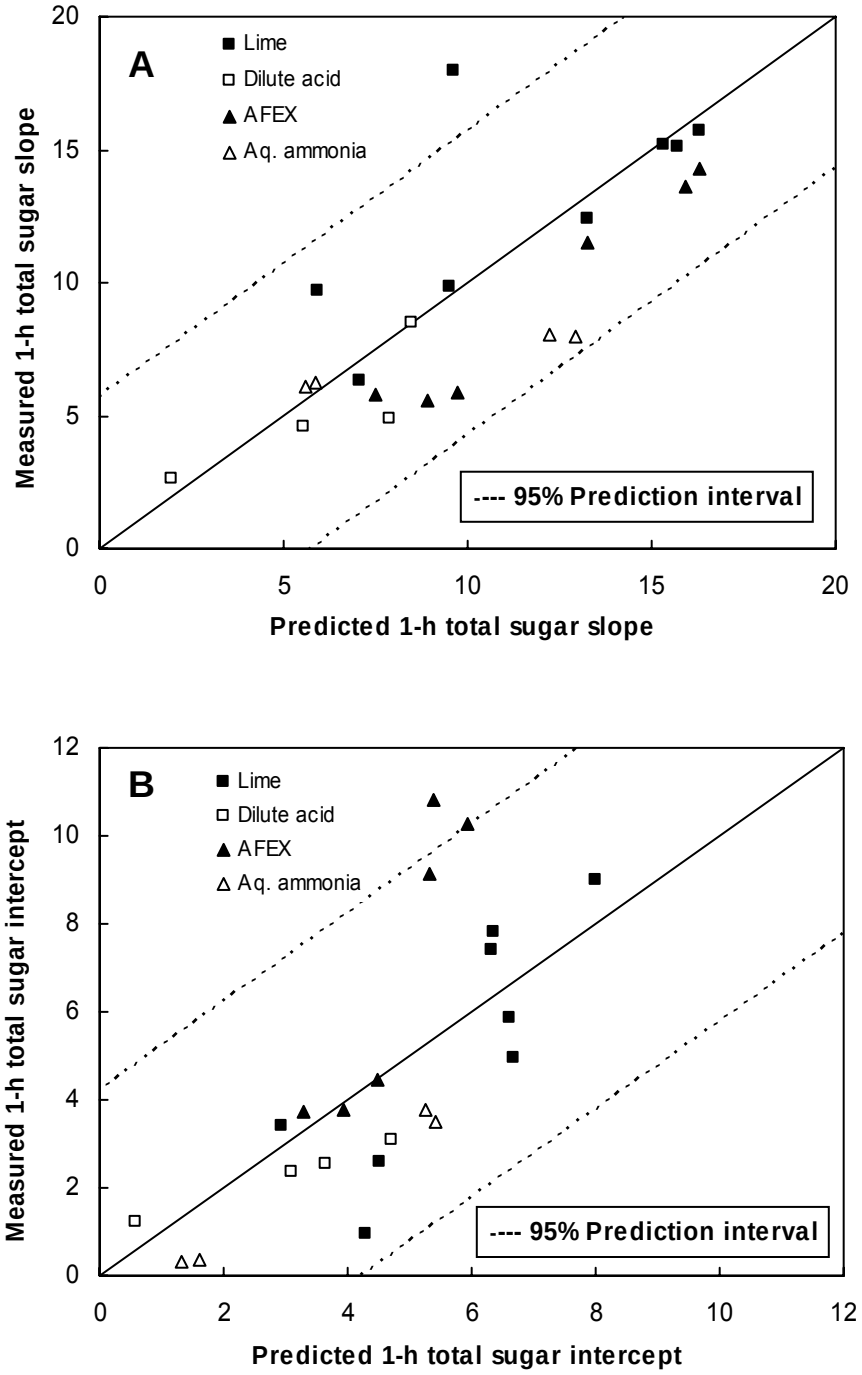

Figure V-17. Prediction of equation V-3 on 1-h slope and intercept of total sugar hydrolysis for corn stover, bagasse, and rice straw treated with lime, dilute acid, AFEX, and aqueous ammonia: (A) slope; (B) intercept.

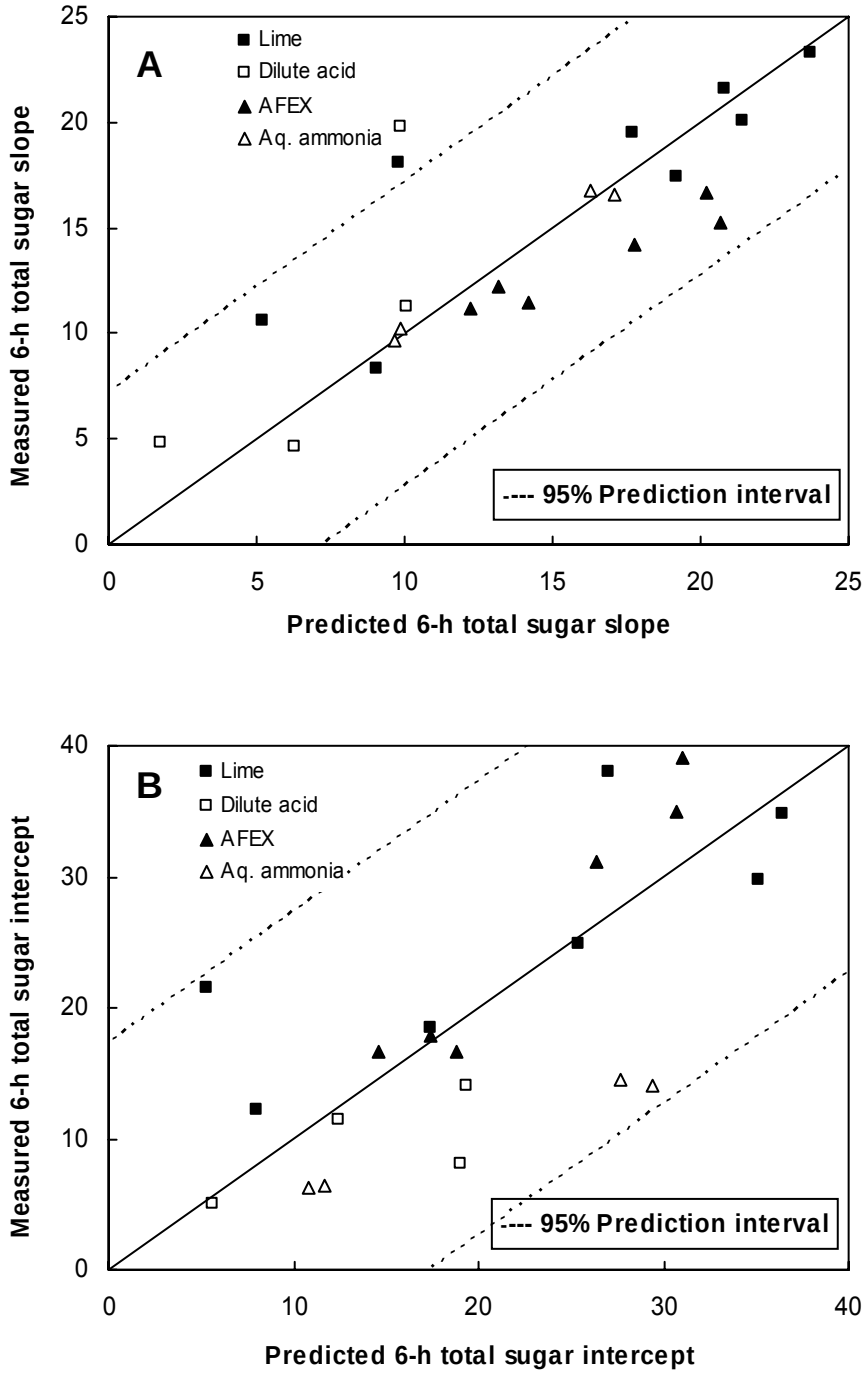

Figure V-18. Prediction of equation V-3 on 6-h slope and intercept of total sugar hydrolysis for corn stover, bagasse, and rice straw treated with lime, dilute acid, AFEX, and aqueous ammonia: (A) slope; (B) intercept.

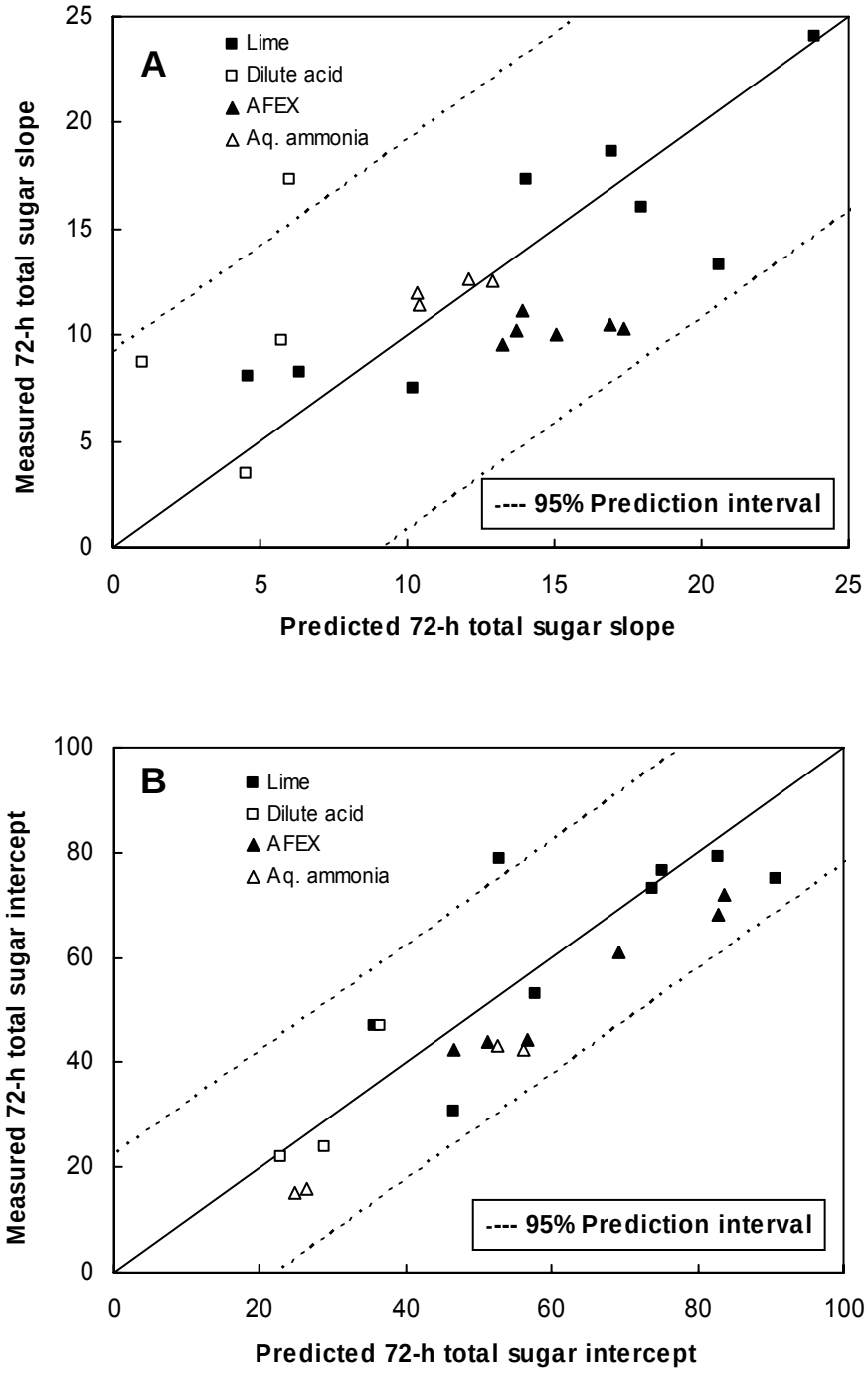

Figure V-19. Prediction of equation V-3 on 72-h slope and intercept of total sugar hydrolysis for corn stover, bagasse, and rice straw treated with lime, dilute acid, AFEX, and aqueous ammonia: (A) slope; (B) intercept.

Prediction of Biomass Digestibility

The primary goal of developing mathematical models is to predict biomass digestibility, which can be calculated by Equation I-3 using the slopes and intercepts predicted by the models. Figure V-20 compares the predicted 1-, 6-, and 72-h total sugar conversions of biomass treated with various techniques and measured conversions as a function of the natural logarithm of cellulase loading. For lime-treated and 72-h ball milled corn stover, the 1- and 72-h predicted sugar conversions agreed well with the measured data at each cellulase loading, the 6-h predicted sugar conversions were higher than the measured values because the predicted straight line had a bigger intercept. For dilute acid-treated rice straw, the 1-, 6-, and 72-h predicted sugar conversions at 1 FPU/g dry biomass fit well with measured data, whereas the error between the predicted and measured conversions increased with the increase in cellulase loading. For AFEX-treated corn stover, Equations I-3 and V-3 predicted 1- and 6-h sugar conversions more satisfactorily than 72-h conversions. Equations I-3 and V-3 also well predicted 1-h sugar conversions of aqueous ammonia-treated bagasse.

Using various enzyme loadings, Figures V-21 to V-23 compare the calculated 1-, 6-, and 72-h glucan, xylan, and total sugar conversions to the measured conversions, respectively. Similar to the prediction of slopes and intercepts, the predicted glucan, xylan, and total sugar conversions of lime and AFEX-treated corn stover fit well with the measured data, whereas the points out of the 95% prediction interval were mainly from lime- and acid-pretreated rice straw and bagasse. Due to the overestimated intercepts of aqueous ammonia-treated bagasse, the predicted glucan, xylan, and total sugar conversions were not as satisfactory as those of lime and AFEX-treated corn stover.

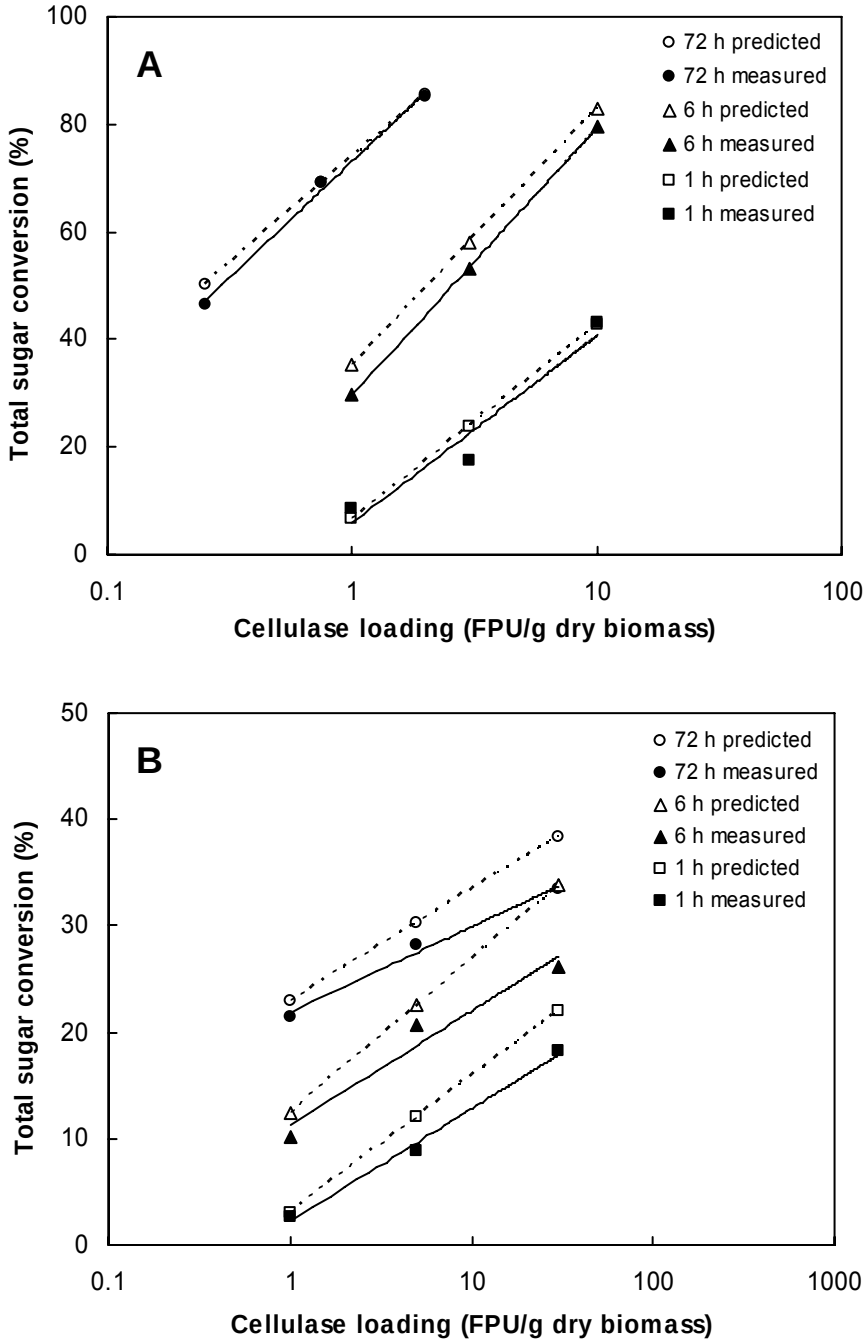

Figure V-20. Prediction of equations I-3 and V-3 on 1-, 6-, and 72-h total sugar conversions: (A) lime-treated and 72-h ball milled corn stover; (B) dilute acid-treated rice straw; (C) AFEX-treated corn stover (60% moisture content, 90°C); (D) aqueous ammonia-treated bagasse.

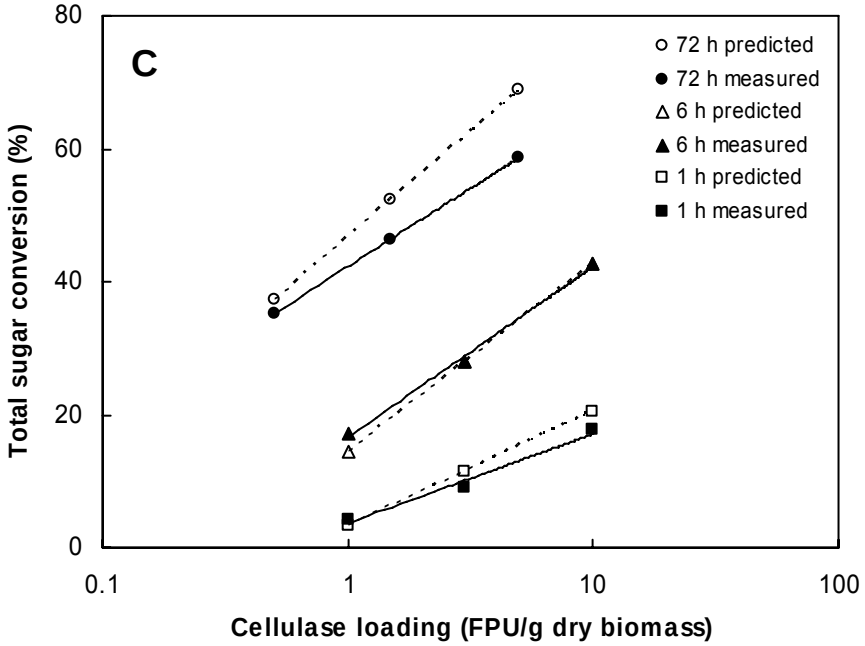

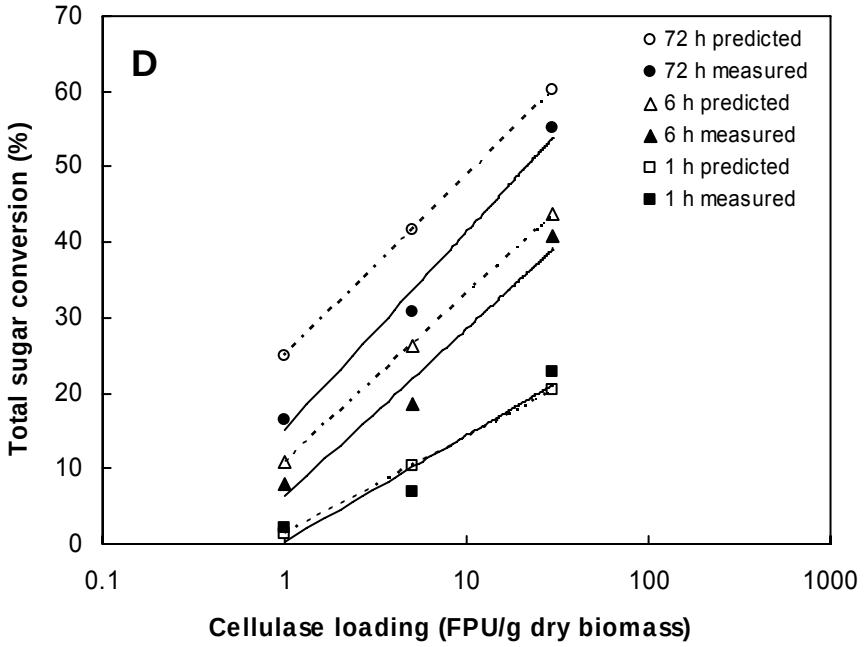

Figure V-20. Continued

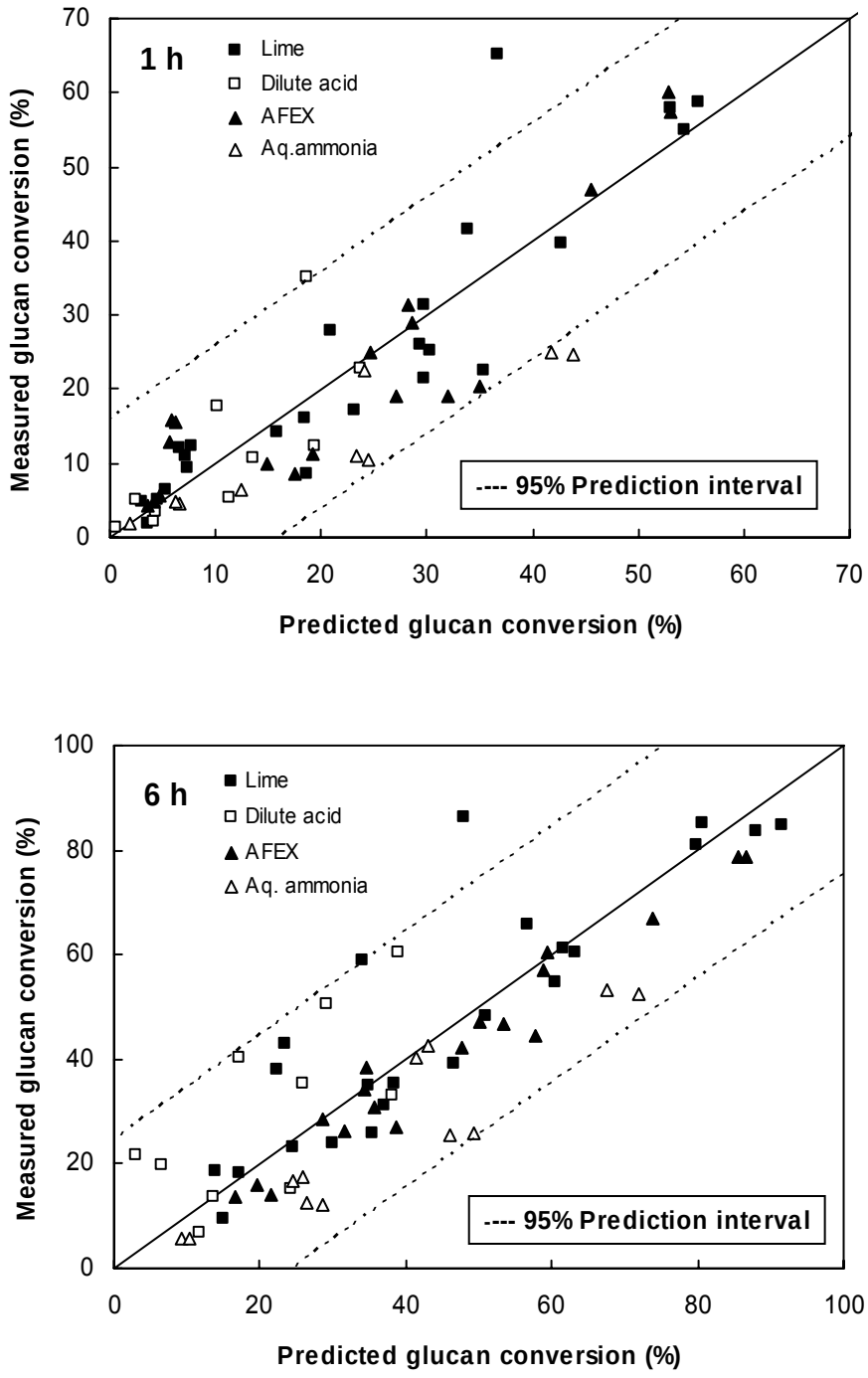

Figure V-21. Prediction of Equations I-3 and V-3 on 1-, 6-, and 72-h glucan conversions for corn stover, bagasse, and rice straw treated with lime, dilute acid, AFEX, and aqueous ammonia.

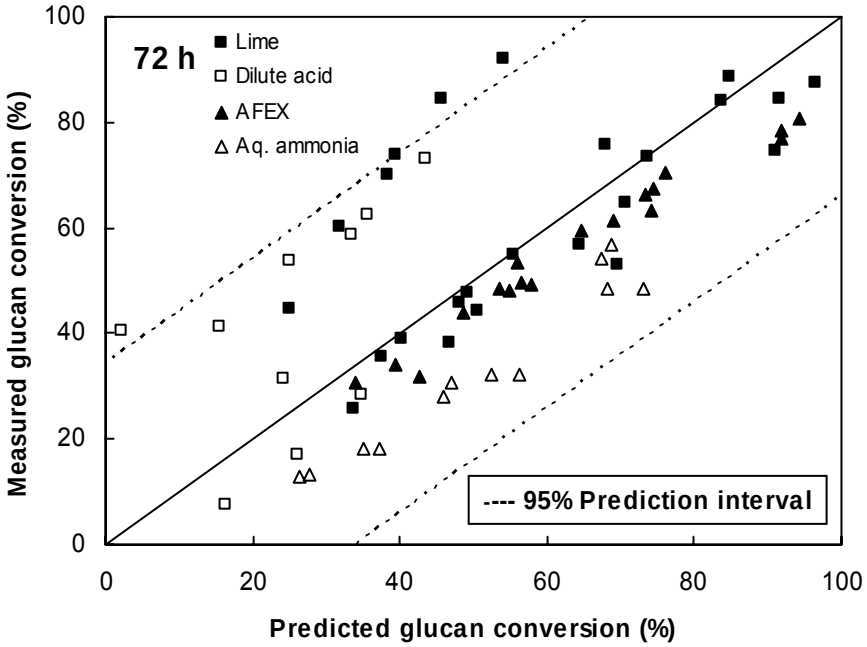

Figure V-21. Continued.

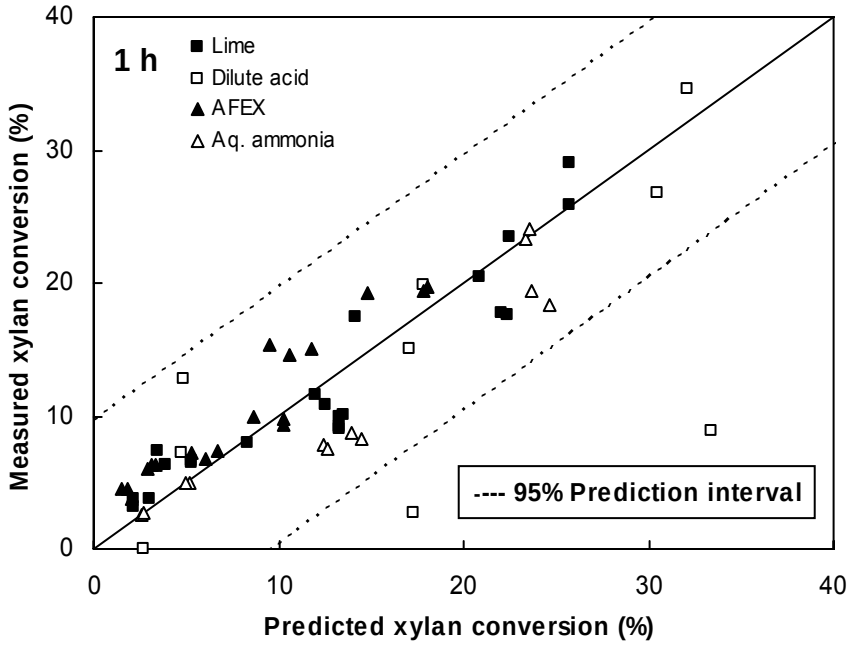

Figure V-22. Prediction of equations I-3 and V-3 on 1-, 6-, and 72-h xylan conversions for corn stover, bagasse, and rice straw treated with lime, dilute acid, AFEX, and aqueous ammonia.

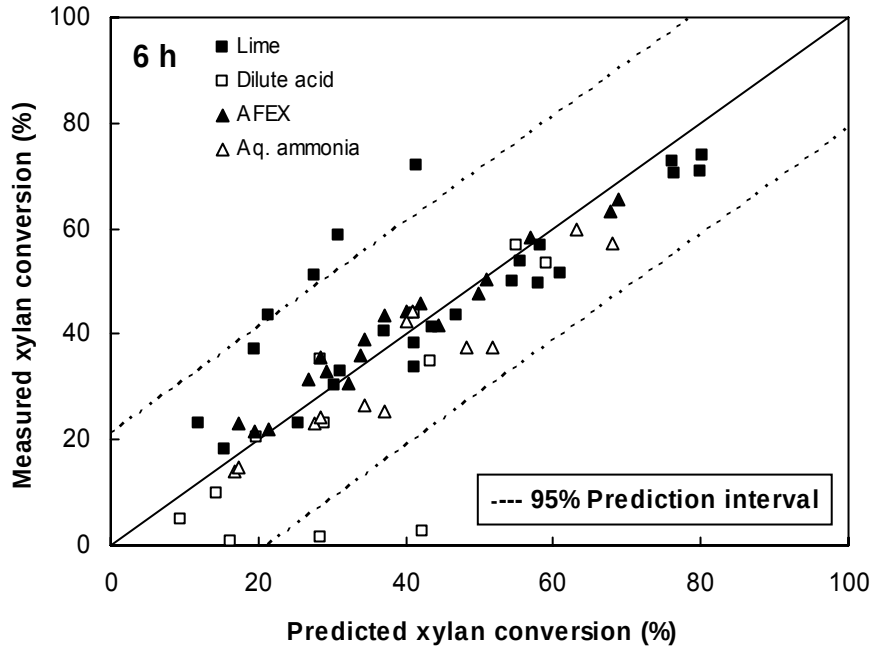

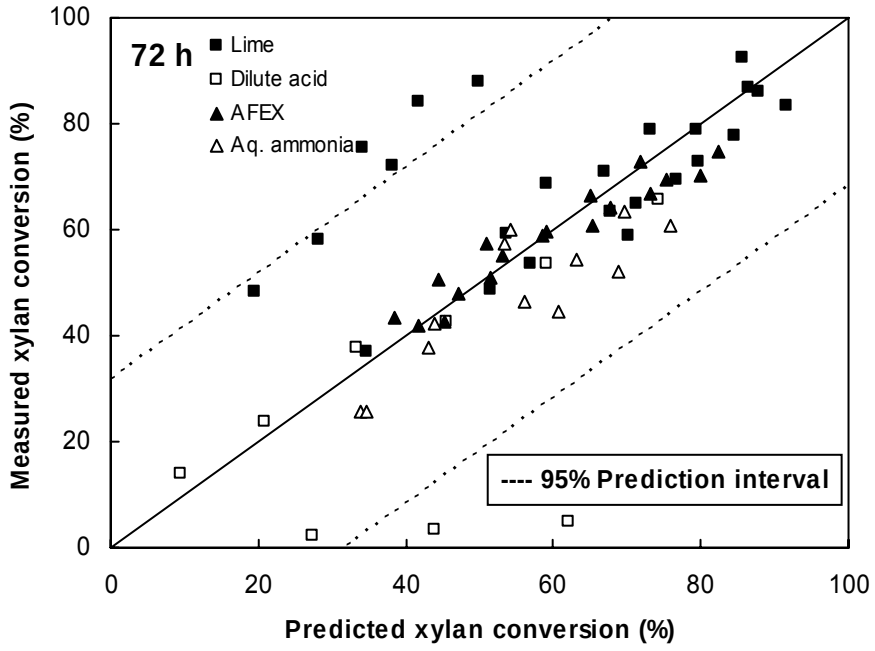

Figure V-22. Continued.

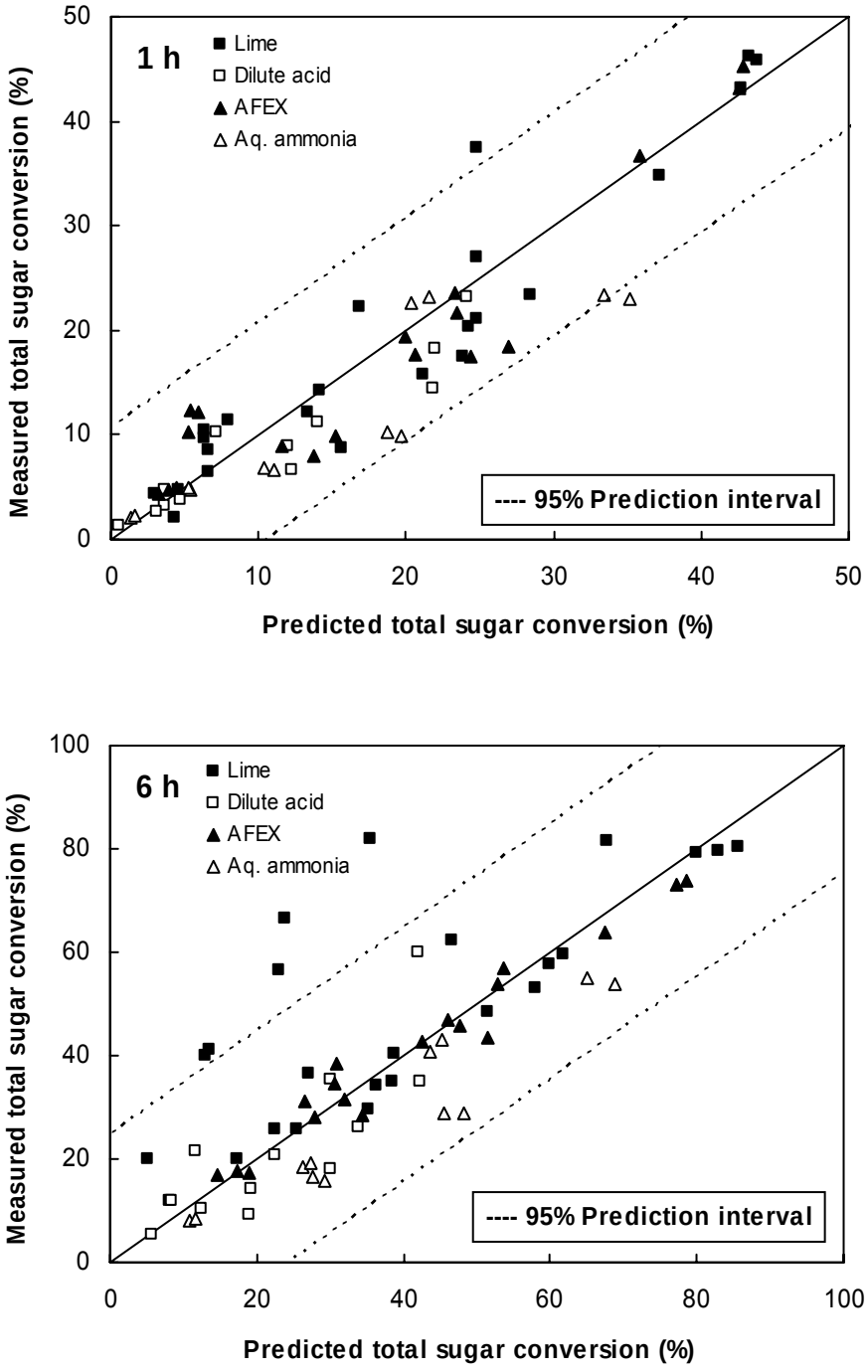

Figure V-23. Prediction of equations I-3 and V-3 on 1-, 6-, and 72-h total sugar conversions for corn stover, bagasse, and rice straw treated with lime, dilute acid, AFEX, and aqueous ammonia.

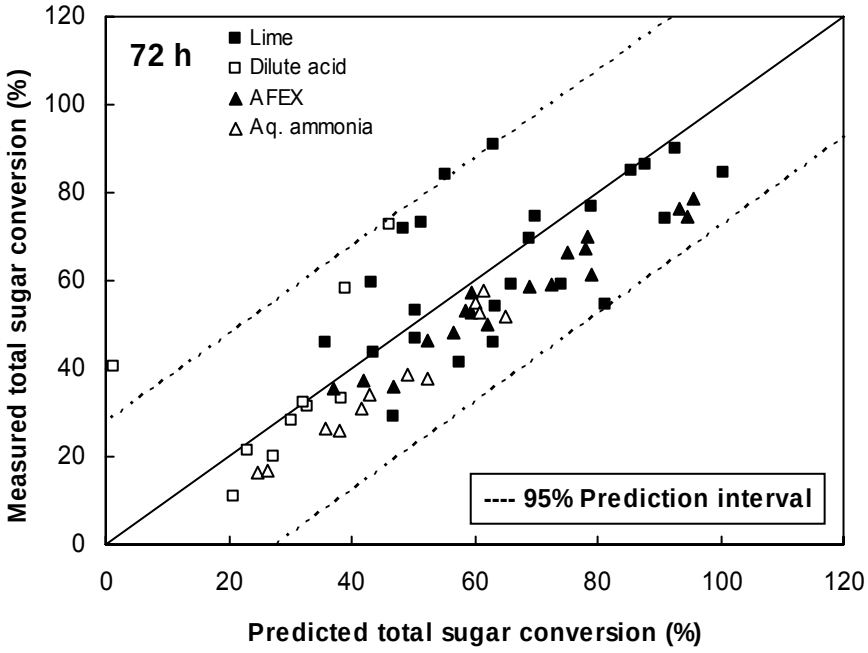

Figure V-23. Continued.

Table V-12 compares the predictive abilities of the parametric and nonparametric models on carbohydrate conversions. The MSE value indicates that the parametric models show better predictive ability than the nonparametric models. The plots of carbohydrate conversion predicted by the nonparametric models vs the measured data (not shown) were similar to Figures V-21 to V-23 with the larger MSE values giving wider 95% prediction intervals.

Table V-12. Comparison of predictive ability of the parametric and nonparametric models on carbohydrate conversions

Carbohydrate	Incubation period (h)	MSE	
		Parametric model	Nonparametric model
Glucan	1	64	100
	6	149	186
	72	287	290
Xylan	1	23	19
	6	112	105
	72	250	261
Total sugar	1	28	49
	6	152	132
	72	192	266

IMPLEMENTATIONS

The primary implementation of the models is to predict the quantity of enzyme required to achieve the desired conversion or sugar conversions at a given enzyme loading for biomass with specific structural features resulting from pretreatment. This allows the pretreatment and hydrolysis processes to be optimized.

Figures V-24 to V-26 illustrate the calculated total sugar conversions as a function of the logarithm of cellulase loadings at various lignin contents for 1-, 6-, and 72-h hydrolysis, respectively. The sugar conversions were calculated using Equations I-3 and V-3 and the parameters in Table V-3 with a typical pretreated biomass composition (glucan: xylan = 45:20; CrI_B = 55%; acetyl content = 0%). Ball milling can effectively reduce biomass crystallinity without changing biomass composition (glucan: xylan = 45:20; CrI_B = 15%; acetyl content = 0%). However, these figures are only illustrations. The composition change during a chemical pretreatment is very complex, causing the ratio of glucan to xylan and biomass crystallinity to vary with the extent of delignification.

Figure V-24 shows that decrystallization has a more significant effect on the initial hydrolysis rate than delignification. As cellulase loading increase from 10 to 100 FPU/g dry biomass, the initial hydrolysis rate of the highly-crystalline (i.e., 55%) biomass sample only increases around 2 times regardless of lignin content. Decrease in biomass crystallinity from 55% to 15% enhances the initial hydrolysis rate of high-lignin biomass sample 3 times at both enzyme loadings of 10 and 100 FPU/g dry biomass; whereas the initial hydrolysis rate of the low-lignin biomass sample only increases about 1.7 times. Moderate delignification (i.e., 15%) greatly enhances the initial hydrolysis rate of highly-crystalline (i.e., 55%) and low-crystalline (i.e., 15%) biomass sample, whereas extensive delignification (i.e., 5–10%) does not improve the initial hydrolysis rate. Decrystallization significantly reduces the amounts of enzyme required to achieve certain hydrolysis rate. The 1-h total sugar conversion of low-crystalline biomass with lignin content of 15% can attain 80% with enzyme loading of 100 FPU/g dry biomass, thus the hydrolysis time can be reduced from 72 h to 1 h and the enzyme can be reused.

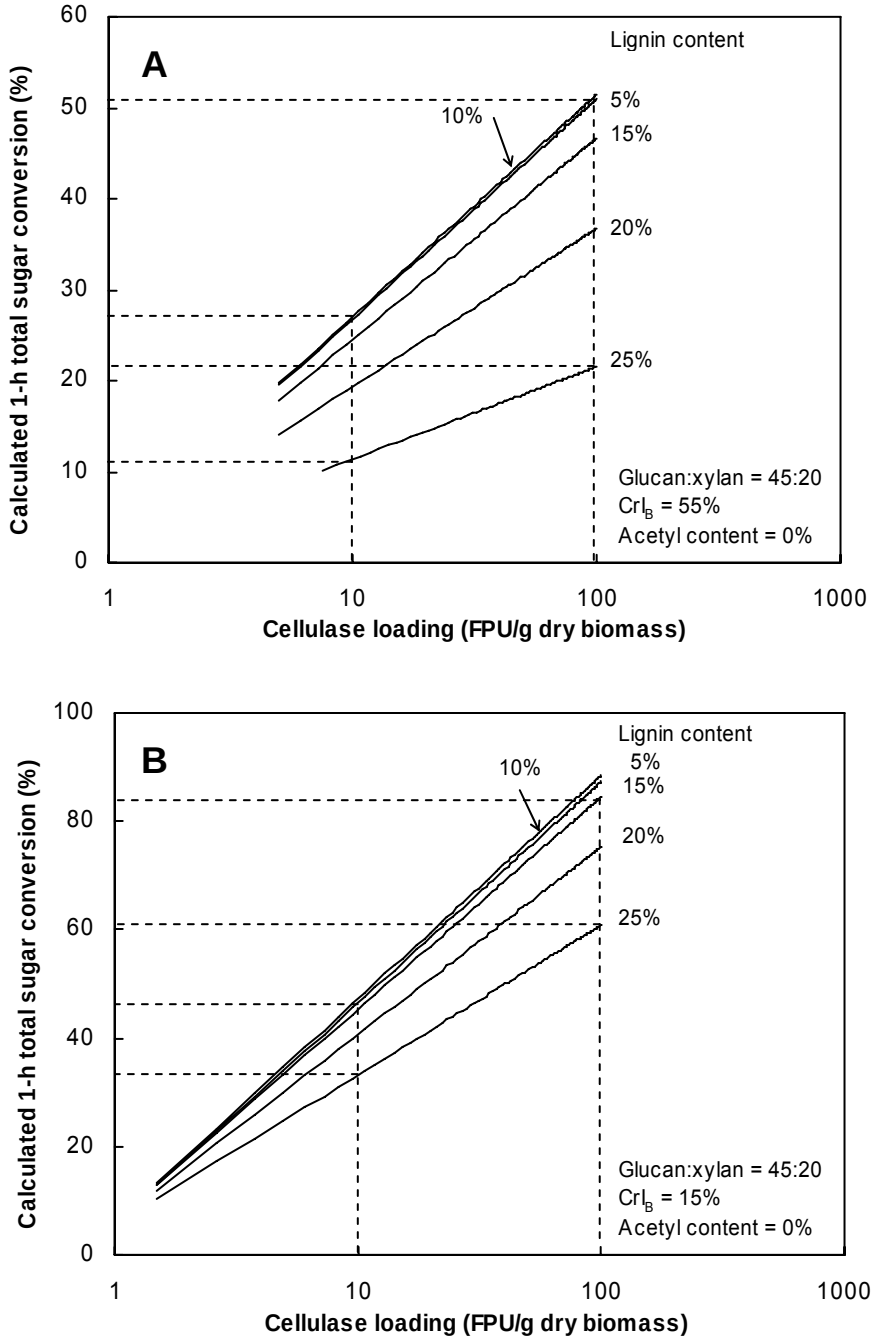

Figure V-24. Calculated 1-h total sugar conversions as a function of cellulase loading at various lignin contents using equations I-3 and V-3: (A) high-crystallinity biomass samples; (B) low-crystallinity biomass samples.

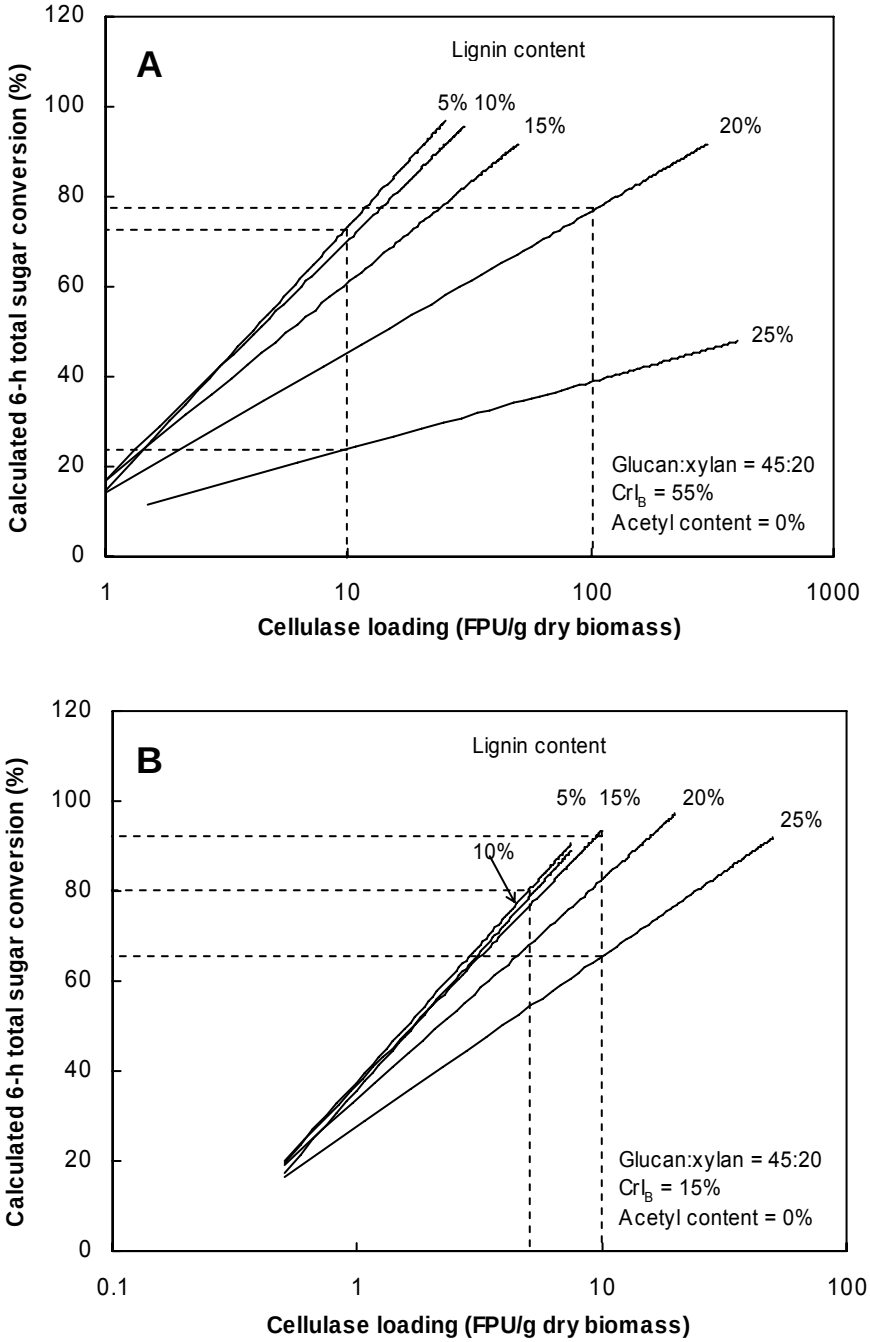

Figure V-25. Calculated 6-h total sugar conversions as a function of cellulase loading at various lignin contents using equations I-3 and V-3: (A) high-crystallinity biomass samples; (B) low-crystallinity biomass samples.

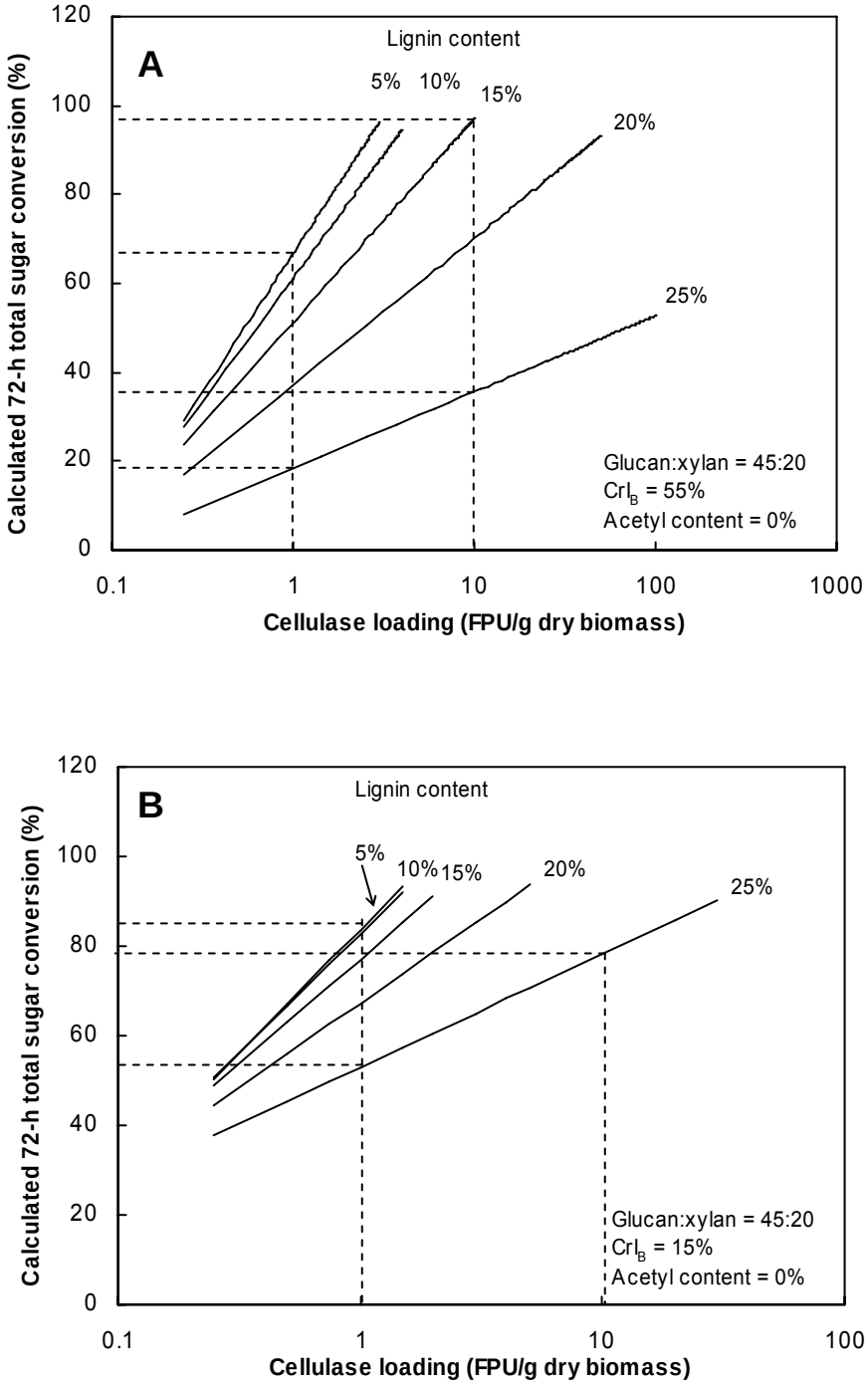

Figure V-26. Calculated 72-h total sugar conversions as a function of cellulase loading at various lignin contents using equations I-3 and V-3: (A) high-crystallinity biomass samples; (B) low-crystallinity biomass samples.

Figure V-25 demonstrates that lignin reduction from 25% to 10% increases the 6-h total sugar conversion of the highly-crystalline biomass sample from 23% to 70% with an enzyme loading of 10 FPU/g dry biomass. For the low-crystalline biomass sample, the 6-h total sugar conversion increases from 65% to 93% at a cellulase loading of 10 FPU/g dry biomass as lignin content decreases from 25% to 15%. These data indicate that delignification has more impact on the digestibility of highly-crystalline biomass sample than on low-crystalline biomass sample. For the high-lignin (i.e., 20%) and high-crystallinity (i.e., 55%) biomass sample, the enzyme loading required to achieve the 6-h total sugar conversion of 80% is 100 FPU/g dry biomass, whereas 5 FPU/g dry biomass is sufficient for low-lignin (i.e., 10%) and low-crystallinity (i.e., 15%) biomass to achieve the same sugar conversion. Severe delignification (i.e., 5–10%) does not improve the 6-h total sugar conversion of the decrystallized biomass sample.

Figure V-26 shows that decreasing lignin content from 25% to 5% greatly enhances the hydrolysis extent of highly-crystalline biomass sample (i.e., from 18% to 67%) with a cellulase loading of 1 FPU/g dry biomass. Nearly complete hydrolysis is possible for highly-crystalline biomass sample with lignin content of 10–15% with cellulase loading less than 10 FPU/g dry biomass; whereas severe delignification (i.e., lignin content of 5%) incurs extra cost with slight decrease in enzyme loadings. Reducing biomass crystallinity from 55% to 15% increases the hydrolysis extent of high-lignin (i.e., 25%) biomass sample to great extent, for example, from 18% to 57% with a cellulase loading of 1 FPU/g dry biomass and from 36% to 78% at a cellulase loading of 10 FPU/g dry biomass. Lignin content must be reduced to 15% for the highly-crystalline biomass sample to attain nearly complete hydrolysis with a cellulase loading of 10 FPU/g dry biomass; whereas a cellulase loading of 1 FPU/g dry biomass is sufficient for low-lignin and low-crystallinity biomass to achieve 85% total sugar conversion. Therefore, for the moderately delignified biomass (i.e., 15–20%), decrystallization reduces the required amounts of enzyme to achieve nearly complete hydrolysis. However, extensive delignification (i.e., 5–10%) does not improve the hydrolysis extent of decrystallized biomass samples.

Figures V-24 to V-26 show that either delignification or decrystallization significantly increases digestibility. However, selecting a delignifying or decrystallizing pretreatment depends on economics. This research provides the models to help reduce production costs by optimizing the pretreatment and enzymatic hydrolysis processes.

CONCLUSIONS

The parametric and nonparametric models can satisfactorily correlate the 1-, 6-, and 72-h slopes and intercepts of glucan, xylan, and total sugar hydrolyses with lignin content, acetyl content, cellulose crystallinity, and carbohydrate content (only for the parametric models). Based on the variables selected in the parametric models, lignin content and cellulose crystallinity show more significant effects on the slopes and intercepts (i.e., carbohydrate conversions) than acetyl content. The smaller MSE values in the parametric models indicate that they are superior to the nonparametric models.

The predictive ability of models was evaluated for a variety of biomass feedstocks (corn stover, bagasse, and rice straw) treated with lime, dilute acid, AFEX, and aqueous ammonia. The models can well predict the 1-, 6-, and 72-h slopes and intercepts, and carbohydrate conversions. The agreement between the measured and predicted values indicates that lignin content, acetyl content, and cellulose crystallinity are key factors that determine biomass digestibility. Biomass digestibility can be determined over a wide range of enzyme loadings at 1, 6, and 72 h on the basis of the simplified HCH-1 model.

CHAPTER VI

CONCLUSIONS

The addition of supplemental cellobiase to the enzyme complex significantly increased the initial rate and ultimate extent of biomass hydrolysis. It also increased the filter paper activity of the enzyme complex by converting the strong inhibitor, cellobiose, to glucose. Highly excessive addition of cellobiase enhanced digestibility and the filter paper activity only slightly. A cellobiase loading of 28.4 CBU/g dry biomass was sufficent to eliminate the inhibitiory effect of cellobiose at an incubation period of 1 h. By adding cellobiase, the extents of glucan and xylan hydrolyses were essentially identical regardless of substrate concentration. Low substrate concentrations such as 10–20 g/L are often used in laboratory investigations to prevent end-product inhibition of cellulase by cellobiose and glucose when cellobiase activity is low in the enzyme complex.

The infuence of enzyme loading on biomass digestibility highly depends on structural features resulting from pretreatment. A low enzyme loading of 2 FPU/g dry biomass is sufficient for high-digestibility biomass (low lignin content and low crystallinity) to achieve nearly complete hydrolysis at 72 h. To some extent, digestibility of biomass with structural features recalcitrant to enzymatic hydrolysis can be improved by increasing enzyme loading (50 FPU/g dry biomass); however, nearly complete hydrolysis cannot be achieved even at an enzyme loading of 180 FPU/g dry biomass. Severe delignification combined with decrystallization is not necessary to achieve high sugar yields.

The 1-, 6-, and 72-h glucan, xylan, and total sugar conversions were proportional to the natural logarithm of cellulase loadings from 10–15% to 90% conversions, indicating that the simplified HCH-1 model can predict enzymatic hydrolysis of lignocelluloses with various structural features. Because of the wide spectrum of

structural features, the enzyme loadings that produce 1-, 6-, and 72-h carbohydrate conversions in the range of 10–15% to 90% varied.

Lignin content and crystallinity play more significant roles in biomass digestibility than acetyl content. Decrystallization has a greater effect on the initial glucan hydrolysis rate, whereas delignification has a greater effect on xylan hydrolysis. Decrystallization tremendously increased biomass digestibility during shorter reaction times whereas delignification greatly enhanced the ultimate extent of biomass hydrolysis. Severe delignification or decrystallization incurrs an extra cost with no significant improvement in ultimate sugar conversion. The effects of lignin content, acetyl content, and crystallinity on biomass digestibility are, to some extent, interrelated. Delignification shows less effect on the digestibility of low-crystalline biomass than it does on the digestibility of high-crystalline biomass. Deacetylation has an insignificant influence on the digestibility of biomass with low lignin content or low crystallinity.

Compared to deacetylation, both delignification and decrystallization show more significant effects on the 1-, 6-, and 72-h slopes and intercepts of total sugar hydrolysis. The large 72-h intercept and relatively small 72-h slope for the decrystallized biomass samples indicate that small amounts of enzyme are required to achieve the desired carbohydrate conversion; the large 72-h slope for the delignified biomass samples signifies that the ultimate extent of carbohydrate hydrolysis could be virtually complete at high enzyme loadings. Decrystallization greatly accelerated the initial hydrolysis rate because the 1-h slope and intercept increased as crystallinity decreased. Both delignification and decrystallization significantly influenced the 6-h slope and intercept of total sugar hydrolysis.

The parametric and nonparametric models can satisfactorily correlate the 1-, 6-, and 72-h slopes and intercepts of glucan, xylan, and total sugar hydrolyses with lignin content, acetyl content, cellulose crystallinity, and carbohydrate content (only for the parametric models). Based on the variables selected in the parametric models, lignin content and cellulose crystallinity show more significant effects on the slopes and

intercepts (i.e., carbohydrate conversions) than acetyl content. The smaller MSE in the parametric models indicates that they are superior to nonparametric models.

The predictive ability of the models was evaluated for a variety of biomass feedstocks (corn stover, bagasse, and rice straw) treated with lime, dilute acid, AFEX, and aqueous ammonia. The measured 1-, 6-, and 72-h slopes and intercepts, and carbohydrate conversions agreed well with the values predicted by the models, indicating that lignin content, acetyl content, and cellulose crystallinity are key factors that determine biomass digestibility. Biomass digestibility can be determined over a wide range of enzyme loadings based on the simplified HCH-1 model.

CHAPTER VII

FUTURE WORK

Although the predictive ability of the models is satisfactory, the following are recommendations for future work to improve the models and their predictive ability:

1. Because the addition of cellobiase into the enzyme complex can increase cellulase activity, it is desirable to determine the cellulase activity as cellobiase is supplemented. The ratio of cellobiase to cellulase (v/v) should be kept constant at various cellulase loadings during enzymatic hydrolysis of lignocellulosic biomass.
2. The xylanase activity in the enzyme complex and the supplemental cellobiase should be determined when correlating xylan digestibility with structural features.
3. Because biomass digestibility can be improved as the incubation period increases, digestibility at longer incubation periods, such as 120 and 144 h, should be correlated with structural features.
4. For sugar conversion from 0–100%, the plot of sugar conversion versus the natural logarithm of enzyme loading is actually sigmoidal, not linear. The parameters that describe sigmoidal plots could be correlated with structural features.

REFERENCES

Bailey MJ, Biely P, Poutanen K. 1992. Interlaboratory testing of methods for assay of xylanase activity. J Biotech 23: 257-270.

Blakeney AB, Matheson NK. 1984. Some properties of the stem and pollen starches of rice. Starke 36: 265-269.

Breiman L, Friedman JH. 1985. Estimating optimal transformations for multiple regression and correlation. J Am Stat Assoc 80: 580-598.

Breuil C, Saddler J. 1985. Limitations of using the D-glucose peroxidase method for measuring glucose derived from lignocellulosic substrates. Biotech Lett 7: 191-196.

Breuil C, Chan M, Gilbert M, Saddler J. 1991. Influence of β-glucosidase on the filter paper activity and hydrolysis of lignocellulosic substrate. Biores Technol 39: 139-142.

Caulfield DE, Moore WE. 1974. Effect of varying crystallinity of cellulose on enzymic hydrolysis. Wood Sci 6: 375-379.

Chang VS, Burrm B, Holtzapple MT. 1997. Lime pretreatment of switchgrass. Appl Biochem Biotechnol 63-65: 3-19.

Chang VS, Holtzapple MT. 2000. Fundamental factors affecting biomass enzymatic reactivity. Appl Biochem Biotechnol 84-86: 5-37.

Chum HL, Johnson DK, Black S, Baker J, Grohmann K, Sarkanen KV. 1988. Organosolv pretreatment for enzymatic hydrolysis of poplars: 1. Enzymatic hydrolysis of cellulosic residues. Biotech Bioeng 31: 643-649.

Coward-Kelly G, Aiello-Mazzari C, Kim S, Granda C, Holtzapple MT. 2003. Suggested improvements to the standard filter paper assay used to measured cellulase activity. Biotechnol Bioeng 82(6): 745-749.

Dale BE, Moreira MJ. 1982. A freeze-explosion technique for increasing cellulose hydrolysis. Biotech Bioeng Symp 12: 31-43.

Datta R. 1981. Energy-requirement for lignocellulose pretreatment processes. Process Biochem 16:19-25.

Dische Z, Borenfreund E. 1957. A new color reaction for the determination of

aldopentose in presence of other saccharides. Biochim Biophys Acta 23: 639-642.

Douglas SG. 1981. A rapid method for the determination of pentosans in wheat flour. Food Chem 7: 139-145.

Draude KM, Kurniawan CB, Duff STB. 2001. Effect of oxygen deliginification on the rate and extent of enzymatic hydrolysis of lignocellulosic material. Biores Technol 79: 113-120.

Dubois M, Gilles KA, Hamilton PA, Smith F. 1956. Colorimetric method for determination of sugars and related substances. Anal Chem 28: 350-356.

Eubank RL. 1988. Spline smoothing and nonparametric regression. New York: Dekker.

Fan LT, Lee YH, Beardmore DH. 1981. The influence of major structural features of cellulose on rate of enzymatic hydrolysis. Biotechnol Bioeng 23: 419-424.

Fan LT, Gharpury MM, Lee YH. 1987. Nature of cellulose materials and enzymatic hydrolysis. In: Cellulose hydrolysis. Berlin: Springer-Verlag. pp 5-69.

Gharpuray MM, Lee YH, Fan LT. 1983. Structural modification of lignocellulosics by pretreatments to enhance enzymatic hydrolysis. Biotechnol Bioeng 25: 157-172.

Granda CB. 2004. Sugarcane juice extraction and preservation, and long-term lime pretreatment of bagasse. Ph.D. dissertation, Texas A&M University, College Station.

Grethlein HE. 1985. The effect of pore size distribution on the rate of enzymatic hydrolysis of cellulosic substrates. Bio/Technol 3: 155-160.

Grethlein HE, Converse AO. 1991. Common aspects of acid prehydrolysis and steam explosion for pretreating wood. Bioresource Technol 36:77-82.

Grohmann K, Mitchell DJ, Himmel ME. 1989. The role of ester groups in resistance of plant cell wall polysaccharides to enzymatic hydrolysis. Appl Biochem Biotechnol 20/21: 45-61.

Gusakov AV, Sinitsyn AP, Klyosov AA. 1985. Kinetics of the enzymatic hydrolysis of cellulose: 1. A mathematical model for a batch reactor process. Enzyme Microbiol Technol 7: 346-352.

Gusakov AV, Sinitsyn AP, Manenkova JA, Protas OV. 1992. Enzymatic saccharification of industrial and agricultural lignocellulosic wastes. Appl Biochem Biotechnol 34/35: 625-637.

Holtzapple MT, Humphrey A. 1983. Determination of soluble and insoluble glucose oligomers with chromotropic acid. Anal Chem 55: 584-585.

Holtzapple MT, Caram H, Humphrey A. 1984. The HCH-1 model of enzymatic cellulose hydrolysis. Biotechnol Bioeng 26: 775-780.

Holtzapple MT, Cognata M, Shu Y, Hendrickson C. 1990. Inhibition of *Trichoderma reesei* cellulase by sugars and solvents. Biotechnol Bioeng 36: 275-287.

Holtzapple MT, Jun J, Ashok G, Patibandla SL, Dale BE. 1991. The ammonia freeze explosion (AFEX) process. A practical lignocellulose pretreatment. Appl Biochem Biotechnol 28/29: 59-74.

Holtzapple MT. 1993a. Cellulose. In: Macrae R, Robinson R K, Sadler MJ, editors. Encyclopedia of food science, food technology and nutrition, vol. 2. London: Academic Press. pp 2731-2738.

Holtzapple MT. 1993b. Hemicellulose. In: Macrae R, Robinson R K, Sadler MJ, editors. Encyclopedia of food science, food technology and nutrition, vol. 2. London: Academic Press. pp 2324-2334.

Holtzapple MT. 1993c. Lignin. In: Macrae R, Robinson R K, Sadler MJ, editors. Encyclopedia of food science, food technology and nutrition, vol. 2. London: Academic Press. pp 758-767

Holtzapple MT, Ripley E, Nikolaou M. 1994. Saccharification, fermentation, and protein recovery from low-temperature AFEX-treated coastal bermudagrass. Biotechnol Bioeng 44: 1122-1131.

Holtzapple MT, Ross MK, Chang NS, Chang VS, Adelson SK, Brazel C. 1997. Biomass conversion to mixed alcohol fuels using the MixAlco Process. In: Saha BC, Woodward J, editors. Feuls and chemicals from biomass. Washington DC: American Chemical Society. pp 130-142.

Honda S, Chiba H, Kakehi K. 1981. Selective determination of pentoses, hexoses and 6-deoxyhexoses by dual-wavelength spectrophotometry with the cysteine-phenol-sulfuric acid system. Anal Chim Acta. 131: 205-211.

Hsu TA. 1996. Pretreatment of biomass. In: Wyman CE, editor. Handbook on bioethanol, production and utilization.Washington DC: Taylor & Francis. pp 179-212.

Huang X, Penner MH. 1991. Apparent substrate inhibition of the *Trichoderma reesei*

cellulase system. J Agric Food Chem 39: 2096-2100.

Ingram LO, Doran JB. 1995. Conversion of cellulosic materials to ethanol. FEMS Microbiology Review 16: 235-241.

Joglekar AV, Karanth NG, Srinivasant MC. 1983. Significance of β-D-glucosidase in the measurement of exo-β-D-glucanase activity of cellulolytic fungi. Enzyme Microb Technol 5: 25-29.

Kim S. 2004. Lime pretreatment and enzymatic hydrolysis of corn stover. Ph.D. dissertation, Texas A&M University, College Station.

Kim TH, Kim JS, Sunwoo C, Lee YY. 2003. Pretreatment of corn stover by aqueous ammonia. Biores Technol 90: 39-47.

Kirk TK, Farrell RL. 1987. Enzymatic combustion: The microbial degradation of lignin. Annu Rev Microbiol 41: 465-505.

Klein B, Weissman M. 1953. New color reagent for determination of hexoses. Anal Chem 25(5): 771-774.

Kong F, Engler CR, Soltes EJ. 1992. Effect of cell-wall acetate, xylan backbone, and lignin on enzymatic hydrolysis of aspen wood. Appl Biochem Biotechnol 34/35: 23-35.

Koullas DP, Christakopoulos PF, Kekos D, Macris BJ, Koukios EG. 1990. Effect of cellulose crystallinity on the enzymic hydrolysis of lignocellulosics by *Fusarium oxysporum* cellulases. Cellulose Chem Technol 24: 469-474.

Koullas DP, Christakopoulos PF, Kekos D, Macris BJ, Koukios EG. 1992. Correlating the effect of pretreatment on enzymatic hydrolysis of wheat straw. Biotechnol Bioeng 39: 113-116.

Lee YH, Fan LT. 1982. Kinetic-studies of enzymatic-hydrolysis of insoluble cellulose-analysis of the initial rates. Biotechnol Bioeng 24: 2383-2406.

Lu Y, Yang B, Gregg D, Saddler JN, Mansfield SD. 2002. Cellulase adsorption and an evaluation of enzyme recycle during hydrolysis of steam-exploded softwood residues. Appl Biochem Biotechnol 98-100: 641-652.

Lynd LR, Weimer PJ, van Zyl WH. 2002. Microbial cellulose utilization: Fundamentals and biotechnology. Microbiol Mol Biol Rev 66(3): 506-565.

Mandels M, Medeiros JE, Andreotti RE, Bissett FH. 1981. Enzymatic hydrolysis of cellulose: Evaluation of cellulose culture filtrates under use conditions. Biotechnol Bioeng 23: 2009-2026.

Manonmani HK, Sreekantiah KR. 1987. Saccharification of sugar-cane bagasse with enzymes from *Aspergillus ustus* and *Tricholderma viride*. Enzyme Microb Technol 9: 484-488.

McCleary BV, Shameer I, Glennie-Holmes M. 1988. Measurement of (1→3), (1→4)-β-D-glucan. In: Methods in enzymology, vol. 160. New York: Academic Press. pp 545-551.

Meunier-Goddik L, Penner M H. 1999. Enzyme-catalyzed saccharification of model celluloses in the presence of lignacious residues. J Agric Food Chem 47: 346-351.

Miller GL. 1959. Use of dinitrosalicylic acid reagent for determination of reducing sugars. Anal Chem 31: 426-428.

Millet MA, Baker AJ, Satter LD. 1976. Physical and chemical pretreatments for enhancing cellulose saccharification. Biotech Bioeng Symp 6: 125-153.

Mitchell DJ, Grohmann K, Himmel ME, Dale BE, Schroeder HA. 1990. Effect of the degree of acetylation on the enzymatic digestion of acetylated xylan. J Wood Chem Technol 10 (1):111-121.

Mooney CA, Mansfield SD, Touhy MG, Saddler JN. 1998. The effect of initial pore volume and lignin content on the enzymatic hydrolysis of softwoods. Biores Technol 64: 113-119.

Nguyen QA, Saddler JN. 1991. An integrated model for the technical and economic evaluation of an enzymatic biomass conversion process. Biores Technol 35: 275-282.

Nidetzky B, Steiner W. 1993. A new approach for modeling cellulase-cellulose adsorption and the kinetics of the enzymatic hydrolysis of microcrystalline cellulose. Biotechnol Bioeng 42: 469-479.

National Renewable Energy Laboratory. 2004. Chemical analysis & testing standard procedure. Golden, CO.

O'Dwyer JP. 2005. Developing a fundamental understanding of biomass structural features responsible for enzymatic digestibility. Ph.D. dissertation. Texas A&M University, College Station.

Ooshima H, Burns DS, Converse AO. 1990. Adsorption of cellulase from *Trichoderma reesei* on cellulose and lignacious residue in wood pretreated by dilute sulfuric acid with explosive decompression. Biotechnol Bioeng 36: 446-452.

Ortega N, Busto MD, Perez-Mateos M. 2001. Kinetics of cellulose saccharification by *Trichoderma reesei* cellulases. Int Biodeter Biodegr 47: 7-14.

Pfeifer PA, Bonn G, Bobleter O. 1984. Influence of biomass degradation products on the fermentation of glucose to ethanol by *Saccharomyces carlsbergensis W 34*. Biotech Lett 6(8): 541-546.

Puri VP. 1984. Effect of crystallinity and degree of polymerization of cellulose on enzymatic saccharification. Biotechnol Bioeng 26: 1219-1222.

Reese ET, Mandels M. 1971. Enzymatic degradation. In: Bikales N, Segal L, editiors. Cellulose and cellulose derivatives, vol. 5. New York: Wiley. pp 1079-1094.

Saha SK, Brewer CF. 1994. Determination of the concentrations of oligosaccharides complex type carbohydrates and glycoproteins using the phenol-sulfuric acid method. Carbohydrate Research 254:157-167.

Sattler W, Esterbauer H, Glatter O, Steiner W. 1989. The effect of enzyme concentration on the rate of the hydrolysis of cellulose. Biotechnol Bioeng 33: 1221-1234.

Schell DJ, Ruth MF, Tucker MP. 1999. Modeling the enzymatic hydrolysis of dilute-acid pretreated Douglas fir. Appl Biochem Biotechnol 77-9: 67-81.

Schwald W, Breuil C, Brownell HH, Chan M, Saddler JN. 1989. Assessment of pretreatment conditions to obtain fast complete hydrolysis on high substrate concentrations. Appl Biochem Biotechnol 20/21: 29-44.

Segal L, Creely JJ, Martin Jr AE, Conrad CM. 1959. An empirical method for estimating the degree of crystallinity of native cellulose using the X-Ray diffractometer. Text Res J 29: 786-794.

Sewalt VJH, Glasser WG, Beauchemin KA. 1997. Lignin impact on fiber degradation. 3. Reversal inhibition of enzymatic hydrolysis by chemical modification of lignin and by additives. J Agric Food Chem 45: 1823-1828.

Sinitsyn AP, Gusakov AV, Vlasen EY. 1991. Effect of structural and physico-chemical features of cellulosic substrates on the efficiency of enzymatic hydrolysis. Appl Biochem Biotechnol 30: 43-59.

South CR, Hogsett DAL, Lynd LR. 1995. Modeling simultaneous saccharification and fermentation of lignocellulose to ethanol in batch and continuous reactors. Enzyme Microb Technol 17: 797-803.

Takagi M, Abe S, Suzuki S, Emert GH, Yata N. 1997. A method for production of alcohol directly from cellulose using cellulase and yeast. In: Ghose TK, editor. Bioconversion of cellulosic substances into energy. Delhi: Indian Institute of Technology. pp 551-571

Taylor KA. 1995. A modification of the phenol/sulfuric acid assay for the total carbohydrates giving more comparable absorbance. Appl Biochem Biotechnol 53: 207-214.

Tengborg C, Galbe M, Zacchi G. 2001. Influence of enzyme loading and physical parameters on the enzymatic hydrolysis of steam-pretreated softwood. Biotechnol Prog 17: 110-117.

Teymouri F, Laureano-Perez L, Alizadeh H, Dale BE. 2004. Ammonia fiber explosion treatment of corn stover. Appl Biochem Biotechnol 113-116: 951-963.

Thompson DN, Chen HC. 1992. Comparison of pretreatment methods on the basis of available surface area. Biores Technol 39: 155-163.

Tibshirani R. 1988. Estimating optimal transformations for regression via additivity and variance stabilization. J Am Stat Assoc 83: 394-405.

Torget R, Walter P, Himmel M, Grohmann K. 1991. Diluted-acid pretreatment of corn residues and short-rotation woody crops. Appl Biochem Biotechnol 28/29: 75-86.

Tran AV, Chambers RP. 1986. Ethanol fermentation of red oak acid prehydrolyzate by the yeast *Pichia stipitis* CBS 5776. Enz Microbiol Tech 8(7): 439-444.

Vidal PF, Molinier J. 1988. Ozonolysis of lignin-improvement of *in vitro* digestibility of poplar sawdust. Biomass 16: 1-17.

Wald S, Wilke CR, Blanch HW. 1984. Kinetics of the enzymatic hydrolysis of cellulose. Biotechnol Bioeng 26: 221-230.

Wang D, Murphy M. 2004. Estimating optimal transformation for multiple regression using the ACE algorithm. J Data Sci 2: 329-346.

Weimer PJ, Weston WM. 1985. Relationship between the fine structure of native cellulose

and cellulose degradability by the cellulase complexes of *Trichoderma reesi* and *Clostridium thermocellum*. Biotechnol Bioeng 27: 1540-1547.

Wright JD, Wyman CE, Grohmann K. 1988. Simultaneous saccharification and fermentation of lignocellulose. Appl Biochem Biotechnol 18: 75-90.

Wu CH, Soto RD, Valko PP, Bubela AM. 2000. Non-parametric regression and neural-network infill drilling recovery models for cobonate reservoirs. Computers and Geosciences 26: 975-987.

Xue G. 1997. Integrated reservoir characterization using optimal nonparametric transformations and structure preserving inversion. Ph.D. dissertation, Texas A&M University, College Station.

Yoon HH, Wu ZW, Lee YY. 1995. Ammonia-recycled percolation process for pretreatment of biomass feedstock. Appl Biochem Biotechnol 51/52: 5-19.

APPENDIX A

PRETREATMENT PROCEDURE

Short-Term Oxidative Lime Pretreatment

Lignocellulosic biomass was pretreated with lime (calcium hydroxide) in the presence of water and air. The pretreatment conditions were temperature = 100^{o}C, time = 2 h, lime loading = 0.1 g/g dry biomass, and water loading = 10 mL/g dry biomass.

Apparatus and Materials

Corn stover provided by NREL

Calcium hydroxide: Fisher Scientific

Glacial acetic acid

Bunsen burner

Stainless tank

Glass rod

Centrifuge machine, Beckman, J-6B.

Centrifuge bottle, 1-L, Fisher Scientific

Beaker, 3-L, Fisher Scientific

pH meter

Convection drying oven, with temperature control of 45 ± 1^{o}C

Procedure

1. Place 250 g of corn stover (-40 mesh) and 25 g of lime, 2.5 L of 50–60^{o}C distilled water in a stainless steel tank, mix them thoroughly with a glass rod to ensure even distribution of lime and water.
2. Heat the slurry with two Bunsen burners, and allow it to boil for 2 h with occasional stirring. A cover is necessary to reduce water evaporation.
3. Turn off the burners, and allow the mixture to cool to room temperature.

4. Adjust the pH of the mixture to 5.5 to 6.0 by adding 65 mL of dilute glacial acetic acid (glacial acetic acid: distilled water = 1: 2 (v/v)).
5. Transfer the pretreated biomass slurry to eight 1-L centrifuge bottles and add 800 mL of distilled water to each bottle. Stir them for 15 min.
6. Centrifuge the water-biomass mixture at 4,000 rpm for 20 min.
7. After centrifuging, decant the water to the sink.
8. Repeat Steps 5 through 7 until the filtrate becomes clear. It normally takes 10 cycles.
9. After being completely washed, transfer all the biomass in the centrifuge bottles into a flat container.
10. Dry biomass at 45^{o}C for 48 h or longer if necessary.

Long-Term Oxidative or Nonoxidative Lime Pretreatment

The whole process is described by Kim (2004).

1. Fill water into the water tank to cover the heating element. Turn on the centrifugal pump to circulate water. Fill sufficient water into the tank to maintain a nearly full level.
2. Turn on the temperature controller to heat up the circulating water to the set temperature.
3. Operate the whole system to reach a steady state.
4. Steps 1 to 3 can be skipped for the pretreatment at 25°C.
5. Place 15.0 g dry weight of the raw biomass and 7.5 g of calcium hydroxide in a beaker. Pour 70 mL of distilled water into the beaker and thoroughly mix them using a spatula.
6. Transfer the mixture of biomass and calcium hydroxide into a reactor using a funnel. Wash the beaker and the spatula with 80 mL of distilled water to transfer all remnants in the reactor through the funnel.

7. Tightly cap the reactor and connect the bubble indicator (it is filled with 20–25 mL of distilled water in a 50-mL plastic tube) to measure the gas flow rate.
8. Slowly open the appropriate valve to supply nitrogen for non-oxidative pretreatment or air for oxidative pretreatment. Confirm bubble formation in the bubble indicator. Adjust the gas flow rate to achieve at 2–3 bubbles/s using a clamp, which is placed at the tube in the bottom of the reactor.
9. Regularly check the gas pressure (4.5–5.0 psi for nitrogen gas and 60–80 psi for in-line air), gas flow rate, seals, and water levels in the cylinder filled with water and in the tank, and working temperatures.
10. At certain pretreatment periods, remove the reactors and cool down to ambient temperature.

Aqueous Ammonia Pretreatment

Lignocellulosic biomass was pretreated with 15% aqueous ammonia. The pretreatment conditions were temperature = 60^{o}C, time = 12 h, liquid loading = 6 mL/g dry biomass.

Apparatus and Materials

Bagasse
30% aqueous ammonia: Fisher Scientific
500-mL wide-mouth Pyrex bottle
Glass rod
Centrifuge machine, Beckman, J-6B.
Centrifuge bottle, 1-L, Fisher Scientific
pH meter
Convection drying oven, with temperature control of 45 ± 1^{o}C

Procedure

1. The following steps should be done in a fume hood: prepare 15% aqueous ammonia by mixing 250 mL of distilled water and 250 mL of 30% aqueous ammonia solution
2. Place 40 g of ground bagasse and 240 mL of 15% aqueous ammonia in a 500-mL wide-mouth Pyrex bottle with orange cap.
3. Stir the slurry with a glass rod to mix them well and place the bottle in the oven set at 60^{o}C for 12 h.
4. Remove the bottle from the oven, allowing the mixture to cool to room temperature.
5. Follow Steps 5 to 10 in Short Term Oxidative Lime Pretreatment to wash and dry pretreated biomass.

Ammonia Fiber Explosion (AFEX)

The AFEX treatment procedure is described by Teymouri et al.(2004).

1. Corn stover (passed through a 6-mm screen) is wetted to obtain the moisture content of 40% or 60%.
2. Load prewetted corn stover into a 300-mL stainless steel pressure vessel. The vessel was topped up with stainless steel spheres (1 mm in diameter) to occupy the void space and thus minimize transformation of the ammonia from liquid to gas during loading.
3. The lid is then bolted shut.
4. Deliver the predetermined amount of liquid ammonia to the vessel using the precalibrated ammonia sample cylinders.
5. Heat the vessel to the desired temperature using a 400-W Parr heating mantle.
6. After holding the vessel at the target temperature for the selected residence time, rapidly open the exhaust valve to relieve the pressure and accomplish the explosion.
7. Both the pressure and temperature drop very rapidly.

8. Remove the treated biomass from the vessel and allow them to stand overnight in a fume hood to evaporate the residual ammonia.
9. Keep the treated biomass in plastic bags in a refrigerator.

Dilute Acid Pretreatment

Apparatus and Materials

Bagasse

96% H_2SO_4: Fisher Scientific

500-mL wide-mouth Pyrex bottle

Glass rod

Centrifuge machine, Beckman, J-6B.

Centrifuge bottle, 1-L, Fisher Scientific

Autoclave, set to 121 ± 3°C

pH meter

Convection drying oven, with temperature control of 45 ± 1°C

Procedure

1. Place 500 mL of distilled water in a 1-L volumetric flask, and then 5.66 mL of 96% H_2SO_4.
2. Complete to 1 L using distilled water.
3. Place 15 g of ground bagasse and 300 mL of 1% H_2SO_4 in a 500-mL wide-mouth Pyrex bottle with orange cap.
4. Stir the slurry with a glass rod to mix them well.
5. Autoclave the samples for 2 h at 121 ± 3°C.
6. Remove the bottle from the oven, allowing the mixture to cool to room temperature.
7. Follow Steps 5 to 10 in Short-Term Oxidative Lime Pretreatment to wash and dry pretreated biomass.

APPENDIX B

ENZYMATIC HYDROLYSIS

Enzymatic Hydrolysis Procedure for Fundamental Study of Structural Features

Enzymatic hydrolysis of pretreated biomass was performed in 50-mL Erlenmeyer flasks at 50°C on a shaking air bath agitated at 100 rpm. The hydrolysis experiments were performed at 10-g/L solid concentration in 0.05-M citrate buffer (pH 4.8) supplemented with 0.01-g/mL sodium azide to prevent microbial contamination. Hydrolysis was initiated by adding appropriately diluted cellulase and excess cellobiase, which prevents end-product inhibition by cellobiose. A series of experiments were conducted with strategic cellulase loadings based on biomass structural features. After the incubation periods (1, 6, and 72 h), the reaction in the sealed Erlenmeyer flasks was quenched in boiling water. Then sugar yields were measured at each time point. See the following complete hydrolysis procedure.

Apparatus

Analytical balance, accurate to 0.1 mg

Convection drying oven, with temperature control of 105 ± 3^{o}C

100-rpm shaking air bath, Amerex instrument, GM 706

Centrifuge machine, Beckman, J-6B.

Adjustable pipettors, covering ranges of 0.02 to 5.00 mL

Bunsen Burner

Erlenmeyer flask, 50-mL

Centrifuge tubes, 15-mL

Plastic vials, 2-mL

Long sleeve rubber stopper, 19-mm, VWR

Hose Clamps, SNP-19, Cole Parmer, Cat No. 06832-20

Materials

Citric acid monohydrate, Fisher Scientific

Glacial acetic acid, G. R., 99.7%, EM Science

Sodium hydroxide, Beads, Fisher Scientific

Sodium azide, Fisher Scientific

Cellulase, Spezyme CP, Lot No. 301-00348-257, Genencor, USA, activity ≅ 65 FPU/mL

Cellobiase, "Novozyme 188", activity ≅ 321 CBU/mL

Procedure

1. Determine the moisture contents of biomass using NREL standard procedure No. 001 (2004).
2. Prepare 1 L of 1-M citrate buffer and 250 mL of 0.01-g/mL sodium azide following NREL standard procedure No. 006 (2004).
3. Place 0.2 g dry biomass and 18 mL of distilled water in 50-mL Erlenmeyer flasks. Label each flask with enzyme loading and incubation period.
4. Add 1.0 mL of 1-M citrate buffer and 0.6 mL of 0.01-g/mL sodium azide into the flasks to keep the pH constant and prevent the growth of microorganisms, respectively.
5. Measure the pH of the mixture and add glacial acetic acid or sodium hydroxide to adjust pH to 4.8, if necessary.
6. Place the rubber stopper on the top of the Erlenmeyer flasks and preheat the flasks at 50°C in a 100-rpm shaking air bath for 1 h before adding enzymes.
7. Take out the heated flask from the shaker and initiate the enzymatic hydrolysis by adding 0.2 mL of the appropriately diluted cellulase and 0.05 mL of cellobiase (81.2 CBU/g dry biomass). The final volume is 20.0 mL. See Table B-1 to prepare the diluted cellulase solutions at various concentrations.
8. Cap the flasks tightly using a clamp to seal the rubber stopper, so the stopper can stand the pressure during boiling. Place the flasks back into the shaking air bath.

9. After 1 h incubation, take out the flask and vigorously boil the whole flask for 15 min to denature enzymes.
10. Cool the boiled flasks in an ice-water bath for 10 min and transfer 10 mL of the mixture to conical centrifuge tube.
11. Centrifuge the mixture at 4,000 rpm for 5 min to separate the liquid and solid phases.
12. Transfer 1.7 mL of the liquid into a 2-mL plastic vial and store it in the freezer for sugar analysis by DNS or HPLC later. Remember to vortex the sample after thawing.
13. Repeat Steps 9 through 12 at 6 and 72 h to obtain 6 and 72 h digestibility.

Table B-1. Preparation of dilute cellulase solutions

Cellulase concentration in hydrolysis (FPU/g dry biomass)	Original cellulase solution (mL)[a]	Distilled water (mL)
0.25	0.1	25.9
0.5	0.25	32.25
0.75	0.25	21.42
1.0	0.25	16.0
1.5	0.25	10.58
2.0	0.25	7.87
3.0	0.25	5.16
5.0	0.25	3.0
10.0	0.5	2.75
30.0	1.0	1.17
50.0	2.0	0.6

[a] The activity of the original cellulase solution was 65 FPU/mL.

APPENDIX C

EFFECT OF BALL MILLING ON DECRYSTALLIZATION

Introduction

Ball-milling effectively reduces biomass crystallinity by destroying the crystal lattice structure of the cellulose fiber, thus enhancing the amorphous cellulose content (Chang and Holtzapple, 2000; Fan et al., 1981). Although decrystallization has been reported to be less important than lignin removal on sugar yields, decreasing crystallinity significantly increased the initial hydrolysis rate, and to some extent, the ultimate biomass conversion (Chang and Holtzapple, 2000). The use of fine substrate resulting from decrystallization allows a higher slurry concentration so as to reduce the reactor volume (Fan et al., 1981). Even though biomass crystallinity is mainly from highly crystalline cellulose in biomass, the contents of amorphous hemicellulose and lignin influence biomass crystallinity measured by XRD, i.e., removal of lignin or hemicellulose increases biomass crystallinity. It is desirable to measure cellulose crystallinity in lignocellulose that influences biomass digestibility. In this study, the effectiveness of ball milling on decrystallization was evaluated. The correlation between cellulose crystallinity (CrI_C), biomass crystallinity (CrI_B), and the lignin and hemicellulose contents was proposed.

Materials and Methods

Substrate Preparation

Ground and sieved corn stover (-40 mesh) was pretreated at 100°C for 2 h in the presence of 0.1 g lime/g dry biomass and 10 mL water/g dry biomass. The dried corn stover was ground through a 40-mesh sieve. The step-by-step pretreatment procedure is described in Appendix A. Microcrystalline cellulose, xylan (beech wood), and lignin were purchased from Fluka and Sigma, respectively.

Ball Milling Procedure

The rotary ball mill was built with two 1/6-hp, 156-rpm AC gearmotors (Dayton Electric Mfg. Co., Niles, IL). The ball mill consists of four 1-in diameter × 25-in long steel blower shafts enclosed with 1.5-in O.D. Buna-N rubber tubing (McMaster-Carr, Atlanta, GA). A 300-mL porcelain jar was charged with 0.375-in zirconia grinding media (U.S. Stoneware, East Palestine, OH) to ~25% of the jar volume (~258 g of zirconia). The ratio of grinding media to the dry weight of biomass was 43 g zirconia/g dry biomass. Then, the jars were placed between the rollers and rotated at 68 rpm for various periods. A variable AC autotransformer was used to alter the rotation speed of rotary ball mill. About 0.2 g of lime-treated corn stover was taken as a function of time (i.e., 0–9 d). Cellulose placed in four different jars was ball milled for 12, 24, 48, and 72 h, respectively.

Crystallinity Measurements

The mixed biomass was obtained by mixing various amounts of hemicellulose and lignin with cellulose ball-milled for 0, 12, 24, and 48 h. The crystallinity of corn stover and the cellulose, hemicellulose, and lignin mixtures were determined by XRD, described in Chapter II.

Results and Discussion

Figure C-1 shows the effect of milling time on crystallinity of corn stover and cellulose. The crystallinity of corn stover and cellulose decreased proportionally with the increase of ball milling time up to 3 d, and then further increasing milling time did not decrease corn stover crystallinity any more. The effect of ball milling on reducing cellulose crystallinity was more significant than that on corn stover, because corn stover had approximately 50% amorphous materials, such as hemicellulose and lignin that lower biomass crystallinity. The linear relationship between crystallinity reduction and milling time within 3 d agrees with Koullas's conclusion (Koullas et al., 1990). Prolonged ball milling not only consumed much energy but also showed a negative effect on the sugar

yield during enzymatic hydrolysis due to reduced biomass porosity and specific area resulted from long milling.

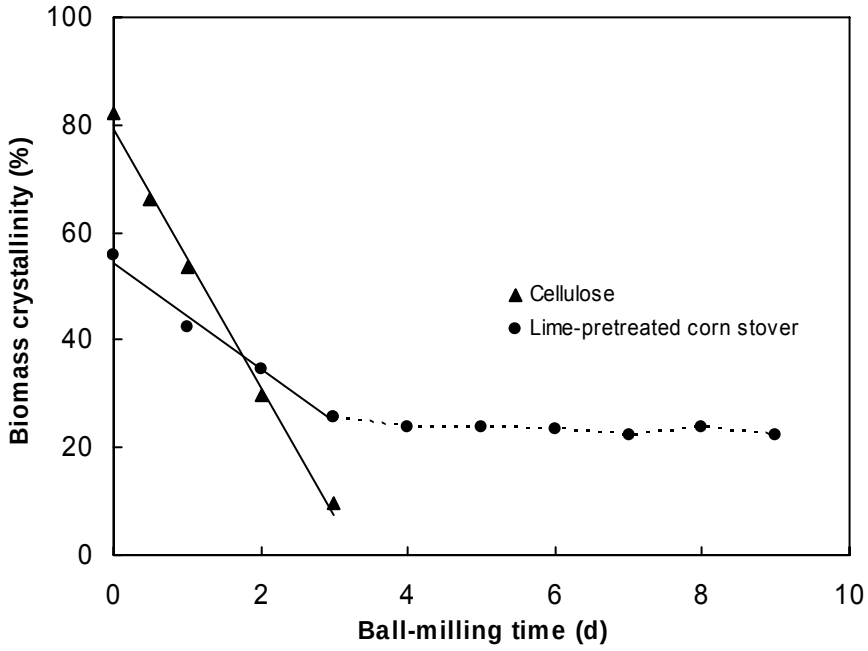

Figure C-1. Effect of ball milling time on biomass crystallinity.

Table C-1 shows the factors that influence corn stover crystallinity during ball milling. As the ratio of grinding media to the dry weight of biomass increased from 43 to 86, biomass crystallinity decreased from 29.5% to 19.9%. This might be due to the larger crushing and shearing action exerted by more grinding media. There was no observable change in biomass crystallinity when the rotation speed was altered from 156 rpm to 68 rpm. Because the rotation speed of the roller was really low, the change in rotation speed was not large enough to cause an observable change in biomass crystallinity. With the constant ratio of grinding media to the dry weight of biomass, more grinding media charged in a porcelain jar increased biomass crystallinity. It could be explained that more grinding media leads to less moving distance of media, thus there is less crushing force to grind biomass.

Table C-1. Effect of ball milling conditions on corn stover crystallinity

Sample	Ratio of zirconia weight to dry weight of biomass	Rotation speed of roller (rpm)	Percentage of the jar volume charged with grinding media (%)	CrI_B[a] (%)
1	43	156	50	36.4
2	43	156	25	30.3
3	43	68	25	29.5
4	86	68	25	19.9

Material: corn stover (-40 mesh) after lime pretreatment.
Ball milling time: 72 h.
[a] Biomass crystallinity.

Table C-2 shows the change in biomass crystallinity with varied contents of each biomass component. For the mixture of lignin, hemicellulose, and ball-milled cellulose, the increase in lignin and hemicellulose contents decreased biomass crystallinity whereas cellulose crystallinity was unchanged. The biomass crystallinity reduction resulting from increasing lignin contents seemed more pronounced than that resulting from increasing hemicellulose contents. Based on the data in Table C-2, cellulose crystallinity is linear with respect to biomass crystallinity, lignin content, and hemicellulose content. Statistically, 98% of crystallinity measured by XRD can be explained by Equation C-1.

$$CrI_C = 1.088 CrI_B + 0.604 HC + 0.4664 LC - 11.01 \quad \text{(C-1)}$$

where CrI_C = cellulose crystallinity (%)

CrI_B = biomass crystallinity (%)

HC = hemicellulose content (%)

LC = lignin content (%)

Table C-2. Influence of biomass composition on biomass crystallinity

Sample	Ball milling time (d)	CrI_C[a]	Composition of biomass (%)			CrI_B[b]
			Cellulose	Hemicellulose	Lignin	
C0-100-0-0	0	82.2	100	0	0	82.2
C0-75-25-0	0	82.2	75.3	24.7	0.0	82.3
C0-75-0-25	0	82.2	75.4	0.0	24.6	81.8
C0-70-25-5	0	82.2	70.1	24.7	5.2	81.3
C0-70-5-25	0	82.2	69.7	5.2	25.1	83.7
C0-65-25-10	0	82.2	65.1	24.6	10.4	82.7
C0-60-10-30	0	82.2	59.9	9.9	30.2	84.1
C0-55-30-15	0	82.2	55.3	29.6	15.1	84.0
C0-55-15-30	0	82.2	55.0	14.7	30.3	82.8
C0-50-50-0	0	82.2	50.4	49.6	0.0	83.5
C0-50-30-20	0	82.2	50.3	29.4	20.3	82.6
C0-50-25-25	0	82.2	50.1	24.6	25.3	81.9
C0-50-0-50	0	82.2	49.6	0.0	50.4	80.2
C0-45-35-20	0	82.2	45.0	34.3	20.7	82.6
C0-40-35-25	0	82.2	40.2	34.5	25.3	82.6
C0.5-100-0-0	0.5	66.1	100	0	0	66.1
C0.5-70-5-25	0.5	66.1	69.6	4.9	25.5	65.0
C0.5-65-25-10	0.5	66.1	65.5	24.5	10.0	65.3
C0.5-60-10-30	0.5	66.1	59.9	9.7	30.4	68.2
C0.5-55-30-15	0.5	66.1	55.1	29.7	15.2	67.0
C0.5-55-15-30	0.5	66.1	55.0	14.8	30.2	66.1
C0.5-50-30-20	0.5	66.1	50.1	29.7	20.2	63.3
C0.5-50-25-25	0.5	66.1	49.9	24.7	25.4	62.7
C0.5-45-35-20	0.5	66.1	45.2	34.6	20.3	62.5
C0.5-40-35-25	0.5	66.1	40.2	34.5	25.3	60.3

Table C-2. Continued

Sample	Ball milling time (d)	CrI_C[a]	Composition of biomass (%)			CrI_B[b]
			Cellulose	Hemicellulose	Lignin	
C1-100-0-0	1	53.4	100	0	0	53.4
C1-70-5-25	1	53.4	69.9	4.9	25.2	52.1
C1-65-25-10	1	53.4	63.8	26.4	9.9	52.9
C1-60-10-30	1	53.4	60.1	9.6	30.3	53.5
C1-55-30-15	1	53.4	55.3	29.6	15.2	47.5
C1-50-30-20	1	53.4	50.2	29.5	20.3	49.9
C1-45-35-20	1	53.4	45.3	34.5	20.3	53.4
C1-40-35-25	1	53.4	40.1	34.6	25.3	53.1
C2-100-0-0	2	29.8	100	0	0	29.8
C2-70-5-25	2	29.8	70.0	4.9	25.1	31.6
C2-65-25-10	2	29.8	65.2	24.6	10.2	28.2
C2-60-10-30	2	29.8	60.0	9.8	30.2	30.8
C2-55-30-15	2	29.8	55.2	29.6	15.2	28.3
C2-50-30-20	2	29.8	50.2	29.5	20.2	33.1
C2-45-35-20	2	29.8	45.3	34.5	20.2	35.3
C2-40-35-25	2	29.8	40.3	34.5	25.2	37.0

[a] Celullose crystallinity.

[b] Biomass crystallinity.

Table C-3 compares the predictive ability of the parametric models with cellulose crystallinity obtained by Equation IV-1 or C-1, respectively. Equation IV-1 presents the correlation of cellulose crystallinity with biomass crystallinity and hemicellulose content, whereas Equation C-3 presents the correlation of cellulose crystallinity with biomass crystallinity, hemicellulose content, and lignin content. Comparing the MSE value, the parametric models with cellulose crystallinity obtained by Equation IV-1 are superior to those with cellulose crystallinity obtained by Equation C-1.

Table C-3. Comparison of predictive ability of the parametric models with cellulose crystallinity obtained by different correlations

Dependent variables		MSE	
		CrI_C [b]	CrI'_C [c]
Glucan	1-h slope	17	19
	1-h intercept	9.6	9.8
	6-h slope	14	15
	6-h intercept	76	84
	72-h slope	14	15
	72-h intercept	228	248
Xylan	1-h slope	4.2	4.1
	1-h intercept	5.0	5.0
	6-h slope	7.3	7.2
	6-h intercept	66	67
	72-h slope	9.3	9.2
	72-h intercept	186	197
Total Sugar	1-h slope	8.2	9.6
	1-h intercept	4.5	4.3
	6-h slope	13	14
	6-h intercept	75	76
	72-h slope	21	21
	72-h intercept	124	141

[a] Data obtained from Equation V-4 and parameters in Tables V-1 to V-3.

[b] Cellulose crystallinity obtained by Equation IV-1.

[c] Cellulose crystallinity obtained by Equation C-1.

Conclusions

It is apparent that ball milling is an effective method to reduce biomass crystallinity. The crystallinity of corn stover and cellulose decreased proportionally with the increase in ball milling time up to 3d; however, prolonged milling did not decrease corn stover crystallinity below 25%. There was no observable change in crystallinity when the rotation speed was altered from 68 to 156 rpm. An increase in the ratio of grinding media to the dry weight of biomass and a decrease in the amount of grinding media charged in the jar are helpful in reducing biomass crystallinity. The linear equation proposed successfully described the dependence of cellulose crystallinity on hemicellulose content, lignin content, and biomass crystallinity. Comparing the MSE value, the parametric models with cellulose crystallinity obtained by Equation IV-1 are superior to those with cellulose crystallinity obtained by Equation C-1.

BALL MILLING PROCEDURE

Ball milling was used to decrease biomass crystallinity. The mill jar was charged with grinding media to 25–50% of the jar volume. A sufficient amount of biomass was placed in the jar to fill the void volume between the media.

Apparatus and Materials

Rotary ball mill
Porcelain jar, 300-mL, Fisher Scientific
Zirconia, 0.375 in, Fisher Scientific
Balance, accurate to 0.1 g
Autotransformer
10-mesh sieve
Spatula

Procedure

1. Place 6.0 g of dry biomass and 258 g of 0.375-in zirconia in a porcelain jar.
2. Cap the mill jar tightly using an O-ring and shake it well.
3. Place the jar between the rollers and rotate it at 74 rpm. Use a variable autotransformer to change the rotation speed.
4. After certain milling periods, remove the mill jar from the rollers and discharge the grinding media and biomass on a 10-mesh sieve.
5. Carefully sieve the grinding media to remove biomass that stuck to the grinding media.
6. Use a spatula to scrape off biomass on the wall of the mill jar.

APPENDIX D

SUGAR MEASUREMENT BY COLORIMETRIC ASSAYS

DINITROSALICYLIC ACID (DNS) ASSAY

Reducing sugar was measured using the dinitrosalicylic (DNS) assay (Miller, 1959). A glucose standard prepared from Sigma 200-mg/dL glucose standard solution was used for the calibration, thus the reducing sugars were measured as "equivalent glucose."

Apparatus and Materials

Spectrophotomer, Milton Roy, Spectronic 1001
Convection drying oven, with temperature control of 45 ± 1^{o}C
Bunsen burner
Adjustable pipettors, covering ranges of 0.1 to 5.00 mL
Glass test tubes, 20 × 150 mm
Dispensor, 0–5.0 mL
3,5-Dinitrosalicylic acid, Sigma
Sodium hydroxide, Fisher Scientific
Sodium potassium tartate (Rochelle salts), Sigma
Phenol, Fisher Scientific
Sodium metabisulfite, Sigma
Glucose standard, Sigma

DNS Reagent Preparation

1. Place 10.6 g of 3,5-dinitrosalicylic acid crystals, 19.8 g of NaOH, and 1416 mL of distilled water in a 2-L amber glass bottle with a magnetic stir bar inside.
2. Stir the mixture vigorously on a stirring plate and add 306 g of Na-K-tartrate.

3. Melt phenol crystals in a fume hood at 50^{o}C using a water bath. Add 7.6 mL of phenol to the above mixture.
4. Add 8.3 g of sodium meta-bisulfite (Na_2S_2O4).
5. Add NaOH, if necessary to adjust the pH of solution to 12.6.
6. Stir the solution until it becomes homogenous and store the bottle in the dark to avoid direct light.

DNS Reagent Calibration

1. Using a 200-mg/dL Sigma glucose standard, prepare 1 mL of glucose standard in test tubes according to Table D-1.
2. Place 0.5 mL of each standard into test tubes.
3. Add 1.5 mL of DNS reagent into each test tube.
4. Place the caps on the tubes and vortex
5. Vigorously boil samples for 5 min right after adding DNS.
6. Cool the test tubes for a few minutes in an ice-water bath or running tape water bath.
7. Add 10 mL of distilled water into each test tube to make the absorbance reading in the range of 0.1 and 0.8. Vortex the mixture.
8. Zero the spectrophotometer at 540 nm with distilled water. (Note: To stabilize the spectrophotometer, it should be turned on at least 1 h before using).
9. Measure the absorbance and prepare a calibration curve.

Reducing Sugar Measurement of Samples

1. Centrifuge samples at 4,000 rpm for 5 min, if necessary.
2. Dilute the samples into test tubes such that the sugar concentration is in the range of 0.2 to 1.0 mg/mL. Vortex the diluted samples.
3. Place 0.5 mL of each diluted sample into test tubes.
4. Repeat Steps 3 to 9 used to prepare the calibration curve.
5. Calculate sugar concentration from the absorbance of the samples using the calibration curve.

6. Calculate the reducing sugar yield by following formula:

$$Y = S \times D \times V / W \quad \text{(D-1)}$$

where Y = reducing sugar yield (mg equivalent glucose/g dry biomass)

S = sugar concentration in diluted sample (mg equivalent glucose/mL)

D = dilution factor

V = working liquid volume (mL)

W = weight of dry biomass (g)

Table D-1. Preparation of glucose standard solutions for DNS assay

Glucose concentration (mg/mL)	200-mg/dL Sigma standard (mL)	Distilled water (mL)
0.2	0.1	0.9
0.4	0.2	0.8
0.6	0.3	0.7
0.8	0.4	0.6
1.0	0.5	0.5

PHENOL-SULFURIC ASSAY

Simple sugars, oligosaccharides, and polysaccharides form an orange-yellow color when treated with phenol and concentrated sulfuric acid (Dubois et al., 1956). This reaction is more sensitive than the DNS method, and has been developed to determine submicro amounts of sugar. The method is simple, rapid, and gives reproducible results. The color produced is stable and it is unnecessary to pay special attention to the control of the conditions.

Apparatus and Materials

Spectrophotomer, Milton Roy, Spectronic 1001

Convection drying oven, with temperature control of 45 ± 1^{o}C

Adjustable pipettors, covering ranges of 0.1 to 5.00 mL

Cuvettes, 1-cm

Glass test tubes, 20 × 150 mm

Phenol, Fisher Scientific

Pyrex orange cap bottle with wide mouth, 250-mL

Concentrated sulfuric acid, Sigma

Standard sugar, Sigma

Procedure

1. Place 5.0 g of phenol and 95 g of distilled water in a Pyrex wide-mouth bottle, mix the mixture well.[a]
2. Prepare 1 mL of sugar standards in test tubes according to Table D-2.
3. Centrifuge samples at 4,000 rpm for 5 min, if necessary.
4. Dilute the samples into test tubes such that the sugar concentration is in the range of 0.05 to 0.25 mg/mL. Vortex the diluted samples.
5. Place 0.5 mL of each sugar standard and diluted sample into test tubes.
6. Add 1 mL of 5% phenol, and then add 5 mL of concentrated H_2SO_4 rapidly. The stream of acid is directed against the surface rather than against the side of the test tube to obtain good mixing.[b]
7. Leave the tubes to stand for 10 min, then shake and place them for 10 to 20 min at room temperature[c] (25 to 30^{o}C) before readings are taken.
8. Measure the absorbance at 490 nm for hexoses and 480 nm for pentoses.
9. Prepare the calibration curve and calculate sugar concentration from the absorbance of the samples using the calibration curve.
10. Calculate the sugar yield following Equation D-1.[d]

Notes:

a. All the procedures should be done in a fume hood to avoid exposure to phenol vapor.

b. The addition sequence of phenol and H_2SO_4, and the phenol concentration in water were modified by other researchers (Honda et al., 1981; Saha and Brewer, 1994; Taylor, 1995).
c. Usually, 20 min incubation is long enough for maximum color development. (See data in Table D-3.)
d. This method cannot separate glucose and xylose in the mixture.

Table D-2. Preparation of sugar standard solutions for phenol-sulfuric acid assay

Sugar concentration (mg/mL)	0.25-mg/mL sugar standard (mL)	Distilled water (mL)
0.05	0.2	0.8
0.10	0.4	0.6
0.15	0.6	0.4
0.20	0.8	0.2
0.25	1.0	0.0

Table D-3. Absorbance of sugar standard in phenol-sulfuric acid assay

Sugar	Incubation period (min)		
	20	50	120
Glucose	0.453	0.460	0.464
Xylose	0.944	0.930	0.928

GLUCOSE OXIDASE/PEROXIDASE (GOD-POD) ASSAY

Glucose can be rapidly measured in the liquid phase after enzymatic hydrolysis of biomass using glucose oxidase (GOD) and peroxidase (POD). This reaction is sensitive, and has been developed to determine submicro amounts of glucose. This enzymatic reaction is very specific; therefore, the presence of xylose in the sample does not influence the glucose measurement. This method can be used to determine the glucan

content in polysaccharides after being appropriately hydrolyzed (Blakeney and Matheson, 1984; McCleary et al., 1988), but the inhibitory effect of lignin in the residue cannot be neglected (Breuil and Saddler, 1985).

Principle

$$\text{Glucose} + O_2 + H_2O \xrightarrow{\text{Glucose oxidase}} \text{Gluconate} + H_2O_2$$

$$2H_2O_2 + p\text{-Hydroxybenzoic acid} + \text{4-Aminoantipyrine} \xrightarrow{\text{Peroxidase}} \text{Quinoneimine Dye} + 4\ H_2O$$

Apparatus and Materials

Spectrophotomer, Milton Roy, Spectronic 1001

Adjustable pipettors, covering ranges of 0.1 to 5.00 mL

Cuvettes, 1-cm

Water bath, set at 40°C

Glass test tubes, 20 × 150 mm

Sugar standard, Sigma

Solution A.

Disodium hydrogen orthophosphate dodecahydrate, 24.8 g

Sodium dihydrogen orthophosphate dehydrate, 12.4 g

Benzoic acid, 4.0 g

p-Hydroxybenzoic acid, 3.0 g

Solution B. One hundred milligrams of glucose oxidase (Roche, 2208121, 250 U/mg) is dissolved in 4 mL of distilled water and then stabilized by adding 2 g of finely ground ammonium sulfate. The enzyme is stable 4°C.

Solution C. Peroxidase (Roche, 108073, 250 U/mg).

Solution D. One hundred milligrams of 4-aminoantipyrine (Sigma, A4382) is dissolved in 5 mL of distilled water. This is made up just before preparation of the reagent.

Procedure

1. Prepare the reagent by mixing 200 mL of Solution A, 0.2 mL of Solution B, 250 U of Solution C, 1.0 mL of Solution D. The working solution is stored in the dark at 4°C. This reagent is stable and gives similar standard curve for about 3 months.
2. Place 0.4 g of benzoic acid and 200 mL of distilled water in a 250-mL beaker to prepare 0.2% benzoic acid. Stir the mixture on a magnetic stir plate.
3. Prepare 1-mg/mL glucose standard in 0.2% benzoic acid. The glucose standard solution can be stored at room temperature for 6 months.
4. With each new batch of glucose oxidase/peroxidase reagent the time for maximum color formation with 0.1-mg/mL glucose is checked. It is usually 20–25 min.
5. Centrifuge samples at 4,000 rpm for 5 min, if necessary.
6. Dilute the samples in test tubes such that the sugar concentration is below 1.0 mg/mL. Vortex the diluted samples.
7. Place 0.1 mL of reagent blank, glucose standard (duplicate), and diluted sample into test tubes. Add 0.1 mL of distilled water into each tube. (Table D-4). These tubes are incubated at 40°C for 15 min.
8. Three milliliters of glucose oxidase/peroxidase reagent is added to each tube at 1-min time intervals and each tube is incubated at 40°C for exactly 20 min.[a] The pink violet color is formed in each tube.
9. Zero the spectrophotometer at 510 nm with reagent blank.
10. Pippet 1 mL of each sample into a 1-cm cuvette, measure the absorbance of each sample at 1-min intervals in the same sequence as Step 8.

Calculation

$$\text{Glucose, } \mu\text{g}/0.1 \text{ mL} = \frac{\text{O.D. Sample}}{\text{O.D. Standard (Glucose, 100 } \mu\text{g)}} \times D \times 100 \qquad \text{(D-2)}$$

where D = dilution factor

Table D-4. Preparation of samples for GOD-POD assay

	Blank	Standard	Sample
Reagent (mL)	3	3	3
Glucose standard (mL)	---	0.1	---
Sample (mL)	---	---	0.1
Water (mL)	0.2	0.1	0.1

Table D-5. Factors influencing absorbance in GOD-POD assay

Enzyme concentration in reagent (U/mL)		Absorbance at various incubation periods in water bath (min)				
GOD	POD	20	30	40	50	60
6.25	1.25	0.227	0.309	0.360	0.390	0.470
6.25	2.5	0.235	0.305	0.399	0.459	0.486
12.5	2.5	0.4	---	---	---	0.692
27.1	1.25	0.734	0.896	0.929	0.974	1.008[b]

Table D-6. Effect of xylose on glucose measurement in GOD-POD assay

Glucose concentration (mg/mL)	0.4	0.4	0.4	0
Xylose concentration (mg/mL)	0.1	0.2	0.4	0.4
Absorbance	0.276	0.281	0.280	0.005

Notes:

a. Use 0.1-mg/mL glucose standard to check the time for maximum color formation. Longer incubation time may be needed, or increase the amount of glucose oxidase (GOD) and peroxidase (POD) in the reagent. The color formed is more sensitive to the change in GOD concentration than to the change in POD concentration. (Data shown in Table D-5.)

b. Only this reading is very stable, others increase as the sample stays at room temperature for a while.

CHROMOTROPIC ACID ASSAY

The total amount of hexoses in the presence of pentoses is measured using 15-M sulfuric acid solution of chromotropic acid to produce a violet color (Klein & Weissman, 1953). The reaction depends on the conversion of hexoses to 5-hydroxymethylfurfural which further degrades to form formaldehyde and furfural. The formaldehyde reacts with the chromotropic acid to form a violet color. Under these circumstances, pentoses which form furfural, incapable of splitting off formaldehyde, do not react. To overcome protein interference and unstable color formation, Holtzapple and Humphrey (1983) improved the Klein and Weissman technique by increasing the chromotropic acid concentration to 2% and the boiling time to 60 min, respectively.

Apparatus and Materials

Spectrophotomer, Milton Roy, Spectronic 1001
Bunsen burner
Adjustable pipettors, covering ranges of 0.1 to 5.00 mL
Cuvettes, 1-cm
Glass test tubes, 20 × 150 mm
Chromotropic acid (Sodium 1, 8-dihydroxynaphthalene-3, 6-disulfonate), Sigma
Concentrated sulfuric acid, ACS reagent, Fisher Scientific
Glucose standard, Sigma

Chromotropic Acid Reagent Preparation

1. Place 20 g of chromotropic acid in a 1-L volumetric flask.
2. Add 100 mL of distilled water to the volumetric flask to dissolve chromotropic acid.
3. Complete to 1 L using 95% H_2SO_4. Cool the volumetric flask under running water and add more H_2SO_4. Repeat until the volume no longer changes upon cooling.
4. The reagent is usable for many months if it is stored in the refrigerator.

Glucose Measurement of Sample

1. Using a 200-mg/dL Sigma glucose standard, prepare 1 mL of glucose standards in test tubes according to Table D-1.
2. Dilute the samples into test tubes such that the sugar concentration is in the range of 0.2 to 1.0 mg/mL. Vortex the diluted samples.
3. Place 0.5 mL of each glucose standard and diluted sample into test tubes.
4. Add 2.5 mL of the reagent.
5. Seal the test tube with an inert cap and mix very well on a vortex mixer.
6. Place the tubes in a vigorously and uniformly boiling water bath for 1 h.
7. Place the tubes in a bath of ice water to stop the reaction.
8. Add 12 mL of distilled water and mix well.
9. Pippet 1 mL of each sample into a 1-cm cuvette, measure the absorbance at 570 nm.
10. Prepare the calibration curve and calculate sugar concentration from the absorbance of the samples using the calibration curve.
11. Calculate the sugar yield following Equation D-1.

Prepare a series of mixtures of glucose and xylose to check whether xylose interferes with glucose measurement. Data in Table D-7 indicate that increasing xylose concentration increases the absorbance of the samples containing the same amount of glucose.

Table D-7. Effect of xylose on glucose measurement in chromotropic-acid assay[a]

Glucose concentration (mg/mL)	0.5	0.5	0.5	0.5	0.5
Xylose concentration (mg/mL)	0.05	0.10	0.15	0.20	0.25
Absorbance	0.355	0.386	0.418	0.456	0.463
Glucose concentration (mg/mL)[b]	0.589	0.647	0.708	0.780	0.793

[a] Chromatropic acid concentration: 2%, heating time: 60 min, assay range: 0–1.2 mg/mL, and diluting samples after cooling with distilled water.

[b] Calculation is based on the glucose calibration curve and measured absorbance.

Follow the procedure of Klein and Weissman (1953) decreasing chromatropic acid concentration to 0.2%, assay range to 0–0.3 mg/mL of glucose, and diluting samples after cooling with 9-M H_2SO_4. Xylose reacts with chromotropic acid to form yellow-brown color. Data of absorbance are shown in Table D-8. Data in Table D-9 are from Klein and Weissman's paper (1953). The source or purity of chromotropic acid may lead to the different results. Figure D-1 indicates that boiling time has more effect on xylose absorbance than glucose absorbance.

Table D-8. Effect of xylose on glucose measurement in chromotropic-acid assay[a]

Glucose concentration (mg/mL)	0.10	0.10	0.10	0.10	0
Xylose concentration (mg/mL)	0	0.05	0.10	0.20	0.20
Absorbance	0.408	0.636	0.829	1.165	0.938
Glucose concentration (mg/mL)[b]	0.098	0.169	0.229	0.334	0.263

[a] Chromatropic acid concentration: 0.2%, boiling time: 60 min, assay range: 0–0.3 mg/mL, and diluting samples after cooling with 9-M H_2SO_4.

[b] Calculation is based on the glucose calibration curve and measured absorbance.

Table D-9. Effect of xylose on glucose measurement in chromotropic-acid assay[a]

Glucose concentration (mg/mL)	0.10	0.10	0.10	0.10	0.10
Xylose concentration (mg/mL)	0	0.05	0.10	0.20	10.2
Absorbance	0.168	0.165	0.168	0.168	Huminization

[a] Data are from Klein and Weissman's Paper (1953).

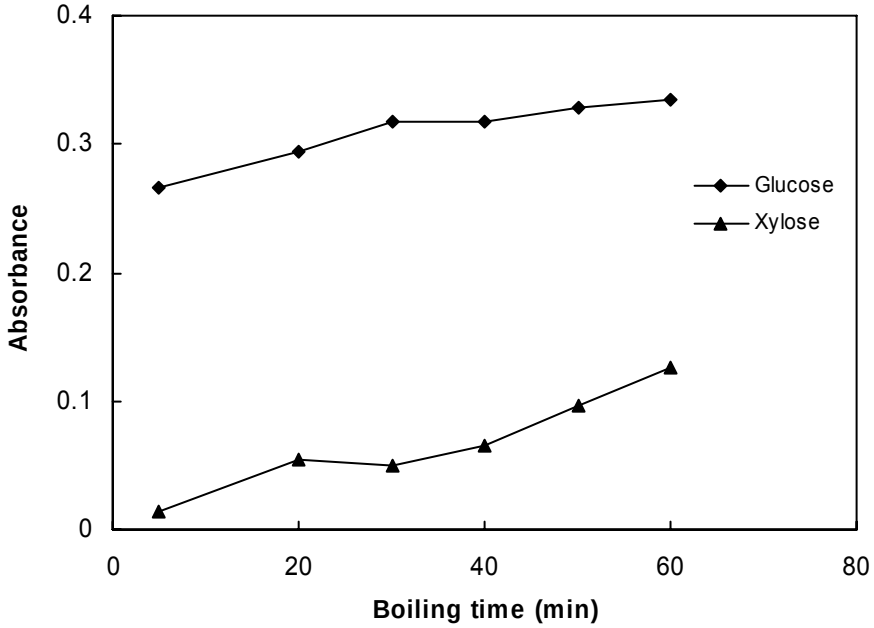

Figure D-1. Effect of boiling time on the absorbance of glucose and xylose. Condition: 0.2% chromotropic acid, 2.5 mL of distilled water for dilution, glucose concentration: 0.2 mg/mL, xylose concentration: 0.2 mg/mL.

PHLOROGLUCINOL ASSAY

Phloroglucinol reagent has been developed for colorimetric measurement of pentosan. The interference from hexoses can be eliminated by reading the absorbance at two wavelengths (Dische and Borenfreund, 1957). This method is simple, rapid, and more convenient to be used to determine xylose derived from lignocellulosic substrates.

Apparatus and Materials

Spectrophotomer, Milton Roy, Spectronic 1001

Adjustable pipettors, covering ranges of 0.1 to 5.00 mL

Bunsen burner

Cuvettes, 1-cm

Glass test tubes, 20 × 150 mm

Glacial acetic acid, Fisher Scientific, Cat No. A38^{S}-500

Fuming hydrochloric acid, Fisher Scientific, Cat No. A144^{S}-500

Phloroglucinol dehydrate (1,3,5-Trihydroxybenzene), ICN biomedicals, Cat No. 102640

Ethanol

Xylose standard, Sigma

Glucose standard, Sigma

Procedure

1. Prepare 0.8% glucose solution (0.8 g of glucose dissolved in 100 mL distilled water) and 5% of phloroglucinol in ethanol solution (0.5 g of phloroglucinol in 10 mL ethanol).
2. Prepare the reagent by mixing 110 mL of glacial acetic acid, 2 mL of concentrated HCl, 1 mL of 0.8% glucose, and 5 mL of 5% phloroglucinol.
3. Prepare 0.5-mg/mL xylose standard and 2-g/L glucose standard.
4. Dilute the samples into test tubes such that the sugar concentration is in the range of 0.02 to 0.1 mg/mL. Vortex the diluted samples.
5. Place 0.4 mL of each xylose standard and diluted sample into test tubes.
6. Add 5 mL of the freshly prepared reagent and mix very well on a vortex mixer.
7. Place the tubes in a vigorously and uniformly boiling waterbath for 15 min.
8. Cool the tubes in tap water.
9. Pippet 1 mL of each sample into a 1-cm cuvette, measure the absorbance at 552 nm and 510 nm, respectively. The absorbance of standards and samples should be read as soon as possible after cooling as a gradual loss in color is noted on standing.
10. Prepare the calibration curve and calculate sugar concentration from the absorbance of the samples using the calibration curve.
11. Calculate the xylose yield following Equation D-1.

Data in Table D-10 indicate that the presence of glucose does not interfere with xylose measurement, because the absorbance is almost same for a series of samples

containing the same amount of xylose but various amounts of glucose. However, this method has the problem of color fading, which may lead to unsatisfactory reproducibility of this method. (See data in Table D-11.) The color of solutions faded approximately 20% over a 60-min period. The proposed modified method (Douglas, 1981) provided better reproducibility by increasing phloroglucinol concentration, glucose concentration, and boiling time.

Table D-10. Effect of glucose on xylose measurement in phloroglucinol assay[a]

Xylose concentration (mg/mL)	0.10	0.10	0.10	0.10	0
Glucose concentration (mg/mL)	0	0.1	0.3	0.5	0.5
Absorbance @ 552 nm	0.795	0.751	0.760	0.763	0.057
Absorbance @ 510 nm	0.244	0.220	0.229	0.231	0.057
Absorbance 552 – 510 nm	0.551	0.531	0.531	0.532	0

[a] Follow Dische's method (1957), boiling time is 15 min, absorbance are quite stable for 5-10 min.

Table D-11. Effect of glucose on xylose measurement in phloroglucinol assay[a]

Xylose concentration (mg/mL)	0.10	0.10	0.10	0.10	0
Glucose concentration (mg/mL)	0	0.1	0.3	0.5	0.5
Absorbance @ 552 nm	0.760	0.784	0.765	0.724	0.109
Absorbance @ 510 nm	0.252	0.257	0.267	0.264	0.124
Absorbance 552 – 510 nm	0.508	0.527	0.498	0.460	-0.015

[a] Follow Dische's method (1957), boiling time is 25 min, absorbance are quite stable for 5-10 min.

APPENDIX E

SUGAR MEASUREMENT BY HPLC

High performance liquid chromatography (HPLC) can separate and quantitate monosaccharide, disaccharide, oligosaccharide in one step, whereas most other assay procedures require the degradation of disaccharide and oligosaccharide and then subsequent quantitation of the resulting monosaccharide. The separation of different sugars was achieved when those components pass through the column. The amount of each sugar was determined by a refractive index (RI) detector with the calibration of each sugar standard. HPLC is a relatively rapid technique and gives reproducible results.

Apparatus

Biorad Aminex HPX-87P column with ionic form H^+/CO_3^- deashing guard column[a]:

Sample injection volume: 20 μL

Mobile phase: 18.3-mΩ-cm reverse osmosis deionized (RODI) water, degassed by vacuum filtration through a 0.2-μm nylon membrane

Flow rate: 0.6 mL/min

Column temperature: 85°C

The equipment used in HPLC are as follows:

Pump: ConstaMetric 3200, LDC Analytical Pump

Autosampler: AS100, Spectra-Physics Analytical

Pulse dampener: LP-21, Scientific Systems/Laballiance, Inc.

Column heater: Jones chromatography

RI detector: Lab Alliance

RODI water: NANOpure Ultrapure Water System, Barnstead/Thermolyne

Materials

Standard sugars: a set of glucose, xylose, cellobiose, Sigma

Adjustable pipettors, covering ranges of 0.1 to 5.00 mL
Disposable nylon syringe filters, 0.2-μm, Fisher Scientific
Polypropylene copolymer (PPCO) centrifuge tubes, 12-mL
Disposable syringe, 5-mL
Autosampler vials, with crimp top seals to fit

Carbohydrate Standard Preparation

1. Prepare carbohydrate stock solutions: dissolve 0.5 g of glucose, 0.1667 g of xylose, and 0.25 g of cellobiose[b] in a 100-mL volumetric flask with mobile phase.
2. Prepare 5-mL standard solutions in test tubes according to Table E-1.
3. Place 1.0-mL standard solutions into autosampler sample vials.
4. Freeze the standard solutions if the analysis will be done later.[c]

Carbohydrate Measurement of Samples

1. Thaw the frozen samples and vortex.
2. Dilute samples using mobile phase with a sugar concentration in the range of carbohydrate standard concentration in 12-mL PPCO centrifuge tubes equipped with appropriate caps.
3. Centrifuge diluted samples at 15,000 rpm for 30 s.
4. Using a syringe, filter the centrifuged diluted samples through a 0.2-μm nylon membrane into autosampler vials. The volume in the vial is 1 mL.
5. Place the samples and the standard solutions in the autosampler. Edit and load a sample file, as explained in "Autosampler Setup." Adjust the cycle time to 20 min for carbohydrate analysis.
6. Press the RUN button to start measurement.
7. Using the standards, prepare a calibration curve, which relates area to sugar concentration. Calculate carbohydrate concentrations of the samples from the area given in the chromatograms and the calibration curve.

Table E-1. Preparation of carbohydrate standard solutions for HPLC

Carbohydrate concentration (mg/mL)			5-mg/mL Stock solution (mL)	Distilled water (mL)
Glucose	Xylose	Cellobiose		
0.5	0.17	0.25	0.5	4.5
1.0	0.33	0.5	1.0	4.0
2.0	0.67	1.0	2.0	3.0
3.0	1.0	1.5	3.0	2.0
4.0	1.34	2.0	4.0	1.0

Equipment Setup

1. Degas 4 L of 18.3-mΩ-cm RODI water by vacuum filtering through a 0.2-µm nylon membrane into a glass jar.[d]
2. Take out the column from refrigerator and expose it to ambient temperature.
3. Turn on the pump, the autosampler, the RI detector for warm-up.
4. After degassing, place the pump inlets with filtering fittings inside the glass jug. Place the glass jug on the stirring plate, cap the jug tightly, and start stirring as slowly as possible.
5. Prime the pump with a syringe by sucking 40 mL of water retained in the tubing from the priming port.
6. Start the pump and increase the flow rate to 2 mL/min to flush air bubbles from the system.
7. Press the PURGE button in the RI detector to allow both the reference and sample cells to be purged with water.
8. After 30–60 min of purging, decrease the flow rate to 0.2 mL/min.
9. Connect the column as described in the Bio-Rad manual, *Guidelines for Use and Care of Aminex Resin Based Columns.*
10. Turn on the column heater and adjust the temperature setting to 85°C. Place a mercury thermometer in the column heater as an independent measurement. Usually it takes about 1 h to reach 85°C.

11. After the column heater reaches 85°C, gradually (i.e., 0.01 mL/min every 30–40 s) increase the flow rate from 0.2 to 0.6 mL/min.[e] Equilibrate the column for 30 min.
12. Turn off the purge in the RI detector to stop circulating liquid through the reference cell and run a base line by hitting computer keyboard spacebar.[f] The baseline recording can be stopped by hitting END key on the computer keyboard.
13. Record the pressure change of the column while the column is in the system.[g]

Autosampler Setup

Editing /Loading Autosampler Files

1. Press the MENU key to display the main menu. Sequentially select FILES, EDIT, and then INJECTION to display the edit menu using the arrow keys to move the cursor and the ENTER key to select the desired option.
2. Adjust the loop size to 20.0 µL and the number of injections per sample to the desired number using the ″+″ key to increase or ″−″ key or decrease the values.
3. Adjust cycle time to 20 min.[h,i]
4. Turn on the built-in refrigerator by pressing the ″+″ key to switch the option from OFF to ON. Gradually (i.e., decrease 5°C each time, stabilize the refrigerator at each temperature point for 10–15 min) decrease the refrigerator temperature from 20°C to 5°C using the ″+″ or ″−″ key. This sequential decrease of refrigerator temperature is important, because the cooler overloads if the temperature is decreased directly to 5°C.
5. Use the default values for other parameters in the autosampler file by continuously pressing the ENTER key.
6. Load the file by selecting FILES and LOAD from the main menu and then pressing the ENTER key.
7. Flush the syringe in autosampler before analyzing samples by selecting FILES and COMMANDS from the main menu.

Editing/Loading Sample Files

1. Press the SAMPLE key to display the sample menu.

2. Specify the sample set number.
3. Adjust the number of injections per sample and the cycle time as explained in "Editing/Loading Autosampler Files."
4. Specify the first sample vial to start with and the number of the samples using the ″+″ or ″−″ key.
5. Add the sample set to the queue by pressing the ENTER key.

Chromatography Data System Setup

Creating Control File

1. Select FILE-PRINT, click on **Channel 1** to edit Channel 1 information. Check the **Print Header** box and select **FORMAT** button. Input **Laboratory name**, **Analysis method**, **Column**, **Carrier,** etc., and check the box next to each file. Check the **Print Chromatogram** box and select **FORMAT** button to edit start and stop time. Input 20.0 min to the right of checkbox. Use the other default values.
2. Select EDIT-CHANNELS and choose Channel 1 as analysis channel by checking **active**, **displayed,** and **integrated** boxes.
3. Select EDIT-CHANNELS-DETAILS, input Channel 1 HPLC in the box of **Description**. Other parameters on the screen: **End time** of 20 min, **Sample rate** of 1 Hz, main **Trigger group**, **Control by** temperature. Input the maximum and minimum value in **default display limits**. Check **Remote start** box. Use the other default values.
4. Select EDIT-CHANNELS-INTEGRATION, **Peak**: 95%, **Baseline**: 60%, **Spike channel**: None, **Area reject**: 5.
5. Creating component tables: Show the Component Details screen by selecting EDIT-CHANNELS-COMPONENTS.
    a. Select **Add** to add a new component, input specific peak parameters including **Peak Number**, **Peak Name**, **Start** time, **End**, and **Expected** time. Other parameters are **Peaks measured** by **Area**, handling of **Multiple peaks** by **showing each peak separately**. Use the other default values.

b. Click on an existing component and select it. Click on the **Change** or **Remove** button to change or remove the parameters of the component respectively.
c. Click on the **Save** button to save a new component file with **.CPT** extension.

6. Select EDIT-CHANNELS-POSTRUN, select the box of **Auto-increment** and **Save file as**, input files name to the right of the checkbox. Check the **Add to results log** by inputting CH1.LOG. Restart run after 20.00 min. Use the other default values.
7. Select EDIT-OVERALL, select the checkboxes of **Show retention windows**, **Abbreviated name**, **Retention time**, **Draw label vertically**, **Postrun file overwrite protection**, and **Reset relays at end of run**. Input 0.0 and 20.0 in the **start** and **end** box respectively in **Default display period**.
8. After setting up all of the user-definable parameters, save these settings as **.CON** files for future use in the FILE-SAVE CONTROL FILE.

Analyzing Samples

1. Click on the icon of **PeakSimple** on the screen to launch Peaksimple and initialize the data acquisition system.
2. Select File-Open Control File to load the control file including the operating setting used for sugar analysis. Check each parameter appropriately set.
3. Select EDIT-CHANNELS-POSTRUN, select the **Save file as** checkbox, and input the file name and path entered in the information field to the right of the checkbox.

Equipment Shut-down

1. After running the samples, decrease flow rate gradually to 0.2 mL/min.
2. Turn off the heater and expose the column to ambient temperature.
3. Disconnect the column from its inlet and outlet tubing when the column has cooled to ambient temperature (usually takes about 30 min).
4. Cap the column and guard column with plastic end screw and store them in the refrigerator.

5. Use the piece of tubing to take the place of the column, and increase the flow rate to 2 mL/min to flush the system for 30 min.[j]
6. Decrease the flow rate to 0.1 mL/min and press the STAND BY button on the pump.
7. Turn off the pump, RI detector, autosampler, and computer.

Notes

a. Deashing guard column is chosen to exchange the cations and anions in the sample with H^+/CO_3^- so as to avoid the formation of precipitate in the column, which leads to ever-increasing pressure of the column. White precipitate is formed when citrate buffer or sodium azide is mixed with lead nitrate. (Note: HPX-87P is H-Lead cationic form resin.) These guard columns also have been found to be effective in eliminating baseline ramping.
b. Dry standards at 45°C convection oven overnight prior to use.
c. Be sure to thoroughly mix the sample after thawing because freezing separates the sugars from the water.
d. Degassed water can avoid bubble formation and keep the baseline from drifting. Mobile phase must be degassed at least every other day, because the water loses its degassed condition after running for a period of time.
e. Do not operate the column at a flow rate higher than 0.2 mL/min at ambient temperature.
f. Check the baseline for noise or drift. If the baseline drifts, the temperature of RI detector may not be stable. If there are spikes in baseline, there maybe bubbles in the system detected by RI detector. Degas the mobile phase and flush the whole system again.
g. Replace the guard column when the pressure of the column increases to certain value (i.e., 800 psi). Check the pressure of the old guard column, and replace it if its pressure is too high.

h. Run the sample for a longer time to let all peaks show up, and adjust the cycle time by eliminating the interference from other compounds with longer retention time to the target carbohydrate in next sample.
i. Run the sample only with denatured cellulase and cellobiase, respectively; determine sugar concentration and retention time of some other peaks in enzymes, if necessary.
j. To prevent salts (from buffer) from drying on the plunger of the pump, flush the system at the flow rate of 2 mL/min for 30–60 min prior to turning off the pump.

APPENDIX F

DETERMINATION OF CARBOHYDRATES AND LIGNIN IN BIOMASS

This method used a two-step acid hydrolysis to fractionate biomass into forms that are more easily quantified. The biomass sample was taken through a primary 72% (w/w) sulfuric acid hydrolysis at 30ºC for 1 h, followed by a secondary dilute acid hydrolysis at 121ºC for 1 h. The resulting sugar monomers and acetyl content were analyzed using HPLC. The acid-soluble lignin was measured by UV-Vis spectroscopy. This method is based on the NREL standard procedure No. 002 (2004).

Apparatus

Analytical balance, accurate to 0.1 mg

Convention drying oven, with temperature control of 45 ± 3^{o}C and 105 ± 3^{o}C

Muffle furnace, set to 575 ± 25^{o}C

Water bath, set at 30 ± 3^{o}C

Autoclave, suitable for autoclaving liquids, set to 121 ± 3^{o}C

HPLC system equipped with RI detector, Biorad Aminex HPX-87P column and Biorad Aminex HPX-87H column

Spectrophotomer, Milton Roy, Spectronic 1001

Materials

Sulfuric acid, 72% w/w (12.00 ± 0.02 M) or specific gravity 1.6389 at 15.6^{o}C

High purity standards: set of D (+) glucose, D (+) xylose

Calcium carbonate, ACS reagent grade

Glacial acetic acid (99.7%), Fisher Scientific

Water, 18.3-mΩ-cm deionized

Glass test tubes, 20 × 150 mm

Glass serum bottles, 125-mL, crimp top with rubber stopper and aluminum seals to fit

pH paper (pH 4–7)

Filtering crucibles, 50-mL, porcelain, medium porosity

Vacuum flask, 1-L

Glass stir rods, 200-mm

Vacuum adapter for crucibles

Crucible tongs

Adjustable pipettors, covering ranges of 0.02 to 5.00 mL

Graduate cylinder, 100-mL

Disposable nylon syringe filters, 0.2-μm

Disposable syringes, 5-mL

Autosampler vials with crimp top seals to fit

Erlenmeyer flasks, 50-mL

Procedure

Preparation of Sample for Analysis and Hydrolysis

1. Determine the moisture content of biomass following NREL standard procedure No.001 (2004). Total solid content is determined as T_f.
2. Weigh 0.3 ± 0.01 g of biomass to the nearest 0.1 mg and place in a glass test tube (W_i).
3. Add 3.00 ± 0.01 mL (or 4.92 ± 0.01 g) of 72% H_2SO_4 to each tube and mix with a glass stirring rod to wet biomass thoroughly.
4. Place the tubes in a water bath set at 30 ± 3°C and incubate the sample for 1 h. Using the stir rod, stir the samples every 5 to 10 min without removing the test tubes from the water bath.[a]
5. After 1-h hydrolysis reaction, transfer each sample to its own serum bottle and dilute to a 4% acid concentration by adding 84 mL of deionized water. Carefully transfer all residues solids along with the hydrolyzed liquor. The total volume of solution (V_f) is 87.0 mL.

6. Prepare a set of sugar recovery standards (SRS)[b]: Weigh 2.0 g of glucose and 0.6 g of xylose (predried at 45°C overnight) to the nearest 0.1 mg. Dissolve sugars with deionized water in a 1-L volumetric flask. Transfer 84 mL of SRS to septum bottle and add 3.00 mL of 72% H_2SO_4.
7. Mix SRS with H_2SO_4 well, and transfer 20 mL of mixture to a 50-mL Erlenmeyer flask.[c]
8. Stopper each bottle and crimp aluminum seals into place.
9. Autoclave the samples and SRS for 1 h at 121 ± 3°C.
10. After autoclaving, allow the hydrolyzates to cool in a water bath to room temperature before removing the seals and stoppers.
11. These autoclaved solution can be used to determinate the acid-insoluble and/or acid-soluble lignin, carbohydrates, and acetyl content.

Analysis of Acid Insoluble Lignin

1. Place filtering crucibles in the muffle furnace at 575 ± 25°C for a minimum of 4 h. Remove the crucibles from the furnace directly into a desiccator and cool for 1 h. Weight the crucibles to the nearest 0.1 mg (W_1).
2. Vacuum filter the autoclaved hydrolysis solution through the previously weighed filtering crucibles. Capture the filtrate in a vacuum flask.
3. Transfer 50 mL of filtrate into a 50-mL Erlenmeyer flask to determine acid-soluble lignin,[d] carbohydrates, and acetyl groups.
4. Use deionized water to transfer all the remaining solids out of the septum bottle into the filtering crucible. Rinse the solids with a minimum of 50-mL fresh deionized water.
5. Dry the crucible and acid-insoluble residue at 105 ± 3°C until a constant weight is achieved, usually a minimum of 4 h.
6. Remove the samples from the oven and cool in a desiccator. Record the weight of the crucibles and dry the residue to the nearest 0.1 mg (W_2).
7. Place the crucibles and residue in the muffle furnace at 575 ± 25°C for 24 ± 6 h.

8. Remove the crucible from the furnace directly into a desiccator and cool for 1 h. Weight the crucibles and ash to the nearest 0.1 mg and record the weight (W_3).

Analysis of Acid Soluble Lignin

1. Measure the absorbance of the filtrate at an appropriate wavelength on a UV-Visible spectrophotometer.
2. Dilute the samples as necessary to bring absorbance into the range of 0.7–1.0. Deionized water or 4% H_2SO_4 maybe used to dilute the sample, but the same solvent should be used as a blank. Record the absorbance to three decimal places.

Analysis of Structural Carbohydrates

1. Transfer 20 mL of filtrate (obtained in insoluble lignin analysis) of each sample into a 50-mL Erlenmeyer flask.
2. Use calcium carbonate to neutralize each sample and the SRS before autoclaving to pH 5–6. (Usually 0.8–1.0 g of calcium carbonate for 20 mL of filtrate.). Avoid neutralizing to a pH greater than 6 by monitoring with pH paper.[e]
3. After reaching pH 5–6, allow the sample to settle, and transfer the supernatant to centrifuge tubes using a pipettor.
4. Centrifuge the supernatant at 4,000 rpm for 5 min.
5. Using a syringe, filter the centrifuged samples through a 0.2-μm nylon membrane into autosampler vials if the hydrolyzate is to be analyzed without dilution.[f] Dilute the hydrolyzate before filtering into autosampler vials, if the concentration of the analyte is expected to exceed the validated linear range.
6. Prepare a series of sugar calibration standards containing the compounds that are to be quantified; the suggested concentration range is 0.1–4.0 mg/mL for each component. Use a four-point calibration. (See Table D-2 for reference.)
7. Analyze the calibration standard and samples using a Biorad Aminex HPX-87P column equipped with the deashing guard column.[g,h]

HPLC condition:

Injection volume: 20 μL

Mobile phase: 0.2-μm filtered and degassed, deionized water

Flow rate: 0.6 mL/min

Column temperature: 85 ^{o}C

Detector: refractive index

Run time: 20 min data collection plus a 15-min post-run

Analysis of Acetyl Content

1. Prepare 0.01-N H_2SO_4 for use as HPLC mobile phase. Add 0.834 mL of concentrated H_2SO_4 and 3 L of deionized water into a 4-L flask. Filter through a 0.2-μm nylon membrane and degas before use.
2. Prepare a series of calibration standards containing the compounds that are to be quantified. Place 0.477 mL of glacial acetic acid in a 1-L volumetric flask and bring to the volume with HPLC-grade water. The concentration of dilute acetic acid is 0.5 mg/mL. Prepare 5-mL standard solutions in test tubes according to Table F-1.
3. Using a syringe, prepare the sample for HPLC analysis by filtering the filtrate through a 0.2-μm nylon membrane into autosampler vials. Seal and label the vials.
4. Analyze the calibration standards and samples by HPLC using a Biorad Aminex HPX-87H column equipped with the H guard column.

Table F-1 Preparation of acetic acid solutions for acetyl content assay

Acetic acid concentration (mg/mL)	0.5 mL/mL acetic acid standard (mL)	HPLC water (mL)
0.02	0.2	4.8
0.1	1.0	4.0
0.2	2.0	3.0
0.5	5.0	0

HPLC conditions:

Injection volume: 20 μL, 50 μL is better for sample with low acetyl content

Mobile phase: 0.01-N H_2SO_4, 0.2-μm filtered and degassed

Flow rate: 0.6 mL/min

Column temperature: 65 °C

Detector: refractive index

Run time: 20 or 50 min

Calculations

1. Calculate the oven dry weight (W_0) of the sample:

$$W_0 = \frac{W_i \times \%T_f}{100} \tag{F-1}$$

where W_0 = oven dry weight

W_i = initial sample weight

T_f = solid content in the initial sample

2. Calculate acid-insoluble lignin (AIL) content:

$$\%\ \text{AIL} = \frac{W_2 - W_3}{W_0} \times 100 \tag{F-2}$$

where W_2 = weight of crucible + acid insoluble residue

W_3 = weight of crucible + ash

3. Calculate acid-soluble lignin (ASL) content:

$$\%\ \text{ASL} = \frac{\text{Abs} \times V_f \times df}{\varepsilon \times W_0} \times 100 \tag{F-3}$$

where Abs = average UV-Vis absorbance for the sample at 205 nm

V_f = volume of filtrate, 87 mL

df = dilution factor

ε = absorptivity value of biomass[i]

4. Calculate the total lignin content:

$$\% \text{ Lignin} = \% \text{ AIL} + \% \text{ ASL} \quad \text{(F-4)}$$

5. Calculate structural carbohydrate:
   a. Create calibration curve by linear regression analysis for each sugar to be quantified. From these curves, determine the concentration in mg/mL of the sugars present in the sample.
   b. Calculate the amount of sugar recovered from each SRS after dilute acid hydrolysis.

$$\% R_{SRS} = C_2/C_1 \times 100 \quad \text{(F-5)}$$

where $\% R_{SRS}$ = % recovery of sugar recovery standard (SRS)

C_1 = concentration of SRS detected by HPLC before hydrolysis, in mg/mL

C_2 = concentration of SRS detected by HPLC after hydrolysis, in mg/mL

   c. Correct sugar concentration obtained by HPLC for each sugar in the hydrolyzed sample by using $\% R_{SRS}$

$$C_{corr} = C_{HPLC} \times 100 / \% R_{SRS} \quad \text{(F-6)}$$

where C_{corr} = concentration of sugar in the hydrolyzed sample corrected, in mg/mL

C_{HPLC} = concentration of sugar in the hydrolyzed sample detected by HPLC, in mg/mL

   d. Calculate the percentage of each sugar in the samples as follows:

$$\%\ \text{Sugar} = \frac{C_{corr} \times A \times V_f \times \frac{1\ \text{g}}{1000\ \text{mg}}}{W_0} \times 100 \qquad \text{(F-7)}$$

where A = anhydro correction of 0.9 (or 162/180) for C-6 sugars and correction of 0.88 (or 132/150) for C-5 sugars

6. Calculate acetyl content:

$$\%\ \text{Acetate} = \frac{C_{AA,HPLC} \times V_f \times C}{W_0} \times 100 \qquad \text{(F-8)}$$

where $C_{AA,HPLC}$ = concentration in mg/mL of acetic acid as determined by HPLC

C = 0.683, the conversion factor from acetic acid to acetate in biomass

Notes

a. Stirring is essential to ensure even acid to particle contact and uniform hydrolysis.
b. SRS go through the diluted H_2SO_4 hydrolysis and are used to correct for sugar losses during dilute acid hydrolysis. SRS sugar concentrations resemble the sugar concentrations in the test tubes.
c. SRS can be stored in a freezer. Thaw and vortex the frozen SRS prior to use. The appropriate amount of acid must be added to the thawed SRS and vortex prior transferring to septum bottle.
d. Acid-soluble lignin determination must be done within 6 h of hydrolysis. If the hydrolysis liquor must be stored, it should be stored in a refrigerator for a maximum of 2 weeks.
e. When neutralizing the filtrate for carbohydrate analysis, add the calcium carbonate slowly with frequent swirling to avoid the problem of foaming.
f. Neutralized samples may be stored in the refrigerator for 3 or 4 days. After this time, the samples should be considered compromised due to microbial growth. Check the

samples for the presence of a precipitate after cold storage. Sample containing a precipitate should be refiltered through 0.2-μm filters, while still cold.

g. Check test sample chromatograms for the presence of cellobiose and oligometric sugars. Cellobiose concentrations greater than 3 mg/mL indicate incomplete hydrolysis. Fresh samples should be hydrolyzed and analyzed.

h. Check test sample chromatograms for the presence of peaks eluting before cellobiose. These peaks may indicate high levels of sugar degradation products in the previous sample, which indicates over hydrolysis. All samples from the batch showing evidence of over-hydrolysis should have fresh samples hydrolyzed and analyzed.

i. In determining the acid-soluble lignin (ASL) content, ε values are different in the NREL standard procedure No. 002 (2004) and No. 002 (2002). In the old procedure, ε value is 110 L/(g·cm) at wavelength of 205 nm for all kinds of biomass; whereas biomass has its own ε values determined at specific wavelength in the new method; therefore the values of ASL are different followed these two methods (See Table F-1).

j. The hydrolyzates being tested will contain low concentrations of HMF and/or furfural. These components will appear as peaks in the chromatogram of the following sample. It is important to verify the HMF and furfural peaks are not interfering with the peaks of interest. If the run is 20 min, the HMF peak and furfural peak will appear at about 10 min and 19 min in the following chromatogram, respectively. If the run time is 50 min, neither peak interferes with the analytes of interest.

Table F-1. Acid-soluble lignin determined at two wavelengths

Sample	Old Method			New Method		
	Wavelength, λ (nm)	Absorptivity, ε (L/(g·cm))	ASL/%	Wavelength, λ (nm)	Absorptivity, ε (L/(g·cm))	ASL/%
Cornstover lime DC3	205	110	1.60	320	30	0.92
Cornstover 12W N_2	205	110	1.38	320	30	0.86
Cornstover 16W Air	205	110	2.36	320	30	1.10
Cornstover AFEX	205	110	5.09	320	30	2.74
Rice straw diluted acid	205	110	1.19	240	15	3.80
Rice straw lime DC0	205	110	2.60	240	15	7.24
Rice straw lime DC2	205	110	2.70	240	15	7.06
Bagasse diluted acid	205	110	0.94	240	15	3.45
Bagasse lime	205	110	1.98	240	15	6.54
Bagasse NH_3 (s/l=1/6)	205	110	1.30	240	15	5.48
Bagasse NH_3 (s/l=1/8)	205	110	1.20	240	15	5.35
Poplar wood[a]	205	110	2.56	240	15	9.80
Poplar wood[b]	205	110	4.31	240	15	17.43

[a] Deacetylation.

[b] Delignification.

APPENDIX G

MEASUREMENT OF XYLANASE ACTIVITIES

Xylanase activity in *Trichoderma reesei* is measured by catalyzing the degradation of xylan in 0.05-M citrate buffer (pH = 4.8) incubated at 50^{o}C for 5 min. Sugar released during the incubation period is determined by the DNS method (Bailey et al., 1992).

Apparatus and Materials

Spectrophotomer, Milton Roy, Spectronic 1001
Bunsen burner
Adjustable pipettors, covering ranges of 0.1 to 5.00 mL
Glass test tubes, 20 × 150 mm
Cuvettes, 1-cm
Citrate buffer, 1-M
Trichoderma reesei , Lot No. 301-00348-257, Genencor, USA
DNS reagent (preparation method is described in Appendix D)
Birchwood glucuronoxylan, Sigma X-502
Xylose standard, Sigma

Substrate Preparation

1. Place 1.0 g of xylan, 80 mL of 0.05-M citrate buffer (pH = 4.8), and a stir bar in a 200-mL beaker.
2. Heat and stir the mixture of xylan and buffer on a heating magnetic stirrer to 60^{o}C.
3. Transfer half of the mixture to a Waring blender with a small volume of stainless steel jar. Put a rubber stopper wrapped with aluminum foil on the top of the jar to ensure no loss of the mixture during blending.

4. Turn on the blender for 1–2 min and then turn it off. Transfer the mixture into another 200-mL beaker.
5. Follow Steps 3 and 4 for the left half of mixture.
6. Heat the mixture to the boiling point on the heating magnetic stirrer.
7. Cover the beaker and cool with slowly stirring overnight.
8. Transfer the mixture from beaker to a 100-mL volumetric flask, and make up to 100 mL with buffer.
9. This substrate can be stored at 4^{o}C for a maximum of 1 week or freeze at –20^{o}C. Mix well after thawing.

Procedure

1. Add 1.8 mL of substrate solution to 15-mL test tubes, and equilibrate tubes in a water bath to 50^{o}C (usually 1 h).
2. Add 0.2 mL of enzyme diluted appropriately in citrate buffer (Table G-1).
3. Incubate at 50^{o}C for exactly 5 min.
4. At the end of the incubation period, remove each assay tube from the water bath and stop the enzyme hydrolysis by immediately adding 3.0 mL of DNS reagent and mixing.
5. Add 0.2 mL of xylose standard, reagent blank, and enzyme blank into their own tubes right after the addition of 3.0 mL of DNS.
6. Boil all tubes for exactly 5 min in a vigorously and uniformly boiling water bath, and then cool in a cold ice-water bath.
7. Measure the absorbance of the samples at 540 nm against the reagent blank.
8. Correct the absorbance (7) for background color in the enzyme blank if necessary.
9. Convert the corrected absorbance to enzyme activity units (nkat/mL).
10. Calculate the activity in the original (undiluted) sample by multiplying activity units by the dilution factors.

Xylose Standard Preparation

1. Place 0.15 g of xylose and 0.05-M citrate buffer in a 100-mL volumetric flask, and make up to 100 mL by buffer.
2. The stock solution is diluted (in buffer) in the following manner:

   0.5 mL + 0.0 mL buffer = 1:1 = 10.0 μ mol/mL → 33.3 nkat/mL

   0.5 mL + 0.5 mL buffer = 1:2 = 5.00 μ mol/mL → 16.7 nkat/mL

   0.5 mL + 1.0 mL buffer = 1:3 = 3.33 μ mol/mL → 11.1 nkat/mL

   0.5 mL + 2.0 mL buffer = 1:5 = 2.00 μ mol/mL → 6.70 nkat/mL

Blank and Controls

1. Reagent blank: 0.2-mL buffer.
2. Enzyme blank: 0.2-mL diluted enzyme.

All enzyme dilutions are made in citrate buffer, pH 4.8, as indicated in the following table from a working enzyme stock solution that had been diluted 1:100 in citrate buffer (0.2 mL of enzyme + 19.8 mL of buffer).

Table G-1. Preparation of diluted enzyme solutions

Dilution #	Citrate buffer (mL)	1:100 Enzyme (mL)	Dilution factor
1	0.2	2.3	1250
2	0.2	2.8	1500
3	0.2	3.8	2000
4	0.2	5.8	3000
5	0.2	7.8	4000

APPENDIX H

EXPERIMENTAL DATA

Effect of Substrate Concentration on Sugar Concentrations with no Supplemental Cellobiase

Table H-1. Effect of substrate concentration on cellobiose concentration[a]

Incubation period (h)	Cellobiose concentrations at various substrate concentrations (g/L)			
	10 -g/L	20-g/L	50-g/L	100-g/L
1	0.45	1.07	1.71	2.09
6	0.56	0.93	1.54	2.38
12	0.42	0.67	1.20	2.28
24	0.20	0.37	0.78	1.46
72	0.03	0.06	0.11	2.09

[a] Data for Figure IV-1 (A).

Hydrolysis conditions: 5 FPU/g dry biomass, 0 CBU/g dry biomass.

Table H-2. Effect of substrate concentration on glucose concentration[a]

Incubation period (h)	Glucose concentrations at various substrate concentrations (g/L)			
	10 -g/L	20-g/L	50-g/L	100-g/L
1	0.19	0.61	1.57	3.27
6	1.03	2.16	5.46	10.7
12	1.64	3.19	7.79	15. 6
24	2.12	4.16	10.1	19.8
72	2.68	5.33	13.2	26.4

[a] Data for Figure IV-1 (B).

Hydrolysis conditions: 5 FPU/g dry biomass, 0 CBU/g dry biomass.

Table H-3. Effect of substrate concentration on xylose concentration[a]

Incubation period (h)	Xylose concentrations at various substrate concentrations (g/L)			
	10 -g/L	20-g/L	50-g/L	100-g/L
1	0.12	0.33	0.71	1.34
6	0.55	1.17	3.04	5.77
12	0.67	1.41	3.88	7.45
24	0.73	1.60	4.39	8.71
72	0.88	1.88	5.21	10.6

[a] Data for Figure IV-1 (C).

Hydrolysis conditions: 5 FPU/g dry biomass, 0 CBU/g dry biomass.

Effect of Substrate Concentration on Sugar Digestibility with no Supplemental Cellobiase

Table H-4. Effect of substrate concentration on glucan digestibility[a]

Incubation period (h)	Glucan conversions at various substrate concentrations (%)			
	10 -g/L	20-g/L	50-g/L	100-g/L
1	13.3	17.6	13.8	11.1
6	32.9	31.2	29.1	27.1
12	42.2	40.2	37.2	36.9
24	47.9	46.9	44.8	43. 9
72	55.2	55.3	54.4	54.1

[a] Data for Figure IV-2 (A).

Hydrolysis conditions: 5 FPU/g dry biomass, 0 CBU/g dry biomass.

Table H-5. Effect of substrate concentration on xylan digestibility[a]

Incubation period (h)	Xylan conversions at various substrate concentrations (%)			
	10 -g/L	20-g/L	50-g/L	100-g/L
1	5.37	7.1	6.2	5.87
6	23.9	25.8	26.8	25.3
12	29.2	31.2	34.1	32.7
24	32.3	35.2	38.5	38.2
72	38.3	41.3	45.7	46.6

[a] Data for Figure IV-2 (B).

Hydrolysis conditions: 5 FPU/g dry biomass, 0 CBU/g dry biomass.

Effect of Substrate Concentration on Biomass Digestibility with Supplemental Cellobiase

Table H-6. Effect of substrate concentration on glucan digestibility[a]

Incubation period (h)	Glucan conversions at various substrate concentrations (%)			
	10 -g/L	20-g/L	50-g/L	100-g/L
1	18.8	23.9	24.7	23.4
6	42.2	43. 7	44.0	44.2
12	48.8	50.0	49.1	48.8
24	53.4	54. 8	54.9	55.5
72	59.8	58.0	60.5	61.8

[a] Data for Figure IV-3 (A).

Hydrolysis conditions: 5 FPU/g dry biomass, 28.4 CBU/g dry biomass.

Table H-7. Effect of substrate concentration on xylan digestibility[a]

Incubation period (h)	Xylan conversions at various substrate concentrations (%)			
	10 -g/L	20-g/L	50-g/L	100-g/L
1	6.19	8.46	8.86	7.83
6	25.5	30.0	32.4	29.6
12	33.0	38.2	39.2	35.9
24	40.3	44.9	45.5	42.9
72	51.1	50.7	52.5	51.3

[a] Data for Figure IV-3 (B).

Hydrolysis conditions: 5 FPU/g dry biomass, 28.4 CBU/g dry biomass.

Effect of Cellobiase Loading on Biomass Digestibility

Table H-8. Effect of cellobiase loading on biomass digestibility[a]

Incubation period (h)	Glucan conversions at various cellobiase loadings (%)			Xylan conversions at various cellobiase loadings (%)		
	0 CBU/g dry biomass	28.4 CBU/g dry biomass	81.2 CBU/g dry biomass	0 CBU/g dry biomass	28.4 CBU/g dry biomass	81.2 CBU/g dry biomass
1	13.8	24.7	26.9	6.20	8.87	11.0
6	29.1	44.0	45.4	26.8	32.4	34.5
72	54.4	60.5	62.2	45.7	52.5	53.8

[a] Data for Figure IV-4 (A) & (B).

Hydrolysis conditions: 5 FPU/g dry biomass, substrate concentration: 50 g/L.

Effect of Supplemental Cellobiase on Filter Paper Activity of Cellulase

Table H-9. Effect of supplementary cellobiase on filter paper activity in the enzyme complex[a]

Ratio of cellobiase to cellulase (v/v)	Filter paper activity of the enzyme complex (FPU/mL)
0	64.8
0.25	75.5
0.5	85.3
1	87.8

[a] Data for Figure IV-5.

Cellulase activity: 65 FPU/mL, cellobiase activity: 321 FPU/mL.

Effect of Lignin Content on Biomass Digestibility

Table H-10. Hydrolysis profiles of poplar wood with various lignin contents[a]

Incubation period (h)	Glucan conversions at various lignin contents (%)			Xylan conversions at various lignin contents (%)		
	10.6%	17.8%	24.5%	10.6%	17.8%	24.5%
1	12.8	8.26	4.72	12.4	11.8	10.5
3	25.5	18.3	7.86	33.5	33.1	22.4
6	39.9	27.1	10.7	51.9	47.6	27.3
12	58.9	39.6	13.7	67.6	61.3	33.1
24	79.0	51.8	16.0	81.1	70.7	34.8
48	88.8	65.4	19.4	93.5	82.3	37.7
72	92.6	70.3	21.1	99.3	86.1	40.0

[a] Data for Figure IV-7 (A) & (B).

Hydrolysis conditions: 5 FPU/g dry biomass, 28.4 CBU/g dry biomass, substrate concentration: 20 g/L.

Table H-11. Effect of lignin content on digestibility of low-crystsllinity biomass [a]

Incubation period (h)	Glucan conversions at various lignin contents (%)			Xylan conversions at various lignin contents (%)		
	10.6%	14.8%	24.5%	10.6%	14.8%	24.5%
1	42.5	35.9	26.2	18.8	17.4	16.5
6	46.7	69.0	83.6	69.2	66.3	60.1
72	93.5	89.8	64.6	95.9	98.8	85.7

[a] Data for Figure IV-8 (A) & (B).

Hydrolysis conditions: 5 FPU/g dry biomass, 81.2 CBU/g dry biomass, substrate concentration: 10 g/L.

Table H-12. Effect of lignin content lower than 10% on biomass digestibility[a]

Incubation period (h)	Glucan conversions at various lignin contents (%)			Xylan conversions at various lignin contents (%)		
	1.5%	4.5%	10.9%	1.5%	4.5%	10.9%
1	9.7	10.3	9.5	17.2	12.9	11.2
6	31.4	37.6	35.6	60	57.8	49.5
72	82.1	89.9	87.1	99.4	99.2	91.4

[a] Data for Figure IV-9 (A) & (B).

Hydrolysis conditions: 5 FPU/g dry biomass, 81.2 CBU/g dry biomass, substrate concentration: 10 g/L.

Effect of Acetyl Content on Biomass Digestibility

Table H-13. Hydrolysis profiles of poplar wood with various acetyl contents[a]

Incubation period (h)	Glucan conversions at various acetyl contents (%)		Xylan conversions at various acetyl contents (%)	
	1.7%	2.9%	1.7%	2.9%
1	6.70	4.01	7.75	6.21
3	13.9	9.67	17.5	13.5
6	19.7	14.9	22.2	18.7
12	29.1	20.7	30.5	24.7
24	37.1	26.3	39.3	31.2
48	44.3	32.3	46.3	37.3
72	47.0	35.8	49.4	40.8

[a] Data for Figure IV-10 (A) & (B).

Hydrolysis conditions: 5 FPU/g dry biomass, 28.4 CBU/g dry biomass, substrate concentration: 20 g/L.

Table H-14. Effect of acetyl content on digestibility of high-lignin biomass[a]

Incubation period (h)	Glucan conversions at various acetyl contents (%)			Xylan conversions at various acetyl contents (%)		
	0.4%	0.9%	1.9%	0.4%	0.9%	1.9%
1	3.3	3.0	1.85	8.3	4.0	0
6	8.3	6.9	5.4	22	8.1	4.9
72	22.3	14.4	10.5	43.8	13.7	6.4

[a] Data for Figure IV-11 (A) & (B).

Hydrolysis conditions: 5 FPU/g dry biomass, 81.2 CBU/g dry biomass, and substrate concentration: 10 g/L.

Table H-15. Effect of acetyl content on digestibility of low-crystallinity biomass[a]

Incubation period (h)	Glucan conversions at various acetyl contents (%)			Xylan conversions at various acetyl contents (%)		
	0.4%	2.5%	2.9%	0.4%	2.5%	2.9%
1	26.2	16.1	16.9	18.8	6.3	6.0
6	46.7	33.9	34.0	60.1	24.4	23.7
72	64.6	48.4	47.5	85.7	39.9	36.0

[a] Data for Figure IV-12 (A) & (B).

Hydrolysis conditions: 5 FPU/g dry biomass, 81.2 CBU/g dry biomass, substrate concentration: 10 g/L.

Effect of Biomass Crystallinity on Digestibility

Table H-16. Hydrolysis profiles of poplar wood with various crystallinities[a]

Incubation period (h)	Glucan conversions at various crystallinities (%)		Xylan conversions at various crystallinities (%)	
	19.1%	55.8%	19.1%	55.8%
1	22.3	12.3	6.2	4.9
3	44.9	20.6	21.7	11.5
6	62.9	29.8	40.1	17.3
12	76.0	44.8	58.5	25.4
24	84.5	58.7	70.7	35.8
48	86.9	70.4	76.0	45.0
72	89.0	73.7	79.7	50.1

[a] Data for Figure IV-13 (A) & (B).

Hydrolysis conditions: 5 FPU/g dry biomass, 28.4 CBU/g dry biomass, substrate concentration: 20 g/L.

Table H-17. Effect of biomass crystallinity on digestibility of biomass with high lignin content[a]

Incubation period (h)	Glucan conversions at various crystallinities (%)			Xylan conversions at various crystallinities (%)		
	14%	22.7%	59.8%	14%	22.7%	59.8%
1	26.5	16.4	2.6	13.6	8.2	0
6	57.3	40.9	6.8	49.6	34.7	6
72	78.1	64.8	15.6	80.2	65.1	12.2

[a] Data for Figure IV-14 (A) & (B).

Hydrolysis conditions: 5 FPU/g dry biomass, 81.2 CBU/g dry biomass, substrate concentration: 10 g/L.

Enzyme Loading Studies on Poplar Wood with Different Structural Features

Table H-18. Enzyme loading studies at 1-h hydrolysis for high-digestibility poplar wood[a]

Enzyme loading (FPU/g dry biomass)	Carbohydrate conversions (%)		
	Glucan	Xylan	Total sugar
1.2	11.1	8.16	10.4
3.5	25.2	12.4	22.1
5.9	37.8	17.5	33.0
11.8	58.3	27.0	50.8

[a] Data for Figure IV-16 & IV-21.

Hydrolysis conditions: 81.2 CBU/g dry biomass, substrate concentration: 10 g/L.

Table H-19. Enzyme loading studies at 1-h hydrolysis for medium-digestibility poplar wood[a]

Enzyme loading (FPU/g dry biomass)	Carbohydrate conversions (%)		
	Glucan	Xylan	Total sugar
1	2.76	3.58	2.9
3	5.91	13.4	7.18
5	9.47	17.1	10.8
10	13.9	22.7	15.4
30	29.6	37.2	30.9

[a] Data for Figure IV-16 & IV-20.

Hydrolysis conditions: 81.2 CBU/g dry biomass, substrate concentration: 10 g/L.

Table H-20. Enzyme loading studies at 1-h hydrolysis for low-digestibility poplar wood[a]

Enzyme loading (FPU/g dry biomass)	Carbohydrate conversions (%)		
	Glucan	Xylan	Total sugar
1	1.15	0	0.87
3	2.67	0	2.02
5	3.84	2.97	3.63
10	6.07	4.38	5.66
30	10.1	10.4	10.1
50	11.9	11.6	11.9

[a] Data for Figure IV-16 & IV-22.

Hydrolysis conditions: 81.2 CBU/g dry biomass, substrate concentration: 10 g/L.

Table H-21. Enzyme loading studies at 6-h hydrolysis for high-digestibility poplar wood[a]

Enzyme loading (FPU/g dry biomass)	Carbohydrate conversions (%)		
	Glucan	Xylan	Total sugar
1.2	33.1	46.6	36.4
3.5	66.1	61.9	65.1
5.9	83.3	71.4	80.4
11.8	89.6	82.8	88.0

[a] Data for Figure IV-17 & IV-21.

Hydrolysis conditions: 81.2 CBU/g dry biomass, substrate concentration: 10 g/L.

Table H-22. Enzyme loading studies at 6-h hydrolysis for medium-digestibility poplar wood[a]

Enzyme loading (FPU/g dry biomass)	Carbohydrate conversions (%)		
	Glucan	Xylan	Total sugar
0.3	2.15	19.3	5.07
0.6	4.14	25.2	7.73
1	8.48	33.2	12.7
2.4	13.8	41.2	18.5
3	19.9	49.2	24.9
5	31.4	60.0	36.3
10	51.8	70.1	54.9
30	79.2	89.2	80.9
59.1	84.6	94.0	86.2
88.6	85.7	94.7	87.2
118.2	86.5	95.6	88.1

[a] Data for Figure IV-17 & IV-20.

Hydrolysis conditions: 81.2 CBU/g dry biomass, substrate concentration: 10 g/L.

Table H-23. Enzyme loading studies at 6-h hydrolysis for low-digestibility poplar wood[a]

Enzyme loading (FPU/g dry biomass)	Carbohydrate conversions (%)		
	Glucan	Xylan	Total sugar
1	3.50	4.56	3.76
3	8.95	9.32	9.04
5	11.4	10.4	11.1
10	15.2	13.3	14.8
30	23.1	22.0	23.0
50	26.4	26.2	26.3

[a] Data for Figure IV-16 & IV-21.

Hydrolysis conditions: 81.2 CBU/g dry biomass, substrate concentration: 10 g/L.

Table H-24. Enzyme loading studies at 72-h hydrolysis for high-digestibility poplar wood[a]

Enzyme loading (FPU/g dry biomass)	Carbohydrate conversions (%)		
	Glucan	Xylan	Total sugar
0.1	31.2	71.1	40.7
0.3	56.6	76.0	61.2
0.6	73.4	80.9	75.2
0.9	84.3	84.6	84.4
2.4	91.4	95.3	92.3

[a] Data for Figure IV-18 & IV-21.

Hydrolysis conditions: 81.2 CBU/g dry biomass, substrate concentration: 10 g/L.

Table H-25. Enzyme loading studies at 72-h hydrolysis for medium-digestibility poplar wood[a]

Enzyme loading (FPU/g dry biomass)	Carbohydrate conversions (%)		
	Glucan	Xylan	Total sugar
0.06	3.83	40.4	10.1
0.1	6.08	39.9	11.8
0.25	12.7	48.6	18.8
0.5	22.4	60.0	28.8
1	38.1	72.8	44.0
1.5	47.9	80.0	53.4
2.5	68.1	90.9	72.0
5	87.1	94.0	90.0
11.8	89.2	94.5	91.5
30	88.9	95.8	91.4

[a] Data for Figure IV-18 & IV-20.

Hydrolysis conditions: 81.2 CBU/g dry biomass, substrate concentration: 10 g/L.

Table H-25. Enzyme loading studies at 72-h hydrolysis for low-digestibility poplar wood[a]

Enzyme loading (FPU/g dry biomass)	Carbohydrate conversions (%)		
	Glucan	Xylan	Total sugar
0.12	2.70	3.64	2.93
0.3	6.97	7.69	7.14
0.6	10.4	10.8	10.5
1	14.6	14.5	14.6
3	22.8	21.6	22.5
5	28.5	28.3	27.5
10	33.1	32.5	32.7
30	47.1	46.9	47.1
50	52.4	50.3	51.9
88.6	58.6	59.0	58.7
118.2	61.5	61.2	61.4
177.3	63.8	62.4	63.5

[a] Data for Figure IV-18, IV-19, and IV-22.

Hydrolysis conditions: 81.2 CBU/g dry biomass, substrate concentration: 10 g/L.

Reproducibility of Enzymatic Hydrolysis

Table H-26. Reproducibility of sugar conversion during enzymatic hydrolysis[a]

Incubation period (h)	Enzyme loading (FPU/d dry biomass)	Glucan		Xylan		Total sugar	
		Conversion (%)	Standard deviation	Conversion (%)	Standard deviation	Conversion (%)	Standard deviation
1	1.5	3.44	0.38	5.8	0.37	4	0.22
	5	9.07	0.5	13.0	0.49	10.0	0.4
	10	15.8	0.6	20.8	0.75	17.0	0.60
6	1.5	12.4	0.4	34.5	0.33	17.6	0.34
	5	32.5	0.85	51.8	0.80	37	0.76
	10	54.0	1.1	65.1	0.89	56.6	1.0
72	0.25	26.1	0.72	56.0	1.46	33.2	0.89
	1.5	53.2	1.05	73.5	1.31	58.0	1.09
	5	79.2	2.33	93.1	2.83	82.5	2.44

[a] Data for Figure IV-23.

Hydrolysis conditions: 81.2 CBU/g dry biomass, substrate concentration: 10 g/L.

Effect of Ball Milling Time on Biomass Crystallinity

Table H-27. Effect of ball milling time on biomass crystallinity[a]

Biomass	Ball milling time (d)										
	0	0.5	1	2	3	4	5	6	7	8	9
Corn stover	55.8	---	42.5	34.6	25.6	23.7	23.9	23.3	22.4	23.8	22.4
Cellulose	82.2	66.1	53.4	29.8	9.5	---	---	---	---	---	---

[a] Data for Figure C-1.

APPENDIX I

COMPARISON OF CORRELATION PARAMETERS

Table I-1. Comparison of correlation parameters determined by the parametric models

Dependent variables		L^a, A^b, CrI_C^c, carbohydrate content[d]		L^a, A^b, CrI_C^c	
		R^2	MSE	R^2	MSE
Glucan	1-h slope	0.95	2.5	0.94	2.6
	1-h intercept	0.72	1.0	0.69	1.1
	6-h slope	0.93	4.3	0.93	4.3
	6-h intercept	0.95	7.1	0.93	8.6
	72-h slope	0.9	6.9	0.89	7.3
	72-h intercept	0.96	22	0.96	24
Xylan	1-h slope	0.69	1.1	0.66	1.2
	1-h intercept	0.71	1.3	0.72	1.3
	6-h slope	0.86	3.4	0.86	3.4
	6-h intercept	0.9	15	0.91	15
	72-h slope	0.63	6.3	0.6	6.5
	72-h intercept	0.95	35	0.95	34
Total Sugar	1-h slope	0.94	1.9	0.94	1.9
	1-h intercept	0.74	0.9	0.7	1.0
	6-h slope	0.93	3.6	0.93	3.6
	6-h intercept	0.95	5.9	0.94	8.0
	72-h slope	0.88	5.6	0.88	5.6
	72-h intercept	0.96	25	0.96	24

[a] Lignin content.

[b] Acetyl content.

[c] Cellulose crystallinity.

[d] Carbohydrate content: glucan, xylan, and total sugar. Total sugar = glucan + xylan.

Table I-2. Summary of correlation parameters for slopes and intercepts of xylan hydrolysis determined by the parametric models

Independent variables	Correlation coefficients	1 h		6 h		72 h	
		Slope	Intercept	Slope	Intercept	Slope	Intercept
L^a, A^b, $CrI_C{}^c$	R^2	0.66	0.72	0.86	0.91	0.6	0.95
	MSE	1.2	1.3	3.4	15	6.5	34
L^a, A^b, $CrI_C{}^c$, predicted data of glucan	R^2	0.71	0.72	0.88	0.91	0.72	0.92
	MSE	1.1	1.3	2.9	15	4.7	55

[a] Lignin content.

[b] Acetyl content.

[c] Cellulose crystallinity.

Table I-3. Predictive ability of the parametric models on slopes and intercepts of carbohydrate hydrolysis

Dependent variables		MSE		
		L^a, A^b, CrI_C^c, carbohydrate content[d]		L^a, A^b, CrI_C^c
		CrI_C^b	CrI_B^c	
Glucan	1-h slope	17	23	19
	1-h intercept	9.6	10	13
	6-h slope	14	19	14
	6-h intercept	76	97	87
	72-h slope	11	18	11
	72-h intercept	211	310	247
Xylan	1-h slope	4.2	15	4.4
	1-h intercept	5.0	7.5	5.0
	6-h slope	7.3	7.7	11
	6-h intercept	66	65	65
	72-h slope	9.3	8.7	19
	72-h intercept	186	194	200
Total Sugar	1-h slope	8.2	11	9.8
	1-h intercept	4.5	4.8	6.6
	6-h slope	13	17	13
	6-h intercept	75	88	66
	72-h slope	21	24	20
	72-h intercept	124	176	208

[a] Lignin content.

[b] Acetyl content.

[c] Cellulose crystallinity.

[d] Carbohydrate content: glucan, xylan, and total sugar. Total sugar = glucan + xylan.

Table I-4. Comparison of predictive ability of the parametric and nonparametric models on carbohydrate conversions

Carbohydrate	Incubation period (h)	MSE		
		Parametric model		Nonparametric model
		L[a], A[b], CrI_C[c], carbohydrate content[d]	L[a], A[b], CrI_C[c]	L[a], A[b], CrI_C[c]
Glucan	1	64	81	100
	6	149	165	186
	72	287	275	290
Xylan	1	23	22	19
	6	112	118	105
	72	250	246	261
Total sugar	1	28	39	49
	6	152	130	132
	72	192	263	266

[a] Lignin content.

[b] Acetyl content.

[c] Cellulose crystallinity.

[d] Carbohydrate content: glucan, xylan, and total sugar. Total sugar = glucan + xylan.

APPENDIX J

SAS PROGRAMMING FOR VARIABLE SELECTION AND COEFFICIENT ESTIMATION

```
Data DC0;
Input y1 y2 x1 x2 x3 x4;
z1=x1*x1; z2=x1*x2; z3=x1*x3;z4=x2*x2; z5=x2*x3; z6=x3*x3; z10=x4*x4;
Cards;
data
Proc reg; model y1=x1 x2 x3 x4 z1 z2 z3 z4 z5 z6 z10/selection=CP;

Proc reg; model y2=x1 x2 x3 x4 z1 z2 z3 z4 z5 z6 z10/selection=CP;

run;


Data DC0;
Input y1 y2 x1 x2 x3 x4;
z1=x1*x1; z2=x1*x2; z3=x1*x3;z4=x2*x2; z5=x2*x3; z6=x3*x3; z10=x4*x4;
Cards;
data
Proc reg; model y1=x1 x2 x3 x4 z1 z2 z3 z4 z5 z6 z10/p;

Proc reg; model y2=x1 x2 x3 x4 z1 z2 z3 z4 z5 z6 z10/p;

run;
```

VITA

Li Zhu received a BS in chemical engineering from Beijing University of Chemical Technology in 1993 and her MS in organic chemical engineering from Research Institute of Petroleum Processing in 1996. She worked as a chemical engineer in the Fine Chemical Department at Research Institute of Petroleum Processing. In August 2000, she started her Ph.D. in the Department of Chemical Engineering at Texas A&M University, completing this degree in August 2005.

Her current address is
1100 Hensel DR Apt U2C,
College Station, TX 77840
Phone number: 1-979-862-9448.
Her current email address is roseyeah@yahoo.com